Neural pathways of movement fractionation

Lauren R. Dean

Submitted for the degree of
Doctor of Philosophy

September 2014

Institute of Neuroscience
Faculty of Medical Sciences
Newcastle University
Newcastle Upon Tyne, UK

Supervisors:
Prof. Stuart N. Baker
Dr Andrew Jackson

Abstract

Stroke is a common neurological event which often results in motor deficits of the hand and arm. The reticulospinal tract (RST) may partly underlie residual hand and arm movement ability after a stroke but remains poorly characterised. A greater understanding of the RST could inform work to improve motor recovery. Additionally, the development of non-invasive methods of probing the RST in humans should allow comparison of the characteristics of the RST across species.

It has been suggested that the RST is involved in mediating muscle responses to auditory startle, experimentally known as the StartReact paradigm. However, it was not clear how this pathway was involved. A human experiment presented here suggests that the RST comprises the final pathway in the StartReact effect, confirming it as a technique to probe the RST in humans. Other factors such as habituation and the validity of a marker of the StartReact effect were also further explored; these findings may inform future use of the technique.

The output divergence, co-activation patterns, level of fractionation and synergies produced by the RST were further characterised in macaques and baboons; these factors had previously been mostly unexplored. In macaques, two subdivisions of primary motor cortex (M1) were also characterised in order to compare to the RST. These subdivisions are based upon the presence of corticomotoneuronal (CM) cells, and consist of 'old' (CM cells absent) and 'new' (CM cells present) M1. Stimulation of new M1 produced a higher level of fractionation of movement than stimulation of old M1 and the reticular formation (RF). The RF is suggested to produce slightly more fractionated behaviour than old M1, though the baboon RF responses may be less fractionated than those from macaque old M1. Output divergence of the RF as well as old and new M1 was also explored. However, methodological limitations may have biased the results towards muscles with more excitable motoneurons, or monosynaptic connections.

In baboons, threshold stimulation elicited responses in upper limb and axial muscles only, with higher stimulation intensities or trains of pulses required to activate leg muscles. In contrast to long-held beliefs about RST output, distal upper limb muscles were more commonly activated than proximal ones.

Previously reported attempts to record natural electromyography (EMG) data from macaques were limited to controlled experimental settings, and hence may have differed from EMG observed during truly natural behaviours. Here, EMG was recorded from 18 muscles in one macaque over several hours of natural, untrained activity in her home cage. Two matrix decomposition algorithms extracted three to four dominant synergies from the data. This number is comparable to that previously described for 'natural' behaviour in more controlled conditions, suggesting that it accurately reflects the dominant synergies used across both conditions.

Future work should aim to delineate the respective contributions of the RST and corticospinal tract to natural movement and to develop approaches to manipulate RST projections in humans to improve post-stroke motor outcomes.

Dedicated to my parents and sister.

Acknowledgements

Firstly I would like to thank my supervisor, Stuart Baker, for his tirelessly cheerful support, help and patience over the past four years.

My macaque work would have been impossible without the daily help of the laboratory technicians, Terri Jackson and Lee Reed. Felipe De Carvalho deserves a special mention for developing and trouble-shooting the datalogging hat, as does Norman Charlton for aiding in its manufacture. Norman also supplied a multitude of other monkey-related items, often at short notice.

Veterinary advice from Henri Bertrand, Paul Flecknall and Aurelie Thomas, as well as surgical support from Denise Reed and Caroline Fox were invaluable during implant surgery and beyond. For the work on baboons in Kenya, I would like to thank George Omondi and Ngalla Jillani for their assistance. I would also like to acknowledge the frequent help provided by the past and present post-docs of the lab, Karen Fisher, Demetris Soteropoulos, Claire Witham and Boubker Zaaimi, and their assistance during acute experiments.

My time here in the lab just would not have been the same without the daily interactions with all of those named above, as well as John Barrett, Kenneth Brown, Georgia Collins, Cyril Eleftheriou, Michael Fisher, Ferran Galán, Bonne Habekost, Thomas Hall, Kia Nazarpour, Tobias Pistohl, Claire Schofield, Harbaljit Sohal, Edina Tozser and Jonas Zimmermann, who I must also thank for the entertainment, laughter and drinking companionship they provided.

I thank my parents Martin and Andrea and sister Nigella for their support and encouragement throughout my education, and for tolerating my infrequent visits during busy times; I could not have survived eight years of university without them. Finally I would like to thank Stephan for his love and advice since the very beginning of my PhD.

Lauren R. Dean

Presentations to learned societies

Dean LR and Baker SN (2012). Fractionation of muscle activity in the StartReact paradigm. *Society for Neurosciences,* New Orleans, USA. Poster presentation.

Dean LR, Omondi G, Jillani N and Baker SN (2014). Divergent projections to fore- and hindlimb from the primate reticular formation. *Neural Control of Movement*, Amsterdam, the Netherlands. Poster presentation.

Reed L, Jackson T, **Dean LR** and Baker SN (2014). Refined techniques for acclimatizing female macaques to restraint. *Animal Concepts Workshop,* The Hague, the Netherlands. Poster presentation.

Dean LR, Omondi G, Jillani N and Baker SN (2014). Divergent projections to fore- and hindlimb from the primate reticular formation. *Northern Neural Control of Movement 2014*, Leeds, UK. Oral presentation.

Contents

List of Figures

List of Tables

List of Abbreviations

1DI	First dorsal interosseous
2DI	Second dorsal interosseous
AbPL	Abductor pollicis longus
ABR	Auditory blink reflex
ADM	Abductor digiti minimi
APB	Abductor pollicis brevis
BR	Brachioradialis
CDP	Cumulative distribution plot
CM	Corticomotoneuronal
CPG	Central pattern generator
CST	Corticospinal tract
DC	Direct current
EAO	External abdominal oblique
EDC	Extensor digitorum communis
ECR	Extensor carpi radialis
ECRB	Extensor carpi radialis brevis
ECRL	Extensor carpi radialis longus
ECU	Extensor carpi ulnaris
ED2,3	Extensor digitorum 2,3
ED4,5	Extensor digitorum 4,5
EDC	Extensor digitorum communis
EMG	Electromyography
EPB	Extensor pollicis brevis
EPSP	Excitatory post-synaptic potential
eRT	Earliest reaction time
FA	Factor analysis
FCR	Flexor carpi radialis
FCU	Flexor carpi ulnaris
FDL	Flexor digitorum longus
FDP	Flexor digitorum profundus
FDS	Flexor digitorum superficialis

FPL	Flexor pollicis longus
IAL	Interaural line
IC	Independent component
ICA	Independent component analysis
ICMS	Intracortical microstimulation
IPSP	Inhibitory post-synaptic potential
LGS	Lateral-gastrocnemius/soleus
M1	Primary motor cortex
MLF	Medial longitudinal fasciculus
MRI	Magnetic resonance imaging
MVC	Maximum voluntary contraction
NMDA	N-methyl-D-aspartate
NNMF	Non-negative matrix factorisation
OOc	Orbicularis oculi
PC	Principal component
PCA	Principal component analysis
PL	Palmaris longus
PM	Pectoralis major
PnC	Caudal pontine nucleus
PNs	Propriospinal neurons
PPN	Pedunculopontine nucleus
PVE	Percentage of variance explained
PT	Pyramidal tract
RF	Reticular formation
RST	Reticulospinal tract
RT	Reaction time
SCM	Sternocleidomastoid
S-ICMS	Single pulse intracortical microstimulation
spikeTA	Spike triggered-average
stimulusTA	Stimulus triggered-average
TMS	Transcranial magnetic stimulation

1 General introduction

In this Chapter I review the scientific background of this thesis. Starting from an overview of the motor system, I focus on the reticulospinal tract and its potential to contribute to movement recovery in stroke patients. Methods of probing this pathway in humans and non-human primates are also explored, with an emphasis on the value of non-human primates for motor systems research. Finally, an outline of each subsequent Chapter presented in this thesis is given to conclude.

1.1 Introduction

Roughly every five minutes someone in the UK suffers a stroke. This equates to over 150,000 new patients every year, adding to the 1.1 million people currently nationwide who have been affected by a stroke in the past (Stroke Association 2012). Such individuals are often left with impaired movement, including of the hands, which is one of the most frequently cited factors limiting quality of life. This underscores the importance of efforts to restore movement in these patients.

Several distinct pathways project to spinal motoneurons which innervate the peripheral musculature. Strokes resulting in motor impairments often damage the largest and most recently evolved of these pathways, the corticospinal tract (CST), which originates in the primary motor cortex. By contrast, they leave intact the pathways controlled by the brainstem, including the reticulospinal tract (RST), and there is some evidence suggesting that the RST may be responsible for residual motor function post-stroke. Some stereotypical motor behaviours observed after a stroke resemble those expected from RST output, for example maladaptive muscle co-activations or 'synergies' (Dewald et al., 1995). Furthermore, reticulospinal connections with the motoneurons of selected muscles strengthen after CST lesion (Zaaimi et al., 2012). Therefore, the RST already has some control over motor function after stroke and constitutes a potential basis for efforts to improve recovery.

Regaining hand and finger control after loss of its function is particularly important to people (Anderson, 2004). Hence, any substrate for recovery should ideally have projections to motoneurons of the distal upper limb muscles. The RST, although previously believed to control predominantly axial and proximal muscles, has recently been shown to possess distal projections, including to intrinsic hand muscles. Improved independent or 'fractionated' finger control is another important aspect of recovery. Presently, the full range of muscles controlled by the RST in primates, the combinations in which they are activated and the level of fractionated movement achievable by this tract remain unclear. Investigating these properties is of both basic scientific and clinical interest and is the main aim of the experiments presented here. Further knowledge of these characteristics may prove vital to future efforts to manipulate the RST in order to allow improved motor recovery.

This thesis endeavours to advance the field of motor neuroscience by presenting novel findings on the output divergence, level of fractionation and synergies of the CST and RST. Individual chapters present one line of investigation each in a self-contained manner. However, they do not include comprehensive background of the motor system, the reticulospinal tract, the StartReact phenomenon, synergies or the potential role of the reticulospinal system in post-stroke movement control; these areas are introduced further below.

1.2 The motor system

1.2.1 Cortical areas of motor control

Movement is controlled by both cortical and subcortical regions of the brain. The most highly evolved parts of the human motor system reside in the cortex and consist of the primary motor area (M1) and subsidiary motor areas, including the ventral and dorsal premotor areas and the supplementary motor area (Rizzolatti and Luppino, 2001; Cerri *et al.*, 2003; Chouinard and Paus, 2006, Figure 1.1). M1 is located on the precentral gyrus and – like the rest of the neocortex – is comprised of five layers or laminae, of which the innermost

(layer V) projects to subcortical areas. This projection is composed of the axons of pyramidal cells, which derive their name from the characteristic shape of their somas.

M1 is organised somatotopically, with cells projecting to the leg, arm and face arranged along a mediolateral gradient (Hlustik *et al.*, 2001). This is represented by the human homunculus (Penfield and Rasmussen, 1950) or monkey simiusculus (Woolsey *et al.*, 1952). However, in recent years this strict somatotopic layout has been criticised as too simplistic. Instead, it has been suggested that there is much overlap in the broad somatotopy of different limbs, with multiple representations of muscles arranged in a 'mosaic' alongside representations of other muscles (Andersen *et al.*, 1975; Schieber, 2001). The general somatotopy is deemed to represent sets of muscles which would not be functionally linked, such as the ocular muscles and those of the foot. However, the multiple, interwoven representations of individual muscles within a given area of M1 might allow co-activation of functionally relevant muscles during different movements (Schieber, 2001). This is evidenced by convergent input from multiple M1 areas to one motoneuron pool and experiments using cortical microstimulation showing that distributed regions can produce movements of the same muscles (Donoghue *et al.*, 1992).

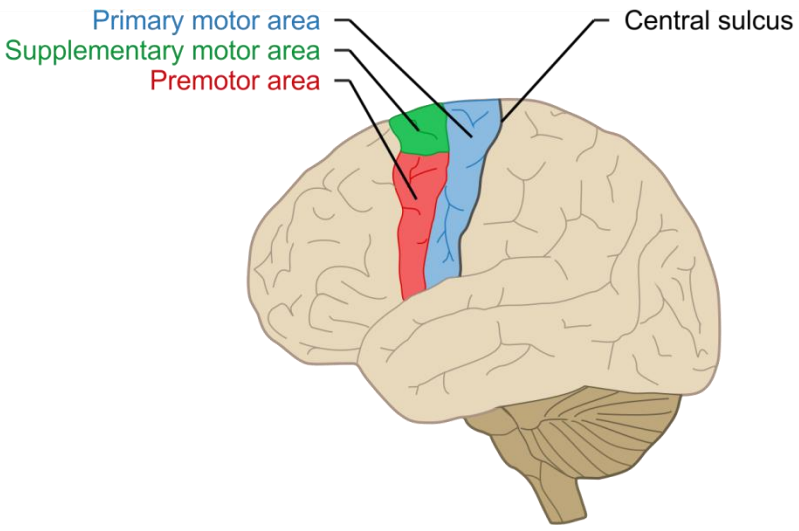

Figure 1.1: The cortical motor areas.

Projections from M1 comprise the corticospinal tract (CST), which extends from the cortex via the internal capsule to the pyramids of the medulla, where approximately 80% of axons decussate, with the remainder continuing ipsilaterally. The pyramids lend their name to the alterative term for the CST (pyramidal tract, PT; coincidentally the same name as pyramidal cells). The crossed pathway continues in the lateral funiculus of the spinal cord, with axons synapsing with motoneurons (MNs) either directly (Landgren *et al.*, 1962) or indirectly via excitatory or inhibitory interneurons in the intermediate zone (Jankowska *et al.*, 1976; Isa *et al.*, 2006). Many CST fibres also send collaterals to subcortical areas, including the thalamic nuclei, inferior olive and reticular formation; these will be discussed further below (Keizer and Kuypers, 1989; Canedo and Lamas, 1993; Lamas *et al.*, 1994).

Cortical cells making excitatory monosynaptic connections onto motoneurons, often referred to as corticomotoneural (CM) cells, permit selective muscle facilitation and are thought to underlie fractionated finger movements (Buys *et al.*, 1986; Bennett and Lemon, 1996). CM connections are established postnatally in macaques, and their development parallels the ability to carry out independent finger movements (Kuypers, 1962; Armand *et al.*, 1997). Conversely, in humans CM connections are present at birth, although independent finger movements do not develop until 6-12 months postnatally (Eyre *et al.*, 2000). CM connections are thought to have evolved relatively recently; indeed, phylogenetically younger species of monkey have higher numbers of CM cells, which reflects their greater ability to carry out independent finger movements (Kuypers, 1987).

The distribution of CM cells throughout M1 in higher primates is not uniform, leading to the suggestion that M1 can be divided into two distinct areas based on their possession of CM cells (Rathelot and Strick, 2009). The majority of CM cells originate in the more recently evolved anterior bank of the central sulcus, termed ‘new M1’, whereas the phylogenetically older, rostral part of M1 (precentral gyrus, or ‘old M1’) is lacking in these cells. CM cells can project to

more than two motoneuron pools, which can synapse with either proximal and distal muscles or both, and may be located in different spinal segments (McKiernan *et al.*, 1998). The aforementioned overlap in cortical representations of different muscles also pertains to CM cells (Rathelot and Strick, 2009), even between muscles separated as widely as those in the hand and shoulder girdle.

1.2.2 Muscle synergies

Mammals, particularly humans, are capable of producing an extensive repertoire of movements, each of which may involve a range of muscles located throughout the limbs and trunk. During a given movement, separate activation of each muscle at the appropriate time and to the correct level would be expected to require a large amount of processing. This has prompted the suggestion of the existence of synergies, representing functional groups of muscles which can each be activated or suppressed to a particular, predetermined degree (Figure 1.2). Activating various synergies either simultaneously or sequentially could reduce the amount of processing required for execution of a given movement. Synergies might not be used all the time and for all types of movement, but potentially in combination with separate control of individual muscles; in some movements, synergies may not be used at all (Ajiboye and Weir, 2009). Presently, it is not clear to what extent synergies are used in everyday activities. Synergies may be time-varying (Klein Breteler *et al.*, 2007), whereby the onset of activation or inhibition across muscles is staggered according to when each is required throughout a movement, or static, in which all muscles are activated or suppressed at the same time, although still to varying degrees (d'Avella *et al.*, 2003).

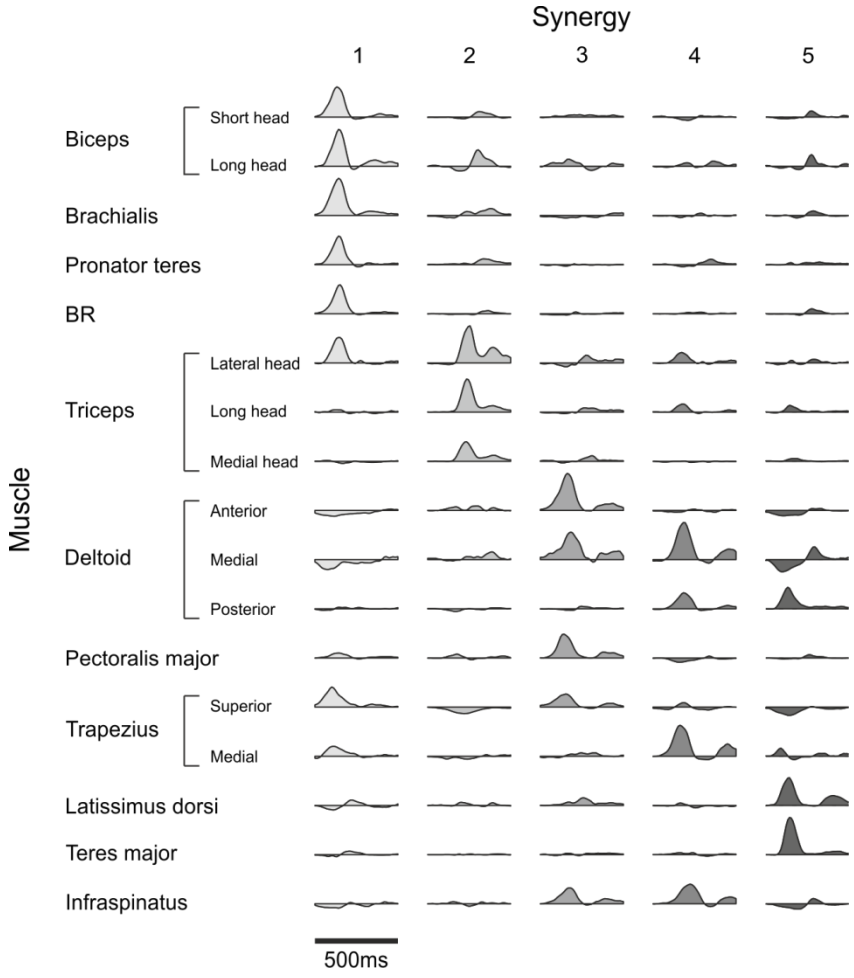

Figure 1.2: Five time-varying muscle synergies, with the level of activation of each muscle over 500ms. Y-axis amplitudes represent activation to a particular coefficient. (Adapted from d'Avella et al. 2006).

Evidence for the existence of synergies has been found in frogs (d'Avella *et al.*, 2003), monkeys (Overduin *et al.*, 2008) and humans (Weiss and Flanders, 2004). Three to five key synergies usually explain most (around 75%) of the variance in the electromyography (EMG) data recorded (d'Avella *et al.*, 2006) and are often consistent between individual animals within a sample. The size of objects lifted in these experiments predicts the synergy amplitude coefficient, showing how the same synergies are adapted for use in different situations (Overduin *et al.*, 2008). Furthermore, grasps of different objects involve the activation of several different synergies, each to a specific degree (Castellini and van der Smagt, 2013). After deafferentation of frogs through ablation of the dorsal spinal roots some synergies are preserved, indicating that they might be modules of central pattern generators (CPGs), which can produce motor output

without sensory input or feedback. However, sensory feedback can also act on synergy recruitment, such as by 'uncoupling' muscles from synergies (Cheung *et al.*, 2005).

Potential substrates Potential anatomical substrates of synergies remain controversial. A spinal origin has been postulated by studies which observed multi-joint movements resulting from intraspinal microstimulation (ISMS, described in detail below) (Zimmermann *et al.*, 2011). Furthermore, patients with cortical strokes have similar synergies in the affected and unaffected arms, suggesting that synergies are generated in a subcortical or spinal site (Cheung *et al.*, 2009). Indeed, both decerebrated (neuraxis transected above the brainstem) and spinalised (neuraxis transected at the base of the medulla) frogs display movements which can be reduced to six synergies, each with two to three dominant muscles, though decerebrated frogs retained 'richer' movements involving fewer muscles (Hart and Giszter, 2004).

Alternatively, a cortical origin has been proposed, as stimulation of M1 produces synergies similar to those found naturally, including hand and finger movements (Overduin *et al.*, 2012). Two potential cortical substrates have been suggested, and these may constitute competing or complementary hypotheses.

Firstly, the representation of each muscle in the motor cortex is repeated in multiple distinct locations, which are linked by long-range horizontal connections, shown anatomically (Huntley and Jones, 1991) and physiologically (Baker *et al.*, 1998). These repeated representations can neighbour cells projecting to anatomically distinct muscles (Rathelot and Strick, 2006), which may reflect involvement of a particular muscle in multiple different synergies, each of which is represented as an anatomically discrete group of cells (Buys *et al.*, 1986; Rathelot and Strick, 2006; Yakovenko *et al.*, 2011; Overduin *et al.*, 2012; Capaday *et al.*, 2013).

Secondly, the muscles activated by CM cells in response to single pulse intracortical microstimulation (S-ICMS, see below) are often the same as those

activated after spontaneous firing of CM cells, although activated to a stronger degree (Cheney and Fetz, 1985). This implies the existence of 'functional clusters' of neighbouring cells. These clusters may be bound together both within and across synergies by intracortical collaterals (Capaday *et al.*, 2013), therefore exciting neighbouring cells when a particular muscle is moved. When a given muscle is moved, excitation of neighbouring cells could serve to bring about postural adjustments or stabilisation, or to activate other muscles required for carrying out the intended movement. Consistent with this, the discharge patterns of single M1 neurons have been correlated with the EMG recorded from a range of arm and hand muscles during a simple reaching task. For individual cells, 'functional linkage vectors' were identified, composed of values which each represented the correlation of the discharge with a particular muscle. Functionally relevant clusters of these neurons were revealed, suggested as representing muscle synergies (Holdefer and Miller, 2002).

Presently, there is no consensus as to whether synergies are represented at a spinal level, a cortical level or both. Alternative suggestions are that synergies are produced by the brainstem or spinal cord in response to activation by the cortex, or that the cortex combines synergies from downstream areas into more complex movements.

Synergy analysis methods In order to examine the synergies underlying EMG data, dimension reduction algorithms such as principal component analysis (PCA), independent component analysis (ICA) and non-negative matrix factorisation (NNMF) are often used. These algorithms find the key structure underlying the data in terms of the main synergies or 'components' that account for most of the variance in the data. These components are composed of a vector of coefficients, with one coefficient for each variable used; in the case of EMG data, these coefficients would represent the degree to which each muscle is involved in a given component. In PCA, these components are orthogonal; in ICA they are not, but the data are assumed to come from a non-Gaussian distribution, and components are sought which are as statistically independent

as possible. These techniques can be used to extract features or separate mixed signals into their original signals (Hyvarinen and Oja, 2000).

EMG synergy studies have used PCA on data recorded from both the lower (Ivanenko *et al.*, 2004) and upper limb (Klein Breteler *et al.*, 2007), finding that four principal components (PCs) explained about 80% of the variance of EMG data, including two key synergies. They argued in favour of using PCA due to its incorporation of reciprocal patterns of EMG in which some muscles are inhibited whilst others are activated, a feature of movement which NNMF does not take into account (Santello *et al.*, 2002; Weiss and Flanders, 2004). ICA was not discussed by these authors, though one study compared the ability of several dimension reduction algorithms (PCA, NNMF, ICA, ICA applied to PCA, and factor analysis) to extract synergies from real and simulated data (Tresch *et al.*, 2006). The algorithm with the best performance was 'ICA applied to the subspace defined by PCA' (ICAPCA) and the worst-performing one was PCA. However, their synthesised data contained only non-negative values, which they argued to reflect both activation and suppression of muscles though how this is true is not clear. The algorithm referred to as ICA in the comparison study did not perform dimension reduction, therefore extracted an equal number of components as sources (Bell and Sejnowski, 1995). The ICAPCA algorithm was essentially the same algorithm but carried out after reducing the dimensionality of the data to four principal components using PCA then reconstructing it. In most Chapters in this thesis, both PCA and ICA were used due to their inclusion of inhibitory effects and the results of both methods compared. The ICA algorithm used here (fastICA) was a different one to that used by Tresch, but reduced the dimensionality of the data using PCA akin to the ICAPCA they used.

1.2.3 Brainstem pathways

Subcortical motor pathways exist in addition to the CST; these are divided into the dorsolateral and ventromedial descending systems (Kuypers, 1982). The lateral brainstem pathways run in the dorsolateral funiculus of the spinal cord

and include the pontospinal tract, projecting from the ventrolateral pontine tegmentum, and the rubrospinal tract originating from the magnocellular red nucleus. The ventromedial brainstem pathways in the ventral funiculus of the spinal cord comprise the medial and lateral vestibulospinal tracts arising from the vestibular nuclei, the interstitiospinal and tectospinal pathways from the midbrain, as well as the reticulospinal tract (RST, Lemon, 2008). Generally, the ventromedial pathways terminate bilaterally in the ventromedial part of the intermediate zone of the spinal cord (Figure 1.3), whereas the dorsolateral pathways project to the dorsal and lateral parts of the intermediate zone. However this strict dichotomy simplifies the extensive overlap seen between termination patterns, as some ventromedial fibres also terminate in the dorsal and lateral parts of the intermediate zone (Kuypers, 1982). Additionally, the dorsolateral pontospinal tract terminates in the dorsal horn, and the RST has additional projections to the medial and lateral motoneuronal cell groups (Holstege and Kuypers, 1982). Kuypers suggested that in macaques the ventromedial pathways provide the basic ability to produce body and whole-limb movements, upon which the dorsolateral pathways add 'resolution', also providing the capacity to make independent limb movements. The CST was proposed to refine the type of movement produced by the dorsolateral pathways, also enabling the ability to make independent finger movements due to its monosynaptic connections with motoneurons (Kuypers, 1982).

Of all these pathways the CST has been researched the most. Little research has been conducted on the interstitiospinal, tectospinal and rubrospinal tracts in humans, indeed there had been no evidence of the existence of the rubrospinal tract in humans until a recent imaging study (Yang *et al.*, 2011). The vestibulospinal tract has received more attention (e.g. Miller *et al.* 2014). However recently, interest in the RST has increased, provoking more thorough investigation as to its role in movement control; this tract will form the focus of this thesis.

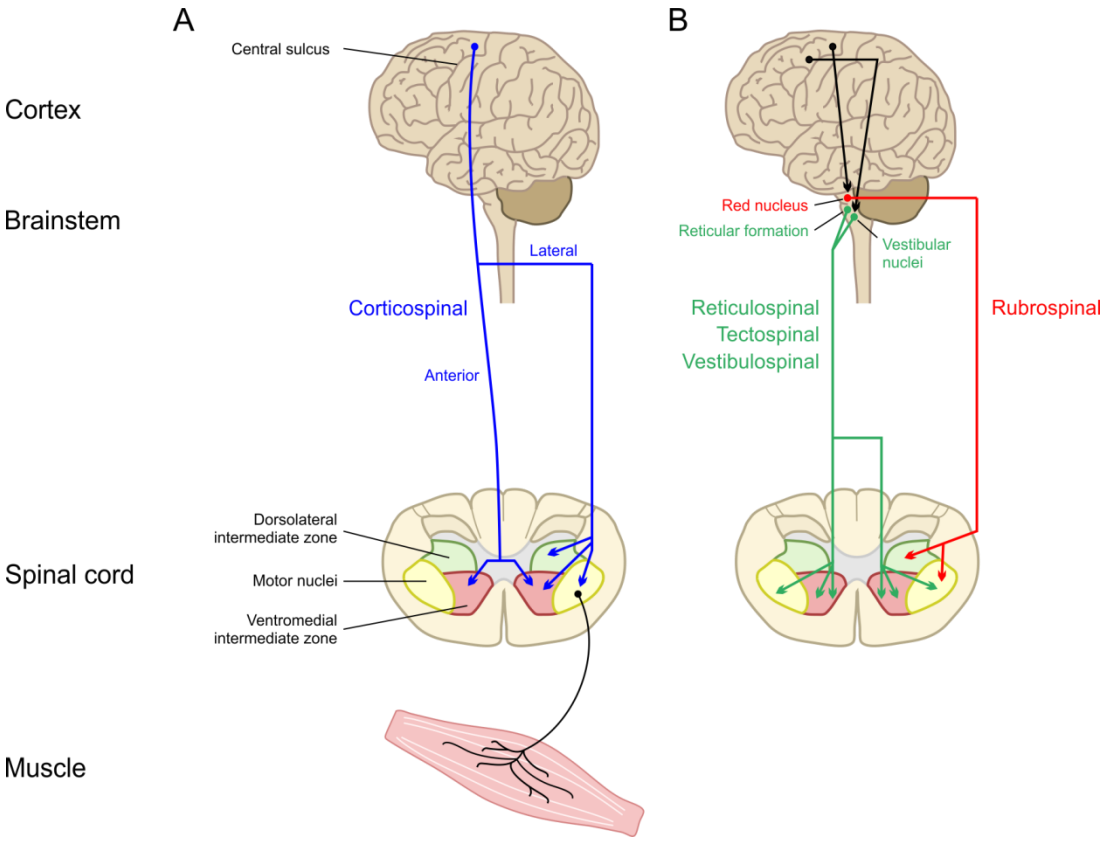

Figure 1.3: Cortical and brainstem motor pathways. The corticospinal tract (A) originates from cortical motor areas and has mostly contralateral projections. It also sends collaterals to brainstem motor pathways (B). Brainstem pathways include the contralaterally descending rubrospinal pathway which terminates in the dorsolateral intermediate zone, as well as the reticulospinal, tectospinal and vestibulospinal pathways, which terminate in the ventromedial intermediate zone, as well as upon some motoneurons directly. Adapted from Lemon (2008). Only corticospinal and reticulospinal pathways are discussed in detail in this thesis.

1.3 The reticulospinal tract

1.3.1 Origins and projections

The RST originates in the reticular formation (RF), a group of nuclei located throughout the brainstem which includes the oral pontine reticular nucleus, the gigantocellular nucleus, the caudal pontine reticular nucleus and the medial pontobulbar reticular formation (Figure 1.4). It travels in the medial longitudinal fasciculus (MLF) before continuing in the ventromedial funiculus of the spinal cord (Canedo, 1997), where individual axons terminate at multiple spinal segments in laminae VII-IX (Grillner *et al.*, 1968; Matsuyama *et al.*, 1997), usually ipsilaterally but often with contralateral collaterals (Peterson *et al.*, 1975). Connections to motor units are mono- or polysynaptic. Control of

contralateral muscles by the RST is possible via inhibitory or excitatory commissural interneurons (Bannatyne *et al.*, 2003). Therefore single RST neurons can co-activate functionally and anatomically distinct muscles, such as those in the fore- and hind-limbs, on either side of the body (Drew *et al.*, 1986; Drew, 1991). Commonly observed EMG patterns elicited from RF stimulation include activation of ipsilateral flexors and contralateral extensors (Herbert *et al.*, 2010).

The RF receives inputs from the cortex, mainly the premotor areas, via the corticoreticular pathway (shown in humans by Yeo *et al.*, 2012); additionally, CST axons send collaterals to the RF (Keizer and Kuypers, 1989). Therefore the control of movement by the RF may be influenced by the cortex, although the extent of this influence is not yet known.

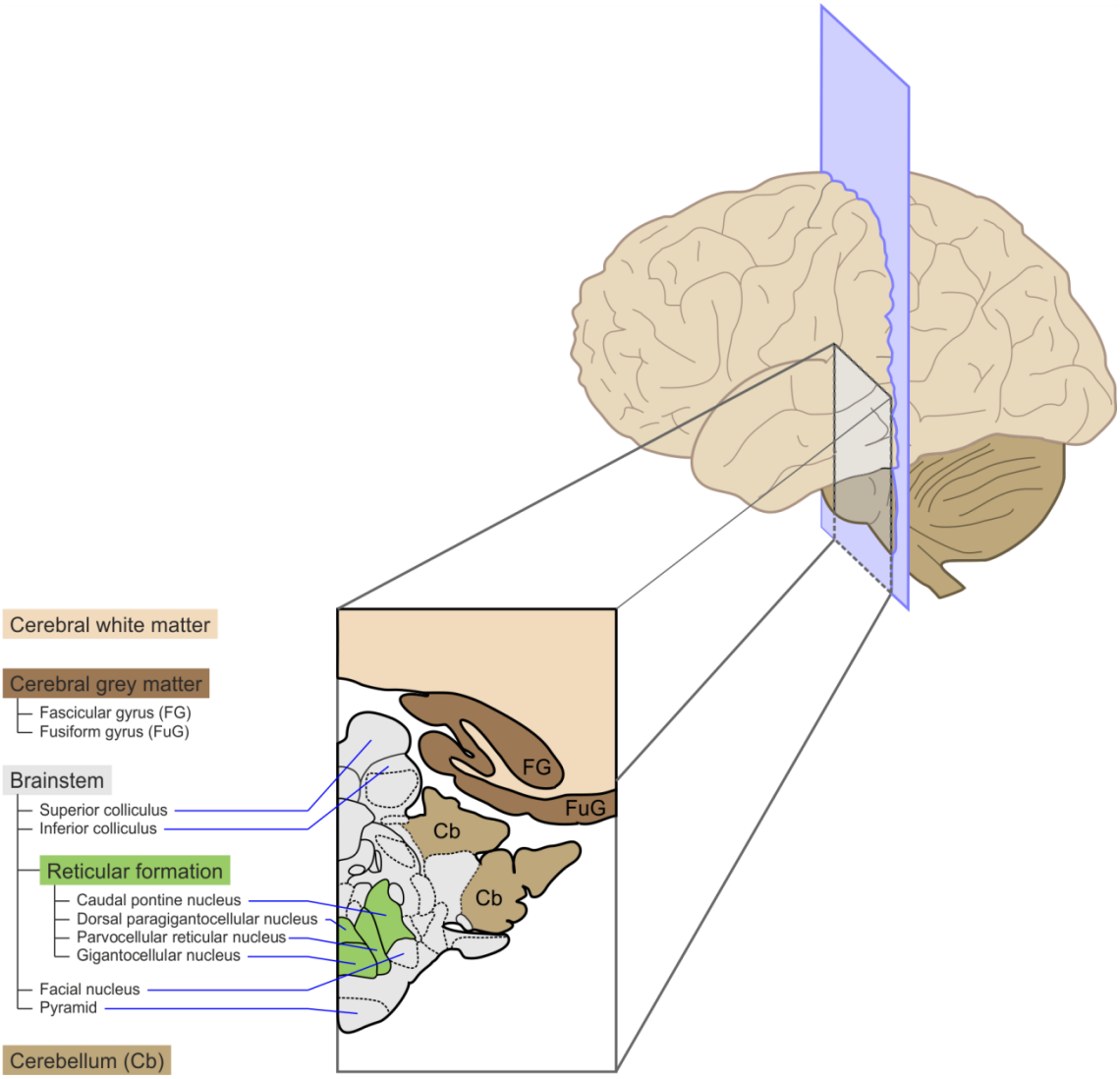

Figure 1.4: Map of the nuclei of the reticular formation and its relative location in the brainstem, (adapted from Martin and Bowden 1996) taken from a coronal slice through the brainstem, cerebellum and cortex.

1.3.2 Excitatory and inhibitory RST projections

The RST forms both excitatory and inhibitory projections onto motoneurons. Stimulation of the RF causes mono- and disynaptic excitatory post-synaptic potentials (EPSPs) (Riddle *et al.*, 2009) and potentially monosynaptic IPSPs (inhibitory post-synaptic potentials, Peterson *et al.*, 1979) in forelimb motoneurons, and monosynaptic EPSPs as well as di- and polysynaptic IPSPs in hindlimb motoneurons (Peterson *et al.*, 1979). Single RF cells have an inhibitory effect via inhibitory interneurons on motoneurons located in multiple spinal

segments, typical of the widely branching nature of the RST (Takakusaki *et al.*, 1994).

1.3.3 Role in movement control

For several decades the RST was thought to contribute mainly to the control of gross movements involved in locomotion and postural adjustments in cats (Shimamura *et al.*, 1982; Shimamura and Kogure, 1983; Schepens and Drew, 2004; Schepens *et al.*, 2008) and lamprey (Brocard and Dubuc, 2003; Pflieger and Dubuc, 2004) and during reaching in primates (Davidson *et al.*, 2007). This view originated from classical studies in macaques demonstrating a marked loss of fine finger movements, such as grasping food from wells on a food board, after combined lesions of the CST and rubrospinal tract (Lawrence and Kuypers, 1968). The loss of fine finger movements became the focus of the work, and it was concluded that such movements depend on the CST and rubrospinal tracts in monkeys. The fact that the macaques retained sufficient grasping ability to climb around their cages and feed themselves was ignored until recently. Although some fractionation of movement had been lost, a substantial degree of hand function was preserved despite damage to the CST; this must have been mediated by the only intact major pathway, the RST. Subsequent investigations into the contribution of the RST to hand control discovered that cervical horn motoneurons projecting to muscles in the forearm and hand derive input not only from CST cells but also from the RST, including both monosynaptic and disynaptic connections (Riddle *et al.*, 2009). Additionally, it was found that RST cells project to spinal cord interneurons also receiving projections from CST neurons, and that these interneurons ultimately connect to distal muscles such as those in the hand (Riddle and Baker, 2010). Single cells in the RF have even been shown to modulate discharge with index finger flexion and extension, and RF stimulation leads to EMG responses in intrinsic hand muscles (Soteropoulos *et al.*, 2012). Hence, it is clear that the RST has some control of intrinsic hand muscles, although probably limited to grosser movements.

1.4 Stroke

The World Health Organization defined a stroke as 'rapidly developing clinical signs of focal (or global) disturbance of cerebral function, lasting more than 24 hours or leading to death, with no apparent cause other than that of vascular origin' (Sacco *et al.*, 2013). Strokes can affect cortical regions, subcortical regions or both. The majority of strokes are ischaemic, i.e. blood flow to a cerebral region is impeded or blocked by thrombus within the feeding artery. A lesser proportion is haemorrhagic, caused by bleeding from a cerebral blood vessel. In more than 50% of cases, patients are left with a disability (Adamson *et al.*, 2004), which may affect motor, sensory, linguistic, emotional or memory function, depending on the territory affected (Steinke and Ley, 2002). Disability results from damage to fibres projecting from their controlling (sub)cortical area to their target location, therefore preventing signal transmission and consequently impairing function. Stroke patients who regain good motor function are thought to have incomplete lesions of M1 or the CST. Those who are only able to produce synergistic movements may have more complete damage to these areas but retain intact projections from other cortical motor areas to brainstem motor pathways, and those who exhibit little or no functional recovery are likely to have lesions affecting most of M1 and the premotor areas, leading to an inability to send motor commands to brainstem pathways.

In humans, strokes typically cause an immediate loss of function of the affected limb(s), accompanied by a reduction in tendon reflexes and a loss of ability to resist passive movement. This flaccid phase is often followed by spasticity and a gradual recovery of function (Twitchell, 1951). Movements made by spastic stroke patients have inaccuracies in the direction of movement and a reduction in the range of angles over which the joint can move; these disruptions correlate with the severity of the lesion (Bourbonnais *et al.*, 1989).

One pathological synergy observed in stroke patients consists of contralateral elbow flexion and shoulder abduction (activation of the anterior deltoid), a co-

activation not seen in healthy controls. Other notable pathological synergies include co-contraction of flexors and extensors (agonists and antagonists) at the elbow and co-activation of trapezius and elbow flexors. Pectoralis major is often activated along with elbow extensors in addition to its usual coupling with the elbow flexors (Dewald *et al.*, 1995; Dewald *et al.*, 2001). Most normal muscle synergies are still present in stroke patients, who otherwise exhibit more widespread activation.

As well as abnormalities in gross upper limb function, moderately impaired stroke patients exhibit a loss of individuation of all fingers when performing both flexion/extension as well as adduction/abduction movements (Lang and Schieber, 2003; Lang and Schieber, 2004; Raghavan *et al.*, 2006). This is analogous to the situation in pyramidotomised monkeys who remain able to move their fingers but cannot fully retract other fingers while moving one alone (Lawrence and Hopkins, 1976). This could be explained in terms of the co-activation of agonist and antagonist muscles often seen post-stroke (Dewald *et al.*, 1995). Several reports describe that strokes or CST lesions reduce the individuality of fingers; whilst the range of movement of each finger is maintained, there is an increase in concurrent movement of other fingers (Lawrence and Hopkins, 1976; Zackowski *et al.*, 2004; Schieber *et al.*, 2009). In other words, 'stroke subjects regained the ability to move the instructed digit through a normal range, but unintentional motion of other digits was increased' (Schieber *et al.*, 2009). Similar observations were recorded in PT-lesioned monkeys, who could still perform pincer grip movements but could not tuck the other fingers out of the way as would be expected in independent finger movements (Lawrence and Hopkins, 1976).

Most research into movement ability of patients post-stroke has focussed on the upper limb, with very few papers describing the effects in the lower limb. Neckel *et al.* (2006) found that the main deficit in the legs was in strength. One suggested contributor was the co-contraction of antagonist muscles, which was observed during ankle flexion and extension as well as knee extension. Stroke

subjects also exhibited hip flexion alongside hip abduction, a pathological synergy analogous to the flexion synergies described in the arm. Additionally, the number of muscle synergies used in leg movement is more diverse in stroke patients compared to healthy controls, with abnormal co-activation of hip adductors and knee extensors (Cruz and Dhaher, 2009).

An experimental lesion of the right precentral gyrus in a cebus monkey lead to acute flaccid paralysis (Lashley 1924); this sometimes evolves into a spastic paralysis, thus paralleling the situation in human stroke patients. However, even after large lesions of M1, recovery of arm function is possible, though constraint-induced movement therapy (Dettmers *et al.*, 2005) was used in some studies to aid recovery. Recovery of arm function predominantly pertained to gross movements such as those involved in climbing (Lawrence and Kuypers, 1968) whereas fine finger control remained markedly impaired or impossible after lesions of M1 or the CST (Passingham *et al.*, 1978). Unfortunately, recovery in human stroke patients is often less good than that described in these lesion studies. Potential contributing factors include additional damage to subcortical areas or corticofugal pathways in humans, increased hand dominance compared to monkeys, and stronger interhemispheric inhibition resulting in inhibition of the unaffected hemisphere (Darling *et al.*, 2011).

Suggestions for the neural substrate of recovery include plasticity of the motor areas and the CST ipsilateral to the paretic limb, as well as involvement of brainstem pathways. It is likely that plasticity of the damaged motor cortex leads to better functional recovery than plasticity of the undamaged cortex (Hallett, 2001) but the method in which this recovery is achieved is unclear. An early experiment showed it is possible that neighbouring areas assume control of the muscles previously controlled by the lesioned M1 site (Glees and Cole, 1950). However, this study employed dural surface stimulation with very high currents and thus could have activated large areas of cortex; much more focal effects can be achieved with intracortical stimulation (see Section 1.5.3). Evidence against undamaged parts of M1 taking over control of muscles

previously governed by adjacent lesioned areas was first provided by Leyton and Sherrington (1917), who could not elicit distal arm movements by stimulating the cortex surrounding an M1 lesion. More recently, this was corroborated using ICMS mapping, which showed that the cortical area surrounding a lesion does not assume the role of the lesioned territory (Nudo and Milliken, 1996). It is therefore likely that although reorganisation of the damaged motor cortex is ideal for recovery after stroke, this does not involve surrounding regions assuming the role of the damaged area. Leyton and Sherrington also suggest the possibility of subcortical structures gaining more control after cortical lesion.

Interestingly, neural characteristics exhibited after strokes are similar to those controlled by the RST. Following a CST lesion, EPSPs recorded from the motoneurons elicited by MLF stimulation increase in size for intrinsic hand muscles and flexor but not extensor muscles (Zaaimi *et al.*, 2012). No such increases in ipsilateral CST EPSPs were found, suggesting that changes after a stroke may occur specifically in the RST in order to compensate for loss of CST function. These innervation patterns are reminiscent of the flexor overactivation and extensor weakness characteristically seen in stroke patients.

When comparing synergies between affected and unaffected arms in stroke subjects with different levels of impairment, disparities between both arms increased with the severity of impairment (Cheung *et al.*, 2012). Additionally, more impaired subjects exhibited 'merging' of the synergies, which was attributed to the co-activations seen in stroke patients, including the characteristic shoulder adduction and elbow flexion synergy.

1.5 Methods of probing the reticulospinal tract

Given the potential role of the RST in functional recovery after damage to the CST in stroke, further investigation of muscles and synergies controlled by the RST is warranted. In the future, this knowledge could be used to selectively

strengthen useful synergies and weaken maladaptive ones. Therefore, finding methods of non-invasively investigating and manipulating the RST is important.

1.5.1 Humans: StartReact technique

The central nervous system (CNS) can only be probed non-invasively in live human subjects, thus limiting the range of techniques that may be used. Approaches include functional imaging methods (e.g. functional magnetic resonance imaging, f-MRI, Meier *et al.*) and non-invasive stimulation using transcranial magnetic stimulation (TMS, Loh *et al.*, 2010), transcranial direct-current stimulation (tDCS, O'Shea *et al.*) or potentially ultrasonic stimulation (Tufail *et al.*, 2010). However, these stimulation modalities are predominantly suited to activating cortical rather than deep brain regions. Although ultrasonic stimulation has the theoretical capacity to stimulate deeper regions, it has not been used to stimulate the brainstem in humans so far.

An alternative method causing selective activation of the RF is auditory startle. Everyone has experienced the innate 'jumping' reaction elicited by a sudden loud, 'startling' noise; an evolutionarily protective mechanism in which muscles contract in order to defend vulnerable areas of the body from attack by predators. Startle activates muscles in a descending manner, with the periocular muscles activated first, followed by the sternocleidomastoid (SCM), the masseter, and then the muscles of the trunk, arms and legs (Brown *et al.*, 1991b). Due to the very short muscle reaction times, the startle response must be mediated by a pathway with few synapses (Pellet, 1990). After the cochlea, the ventral cochlear nucleus (Davis *et al.*, 1982) or cochlear root neurons have been proposed as the first of these relays, though there is debate as to exactly which is involved (Yeomans and Frankland, 1995). The caudal pontine nucleus (PnC) has been well-established as another relay (Davis *et al.*, 1982; Wu *et al.*, 1988), implicating the RST as the motor pathway involved. Further evidence for the involvement of the RST includes that the latencies of muscle response to startle match those expected of the RST, and that lesions of the pontine RF abolish startle responses (Hammond, 1973; Groves *et al.*, 1974).

Reaction times (RTs) for executing a motor task in response to an auditory stimulus are markedly lower when the stimulus is startling (a loud noise of sudden onset) than when it is not; this has been termed the 'StartReact effect' (Valls-Sole *et al.*, 1995). RTs of movements cued by a startling stimulus might be too short to be controlled by the CST, as the majority of CST neurons have slow conduction velocities (Davidoff, 1990). It is likely that the faster RST mediates the startle response, and the StartReact paradigm affords a useful means of activating this pathway.

1.5.2 Non-human primates

Unlike research on humans, animal models permit direct, invasive recording of neuronal activity. Two animal models, the macaque and the baboon, are used in the work presented in this thesis. There is evidence both for and against the suitability of these animals in modelling human motor control, particularly of the hand. Nonetheless, I will argue that they are sufficiently similar to be useful, particularly given the lack of alternative approaches.

Many previous studies used cats as a model of the motor system (for example Ethier *et al.* 2007). However, cats are quadrupedal and cannot grasp objects, making them unsuitable for studies of hand control. By contrast, primates can grasp and manipulate objects in a very similar way to humans, and data derived from their motor systems are more readily applicable to humans. The phylogenetic evolution of apes, including humans, and monkeys separated around 25 million years ago (Figure 1.4). Both groups have evolved different modes of movement and walking, which is reflected in several biomechanical differences. Compared to monkeys, apes have a larger range of rotation of the elbow and wrist joints, with a greater proportion of forearm muscle mass dedicated to pronators and supinators. Both monkeys and apes have a much higher proportion of wrist flexors than extensors (Kikuchi, 2010). In the upper arm, apes have a higher percentage of muscle mass made of up elbow flexors, whereas monkeys have larger extensors, with baboons having the lowest

proportion of flexors amongst the monkeys. There are also differences in the way monkeys, apes and humans grasp different objects, with humans being the only species to use the thumb in most grasps (Pouydebat *et al.*, 2009). Despite these differences, monkeys and apes retain very similar muscular anatomy to humans, and given their opposable thumbs grasp in a fashion much more similar to humans than other species.

Macaques Macaques are a genus of Old World monkeys, several species of which are commonly used in neuroscience research (*Macaca nemestrina*, *Macaca mulatta* and *Macaca fascicularis*). Given that macaques have evolved along a phylogenetically distinct lineage for over 25 million years, questions have been raised as to the suitability of using them as an animal model for some types of human motor research (Passingham, 2009).

For example, macaque brains weigh several times less than human brains (Figure 1.5). This translates into a lower overall number of neurons (Herculano-Houzel *et al.*), fewer specialised subregions within each cortical area and less volume for accommodating different synergistic groups of cells within the motor regions. Differences are also seen at a microstructural level, including the density of dendritic spines on pyramidal cells, which affects the number of synapses these cells can receive (Elston *et al.*, 2001).

Most of the described differences between human and macaque brains concern systems such as language and vision. For the motor system, there is considerable evidence that macaques are a suitable animal model, including similarities in the way humans and macaques grasp objects (Pouydebat *et al.*, 2009), the high degree of manual dexterity of macaques, correlating with their dense corticospinal terminations in the ventral spinal grey matter (Heffner and Masterton, 1975; Bortoff and Strick, 1993), and motor subregions homologous to those found in humans, known as areas F1-7 (Rizzolatti *et al.*, 1998; Rizzolatti and Luppino, 2001). The existence of monosynaptic corticomotoneuronal connections in the macaque represents a further important similarity, as it permits the investigation of the neuronal basis of finely fractionated hand

movements (Buys *et al.*, 1986). In addition to these biological similarities, macaques are easy to breed in captivity and can be trained to perform motor tasks.

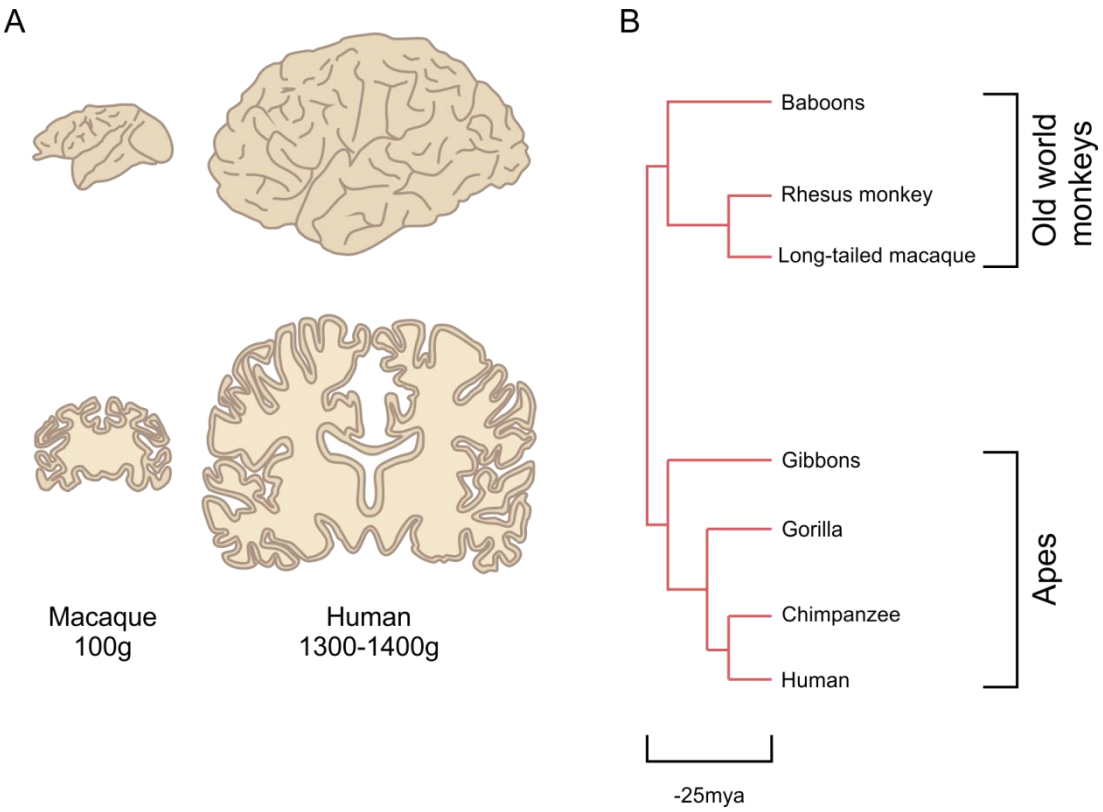

Figure 1.5: Relative sizes and weights of human and macaque brains (A), and a phylogenetic tree showing the divergence of different types of simian from our last common ancestor 25 million years ago (mya, B). Adapted from Rakic (2009).

Baboons Having a closer phylogenetic relationship to humans than macaques, and therefore similar genetic features, baboons are the most widely used primate model in genetic research. They also have very similar physiology in terms of cardiology, ageing and reproductive function (Cox *et al.*, 2013). Baboons have larger and more extensively folded brains compared to macaques and other older species, making them a suitable animal model of humans in neuroscience research (Leigh, 2004). However, motor systems research in baboons has been much more limited than in macaques. As one important similarity to humans, baboons have been shown to have CM connections to muscles of the arm and hand, particularly the intrinsic hand muscles (Landgren *et al.*, 1962; Clough *et al.*, 1968). Known differences include that M1 activates

extensors and inhibits flexors, which is the opposite of the pattern observed in humans (Preston et al. 1967, cited in Capaday *et al.*, 2013). The limited research into the motor system of baboons is probably not indicative of substantial biological differences compared to humans, but may rather be attributable to practical difficulties in working with them experimentally. Baboons are larger, stronger and more aggressive than macaques, which complicates their use in the laboratory.

Comprehensive quantification of the differences between human and primate brains is not currently possible, primarily due to limitations in the extent to which the live human brain can be probed. Pending developments of novel investigative techniques in humans, non-human primate models represent the best method for examining neural systems at a high spatial resolution. In the experiments presented in this thesis, macaques are used for chronic recordings due to their well-established suitability for carrying out motor tasks and their ready availability from UK breeding colonies. In order to ensure the highest scientific gain from these animals, they are also used in terminal acute experiments at the end of their chronic recording life. In this thesis, baboons are used in one terminal acute experiment conducted outside the UK; this experiment required implantation of large numbers of limb electrodes, which was facilitated by the larger limb size of baboons. Use of baboons was limited to terminal acute experiments mostly due to their more aggressive nature and lack of availability in the UK.

1.5.3 Methods of probing the motor systems of non-human primates

Spike- and stimulus-triggered averaging Several techniques have been used to map cortical representations of muscles. Two methods commonly used in awake behaving animals are spike-triggered averaging (spikeTA) and stimulus-triggered averaging (stimulusTA). These involve averaging EMG recordings temporally aligned to naturally-occurring neural spiking or to single pulses of intracortical microstimulation (see below) respectively.

Intra-cortical microstimulation (ICMS) ICMS involves repeated delivery of a small electrical current (typically 5-200μA) to a group of neurons via a penetrating microelectrode. ICMS can be delivered as single pulses or in trains of pulses, and at different frequencies, and is a very useful technique in artificially activating a cortical or subcortical area of interest. Cells can be activated directly by stimulation or indirectly via synaptic connections; the extent to which each technique operates via these pathways is discussed below.

Trains of ICMS A train of pulses to target areas of the motor system can elicit a visible muscle contraction, sometimes of just one muscle if a threshold stimulating intensity is used. When first used, trains of ICMS were thought to achieve much more focal effects than surface stimulation (Asanuma *et al.*, 1976). However, trains (with a small inter-pulse interval) induce temporal summation and activate multiple neurons transsynaptically. This spread increases with the pulse frequency (Jankowska *et al.*, 1975). S-ICMS and trains of ICMS activate different patterns of muscles, with trains more commonly eliciting responses in limb muscles and single pulses more often exciting axial muscles (Herbert *et al.*, 2010); this is again suggested to reflect stimulus trains having polysynaptic effects.

Single-pulse ICMS Trains of pulses have been shown to activate more muscles than seen in spikeTA, and in a dissimilar pattern, whereas single-pulse ICMS (S-ICMS) activates a less widespread pattern of muscles, making it a more suitable method for delineating the output projecting from a given area. For this reason, S-ICMS is used in stimulusTA. It is estimated that currents of 10-20μA can activate around 24 large PT cells, and 4000 smaller cells (Stoney *et al.*, 1968).

Therefore although direct spread of S-ICMS with currents of 20μA is very limited, being confined to the immediate vicinity of the electrode tip (Stoney *et al.*, 1968), responses in cells up to 2mm away from the stimulation site have been found at the same intensity (Baker *et al.*, 1998), suggesting that indirect activation is possible. Knowing the contribution of direct and indirect activation

is important when using ICMS, as any indirect activation could affect conclusions regarding the actual projection output of the target cell or area. Cheney and Fetz have suggested that there are three modes of activation of cells by S-ICMS: direct activation of nearby somas due to current spread; direct activation of nearby axons with remote somas, and indirect activation of cells via directly activated cells (1985). Though it has been reported that ICMS may exert the majority of its effects through indirect activation, which may be brought about even by stimuli too weak (0.1-1.0uA) for direct activation of cells (Jankowska *et al.*, 1975).

Comparison of stimulusTA and spikeTA The pattern of muscle activation in response to S-ICMS was compared to that elicited naturally in spikeTA (Lemon *et al.*, 1987). The longer latencies of the effects induced by stimulusTA may be due to current spread or transynaptic activation of other cells. Though, as mentioned above, current spread from S-ICMS is quite low, so longer latencies are probably more likely to be caused by transynaptic activation.

In one study, post-stimulus facilitation of muscles was more common than post-spike facilitation (even at intensities below 10μA) suggesting that more cells are activated by S-ICMS than by the single CM cells used to investigate post-spike effects (Lemon *et al.*, 1987). This contrasts with another study reporting that S-ICMS induced facilitation (albeit stronger) in the same or similar muscles to spikeTA effects, suggesting that CM cells were 'clustered' in terms of output projection (Cheney and Fetz, 1985). These conflicting results may reflect a genuine difference in different parts of the cortex (involved in the different tasks the two studies used), or be attributable to the smaller population of muscles recorded in the earlier study. The stronger facilitation seen in muscles activated by S-ICMS than in those responding in spikeTA (Lemon *et al.*, 1987) may again be due to activating multiple CM cells projecting to the same muscle. In addition, higher S-ICMS intensities increase the frequency of both facilitatory and suppressive effects. Suppression is observed less commonly than

facilitation, potentially because the muscle needs to be activated in order for suppression to become evident.

Overall, stimulusTA is suggested to elicit responses by both direct and indirect means (Cheney and Fetz, 1985). It allows more accurate delineation of the motor output of a small area than trains of ICMS, and may activate similar muscles to those activated by the area naturally.

Spinal cord and brainstem activation by ICMS Research using ICMS in brainstem regions such as the reticular formation has been limited to a small number of studies delineating the output of the RF in animal models including the cat and macaque (Drew, 1991; Davidson and Buford, 2004; Davidson and Buford, 2006; Herbert *et al.*, 2010). The possibility has been raised that the motoneurons activated by RF stimulation were actually indirectly activated via CST collaterals to the RF. However, the effects of RF stimulation are unchanged after pyramidotomy at a medullary level, or M1 lesions (Shapovalov, 1972), suggesting that activation of the CST via collaterals or current spread does not play a significant role.

Spinal cord stimulation can be applied to the ventral or dorsal surface of the cord, either epidurally, subdurally or intraspinally, the last of which is analogous to intracortical microstimulation. These parameters alter the mode of activation of motoneurons, which could be direct or indirect. However, all of them are usually able to evoke muscle movements (Sharpe and Jackson, 2014). Stimulation (intraspinal microstimulation, ISMS) has been more commonly used in the spinal cord, for example to investigate spinal synergies (Bizzi *et al.*, 2002; Zimmermann *et al.*, 2011).

Therefore, stimulusTA allows a small number of cells in the vicinity to be stimulated, eliciting responses likely to reflect mono-or disynaptic connections. This technique is consequently well-suited for use in investigating the output of specific neural areas. StimulusTA has been used previously to investigate the

motor output of the RF (e.g. Davidson and Buford, 2004; Davidson and Buford, 2006) of macaques carrying out a reaching task. However, using spikeTA may be more suited when investigating the output of individual cells.

1.6 Thesis overview

Chapter 2 presents a human experiment comparing the level of fractionation between voluntary movements and movements elicited by a startling stimulus, aiming to determine whether the final pathway controlling startle-induced movements is the CST or RST. In Chapter 3, I present additional findings which extend existing knowledge of habituation of the StartReact effect, and the validity of using sternocleidomastoid activation as a marker for StartReact. I review previously published findings in the light of my conclusions on marker validity.

Chapters 4 and 5 describe experiments in macaque monkeys. The synergies, output divergence and level of fractionation of muscle responses to stimulation of RF and M1 are presented in Chapter 4. In Chapter 5, I analyse EMG data from a macaque behaving normally in its home cage; PCA and ICA were applied to EMG recordings from 18 muscles to determine the level of fractionation of natural movement.

Chapter 6 details an experiment conducted on baboons in the Institute of Primate Research in Kenya. EMG responses to RF stimulation were recorded from 112 muscles in all four limbs, thus characterising RF projections bilaterally. The level of fractionation and synergies underlying these responses were also analysed.

2 Fractionation of muscle activity in the StartReact paradigm

Exposing subjects to a loud, startling stimulus 'releases' prepared movements more quickly than might be possible under control of the corticospinal tract, an effect known as StartReact. This has prompted suggestions that control is mediated by the reticulospinal tract, but the extent to which this pathway is involved required further investigation. This chapter presents results suggesting that the RST has a key role in the StartReact effect, confirming the potential of the technique to non-invasively probe the reticulospinal tract in humans.

All data in this chapter were collected by me; I also designed the task and carried out all analysis.

2.1 Abstract

Introduction and aims: Movements carried out in response to acoustically startling sounds have significantly shorter reaction times (RTs) than those carried out in response to non-startling acoustic stimuli, a finding known as the StartReact effect. It remains unclear exactly which neural pathways underlie this process; this study aimed to provide further clarification, with a particular focus on the reticulospinal tract (RST).

Methods: Ten subjects were instructed to carry out 32 different motor actions with the right hand and arm as quickly as possible after loud (startling) and quiet (non-startling) auditory cues. Electromyography (EMG) activity was recorded from 15 muscles of the right hand and arm. For each subject, motor task and trial, EMG within a given time window after the earliest RT across muscles was averaged, for each condition. The covariance matrices of these means were subjected to principal component analysis (PCA), which decomposed the data into 15 components, each of which explained a percentage of the variance (PVE) of the EMG. For each condition, PVEs were averaged across subjects. The number of components required to explain the total variance of the data was used as a measure of the level of the movement's fractionation, and was compared between conditions. If patterns of fractionation were similar between conditions, this might suggest that both are

controlled by the same pathway. This process was repeated for four different time windows (0-10ms, 10-20ms, 20-30ms and 50-100ms after RT) to investigate whether the pattern of PVE changed throughout movement.

Results and conclusions: There was a significant difference for some components between loud and quiet conditions for all time windows, with movements cued by the quiet stimulus being significantly more fractionated. We conclude that the RST is likely to be the pathway underlying the startle-induced movements with an early RT in the StartReact effect.

2.2 Introduction and background

2.2.1 StartReact

Certain muscles of the body contract in response to a loud, sudden sound (Li *et al.*, 2001). This is known as the startle response, which has evolved as a mechanism to help protect vulnerable parts of the body from attack by predators. The first muscles to react to a startling stimulus are the orbicularis oculi (OOc) in the auditory blink reflex (ABR), followed by sternocleidomastoid (SCM) (Pilz *et al.*, 1988; Caeser *et al.*, 1989; Pellet, 1990) and then masseter. Trunk and limb muscles are subsequently activated in a rostrocaudal direction (Davis *et al.*, 1982; Brown *et al.*, 1991b). When used to cue a motor task, acoustic startling stimuli significantly decrease RTs compared to non-startling stimuli, an effect termed 'StartReact' (Valls-Sole *et al.*, 1995).

There has been some debate regarding the mechanism underlying StartReact. It has been suggested that the shortened RTs characteristic of StartReact are too short to have involved the cortex, due to known conduction times to the cortex and from the cortex to the arm (Carlsen *et al.*, 2004a). Therefore the effect must be in part controlled by subcortical mechanisms. Two potential mechanisms have been proposed (Carlsen *et al.*, 2011a). The voluntary motor program prepared for the movement task and stored in subcortical structures might be triggered by the loud 'startling' stimulus without cortical involvement (Carlsen *et al.*, 2004a). Alternatively, the activation induced by the startle stimulus might push the motoneurons involved in the prepared movement towards threshold,

thereby speeding up RT. Attempts to clarify this found that differences in RT seen between different cue modalities were not present when startle cues were added. This suggests that startle does not simply speed up processing by bringing neurons closer to threshold; otherwise, differences between the RT in response to cues of different modalities would be expected to remain (Carlsen et al., 2011). An alternative explanation could be that there is a minimum RT that is reached with a startle response, independent of the cue modality. In a simple versus choice RT paradigm, subjects were asked to either make the same movement in response to startling or non-startling cues (simple RT), or to flex or extent the correct hand (right or left) to reach one of two or four targets (choice RT); the latter task type involved cortical processing. RTs decreased with a startling stimulus in the simple RT paradigm but not in the choice RT paradigm, showing that responses must be prepared and stored in order for the StartReact effect to occur (Carlsen *et al.*, 2004a). Subsequently, it was suggested that subcortical structures act as a 'holding pen' for the prepared movement, in order to free up cortical processes (Carlsen *et al.*, 2007).

The reticulospinal tract One of the brainstem movement pathways, the reticulospinal tract, has been implicated in the mediation of the startle response. After a stimulus is received via the cochlea, it is relayed in the ventral cochlear nucleus (Davis *et al.*, 1982) or cochlear root neurons, followed by one of the reticular nuclei, the caudal pontine nucleus (PnC) (Wu et al., 1988). The involvement of the reticular nuclei (particularly the PnC) has been confirmed in lesion studies where the startle response was abolished (Hammond 1973). Further evidence for reticular involvement in mediating startle comes from reduced StartReact responses in patients with Parkinson's disease and gait freezing. The freezing phenomenon has been linked to dysfunction of the RF and pedunculopontine nucleus (PPN); the fact that these patients also exhibit reduced StartReact responses suggests that the RF and/or PPN are involved in StartReact (Nonnekes *et al.*, 2014). Therefore given the likely role of the RF in the startle response, it is possible that RST projections activate motoneurons involved in producing the movements with an early RT in the StartReact effect.

However, the exact pathways underlying the StartReact effect, and whether the RST is involved are still not clear. To help elucidate this, we aimed to find the level of fractionation of movements induced by a startling cue, and compared this to the level of fractionation of movements made in response to a non-startling (quiet) cue. Clarifying the role of the RST would inform the use of the effect as a non-invasive tool for activating the RST. Such non-invasive activation could be useful in exploring the potential of the RST as an alternative pathway for motor control post-stroke (Baker 2011).

Here, PCA was carried out on EMG recorded whilst subjects were carrying out movements in response to loud or quiet cues. This reduced the EMG down to a number of components, each explaining a fraction of the variance of the EMG. The pattern of variance explained by these components was used as a measure of the level of fractionation in the EMG.

A previous study which carried out PCA on EMG recorded while subjects made voluntary static hand positions found that, across five muscles, three components explained 80% of the variance (Weiss and Flanders, 2004). However, no previous work attempted to compare levels of fractionation as revealed by PCA to help identify the underlying pathway of the StartReact paradigm. Additionally, no previous experiment using PCA in humans has recorded EMG from as many as 15 muscles.

As voluntary movements are assumed to be controlled predominantly by the CST, the pattern of fractionation found in movements cued by a quiet stimulus was assumed to represent the level of fractionation of the CST. If the pattern of fractionation found in startle-cued movements were similar to this, it would support the hypothesis that the final pathway of startle-cued movements is the CST.

2.3 Methods

2.3.1 Subjects

Ten human volunteers (5 males, 5 females; age 43±13 years, mean±standard deviation) with no known neurological deficits participated in this experiment. All subjects were right-handed as evaluated through self-report.

Task Subjects were asked to carry out 32 different motor actions as quickly as possible after an auditory cue whilst comfortably seated at a table. The tasks were selected to elicit a wide range of muscle activation patterns and to emulate movements carried out in daily life; these included lifting a mug in a grasp involving multiple fingers, lifting a pen with the thumb and forefinger and simulating the throw of a ball (using upper arm and shoulder muscles, Figure 2.1). The experimenter demonstrated how to carry out each movement and it was ensured that subjects carried out the actions in a consistent manner. The auditory cue was either a quiet beep (80dB), or a loud, startle reflex-inducing beep (115dB; this level being the loudest subjects could tolerate over the many repetitions used) and was delivered via headphones. Movements were carried out in blocks of ten, five in response to each cue. Four different random sequences of loud/quiet cues were used to prevent subjects predicting forthcoming cues; the sequence used for a given trial was also determined randomly.

Electromyography recording EMG was recorded from 15 muscles using bipolar surface electrodes (Bio-Logic M0476; Natus Medical, Mudelein, IL) in a belly-tendon montage and secured with Micropore tape (3M, St. Paul, MN). Muscles recorded from included the first dorsal interosseous (1DI), abductor pollicis brevis (AbPB), abductor digiti minimi (AbDM), flexor digitorum superficialis (FDS), flexor carpi ulnaris (FCU), flexor carpi radialis (FCR), extensor carpi ulnaris (ECU), extensor carpi radialis (ECR), extensor digitorum communis (EDC), brachialis (BR), biceps (BIC), triceps (TRI), anterior deltoid, posterior deltoid and pectoralis major. Muscles were identified by palpation whilst asking subjects to perform hand and arm movements using specific muscles. A unipolar ground electrode was positioned on the dorsum of the right

hand. EMG signals were notch filtered (49-51Hz) to remove mains frequency contamination, band-pass filtered (30Hz-2kHz), amplified by D360 (Digitimer, Welwyn Garden City, UK) amplifiers and digitised at a sampling rate of 5kHz using a micro1401 data capture system connected to a PC running Spike2 software (Cambridge Electronic Devices, Cambridge, UK).

Figure 2.1: The 32 movement tasks subjects were asked to perform. The touch nose task (*) was performed with three different starting positions: with the arm outstretched above the head, with the arm outstretched to the right, and with the arm hanging by the side of the body.

2.3.2 Analysis

EMG recordings were analysed using custom scripts in MatLab (The Mathworks, Natick, MA, USA). A threshold was defined for each muscle as three standard deviations above the mean of the 200ms section of baseline EMG preceding the stimulus marker; the RT for a given trial was defined as the first time after the stimulus marker that the EMG exceeded this threshold. All traces were visually inspected; any RT which appeared to have been inaccurately placed by the automated script was manually corrected. For a given trial, the earliest RT (eRT) across all muscles was used as a starting point from which windows of EMG data were extracted for each muscle (see Figure 2.2B, green

dotted line); windows used were 0-10ms, 10-20ms, 20-30ms and 50-100ms (Figure 2.2B). The mean activity within a given window, minus the mean of the 200ms baseline period, was calculated for each muscle and trial and added to a matrix (*trial x muscle* containing mean EMG activities, Figure 2.2C). Separate matrices were compiled for each movement type, and for loud and for quiet trials.

Any loud trials with an eRT of >100ms were removed from the relevant matrix as they were incompatible with a true startle response. To avoid using an unequal number of trials between conditions, the same number of randomly-selected quiet trials as loud trials was removed. Both matrices were then standardised to Z-scores (using Equation 1), resulting in the final *muscle x trial* matrices containing standardised mean EMG activities.

$$Normalised(d_i) = \frac{d_i - \bar{d}}{\sqrt{\frac{1}{(n-1)}\sum_{i=1}^{n}(d_i - \bar{d})^2}} \quad (1)$$

Where d_i represents the ith data point (i.e. height of the muscle activation at that point) and *n* represents the length of the data.

PCA Covariance matrices for the *muscle x trial* matrices were computed, resulting in *muscle x muscle* matrices of the correlations between all possible pairs of muscles (Figure 2.2D). Each covariance matrix was subjected to PCA, which finds orthogonal eigenvectors and their associated eigenvalues. Each eigenvector represents the direction of a component in n-dimensional space, where n is the number of muscles. Successive components account for progressively less variance, and the amount of variance contributed by each eigenvector is given by its associated eigenvalue. In other words, the eigenvector (or 'component') with the largest eigenvalue explains the highest proportion of the variance in the EMG, and components are ordered by the percentage of variance they explain (PVE). Therefore the first component explains the most variance, and the last component explains the least. The cumulative sum of the PVE was calculated. PCA was performed individually for

every subject. The entire analysis was carried out separately for loud and quiet trials.

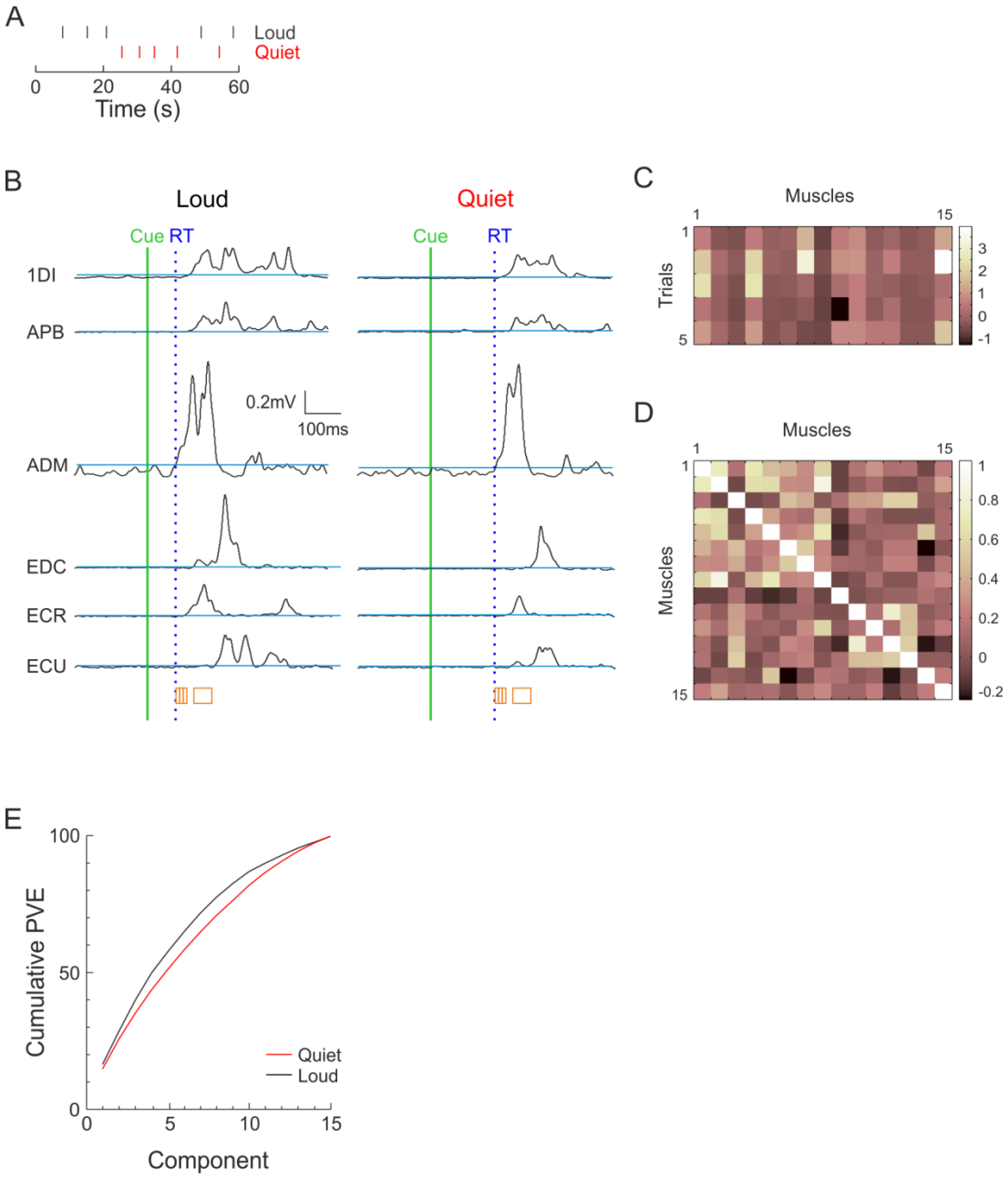

Figure 2.2: The analysis procedure. Firstly, data surrounding the stimulus markers were retrieved (shown by black and red lines, A). RT threshold was defined for each muscle as three standard deviations above mean baseline (pale blue lines, B), and RTs were determined as the first point where traces exceeded this threshold. The earliest RT (eRT) across muscles for each trial was found (dark blue dotted lines, B), after which four different windows of EMG (0-10ms, 10-20ms, 20-30ms and 50-100ms) were taken (orange boxes, B). The mean across each window for each muscle was calculated for each trial and added to a matrix of *muscles x trials* (heat map, C). After Z-score standardisation, the covariance matrix of this matrix was calculated (heat map, D) and PCA was carried out on this. PCA yielded a number of components, each of

which explained a percentage of the variance in the EMG data represented by the matrix shown in C. Components were in descending order of the PVE. The cumulative sum of the PVE was calculated (E).

This resulted in two matrices of *subjects x component* (*10 x 15*) containing PVE values; one matrix per condition. Each matrix was averaged across subjects to yield a row vector (*1 x 15*). The difference between both row vectors was calculated, resulting in a single row vector representing the average difference in PVE between conditions for each component (Figure 2.3A).

Significance testing using Monte Carlo simulations Significance testing was carried out on the null hypothesis that the PVE was not significantly different for any component between both conditions. We used a Monte Carlo approach designed to take multiple comparisons into account.

Rows were randomly shuffled between and within the two *subject x component* matrices representing the loud and quiet stimulus conditions (Figure 2.3B). The single row vector containing the average difference in PVE between both matrices was calculated as outlined above. The shuffling process was repeated 1000 times to generate 1000 such row vectors, and these were stacked to form a matrix of *repeat x component* (1000 x 15). The distribution of values for individual components in the columns of this matrix estimated the distribution of the difference in PVE for each component under the null hypothesis (Figure 2.3B).

Within the *repeat x component* matrix, it was determined whether each value was in the top n_p=25 or bottom n_p=25 values of its column, i.e. whether it was in the most extreme 2*n_p out of 1000 simulated component values. The number of rows where at least one component fulfilled this criterion was counted, expressed as a proportion of the total number of rows, and compared against the set P-value of 50/1000=0.05. If the calculated proportion exceeded 0.05, the value of n_p was decreased by one and the above calculations repeated. Once the calculated proportion was equal to or less than 0.05, the process was completed. Hence, under the null hypothesis, the proportion of row vectors

with at least one component in the top n_p or bottom n_p values of the corresponding column of the simulated null matrix would be P=0.05. At this point, the P value representing the significance level of the differences in PVE between conditions was taken as $2*n_p/1000$. For example if n_p ended up as 15 when the calculated proportion of rows was equal to or less than 0.05, the P value for the difference between PVE for each component would be P<0.03.

For the row vector calculated from the original (non-shuffled) dataset, it was determined whether each value fell within the top or bottom n_p of the column in the simulated null matrix. For values where this was the case, the relevant component was deemed to have a significant difference in PVE between conditions, at the significance level found as explained in the above paragraph.

The above procedure was carried out separately for all time windows.

As described above, loud trials with an eRT of over 100ms were removed, and an equivalent number of randomly selected quiet trials also removed to keep trial numbers balanced between both conditions. The random element in this process led to a slightly different result each time. In order to find a representative result, the selection process, PCA and Monte Carlo analysis were repeated 100 times. A binomial probability distribution was used to find how many repeats out of 100 would be different with a probability of P<0.05:

$$y = F(x|n,p) = \sum_{i=0}^{x} \binom{n}{i} p^i (1-p)^{(n-i)} I_{(0,1,\ldots,n)}(i) \qquad (2)$$

Where *y* is the probability of observing up to *x* criterion values in *n* independent trials, with a probability of observing the criterion value in any one trial is *p*.

It was calculated that if there were a significant difference between conditions for any component in 9 out of 100 analyses, this difference would be significant at the P<0.05 level.

A Wilcoxon rank sum test was used to compare eRTs across muscles for every trial, task and subject between quiet and loud conditions, as they were not found to be normally distributed as assessed by a Kolmogorov-Smirnov test.

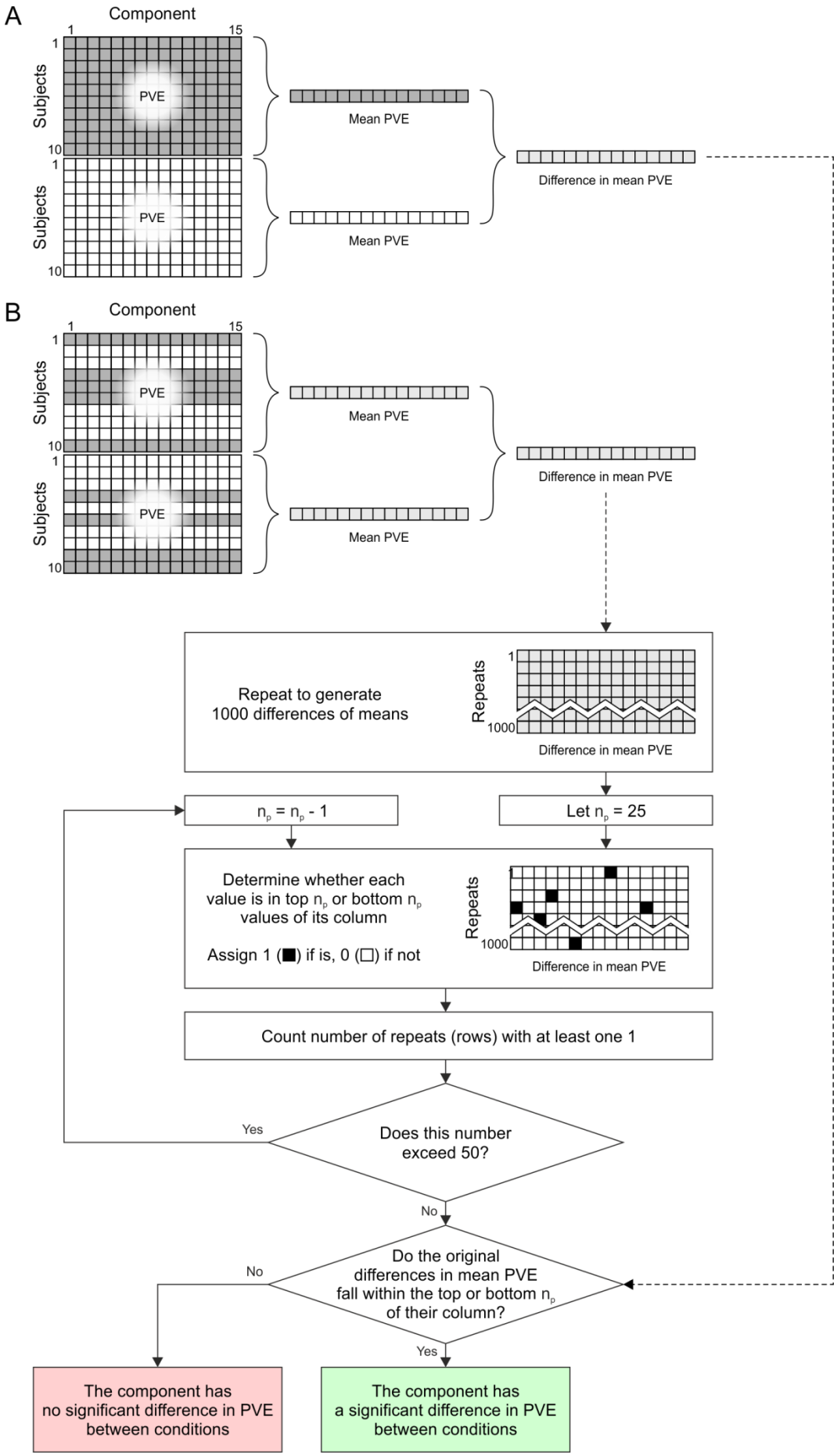
A
Component
1
15
1
Subjects
10
PVE
Mean PVE
Difference in mean PVE
B
Repeat to generate
1000 differences of means
Repeats
1000
$n_p = n_p - 1$
Let $n_p = 25$
Determine whether each value is in top n_p or bottom n_p values of its column
Assign 1 (■) if is, 0 (□) if not
Count number of repeats (rows) with at least one 1
Does this number exceed 50?
Yes
No
Do the original differences in mean PVE fall within the top or bottom n_p of their column?
The component has no significant difference in PVE between conditions
The component has a significant difference in PVE between conditions

Figure 2.3: Flow chart of Monte Carlo simulation for significance testing of difference in mean PVE for each component. Grey boxes represent loud trials, white boxes represent quiet trials. First the mean of each of the original matrices (loud and quiet respectively) was taken and the difference between these found (A). The original matrices were then shuffled and the averaging repeated 1000 times in part (B).

2.4 Results

2.4.1 Reaction times

The mean earliest RT across muscles for each trials, task and subject for the quiet condition was 204±79ms (mean±standard deviation), and for the loud condition was 144±75ms (Figure 2.4). The difference in RT between conditions was significant ($P<0.00001$, Wilcoxon rank sum test). The difference between the mean of these early RTs for each condition was 60ms.

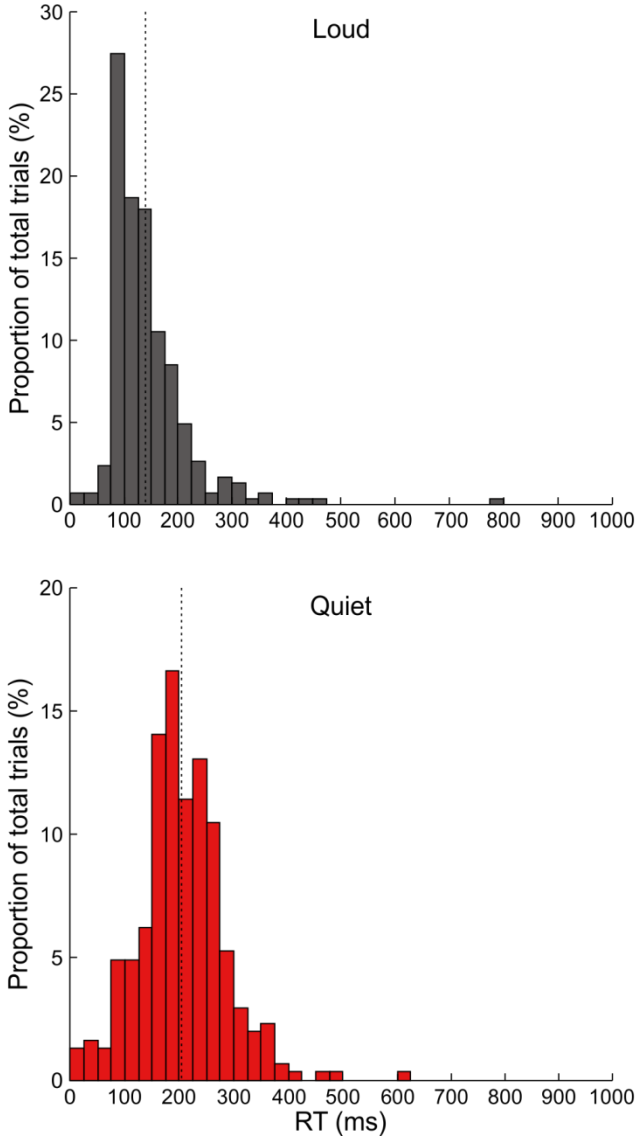

Figure 2.4: Histograms of eRTs for every subject, trials and movement task for each condition. The dotted lines represent the mean eRT for each condition.

2.4.2 Principal component analysis

Principal component analysis was carried out on the mean EMG within each of four different time windows (0-10ms, 10-20ms, 20-30ms and 50-100ms, Figure 2.5).

There were significant differences (indicated by stars) between the PVE of loud and quiet trials for at least one component for every time period, as assessed by Monte Carlo analysis.

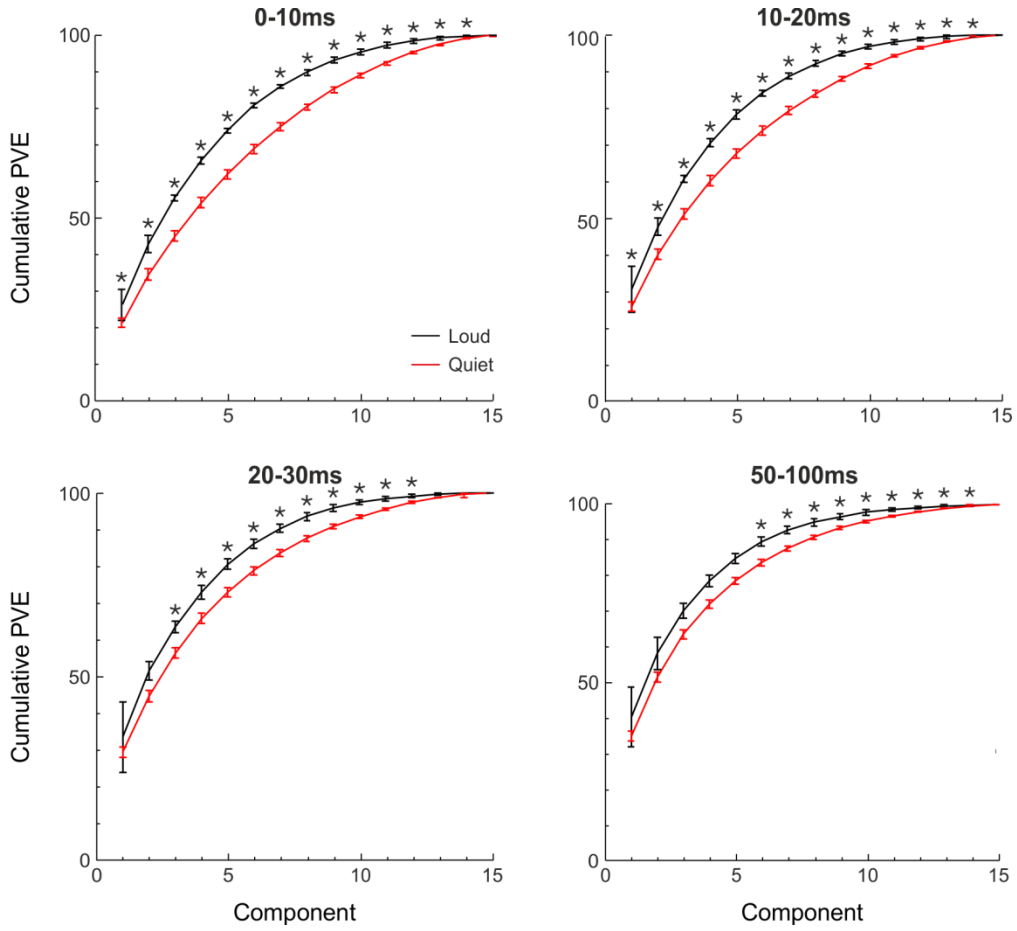

Figure 2.5: The mean cumulative PVE for both loud (black) and quiet (red) stimulus types, as found by PCA carried out on mean EMG from four different time windows. These windows were placed following the eRT for both loud and quiet trials. Stars indicate a significant difference between loud and quiet trials for a given component; the significance level for all time windows was $P<0.004$ as calculated by the Monte Carlo analysis described above. Error bars represent one standard deviation above and below the mean.

2.5 Discussion

2.5.1 Pathways underlying the StartReact effect

The aim of this chapter was to examine the pathways underlying the StartReact paradigm. The approach involved carrying out PCA on EMG from startle-induced and voluntary movements within different time windows, and comparing the pattern of fractionation between both types of movement. Fractionation was assessed as the pattern of PVE by each principal component extracted by PCA. If most of the variance in the muscle responses can be explained by few principal components, the data are said to have a low level of fractionation. Conversely, if many components are required to explain the variance, this implies a higher level of fractionation.

The RST and CST are probably both involved in the control of voluntary movements as well as movements elicited by startling cues. However, the CST is likely to be the predominant pathway underlying voluntary movement, therefore the level of fractionation of such movements is likely to represent the level of fractionation of the CST. As the CST is thought to be a highly fractionated pathway, it would be expected that more components are required to explain the variance in movements it produces. It was hypothesised that if the pattern of fractionation found in movements elicited by startling cues were very similar to that found for voluntary movements, the CST would probably constitute the final pathway for controlling both types of movement. Alternatively, if startle-induced movements have a less fractionated pattern, the RST may be the final pathway underlying these movements.

Significant differences were found between components in all four time windows, with the pattern of fractionation consistently higher for quiet-cued than loud-cued movements. We suggest that this discrepancy arises because startle-induced movements are produced by RST input onto motoneurons. Single RST cells are believed to branch onto more motoneurons than the CST, therefore producing less fractionated movements. Interneurons in macaques alter their firing rates during movement preparation several hundred

milliseconds before movement onset (Prut and Fetz, 1999), suggesting that they are involved in this phase of movement. As it has been previously found that responses must be prepared and stored in order for the StartReact effect to work (Carlsen *et al.*, 2004b), it is possible that the CST provides an initial level of excitation to the motoneurons involved in the prepared movement. When the startling stimulus activates the reticulospinal system, there is a further increase in excitation provided to those motoneurons with common inputs from both the CST and RST. It is possible that, without the initial level of excitation from the CST, the excitation provided by the RST would be insufficient to produce movements.

Alternatively, it is possible that the primary motor cortex stores a copy of the motor program for the movement being prepared in the RF or another subcortical, non-spinal area, which is then released by startle-induced RF excitation. This would support previous suggestions that StartReact does not simply speed up cortical processing but releases a stored plan of the movement (Carlsen *et al.*, 2011a). Indeed, evidence has shown that RF neurons exhibit preparatory-related activity in the cat (Buford and Davidson, 2004), so it is possible that loud cue-induced movements are prepared both in the cortex and RF, but executed by the RST when extra excitation is provided by the startling cue. It has also been shown that the motor cortex gradually builds up excitation after a 'go' cue, over about 80ms before movement execution in a RT paradigm (Starr *et al.*, 1988). Another study found that when a startling stimulus was presented at varying time points before a cue to move, the excitability of three muscles did not change over the 100ms period before the cue (Kumru and Valls-Sole, 2006). It was suggested that these muscles were activated by subcortical structures which must therefore prepare the movement required before a voluntary command is given, when it is known that such a command is forthcoming. This excitation has been found on average 400ms before the 'go' cue, shown by another experiment with similar methods (Valls-Sole *et al.*, 2008). The fact that the cortex only increases excitability 80ms before movement onset suggests that the startle-induced movements are released

from subcortical regions such as the RF instead. This would also put the RST in a position to produce movements with short RTs.

2.6 Conclusions

In conclusion, the level of fractionation of startle-induced movements was significantly and consistently lower than that of quiet-cued movements. Hence, movements elicited by startling cues are suggested to be produced by a less fractionated pathway, which is argued to be the RST. Excitation to motoneurons may be provided entirely by the RST, or involve an initial preparatory contribution from the CST.

3 Habituation and markers of the StartReact paradigm

Exposing subjects to a loud, startling stimulus while a subject is preparing a movement has been found to significantly shorten reaction times of the prepared movement compared to when cued by a quiet stimulus, an effect called the StartReact paradigm. After examining the extent of the involvement of the reticulospinal pathway in the previous chapter, this chapter outlines some further work carried out on habituation of the StartReact effect and the validity of using the SCM marker as an indicator of startle.

All data in this chapter were collected by me; I also designed the task and carried out all analysis.

3.1 Abstract

Introduction and aims: The 'StartReact effect' is the phenomenon of reaction times (RTs) significantly decreasing when subjects are exposed to a loud, startling auditory cue during movement preparation. Habituation of a response occurs when a subject is repeatedly exposed to a particular stimulus. The StartReact effect has so far not been found to habituate across 100 trials, 20 of which were startling; however this is a low exposure rate, and habituation of only a few muscles have so far been examined. The current experiment aimed to expose subjects to 160 trials, half of which were startling, in order to see whether habituation occurs with this exposure rate, and in a range of (four) proximal and distal muscles.

Much of the previous research on StartReact has used activation of the sternocleidomastoid (SCM) muscle as a marker of startle, though with little justification. This experiment also wanted to establish whether this marker is necessary or indeed useful.

In relation to the validity of the SCM marker, previous work has suggested that the StartReact effect does not reduce RTs for individual finger movements, basing their conclusions on the presence or absence of SCM activation. Here the

same methods were repeated and the findings discussed in relation to arguments about the SCM marker.

Methods: Ten subjects carried out 32 different motor actions with the right hand and arm as quickly as they could after two different auditory cues; loud (startling) and quiet (non-startling) while electromyography (EMG) activity from 16 muscles on their right hand and arm was recorded. Cues were presented in blocks of ten, with a 1:1 ratio of loud vs. quiet cue types, pseudo-randomly presented in four different predetermined sequences.

Results and conclusions: The StartReact effect as assessed in four different muscles did not habituate across 160 trials, 50% of which were cued by a loud, 'startling' stimulus. SCM activation was found in trials cued by a quiet, non-startling cue, which formed the basis of the argument that the use of SCM activation as a marker for startle is not a reliable one. Based in part on this premise, the analysis of a previous study showing that the StartReact effect does not work on single finger movements was repeated and the results reassessed. It is argued that the reduction in RT seen between loud- and quiet-cued trials in individual finger movements is due to StartReact, and reflects the RST involvement discussed in Chapter 2.

3.2 Introduction and background

The startle phenomenon is an evolutionary protective mechanism in which certain muscles contract in response to the sudden onset of a very loud noise, trigeminal or vestibular sensation (Li *et al.*, 2001) in order to protect vulnerable areas of the body of an animal from predation. The earliest manifestations of the startle reactions consist of firstly activation of the orbicularis oculi muscle (OOc) in what is known as the auditory blink reflex (ABR). This is shortly followed by sternocleidomastoid (SCM) contraction (Pilz *et al.*, 1988; Caeser *et al.*, 1989; Pellet, 1990), then masseter activation. After this, muscles are activated in a descending pattern as the impulse travels down the body and limbs (Davis *et al.*, 1982; Brown *et al.*, 1991b). Experimentally, the acoustic startle response has been found to significantly decrease RTs when introduced

during the preparation of a simple motor task (Valls-Sole *et al.*, 1995), an effect known as the 'StartReact' paradigm.

3.2.1 Habituation

Often, if a subject is repeatedly exposed to the same stimulus, its effects will diminish or 'habituate' (Abel *et al.*, 1998). Habituation is thought to occur due to a reduction in neurotransmitter release caused by repeated stimulation, which results in reduced post-synaptic potentials (Rimpel *et al.*, 1982); alternatively or additionally, there has been suggestion of an inhibitory side-chain, which is stimulated alongside the habituating neuron, causing it to increase inhibition of the neuron. Evidence from decerebrate rats has shown that short-term habituation of the startle response occurs in the brainstem (Leaton *et al.*, 1985).

Startle has been shown to habituate after being presented two to six times when little or no attention is directed towards the startling stimulus (Brown *et al.*, 1991b; Valls-Sole *et al.*, 1997), however habituation is dramatically reduced or abolished when the stimulus is presented during a reaction time task, or when attention is directed to the stimulus (Valls-Sole *et al.*, 1997; Schicatano and Blumenthal, 1998). It is still not clear exactly how many times a person can be startled before the effect habituates. The most extensive study carried out so far investigating this question involved subjects performing wrist extensions to an auditory tone which was either quiet (control, 85dB) or startling (124dB) for 100 trials, 20 of which were startling. No effect of trial position (1-20 trials) for SCM amplitude was found, and there was no significant difference in RT between the first and the last startling trials (Carlsen *et al.*, 2003). However, habituation increases with increased frequency of stimulus presentation (Thompson and Spencer, 1966); having a ratio of 1:5 startling to non-startling trials may not have been sufficient to allow habituation to occur. Carlsen *et al.* also only looked at a few muscles, the ECR, the FCR, the OOc and the SCM (2003), neglecting upper arm and intrinsic hand muscles. Their analysis was also focussed on the SCM and OOc muscles. Most other research into this area also used a limited number of muscles, usually focussed on the SCM; there is

little evidence showing whether the StartReact effect habituates in other muscles.

Therefore one aim of this analysis was to find whether habituation of the StartReact effect occurs when 160 trials are carried out, 50% of which are startling trials. It also aimed to investigate if this effect habituates in a range of distal and proximal muscles.

Differences in RT were measured between trials cued by loud and by quiet sounds across 160 trials of both trial types. It was hypothesised that if habituation occurred in any of the muscles studied, the difference in RT known as the StartReact effect would diminish or disappear over time.

3.2.2 Sternocleidomastoid activation as a marker for startle

Being one of the most consistent and last responses to habituate (Brown *et al.*, 1991b), the presence of sternocleidomastoid (SCM) muscle activation has been used as an indicator of the startle reflex (Carlsen *et al.* 2010). In fact, there is often a marked reduction in or even no habituation of the SCM response (in terms of response amplitude) when engaged in a RT task, whereas habituation does occur when just sitting quietly (Valls-Sole *et al.*, 1997; Siegmund *et al.*, 2001; Carlsen *et al.*, 2003).

Additionally, trials showing SCM activation (referred to as SCM+) have been shown to have significantly shorter RTs than trials with no activation (referred to as SCM-), an effect which does not diminish over time (Carlsen *et al.*, 2003). Although SCM- trials still showed significantly shorter RTs than trials cued by non-startling cues, overall, in terms of effects on RT, SCM+ trials sometimes induced the most marked change. On this basis, some investigations have argued that SCM activation is evidence of the subjects being startled, and that therefore only those trials showing SCM activation should be included in any analysis (Carlsen *et al.*, 2004a). It has long been shown that RTs decrease when stimulus intensity is increased (Kohfeld, 1969), encouraging the suggestion that some way of distinguishing between RTs which have been shortened due to the

StartReact effect and due to stimulus intensity is required, and that SCM presence is a suitable method of doing this.

However some studies have found a significant decrease in RT between SCM- trials and quiet trials, which has prompted the discussion as to whether the use of SCM activation as a marker of startle is entirely justified. One such study found a large and highly significant difference in RT between voluntary and startle-elicited individual finger movements (Honeycutt *et al.*, 2013). However, it was argued that as there was no significant difference between SCM+ and SCM- startling trials, the StartReact effect did not affect RTs of individual finger movements. Conversely, there was a significant difference between SCM+ and SCM- trials for whole-hand grasps. Honeycutt *et al.* supported the idea of the RST being the final pathway underlying StartReact, activating the motoneurons involved in any responses (2013). Therefore these opposing findings were suggested to be the result of the RST having the projections to finger motoneurons required for whole hand grasps, but not with enough fractionation to produce independent finger movements. However, the differences seen between voluntary and SCM- RTs for both movements were striking, with SCM- movements being shorter than quiet-cued movements by an average of 78ms for finger and 84ms for whole-hand grasps. The differences between SCM+ and SCM- trials, even for the whole hand grasp were tiny in comparison (a difference of 2ms for finger and 9ms for whole-hand grasps). To ignore this large decrease in finger RT and exclude the possibility of it being controlled by the RST is perhaps unfair. In this chapter this analysis was repeated and the suggestions made by the previous authors re-evaluated in light of the conclusions drawn about the validity of the SCM marker.

Therefore, the aims of the analysis presented in this chapter include:

- whether the StartReact effect habituates over 160 trials when presented in a 1:1 ratio of startling: non-startling cues;
- to explore the validity of the presence of SCM activation as a marker of startle;

- to discuss the implications of the SCM marker's validity in assessing whether individual finger movements are affected by StartReact.

3.3 Methods

3.3.1. Subjects

Ten (5 males, 5 females; mean age 43±13 years, mean±standard deviation) human volunteer subjects with no known neurological deficits participated in this experiment. All subjects were right-handed as evaluated through self-report.

3.3.2 Task

Subjects were asked to carry out 32 different motor actions as quickly as possible after an auditory cue whilst comfortably seated at a table. The tasks were selected to elicit a wide range of muscle patterns; these included lifting a mug in a grasp involving multiple fingers, lifting a pen with the thumb and forefinger, simulating the throw of a ball (using upper arm and shoulder muscles) and so forth (Figure 3.1). It was ensured that all subjects carried out the actions with the digits in a consistent pattern, by the experimenter demonstrating how exactly to carry out each movement. The auditory cue was either a quiet beep (80dB) or a loud, startle reflex-inducing beep (115dB; the loudest we found subjects could tolerate for so many repetitions), delivered via headphones. Movements were carried out in blocks of 10; 5 carried out in response to each cue. Four different sequences of loud/quiet cues were used to prevent subjects predicting forthcoming cues.

3.3.3 Electromyography recording

For the duration of the experiment electromyography (EMG) was recorded from 16 muscles in each subject using bipolar surface electrodes (Bio-Logic M0476; Natus Medical, Mudelein, IL, USA) placed in a belly-tendon montage and secured in place with Micropore tape (3M, St. Paul, MN, USA). The muscles recorded from were the first dorsal interosseous (1DI), abductor pollicis brevis (AbPB), abductor digiti minimi (ADM), anterior deltoid, biceps, brachialis (BR),

extensor carpi radialis (ECR), extensor carpi ulnaris (ECU), extensor digitorum communis (EDC), extensor carpi radialis (ECR), flexor carpi radialis (FCR), flexor carpi ulnaris (FCU), flexor digitorum superficialis (FDS), pectoralis major (PM), posterior deltoid, sternocleidomastoid (SCM) and triceps.

Muscles were identified by asking subjects to perform various hand and arm movements which use the muscles and therefore allow their location upon palpation. A unipolar ground electrode was positioned on the dorsum of the right hand. EMG signals were notch filtered (49-51Hz) to remove mains frequency contamination, band-pass filtered (30Hz-2kHz), amplified by D360 (Digitimer, Welwyn Garden City, UK) amplifiers and digitised at a sampling rate of 5kHz using a micro1401 data capture system connected to a PC running Spike2 software (Cambridge Electronic Devices, Cambridge, UK).

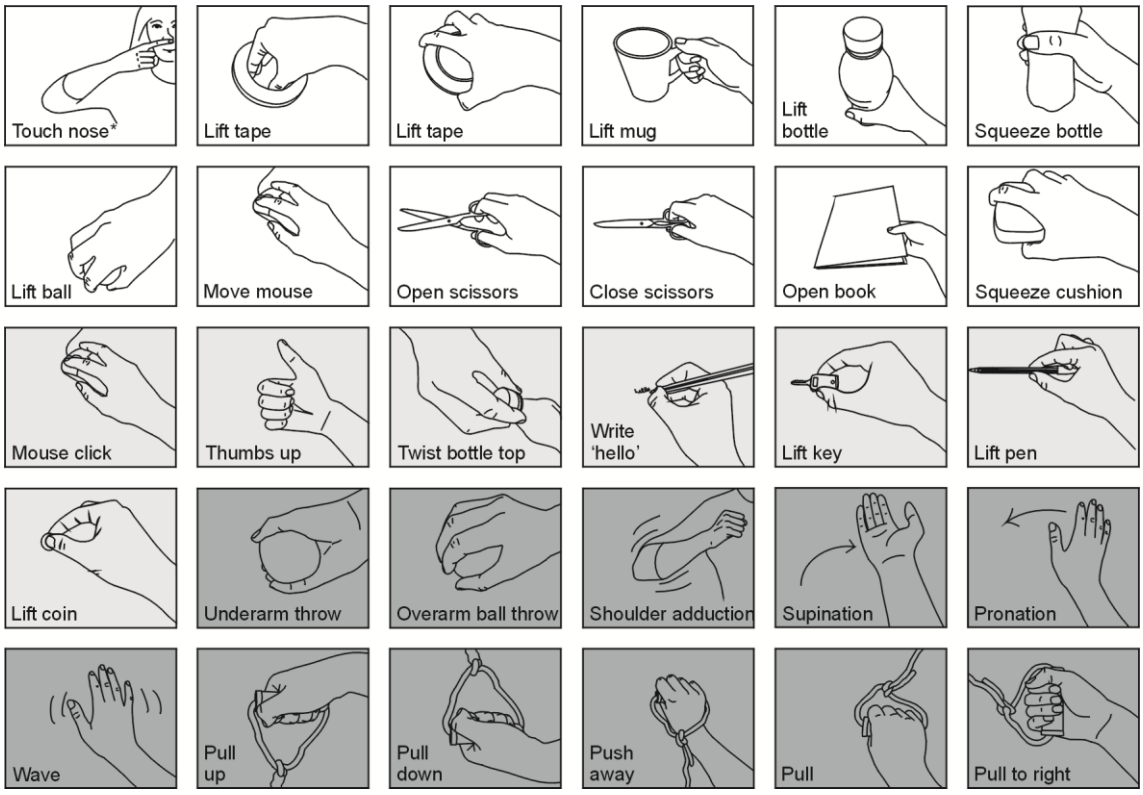

Figure 3.1: The 32 movements subjects were asked to perform. Shaded in pale grey are movements involving distal muscles; shaded in dark grey are movement involving proximal muscles. The touch nose task (*) was performed with three different starting positions: with the arm outstretched above the head, with the arm outstretched to the right, and with the arm hanging by the side of the body.

3.3.4 Analysis

Simple loud and quiet trial analysis Spike2 recordings were analysed using MatLab (The Mathworks, Natick, MA, USA) software. First, a period of the EMG trace for each muscle beginning 200ms before and ending 1000ms following the stimulus marker for each trial was taken and RTs for each cue measured. RTs were defined as the first time after the stimulus marker that the EMG trace exceeded three standard deviations above the mean of the 200ms period of baseline EMG occurring before the marker. Traces were then visually inspected and the RT manually changed if thought to be inaccurately placed by the automated program. The SCM muscle was then removed from all trials, as this was only used in the further analysis explained below.

Analysis of reaction time between loud and quiet-cued trials RTs from neither condition were normally distributed, as measured by a Kolmogorov-Smirnov test. Therefore a Wilcoxon rank sum test was used to test the null hypothesis that RTs from both conditions were the same. The eRTs across muscles (apart from the SCM), for every trial in every movement task and for every subject were included in this analysis.

Analysis of reaction times of trials with and without sternocleidomastoid activation Mean RTs were found across all trials in all subjects for each muscle apart from the SCM, for each task, for three different conditions: all quiet-cued trials with no SCM activation; all loud-cued trials in which the SCM muscle was activated and all loud-cued trials in which the SCM muscle was not activated (the last two conditions termed SCM+ and SCM- trials, respectively). As all groups of RT were not normally distributed as measured by a Kolmogorov-Smirnov test, Wilcoxon rank sum significance tests were performed on RTs between quiet and SCM+, quiet and SCM-, as well as SCM+ and SCM- sets of trials.

Analysis of StartReact habituation In order to find whether the StartReact effect (i.e. significant difference in RT between quiet- and startle-cued trials) was maintained throughout the 160 trials carried out (5 trials for each of the 32

movements), the trials were split into 8 chronologically-ordered groups of 20. This was done separately for each condition. Four different movement tasks were therefore included in each group of 20 trials, though this was unimportant for the purposes of examining habituation. As again the data were not normally distributed, a Wilcoxon signed ranks significance test were carried out on RTs for the two conditions within each of the 8 groups. It was then possible to assess whether the significant difference was maintained over all groups of trials. This would allow the assessment of whether the StartReact effect habituates over time. Additionally, linear regression was carried out over trial number and the mean difference between RT from each cue type.

Assessing the validity of the SCM marker for startle The presence of SCM activation in quiet-cued trials in which startle should not occur was examined in order to see whether the SCM is a reliable marker of startle.

Assessing whether the SCM marker is useful in exploring whether finger movements are affected by StartReact First it was assessed whether RT*s* differed between loud and quiet conditions, for both the 1DI muscle (index finger) in tasks involving the fingers and the anterior deltoid (shoulder) muscle in tasks which required shoulder movements. A Wilcoxon rank sum test was used to test the null hypothesis that the RTs for tasks involving finger movements were the same between conditions for the 1DI muscles. This was repeated for movements involving the shoulder between conditions for the anterior deltoid muscle.

Then an experiment previously carried out into whether the RTs of quiet-cued individual finger movements are reduced by a startling stimulus was repeated. RTs from trials involving the mouse button clicking task and the cushion squeeze task (Figure 3.1) were compared between loud SCM+, SCM- and quiet SCM- conditions for the 1DI muscle only. A Wilcoxon rank sum test was used to test the null hypothesis that there was no difference between all three conditions for each task. This was repeated on the same data but all quiet conditions and all loud trials amalgamated regardless of SCM activation. Again,

Wilcoxon rank sum tests were used to test the null hypothesis that there were no differences in RT between conditions for each task.

3.4 Results

3.4.1 Reaction times

As discussed in Chapter 2, the earliest RT across muscles for every trial, task, and subject were compared in response to loud and to quiet cues. As has been consistently found in the existing literature, there was a significant difference between RTs for movements cued by a quiet and loud stimulus as measured by Wilcoxon rank sum test (significant difference at $P<0.00001$, example trace Figure 3.2, histogram of RTs Figure 3.3). The average RT for quiet trials was 204±79ms, and for loud trials was 144±75ms (mean±standard deviation). The difference between the mean of these early RTs for each condition was 60ms. As the data are not normally distributed and have a positive skew, using the median eRT might be more valid than the mean. The median for the loud condition was 127ms and for the quiet condition was 199ms.

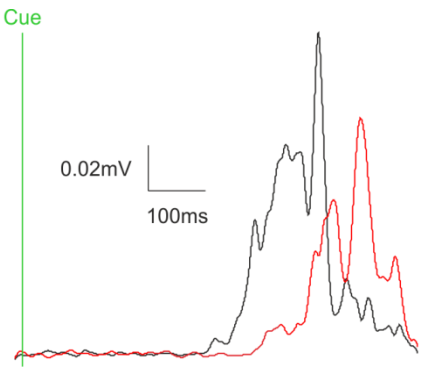

Figure 3.2: Example traces from the 1DI muscle for one subject for one loud trial (black trace) and one quiet trial (red trace) of the 'lift pen' task. The green marker indicates the cue timing.

Then for all tasks and muscles (apart from the SCM muscle which was only used as a marker) the loud trials were separated into SCM- and SCM+ trials and the RTs for these groups were calculated respectively (Figure 3.4). The mean RT for SCM+ trials was 186±123ms (mean±standard deviation) and for SCM- trials was 233±123ms; these were significantly different (Wilcoxon rank sum test,

P<0.0001). The mean RT for all quiet trials with no SCM activation was 289±117ms. The difference in RTs between SCM+ and quiet-cued trials (132ms) as well as between SCM- and quiet-cued trials (117ms) were both significant (Wilcoxon rank sum test, P<0.0001). Activation of the SCM muscle was found in 31% of all loud-cued trials.

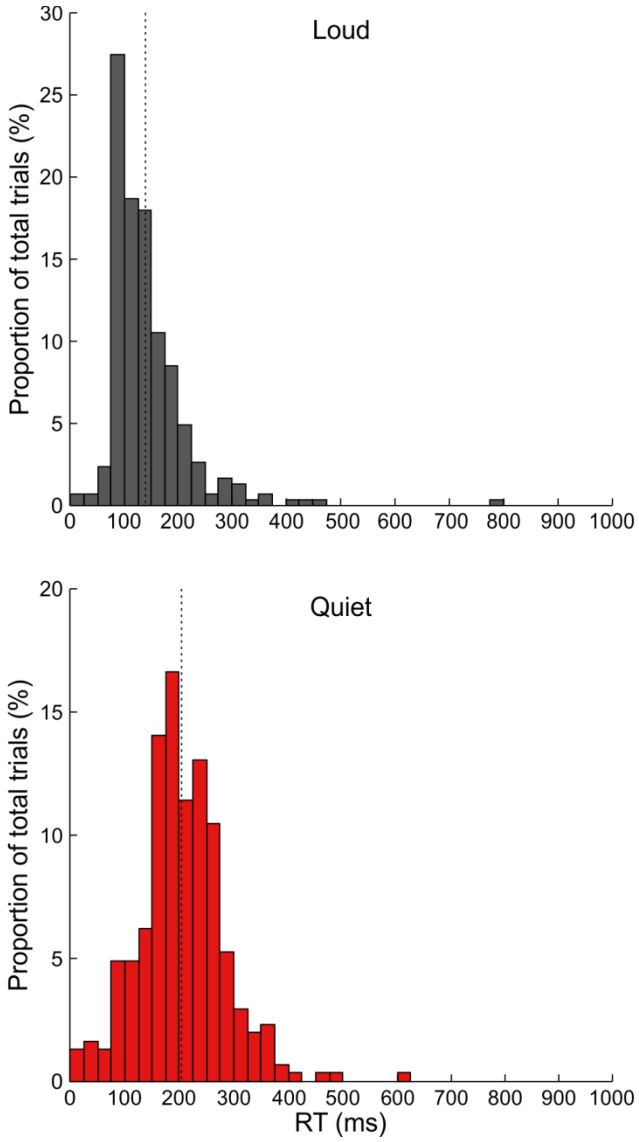

Figure 3.3: Histograms of the earliest RT across muscles for each trial and task for all subjects, for both loud and quiet conditions. The dotted lines represent the mean eRT for each condition.

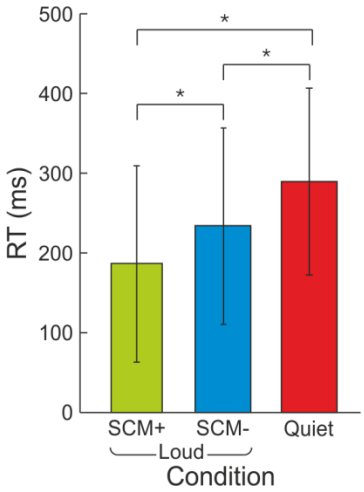

Figure 3.4: Mean RTs across all muscles, trials, tasks and subjects for SCM+ trials, SCM- and quiet trials with no SCM activation, respectively. Error bars represent one standard deviation above and below mean. All conditions were significantly different from each other (P<0.0001).

3.4.2 Habituation of the StartReact effect

It was then investigated whether habituation of the StartReact response was found in different muscles and whether this effect lasted over many trials. For each condition (loud- and quiet-cued) separately, the RT for all trials in chronological order were taken for one muscle and averaged across subjects. This resulted in a vector of 160 trials per condition (5 each of 32 movements); these were split up into 8 equal groups of 20 trials and the means of these plotted (Figure 3.5).

As a Kolmogorov-Smirnov test found the data to be not normally distributed, significance testing of the difference in RT between conditions for each of these groups of trials was carried out using a Wilcoxon signed ranks test. This entire process was repeated on 3 more muscles, resulting in analysis of the 1DI FDS, SCM and biceps muscles. Nearly all groups of trials were significantly different between conditions (P<0.05), with three exceptions in the FDS, SCM and biceps muscles for trials 101-120, 61-80 and 81-100 respectively. In determining the significance between groups of trials, consideration of multiple comparisons must be made. This can be done by using a binomial probability distribution to find the probability of achieving ≥7 significant differences at the level of P<0.05; this results in 0.000006, therefore the differences are highly significant.

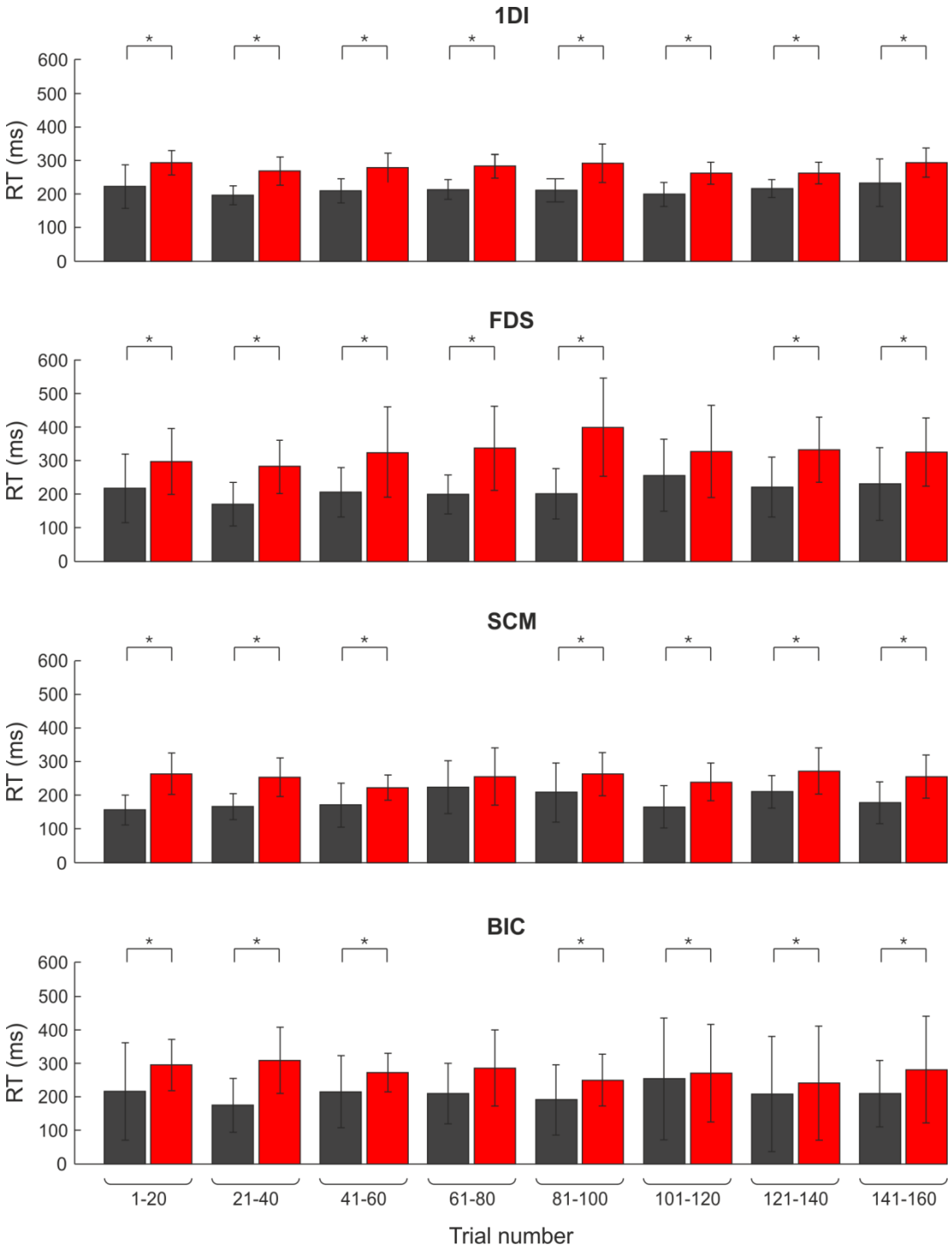

Figure 3.5: Mean RTs across subjects and trials split into eight groups in chronological order for four different muscles. Error bars represent one standard deviation above and below the mean for each group. Stars represent a significant difference between RTs from loud (black bars) and quiet (red bars) conditions (significance level $P<0.05$, Wilcoxon signed ranks test).

The difference in RTs between conditions had a mean of 110ms, 83ms, 88ms and 132ms for the first 20 trials across subjects for the SCM, 1DI, biceps and FDS muscles respectively. The difference in RTs between conditions had a mean

of 74ms, 64ms, 63ms and 85ms for the last 20 trials across subjects for the SCM, 1DI, biceps and FDS muscles respectively.

Across all subjects, out of the first 20 loud trials (giving a total of 200 trials), 65 (33%) had SCM activation. For the last 20 trials, 85 (43%) had SCM activation. There was no significant difference between the number of trials with SCM activation between the first and last ten trials across all subjects (Wilcoxon rank sum test, P=0.516).

Mean differences in RT between loud and quiet conditions were calculated across subjects for each block of 20 trials. Linear regression was then carried out to find whether trial number (1:160 trials in 20 trial blocks) was a predictor of difference in RT between conditions. No significant relationship was found between trial number and the mean difference across subjects in RT between cue conditions for SCM (r^2=0.01, P=0.317), or biceps (r^2=0.01, P=0.140), though this was significant for FDS (r^2=0.05, p<0.005) and 1DI (r^2=0.03, P<0.05, Figure 3.6).

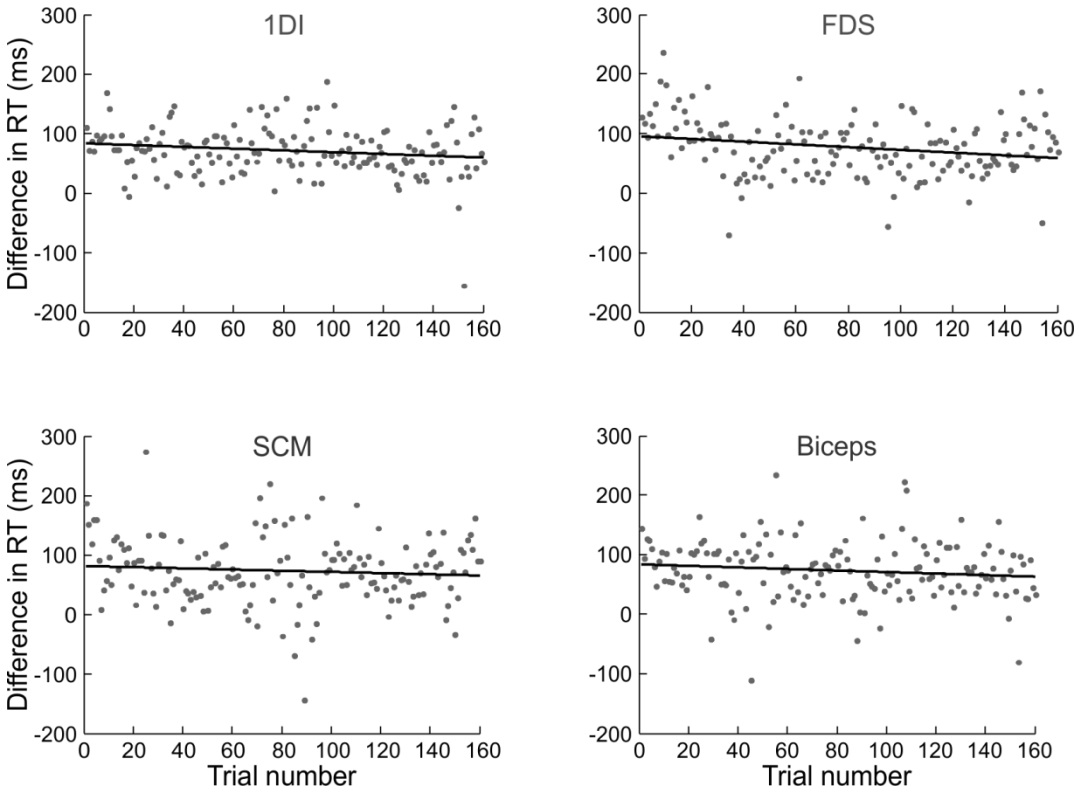

Figure 3.6: Scatterplots of the mean difference in RT between loud and quiet trials across subjects, for four different muscles, with linear regression lines.

3.4.3 Validity of using SCM activation as a startle marker

One way of assessing whether the activation of the SCM muscle is a valid marker to show that startle has occurred is to examine whether it is activated during trials which are non-startling, in this experiment the 80dB 'quiet' cued-trials. It was observed that 7 of the 10 subjects included in this experiment had SCM activation in some quiet trials, totalling 30% of trials across all subjects. SCM activation was found in loud trials in 9 subjects, also totalling 30% of all trials. In some quiet trials, the amplitude of the SCM muscle was higher than that of loud SCM+ trials (Figure 3.7). The two subjects who had the highest percentage of loud trials with SCM activation (94% and 100%) also had the highest percentage of quiet trials with SCM activation (88% and 100%). The mean RT of all the loud trials with SCM activation for these two subjects was 160±92ms, and the mean RT for all quiet trials with SCM activation for the same two subjects was 224±102ms (mean±standard deviation); these groups of trials were significantly different (Wilcoxon rank sum test, $P<0.0001$). The mean RT for quiet trials with no SCM activation for these subjects was 289±117ms.

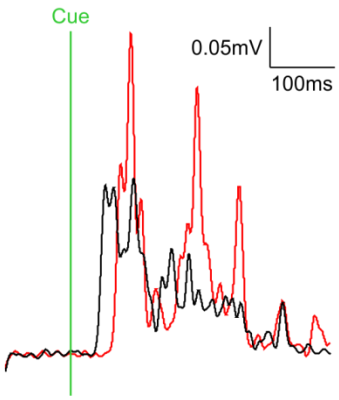

Figure 3.7: Example traces of the SCM muscle showing activation in a loud (black) and quiet (red) trial for the same muscle in the same subject.

The mean RT of the SCM muscle in loud trials across all subjects was 193±133ms and in quiet trials was 258±132ms. The mean difference in RTs between conditions for the SCM muscle was 65ms. There was a significant

difference in RT between conditions (Wilcoxon rank sum test, P<0.00001, Figure 3.8).

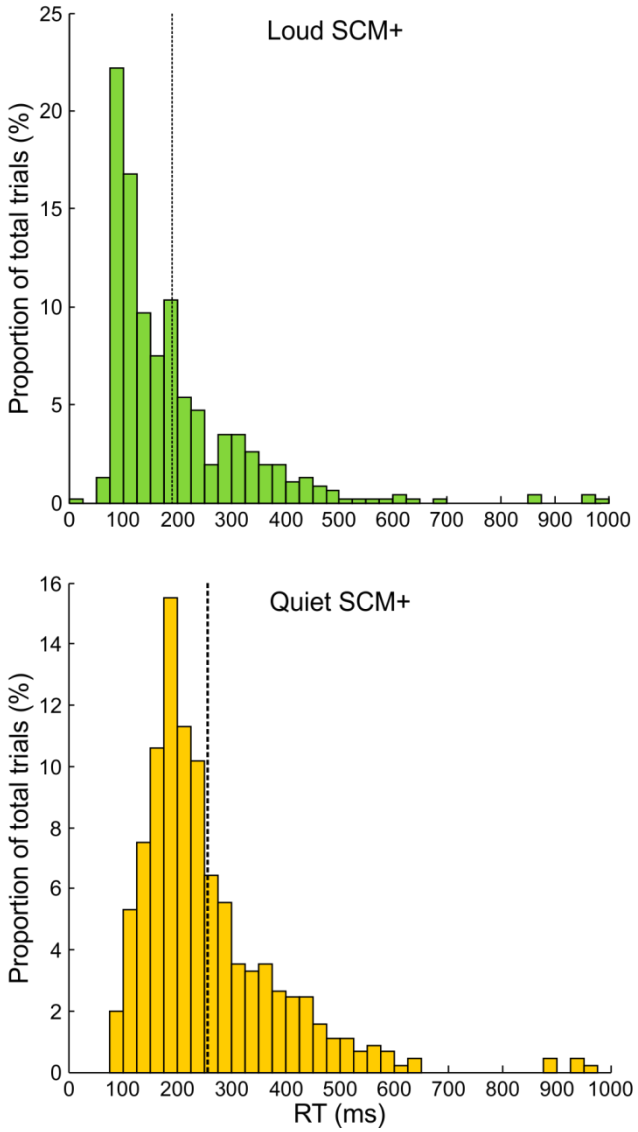

Figure 3.8: Histograms of RTs of the SCM muscle in response to loud cues (top, green) and quiet cues (bottom, yellow). Mean RTs are indicated by the dashed lines in each histogram.

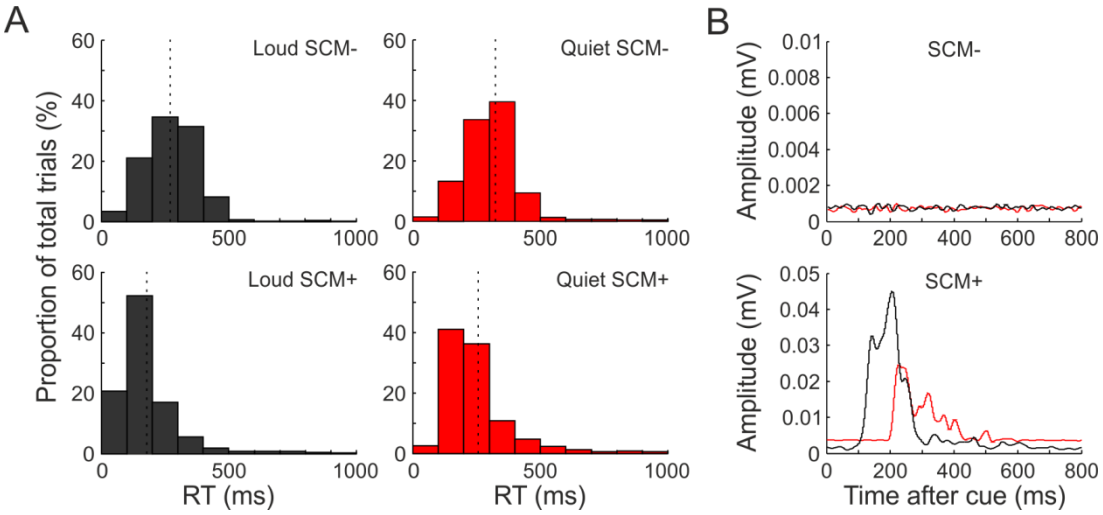

Figure 3.9: Histograms of RTs in four subjects from loud SCM- trials (top left, black), quiet SCM- trials (top right, red), loud SCM+ trials (bottom left, black) and quiet SCM+ trials (bottom right, red); dashed lines indicate the mean of each group (A). Example traces of the SCM muscle from a quiet (red) and loud (black) SCM- trial (top) from one subject, and from a quiet (red) and loud (black) SCM+ trial (bottom), from the SCM muscle in another subject (B).

The presence of SCM activation in quiet trials was found to decrease RT (Figure 3.9), when startle should not occur in response to sounds of only 85dB.

3.4.4 Reaction time differences between proximal and distal muscles

Loud vs quiet conditions It was investigated whether there were differences in RTs between conditions in the 1DI muscle for tasks involving the fingers and the anterior deltoid muscle for tasks which required shoulder movements. Tasks involving the finger included lifting a pen, lifting a key, lifting a coin, making a 'thumbs up', clicking a left mouse button with the index finger, twisting a bottle top and writing 'hello' (Figure 3.1, pale grey boxes). Tasks involving the shoulder comprised of waving, pulling a bungee cord up, down, to the right, in and out, an underarm throw, an overarm throw and making a 'chicken wing' movement consisting of flexing the elbow and abducting/adducting it (Figure 3.1, dark grey boxes).

The mean RT for anterior deltoid for shoulder tasks was 225±156ms (mean±standard deviation) for loud cues and 285±160ms for quiet cues (Figure 3.10), with a difference in means of 60ms. The mean RT for the 1DI muscle for finger-dependent tasks was 206±115ms for loud cues and 270±121ms for quiet

cues, with a difference in means of 64ms. A Wilcoxon rank sum test showed that there was a significant difference between loud and quiet-cued RTs in both the 1DI muscle and anterior deltoid muscle (both P<0.0001).

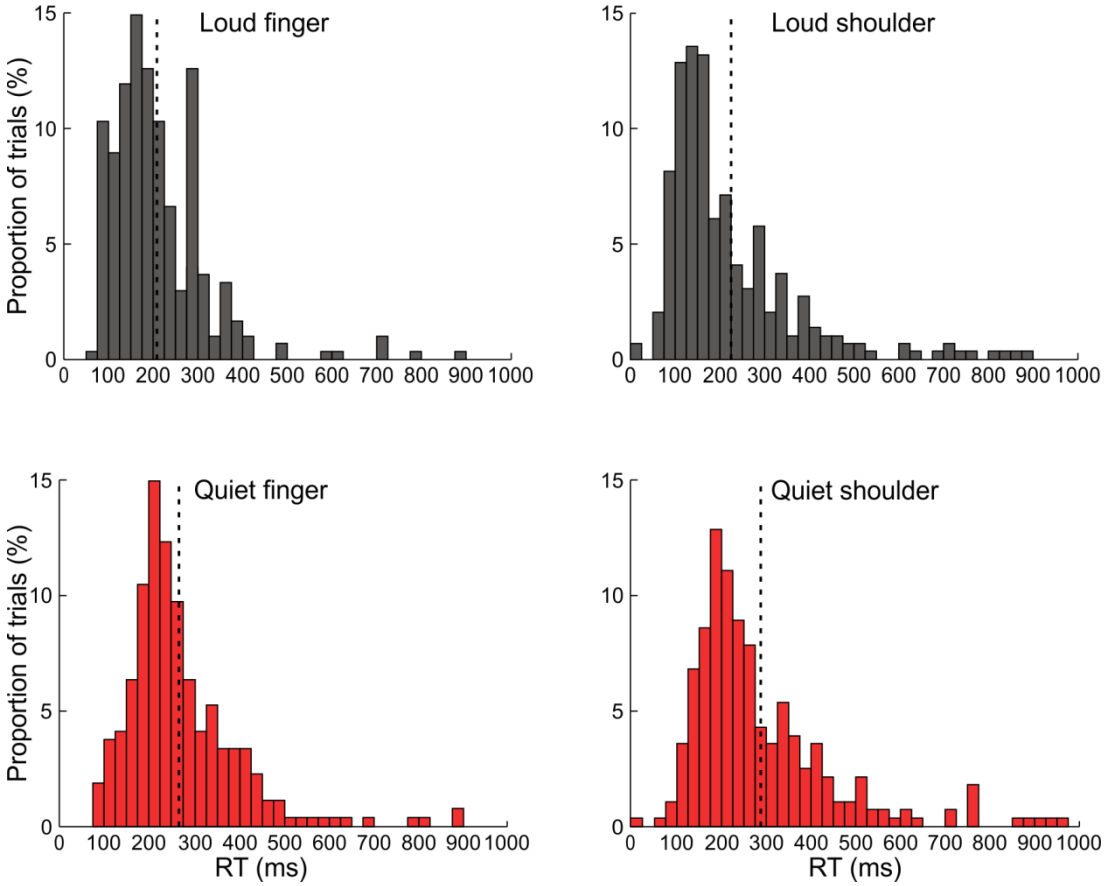

Figure 3.10: Histograms of RTs of 1DI muscle carrying out tasks with finger involvement (left hand histograms) and of anterior deltoid muscle when carrying out movements with strong shoulder involvement (right hand histograms) for 10 subjects.

The difference in RT between conditions for finger and shoulder muscles is also evident from the cumulative probability plots of all RTs these trials (Figure 3.11). For both muscles, there was a clear difference in the probability of a particular RT between conditions, with loud trials resulting in consistently shorter RTs.

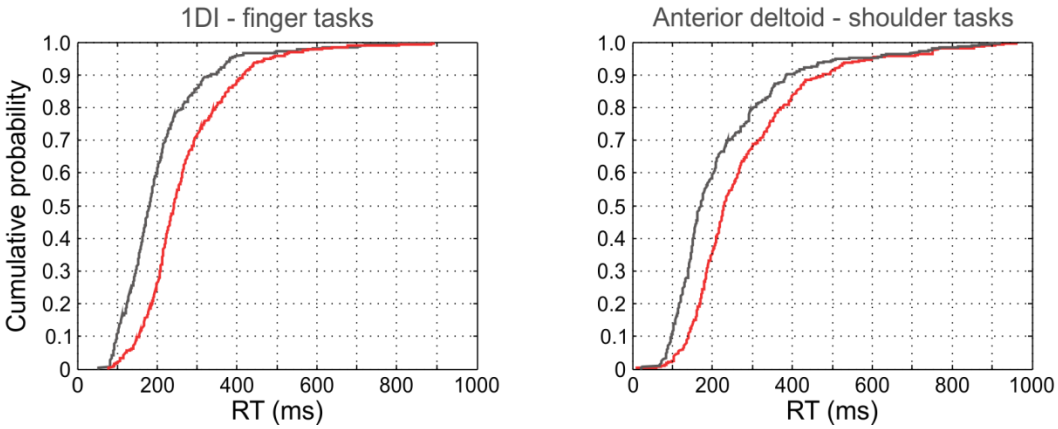

Figure 3.11: Cumulative probability plots of the RT for the 1DI muscle in movements involving the index finger, and the anterior deltoid muscles in movements involving the shoulder, for both loud (black curve) and quiet (red curve) conditions.

Loud SCM+ vs SCM- vs quiet SCM- conditions RTs for the 1DI muscle in SCM+, SCM- and quiet-cued trials with no SCM activation were then examined for two tasks: squeezing a small cushion and clicking the left-hand button on a computer mouse. This was intended to replicate the results of a previous experiment (Honeycutt *et al.*, 2013). The mean RT for the 1DI muscle when carrying out a cushion squeeze in response to a quiet cue was 246±112ms; this was shorter when cued by a loud sound: 124±80ms (mean±standard deviation) in SCM+ trials and 187±131ms in SCM- trials. When clicking a mouse button, the 1DI muscle had a mean RT of 268ms±74ms when cued by a quiet sound: again these RTs decreased when cued by a loud sound, having a mean of 200±106ms in SCM+ trials and 208 ±72ms in SCM- trials (Figure 3.12).

Significant differences were found in the RTs between quiet-cued and SCM- trials for the mouse click task (Wilcoxon rank sum test, $P<0.0001$) but not between quiet and SCM+ trials ($P=0.148$) or SCM+ and SCM- ($P=0.972$). Significant differences were found in the cushion squeeze task between quiet and SCM- ($P<0.0001$), quiet and SCM+ ($P<0.0001$) and SCM+ and SCM- ($P<0.005$).

The lack of significant difference between quiet and SCM+ conditions could be because there were only seven trials across subjects for this movement in which SCM activation was seen, compared to 27 in the quiet condition and 33 in the

SCM- condition (Figure 3.12). Having a small sample size increases the chances of getting a Type II error (falsely accepting the null hypothesis).

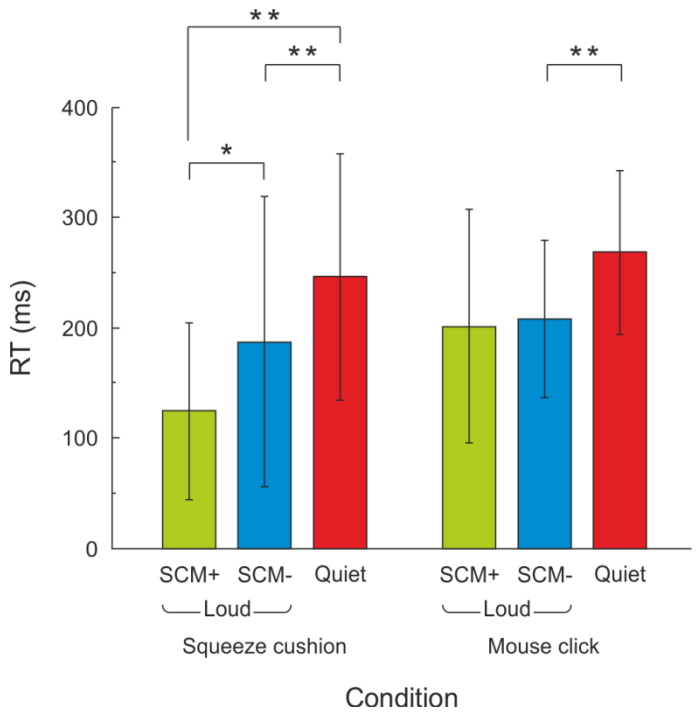

Figure 3.12: RTs for the 1DI muscle when carrying out two different tasks: squeezing a cushion and clicking the left button of a mouse, in SCM+, SCM- and quiet conditions. Error bars represent one standard deviation above and below mean. A single star indicates a significant difference between bracketed conditions at the P<0.005 level, two stars at the P<0.0001 level (Wilcoxon rank sum test).

It was then investigated whether there was a difference in RT between loud and quiet conditions in the 1DI muscle for each task regardless of SCM activation. A decrease in RT was found in both task types when the loud cue was presented compared to the quiet cue. This difference was significant at the P<0.05 level for the cushion squeeze task and at the P<0.005 level for the mouse button click task, tested by Wilcoxon rank sum test (Figure 3.13).

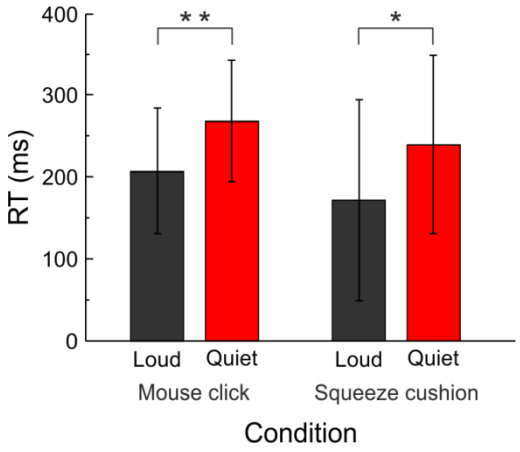

Figure 3.13 Mean RTs for all loud (black) and all quiet (red) trials in all subjects for the 1DI muscle for the mouse click and squeeze cushion tasks. Error bars represent one standard deviation. One star indicate significance at the P<0.05 level; two stars indicate significance at the P<0.005 level.

3.5 Discussion

3.5.1 The effects of a startling stimulus on reaction time

Valls-Solé *et al.* (1999) found that RTs can be decreased by up to 77ms when cued by a startling stimulus; the average decrease in eRT here was 60ms (when no distinction between SCM- and SCM+ trials was made), which is further evidence of the StartReact effect. When loud trials were separated into SCM+ and SCM- trials, the difference in RT between quiet and SCM+ was 132ms and between quiet and SCM- trials was 117ms.

However, the RTs found here in response to either cue type were longer than have been previously reported, with a mean of 204ms for quiet-cued trials and 144ms for loud-cued trials, compared to <70ms for loud trials found in previous reports. RTs for muscles specifically used in particular tasks were lower, for example the mean RT across subjects for the 1DI when carrying out a cushion squeeze in response to a loud cue was 124ms, although this is still higher than seen in previous work. One previous study found 1DI RTs for quiet-cued of 176ms, with 98ms for SCM+ and 96ms for SCM- trials, in an index finger task (Honeycutt *et al.*, 2013).

It is possible that a small factor in the larger RTs was an older subject sample; subjects here were aged 43±13 years (mean±standard deviation), compared to

26±8 years used by Carlsen *et al.* (2007), who found some RTs of 80ms, or 25.9±2.8 years used by (Honeycutt *et al.*, 2013). It has been shown that RTs for the right arm increase by about 40ms with age (Darbutas *et al.*, 2013), though peripheral motor conduction time only increases by 1-2ms between the ages of 20 and 40 (Jaiser *et al.*, 2014). Additionally, for analysis of the current RT data no restrictions on RT were imposed, whereas Honeycutt *et al.,* for example only looked at trials with RTs under 300ms; therefore the inclusion here of all trials may have inflated the mean (Honeycutt *et al.*, 2013).

3.5.2 Habituation of the StartReact effect

The response to a stimulus is often found to decrease or habituate over time if that stimulus is repeatedly presented. This has also been found to occur when subjects are repeatedly exposed to a startling stimulus, though not in the context of a RT task, or when subjects are otherwise planning to execute a motor act (Valls-Sole *et al.*, 1997). This could be explained by the finding that motor areas increase in excitation during motor preparation, whereas after a certain time following the most recent movement made, excitation is lost if no new movement is prepared (Loh *et al.*, 2010). Several studies have looked at habituation of the StartReact response (Brown *et al.*, 1991b; Valls-Sole *et al.*, 1997; Siegmund *et al.*, 2001) however these are all limited in one of two ways.

Firstly, the range of muscles measured in these studies was limited and usually focussed on the SCM. This focus is due to the finding that SCM is one of the last responses out of a range of muscles to disappear when subjects are repeatedly exposed to a startling stimulus (Brown *et al.*, 1991b). However, this experiment involved subjects sitting quietly while the stimuli were presented, so its findings are not applicable in the context of RT tasks (Brown *et al.*, 1991b). It is possible that other muscles take longer to habituate than the SCM during a RT task.

Secondly, most of the existing research on startle habituation has used a small number of trials: Valls-Solé *et al.* (1997) recorded EMG from the masseter, SCM and OOc (orbicularis oculi) muscles and found that the SCM muscle habituated

the least over 5 trials. Another study found no habituation in the SCM, OOc and cervical paraspinal muscles over 14 trials during a RT task of turning the head, though here the use of the SCM is confused due to its involvement in the task. The most extensive study carried out so far on the subject found that the StartReact effect does not habituate in SCM or OOc muscles during a RT task over 100 trials, 20 of which were startling (Carlsen *et al.*, 2003). However this frequency of 1 in 5 is not very high; habituation has been shown to increase when the stimulus is presented with higher frequency (Thompson and Spencer, 1966). Hence it is possible that, were more trials introduced, these muscles would habituate.

Therefore this study aimed to find whether habituation occurs over a larger number of trials and over a range of different muscles. A ratio of 1:1 startle-cued to quiet-cued trials was used, with a total of 160 trials carried out over the 32 different movement tasks. The SCM and three other muscles, the 1DI, FDS and biceps were chosen, based on their distributed location in the hand, forearm and upper arm respectively. As the SCM has been argued as being a marker of startle (discussed below), it was investigated here whether the SCM muscle habituates at all to the StartReact effect, and if so, whether it is the last to habituate. There were no significant differences between the number of trials with SCM activation across subjects between the first and the last ten trials, showing that the SCM muscle does indeed seem not to habituate in a RT task. However none of the muscles studied habituated, as although for all four muscles there was a significant difference between the RTs of the first 20 and the last 20 trials across subjects, the difference in RT actually increased over time. Additionally, linear regression revealed that trial number had no relationship to difference in RT between conditions for two (SCM and biceps) of the four muscles tested. This suggests that the StartReact effect does not habituate over 160 trials when randomly presented in a ratio of 1:1 with quiet cues during a reaction time task. However, as suggested by Carlsen *et al.* (2003), it is still unknown whether habituation would occur if the startling stimulus were presented on every trial. It is perhaps unlikely that if the effect does

habituate, it takes more than the 160 trials studied here to do so, which take about an hour to perform.

The finding that habituation does not seem to occur (at least over 160 trials) when subjects are directing attention towards a motor task could be explained by the involvement of the cortex as well as by increased excitation due to motor preparation (Carlsen *et al.*, 2003). It is known that there is some modulation of the startle response by cortical areas and the cerebellum (Frings *et al.*, 2006), therefore it is possible that these areas provide inhibition of the startle circuit. Further evidence for cortical influences include the finding that the startle response is attenuated by a prior exposure to a weak 'prepulse' stimulus occurring before the actual startling stimulus, an effect called prepulse inhibition or PPI (Swerdlow and Geyer, 1993), which is suggested to be under cortical control (Valsamis and Schmid, 2011). This is one example of directing attention towards the stimulus modality of the startle (which can be auditory, visual or vestibular), which may increase the excitability of that sensory system, making it more resistant to habituation (Richards, 2000). However the possibly more compelling argument for reduced or absent habituation of startle during a RT task is the fact that subjects are preparing to carry out the movement, meaning that the associated motor areas have increased excitation (Chen *et al.*, 1998). This increase has been found 80-120ms before the motor task is carried out (Chen and Hallett, 1999; Leocani *et al.*, 2000).

3.5.3 Use of sternocleidomastoid activation as a marker for startle reflex

Activation of the SCM muscle is often used as a marker of startle, however its use has not been very well justified. Here, several lines of investigation were followed to ascertain its worth more fully.

It has been argued that startle trials without SCM activation could be the result of stimulus intensity effects, whereby increasing stimulus intensity decreases RT, however not as much as when SCM activation is also present (Kohfeld, 1969; Carlsen *et al.*, 2007). Carlsen *et al.* used stimulus intensities of 83-123dB,

finding that SCM activation was present in intensities of 93dB or above (2007). However here it was found that there was SCM activation on many quiet trials of 85dB, indeed the two subjects with the highest percentage of SCM activation in loud trials also had the highest percentage of quiet trials with SCM activation. Quiet trials with SCM activation (for two subjects) had a mean RT of 224±102ms, whereas mean RT for quiet trials with no SCM activation was 289±117ms. This is a difference of about 66ms, which is very similar to the 72ms difference between loud trials with and without SCM activation. Therefore clearly there is some reason why RTs of trials in both loud and quiet conditions are shorter when SCM activation is present. This could be due to startle, with the StartReact effect occurring at intensities as low as 85dB; this would then not preclude the possibility that SCM is a marker of startle. Though as startle is generally found at intensities of 115dB and above (Carlsen *et al.*, 2011b), this might not be a likely conclusion. Additionally, the 85dB cue through headphones was really not very loud. Instead, it is possible that no startle is induced with 85dB cues, and therefore as SCM is still sometimes activated at this intensity, it is not a reliable marker.

Alternatively, it is possible that the activation of this muscle was simply caused by the way in which subjects carried out their tasks, perhaps involving some head and neck postural adjustments when reaching movements were made. The fact that the SCM muscle could be activated by the movement task involved even when no acoustic cues at all are used makes reliance upon it when judging presence of startle risky.

Furthermore, Honeycutt *et al.* (2013) state that 'a latency difference between the SCM+ and SCM- trials indicates that the task is susceptible to StartReact, i.e. that the presence of startle triggers a rapid involuntary release of the planned movement'; this suggests that not only is SCM activation required, but there must be a significant latency difference between SCM+ and SCM- conditions for the SCM+ trials to signify startle has occurred. This distinction is argued to distinguish between trials in which startle and stimulus-intensity effects have caused RTs to shorten (Carlsen *et al.*, 2007); though in Carlsen's study, loud

SCM- decreases in RT relative to quiet cues were about 20ms, whereas here differences of >50ms were found between these conditions. If SCM activation is a marker for startle, then it is also hard to explain the finding that the mean SCM- RT was shorter than the mean SCM+ RT (although not significant) in the 1DI muscle for an index finger task found by Honeycutt *et al.* (2013). Furthermore, here there was no significant difference in RT between SCM- and SCM+ conditions in the 1DI muscle when carrying out a whole-hand grasp (the squeeze of a cushion), which was found by Honeycutt *et al.* (2013); this may suggest that the presence of SCM activation is not a reliable or particularly useful indicator, as RTs when it is present are often not that much shorter than in its absence, and may even be longer.

It is therefore argued here that the presence of SCM activation is not a useful indicator. It has already been shown that the RST has excitatory inputs to motoneurons projecting to intrinsic hand muscles (Riddle *et al.*, 2009), therefore it is possible that the RST could provide the extra excitation required to boost an already prepared but subthreshold finger motoneuron. Even though the RST projections to finger motoneurons are suggested to be widely divergent, if the level of excitation for that finger muscle is already increased due to movement preparation, the extra excitation provided by the RST-mediated startle input could push it above threshold, whereas with perhaps no existing excitation the other muscles projected to would not be pushed above threshold.

3.5.4 Reaction time differences between proximal and distal muscles

It has been suggested that the StartReact effect occurs by the loud startling stimulus triggering pre-programmed motor commands stored subcortically, which then in turn activate the muscles required for the prepared movement via reticulospinal connections (Carlsen *et al.*, 2004a). It has been suggested that fine finger movements are mainly controlled by monosynaptic corticomotoneuronal connections (Bennett and Lemon, 1996; Lemon *et al.*, 2004), leading to the argument that muscles involved in these movements, such as the intrinsic hand muscles, would not have the reticular inputs required to be

susceptible to the StartReact effect (Carlsen *et al.*, 2009). However, research has recently shown that RST connections to hand motoneurons are as common, if not more numerous than those to more proximal muscles (Riddle *et al.*, 2009), therefore it is possible that finger RTs could decrease in StartReact.

To date, two papers have explored this issue. One experiment required subjects to perform an index finger flexion or an arm extension movement in response to a startling, loud go cue and a quiet go cue (Carlsen *et al.*, 2009). It was found that the significant decrease in RT found in arm movements was not true for finger movements; finger RTs were found to be on average 106ms, sufficient time for cortical structures to be in control of the action. In conclusion, the authors argue that there are only 'weak' subcortical-distal muscle projections to finger muscles, which are not susceptible to startle (Carlsen *et al.*, 2009). This view is supported by the 'disproportionally' long latencies that finger muscles have shown in response to startle, found by another group (Brown *et al.*, 1991b). The second study investigating whether individual finger movements are susceptible to StartReact has also shown decreases in coordinated whole-hand grasps which were not found in single finger movements (Honeycutt *et al.*, 2013). However, both of these experiments determined whether or not a decrease in RT was seen by comparing the reaction times of the loud-cued SCM+ trials with SCM- trials, despite the finding that the finger-movement tasks as well as the whole-hand ones showed a significant decrease in RT between quiet-cued and loud-cued trials.

Here it was found that for two types of task (a precise finger movement: clicking a mouse button and a whole-hand grasp: squeezing a small cushion) there was a significant difference in RTs for the 1DI muscle between loud and quiet trials. After separating loud trials into SCM+ and SCM-, there were significant differences between quiet and SCM- trials for both tasks, but only between quiet and SCM+ trials for the cushion squeeze task. This may be because there were very few 1DI trials with SCM activation for the mouse click task. Although Honeycutt *et al.* found a difference between SCM+ and SCM- trials for a whole-hand grasp task, here there were no significant differences between SCM- and

SCM+ trials for either movement (Honeycutt *et al.*, 2013). In addition, here movement types were separated into those involving the shoulder, and those involving precise finger movements, and the differences in loud- and quiet-cued RTs of the anterior deltoid and 1DI muscle in these trials respectively assessed. There was a significant difference between conditions for both categories of movement for their respective muscles.

For the reasons outlined above it is argued here that classifying trials according to the presence or absence of SCM activation is not useful and that it is possible that the difference between quiet-cued and loud-cued RTs in finger movements is the result of startle, reflecting the reticulospinal connections to finger muscle motoneurons shown by Soteropoulos *et al.* (2012).

3.6 Conclusions

Three main points are argued by this chapter. Firstly, that habituation of the StartReact effect does not seem to occur over 160 RT-task trials, 50% of which are startle-cued. This was true for four different muscles studied here: the SCM, 1DI, FDS and BIC muscles. There is no reason to believe the same is not true for any other muscle. This extends previous research which found the effect not to habituate over 100 trials, 20% of which were startle-cued.

Secondly, it is clear that the use of the presence of SCM activation as a marker of startle may not be completely valid or indeed even useful, as even in its absence, startle-induced movements have significantly shorter RTs than quiet-cued movements. Additionally, SCM activation has also been elicited by non-startling 85dB cues.

The third conclusion is that if it is true that SCM activation is an invalid marker of startle, previous findings based upon the SCM+/- distinction that single finger 1DI movements are not susceptible to StartReact might be incorrectly interpreted. Here, even significant differences between SCM- and quiet trials for single finger movements were found, which are argued to be caused by RST

inputs to finger motoneurons. The findings from this Chapter might be useful in informing future research using the StartReact as a technique to probe the RST.

4 Stimulus-triggered average effects from the reticular formation and primary motor cortex

This chapter details an experiment in which the RF and two subdivisions of M1 were stimulated and the output measured in 18-21 muscles of the hand, arm, shoulder and back of two macaque monkeys, with the aim of examining more closely the level of fractionation and motor synergies produced by these two brain regions.

I collected and analysed all data presented in this chapter. I also carried out the majority of the monkeys' task training, with the help of the laboratory animal technicians Terri Jackson and Lee Reed. Surgical techniques were carried out with the help of Stuart Baker.

4.1 Abstract

Introduction and aims: Although recently interest in the reticulospinal tract (RST) in primates has grown, little is still known about the output divergence, level of fractionation and synergies underlying motor output from the reticular formation. Additionally, most previous work on primary motor cortex (M1) projections has focussed on the output of corticomotoneuronal (CM) cells, with little attention paid to the 'old' subdivision of M1 lacking these cells. Therefore this experiment aimed to investigate and compare the output divergence, level of fractionation and synergies produced by the RST, as well as the two subdivisions of M1.

Methods: Two macaque monkeys were trained on a 'reach and grasp' task, which they performed to produce background activity while single pulse microstimulation was applied via a penetrating electrode to the RF, or one of two subdivisions of M1. Electromyography (EMG) responses to this stimulation were recorded in 21 (monkey Sa) or 18 (monkey Uw) muscles of the hand, arm and trunk. Principal component analysis (PCA) and independent component analysis (ICA) were carried out on the resulting stimulus-triggered averages in order to find the underlying muscle synergies and the percentage of variance in all responses accounted for by these synergies, which was used as a measure of

the pathway's level of fractionation. The synergies and patterns of variance explained were then compared between pathways.

Results and conclusions:

In conclusion, of all three regions, old M1 most commonly activated only one muscle, followed by new M1 then the RF. There was a gradient of level of co-activation from RF to old M1 to new M1. Support was found for previous findings about particular co-activation patterns of new M1 and the RF. Fractionation is suggested to be higher in new M1 than old M1 and the RF, which had roughly similar levels of fractionation, though it is suggested that the RF might produce slightly more fractionated movement than old M1.

4.2 Introduction and background

Reticular formation The reticular formation is a collection of nuclei located throughout the brainstem responsible for a number of functions including the sleep-wake cycle (Watson *et al.*, 2011), consciousness (Parvizi and Damasio, 2001) and motor control (Schepens *et al.*, 2008). Motor control is exerted via the reticulospinal tract (RST), which descends bilaterally and terminates upon interneurons and motoneurons in multiple spinal segments (Galea *et al.*, 2010). The RST has long been thought to contribute predominantly to control of axial and postural muscles (Prentice and Drew, 2001), though more recently it has been shown to have a role in reaching (Davidson and Buford, 2004; Davidson and Buford, 2006; Davidson *et al.*, 2007), hand movements (Buford and Davidson, 2004), and even finger movements (Soteropoulos *et al.*, 2012). However despite these recent developments not much is currently known about the muscle projection patterns of the RST, its level of fractionation, or any synergies that it might control, and how these compare to those produced by M1.

Primary motor cortex The primary motor cortex (M1) is located on the anterior bank of the central sulcus, extending out onto the precentral gyrus. Along with supplementary motor areas and regions from the sensory cortex, projections from M1 comprise the descending corticospinal tract (CST) (Dum

and Strick, 1991). The CST has a long-established role in movement control, particularly in imposing finer, more fractionated muscle control on top of existing motor pathways (Lawrence and Kuypers, 1968); this is primarily carried out via corticomotoneuronal (CM) connections which terminate directly onto motoneurons (Maier *et al.*, 1997). The gyrus and sulcus of M1 have been subdivided into two regions based on the presence or absence of CM cells. The gyrus lacks CM cells and is therefore considered an evolutionarily older area (termed 'old' M1) probably present in all mammals. The sulcus contains CM cells so is thought to have evolved more recently and has thus been termed 'new M1' (Rathelot and Strick, 2009).

Movement fractionation and synergies Movements are produced as the result of a particular combination of muscles activated or inhibited to different degrees over a particular time period. Controlling individual muscles or even motor units throughout each movement would therefore require a significant amount of processing. In order to simplify control, it has been suggested that the motor system does not activate each muscle involved in a given movement individually, but instead recruits a flexible combination of predetermined groups of muscles, called muscle synergies. These synergies can be considered 'building blocks' of movement, and evidence for their existence has been shown in many animal models including frogs (d'Avella and Bizzi, 2005), macaques (Overduin *et al.*, 2008) and humans (Weiss and Flanders, 2004). However, it is not yet clear whether they are produced by the cortex, subcortical areas and/or the spinal cord.

The level of fractionation of a motor pathway is defined as its ability to produce precise movements involving few muscles, whereby a highly fractionated pathway would be expected to control many synergies each containing a small number of muscles. Conversely, a pathway with low fractionation would be expected to activate many muscles in a given synergy, producing grosser movements. Movements produced by a pathway with low fractionation might therefore result from a combination of few synergies.

Normalisation Due to factors affecting the size of signal recorded from each muscle, such as number of active motor units in the vicinity of the electrode and the size of the muscle, the measurement of muscle activity in mV is usually not considered comparable between muscles and individuals. Instead, EMG data must be normalised to a more standardised unit. Most commonly each data point is converted to a proportion of the maximum voluntary contraction (MVC) for that muscle (Halaki and Ginn, 2012). Alternatively, Z-score normalisation is used, involving subtraction of the mean and division by the standard deviation for each muscle. Both methods allow recordings from different subjects or different muscles to be compared more accurately. Therefore in this Chapter, as in the next two Chapters, normalisation both by Z-score and by MVC for each muscle was carried out. However there was a possibility of high-amplitude stimulus artefacts being captured in the recordings. These were likely to be higher in amplitude than actual muscle activity, therefore in order to avoid normalising by any artefacts, the 97th percentile value of a cumulative distribution plot (CDP) for each muscle was used instead of the 100% MVC value.

Stimulus-triggered averaging The key methodological technique used in this Chapter is stimulus-triggered averaging (stimulusTA). As detailed in Chapter 1, this involves averaging the muscle responses elicited by stimulation of a particular (sub)cortical site (Davidson and Buford, 2004; Davidson and Buford, 2006), allowing the muscles activated by the site to be characterised. Single pulse stimulation (at frequencies such as 9Hz) is usually used in stimulusTA, in order to avoid temporal summation, and therefore to stimulate as small an area as possible. Compared to trains of stimulation, single pulses produce responses in fewer muscles when applied to a neural region, thought to be the result of trains acting via polysynaptic pathways (Herbert *et al.*, 2010). On the other hand, single pulses of stimulation are thought to activate cells directly and indirectly, with comparable numbers of muscles activated to those responding to the spontaneously-occurring action potentials of individual cells (studied in spike-triggered averaging or spikeTA, Cheney and Fetz, 1985).

Previous work has sought to find the motor output of the reticular formation using stimulus-triggered averaging, (Davidson and Buford, 2006). However although this study recorded EMG from bilateral arms, the number of muscles implanted was limited to twelve in each arm, and did not include any intrinsic hand muscles, which will be studied here. Additionally, no focus was given to the level of fractionation of the motor output of the RF, and how this compares to other movement pathways.

Stimulus-triggered average studies have also been carried out on M1 in macaques, though these have either been confined to CM cells or no distinction made between old and new M1 (Park *et al.*, 2004). Again, these experiments did not investigate the level of fractionation of M1 output, or any underlying synergies other than co-activations.

Therefore the current experiment aimed to investigate the output divergence, level of fractionation and synergies underlying the RF and both 'old' and 'new' subdivisions of M1. As in other Chapters, PCA was carried out on the EMG responses to stimulation of these areas to find the level of fractionation, judged by the pattern of variance explained by each synergy or 'component'. The synergies comprising each component were also examined and compared between brain regions.

4.3 Methods

Two purpose-bred female macaques (*Macaca mulatta*, Uw and Sa, weight ca. 5.5kg each) were used in this experiment. All procedures adhered to the UK Animals (Scientific Procedures) Act (ASPA, 1986, amended 2012), and at all times efforts were made to follow the recommended '3Rs' of reduction in number of animals used, replacement of animals where possible, and refinement of techniques. The experiment had the approval of the Animal Welfare and Ethical Review Board of Newcastle University.

4.3.1 Surgery

Surgery was required to implant a headpiece and EMG wires in each animal. Macaque Sa was implanted first, followed by macaque Uw when chronic recordings were completed in macaque Sa.

Headpiece implant As this experiment required making electrode penetrations into the brain, preventing head movement was paramount. This was done by implanting a headpiece (Figure 4.1) onto each animal (Lemon, 1984), which could be fixed to the recording rig thus enabling stable recordings (Figure 4.2). To make electrode penetrations, craniotomies (the removal of small sections of skull) were also required; the removal of skin involved in implanting a headpiece provides access to the skull to make these craniotomies. A headpiece also provides a base onto which EMG connectors can be affixed. Structural magnetic resonance images (MRI) were used as a guide to custom-make TekaPeek headpieces to fit the skull of each monkey.

Headpieces were implanted in a sterile theatre under general anaesthesia, after sedation with ketamine (10mg/kg). The animals were then prepared for monitoring and maintenance during the course of the surgery, which included temperature monitoring using a rectal thermometer; heat was maintained using a heat blanket placed underneath the body as well as an over-body warm air blanket (Bair Hugger, 3M, St. Paul, MN, USA) heated to 38°C. Pulse rate and 0_2 saturation were measured by pulse oximetry, a capnograph was used to measure end-tidal CO_2, and blood pressure was monitored using a sphygmomanometer. Intubation was performed to allow artificial ventilation, after an intramuscular injection of metacam (0.3mg/kg).

Anaesthesia was then commenced with an intravenous bolus of propofol (8mg/kg) and maintained on sevo-flourane (1.8-2.5% mixed with 100% O_2), alongside an infusion of methylprednisolone (5.4mg/kg/hr) to minimise brain oedema. An infusion of alfentanil was also administered for pain relief (0.2-0.3µg/kg/min). Every two hours throughout surgery, an intravenous bolus of cefotaxime (50mg/kg) was given.

The animal was then placed into a stereotaxic frame, a midline skin incision made longitudinally down the length of the skull and the temporalis muscle trimmed on either side of the incision. Each headpiece has four slots into which screws fixed into the skull can fit, providing the method of securing the headpiece to the skull. The skull screws were fitted by drilling out four circular craniotomies in the skull, through which four discs were inserted. These were each pushed under the bone, away from the craniotomy and towards a smaller drilled hole. Small bolts were then screwed into the discs through the smaller drilled holes and tightened so their expanding flanges secured them into the skull (Lemon, 1984). Once these four screws were in place, the headpiece was manoeuvred into position over them, and further nuts tightened over the top. Stainless steel chambers for craniotomies (Figure 4.1B and C) were then fitted within the headpiece, and the surrounding area covered in acrylic for further strength. The skin surrounding the headpiece was then closed with sutures and the administration of alfentanil and methylprednisolone was stopped. A single dose of buprenorphine (20μg/kg) was given intravenously. Once the animal was breathing independently, the sevo-flourane was stopped and the monkey extubated. In the few days following surgery, monkeys received metacam (0.3mg/kg) and ceftiofur sodium (3mg/kg) as advised by resident Veterinary surgeons.

During later daily recordings, fixation of the head was enabled by the three bolts on the headpiece (Figure 4.1B1), over which a metal disc was fitted. This disc could then be slotted into a space in the recording rig and secured (Figure 4.2).

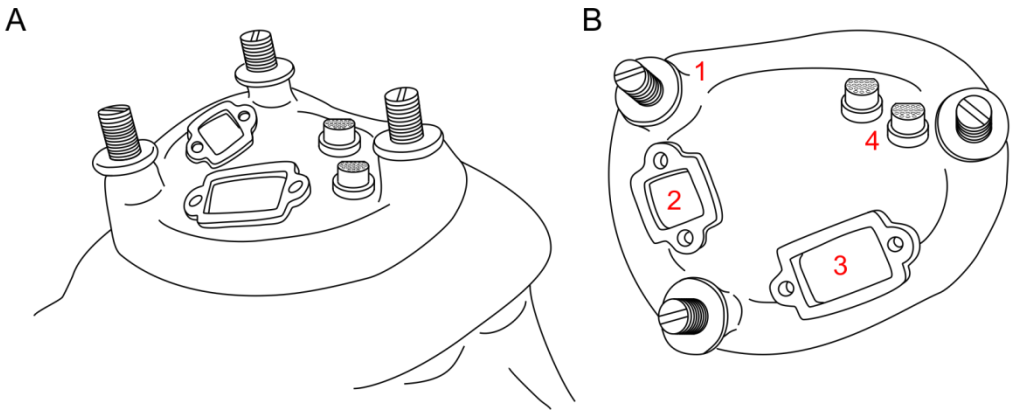

Figure 4.1: Headpiece viewed from the side (A) and from above (B). Includes bolts (1) used to secure the head to the recording rig; a posterior chamber for electrodes targeting reticular formation (2); a lateral chamber for electrodes targeting M1 (3, here located on the right side of the brain instead of the left as required in this experiment) and EMG connectors (4).

Craniotomies Two stainless steel frames or 'chambers' were implanted for the recordings carried out here; one located at the posterior of the headpiece to access the RF and the other on the lateral side of the headpiece, contralateral to the hand trained to carry out the task (right in monkey Uw), to access the left M1. Within these chambers in a separate surgery (ketamine anaesthesia, 10mg/kg delivered intramuscularly) a small area of bone was drilled out to allow electrode penetration in recording sessions. The craniotomies were cleaned during daily recording sessions and treated with 5-fluorouracil to minimise dura thickening (Spinks *et al.*, 2003). At all times when not in the recording chair, chambers were filled with gentamicin drops and sealed with a lid secured to the chamber by screws.

EMG implant In each monkey, pairs of EMG electrodes were implanted into muscles of the hand, arm, shoulder and back. Electrodes consisted of 150µm stainless-steel, Teflon-insulated wire (AISI316, Advent Research Materials, Oxford, UK) with a loop tied at one end followed by a bared stretch of wire hooked over. The other ends of the wires were soldered onto connectors. During surgery, incisions were made on the back, the biceps and triceps sides of the upper arm, the flexor and extensor sides of the forearm, at the wrist and at the three locations on the hand. Muscles were located using observation of surface stimulation effects and anatomical position. When a muscle was

identified, the bare hook of an electrode was fed into sterile 23 gauge needle which acted as an introducer, allowing the wire to be pushed into the muscle and anchored by the hook. Once the wire was anchored, the needle was removed. The loop of each wire was then sutured to the muscle to ensure the hooks could not be easily pulled out. Once all muscles were implanted, the lengths of the wires were tunnelled subcutaneously to the headpiece, where the attached connectors were secured using acrylic. All incisions were closed. Surgical preparation, monitoring and post-operative pain relief were similar to that used for headpiece implant.

In Sa, 21 EMGs were successfully implanted in muscles biceps long, biceps short, pectoralis major (PM), anterior deltoid, posterior deltoid, latissimus dorsi, coracobrachialis, brachioradialis (BR), flexor digitorum longus (FDL), flexor carpi ulnaris (FCU), abductor pollicis brevis (APB), brachialis, extensor digitorum communis (EDC), abductor digiti minimi (ADM), first dorsal interosseous (1DI), extensor digitorum 2,3 (ED2,3), extensor digitorum 4,5 (ED4,5), pronator teres, flexor digitorum profundus (FDP), flexor carpi radialis (FCR), palmaris longus (PL). Uw had EMG wires successfully implanted in 18 muscles, including latissimus dorsi, infraspinatus, anterior deltoid, posterior deltoid, biceps long, triceps, EDC, ECU, ECR (extensor carpi radialis), BR, 1DI, ADM, PM, flexor digitorum superficialis (FDS), FCU, FCR, FDP and APB (see Appendix A).

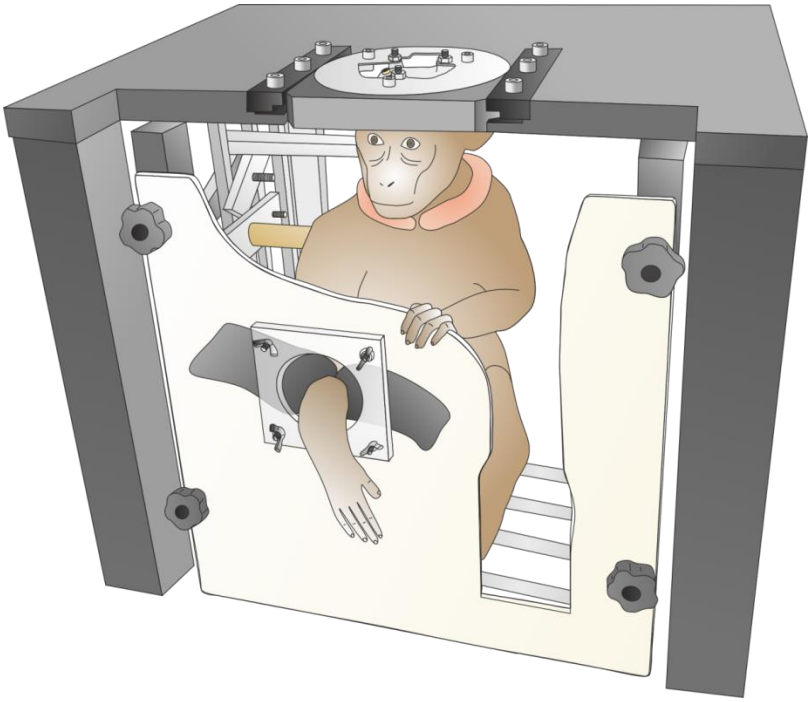

Figure 4.2: Monkey Sa set up in the recording rig, with head fixation as described in section 4.3.1.

4.3.2 Task

Both animals were trained over a period of >1 year to carry out a motor task (Figure 4.3). This involved using the instructed hand to pull the lever on a task box which would result in a door in the box opening, revealing a piece of fruit located in a food well, inserted by the experimenter (Riddle and Baker, 2010). The monkey would then perform a precision grasp to retrieve the piece of fruit from the food well. The monkey then removed her hand from the food well, a movement detected by infra-red beams located on either side of the food well which triggered the closure of the door; the task would then be repeated. This task was designed to elicit background activity in a range of muscles, as it involves use of the fingers, hand, arm and shoulder (EMG shown in Figure 4.4).

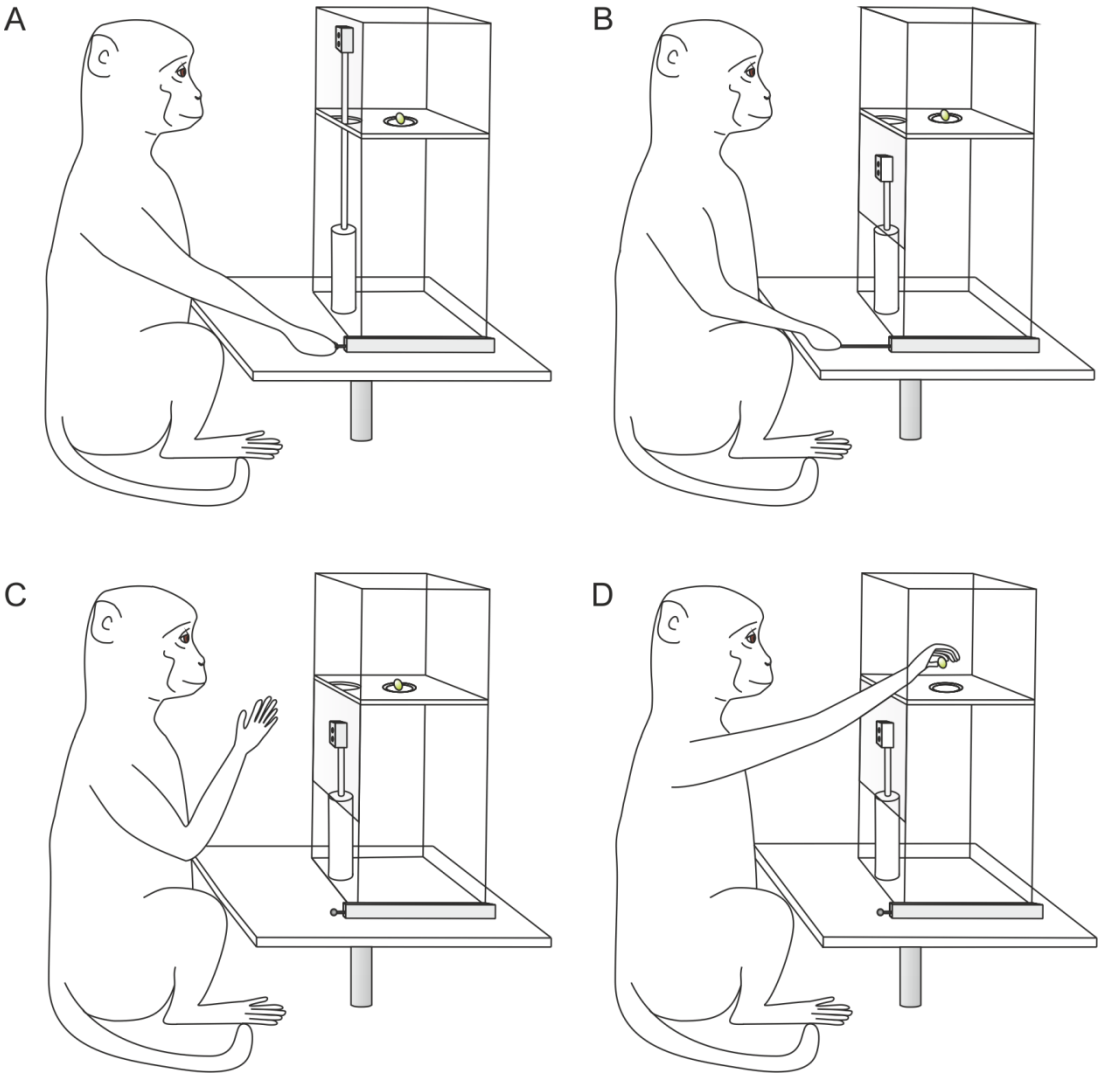

Figure 4.3: The behavioural 'reach and grasp' task. The monkeys were trained to pull a lever connected to the task box (A). This controlled the opening of a door (B) which revealed a food well with a piece of fruit placed inside by the experimenter (C). A precision grasp was then required to retrieve the piece of fruit (D), after which the door closed and the task was repeated.

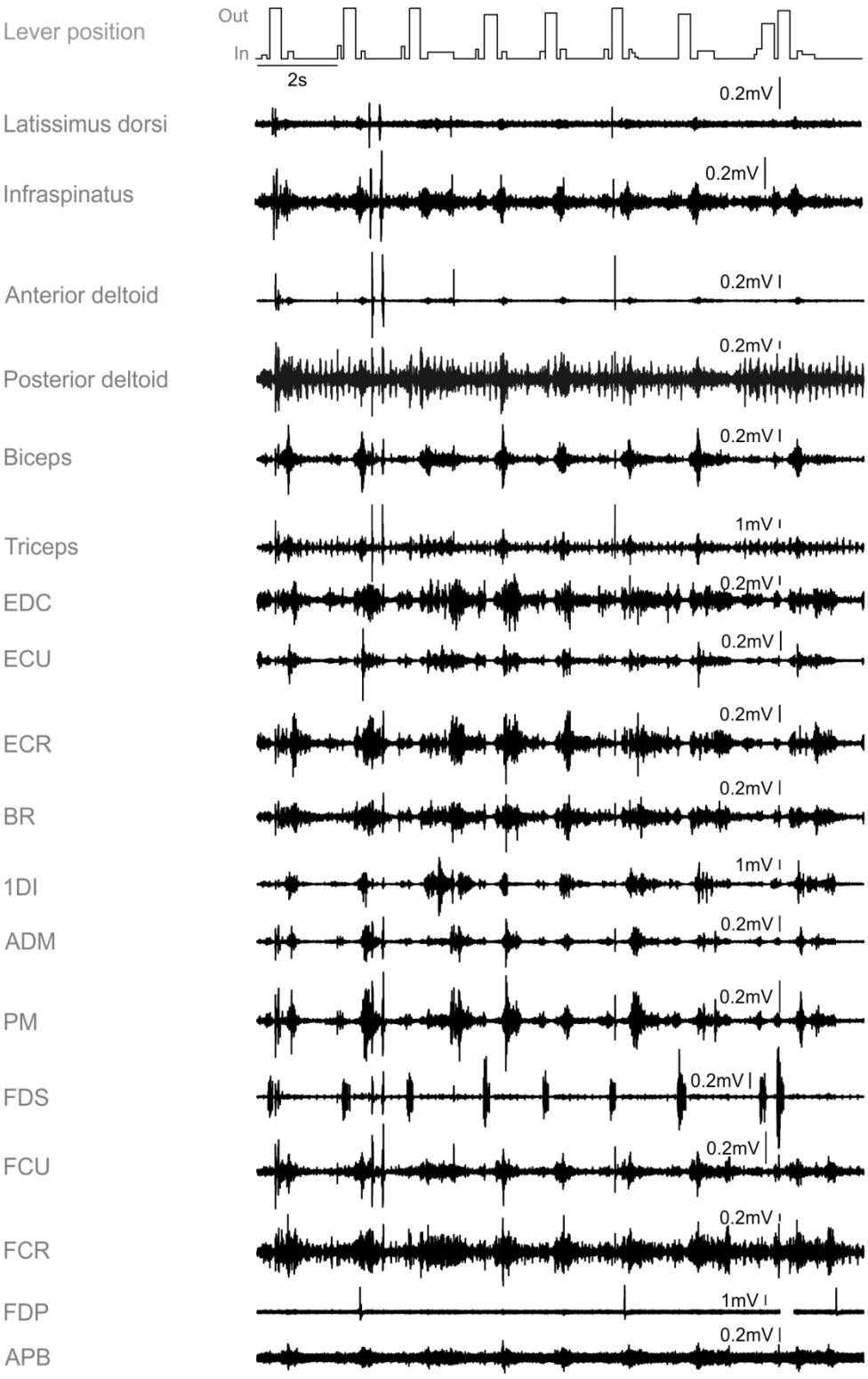

Figure 4.4: Example EMG traces of 18 muscles recorded from monkey Uw while carrying out the reach and grasp task shown in Figure 4.3. Top trace shows lever position.

4.3.3 Recording sessions

After a post-surgical recovery period of around one month, each macaque was taken into the lab for daily recording sessions. At the beginning of each recording session the animal was restrained using a collar which closed around the neck and was secured to the side of the training cage. The sides and lid of the training cage were then removed and it was lifted into a recording rig, then the animal was head-fixed as described earlier.

4.3.4 Reticular formation stimulation

In order to find the location of the RF in the monkeys used, stereotaxic coordinates of the RF (anterior-posterior, medial-lateral position and depth) relative to inter-aural line (IAL) were taken from an atlas of the macaque brain (Martin and Bowden, 1996). Location of the RF chamber (Figure 4.1B) relative to IAL on the monkey was calculated using the stereotaxic coordinates measured during headpiece surgery. It was then possible to calculate the required point of penetration within the chamber, as well as the depth needed to travel into the brain, in order to reach the RF. Once the area had been located, on each recording day an electrode was penetrated in a slightly different place within the RF; the location of daily penetration points relative to the chamber mark (in terms of anterior-posterior (AP), medio-lateral (ML) coordinates and height) were noted to ensure a thorough coverage of the target area. Single stainless-steel electrodes (300µm shaft diameter, 3µm tip diameter, 0.1MΩ impedance: MicroProbes, Gaithersburg, MA, USA), held in place with a manipulator (Stoelting, Wood Dale, IL, USA), were used for penetration and subsequent stimulation. Trains of intra-cortical microstimulation (ICMS) were applied through the electrode (13-18 biphasic pulses, 300Hz, 0.2ms per pulse) as it was penetrated and the resulting stimulation effects as the electrode travelled through different landmarks observed to judge its location. Confirming that the electrode had reached the RF was possible as it has characteristic stimulation responses affecting multiple muscles, often bilaterally located.

Once the target location had been reached, the threshold of the area to trains of ICMS was first defined; this was the lowest stimulation intensity which produced observable stimulation effects in terms of muscle twitches. This intensity was then used as a starting point in finding the threshold intensity of single-pulse stimulation. During single-pulse stimulation (9Hz) the animal carried out the 'reach and grasp' task to create background EMG activity. Task trials were carried out for 1-2mins during single-pulse stimulation for each stimulation intensity while EMG was recorded. The resulting EMG was analysed using a custom program (MatLab, Mathworks Inc., Natick, MA, USA) to find any significant muscle responses. In order to determine significant responses for any one site, the program compiled an average rectified trace for each muscle across stimuli within a window of 100ms before to 150ms after the stimulus pulse. The 100ms of EMG before the pulse was defined as the baseline period. The program then searched for any points of the average trace which exceeded three standard deviations of the baseline above or below the mean of the baseline, during the period 5-25ms after the stimulus pulse. If a response within these limits was found, the section of EMG falling between the first and last points of the response was taken following each stimulus pulse. A window of the same length was taken preceding each stimulus pulse, and the mean taken for each window. This was repeated for each muscle for a particular site. A paired *t*-test was carried out on the two sets of data, testing the null hypothesis that there was no significant difference between response and baseline for that muscle, with a significance level of $P<0.05$.

If a significant response was found for ≥1 muscles, the stimulus intensity was reduced, stimulation and trials repeated and the analysis rerun. This process was repeated until an intensity was reached at which no more responses were elicited. Stimulation threshold was then defined as the lowest intensity at which responses could be seen, when no responses were present at an intensity ≤5μA. When the threshold of a particular site was found, 50 trials at that intensity and the intensity below were recorded. If there were no significant responses at a site, the intensity was increased and the process repeated; if no significant responses were found for a maximum intensity of 200μA, a new site was found.

For the RF, the site along a particular track with the strongest visible responses to trains of ICMS was used; thus no two sites were on one track.

When recording of the EMG responses to a site was complete, the electrode was then withdrawn from the brain and a new location was targeted. Penetrations were repeated until an adequate coverage of the left side of the RF was achieved. As the left arm was implanted with EMGs, all responses seen where therefore ipsilateral.

4.3.5 Primary motor area stimulation

In order to pinpoint M1 on the left hemisphere, the stereotaxic location as provided in the macaque brain atlas (Martin and Bowden, 1996) as well as the individual animal's MRI were used as a guide of the location of the precentral gyrus. The area of the brain at these stereotaxic coordinates was then used as a starting point for electrode penetrations. Once M1 was located, the same stimulation protocol as used for the RF was carried out. However instead of a stainless steel microelectrode, here a five-channel Eckhorn drive loaded with glass-insulated tungsten microelectrodes was used (80μm diameter, Thomas Recording GmBH, Germany). In daily recording sessions, new penetration sites were based on the previous day's findings; if a yielding site with clear responses to the single-pulse ICMS were seen the day before, a site close to this one was chosen on the current day. However if an area proved to be lacking in responses, a larger jump in location was made next. Penetrations were made until an adequate coverage of the M1 was achieved; both the bank (new M1) and the crest (old M1) of the central sulcus were investigated, by choosing sites at both superficial and deep locations.

For M1, a few sites with different visible responses to trains of ICMS were found on the same penetration tracks. Therefore some sites were found at the same AP, ML location but at different depth. The distance between such sites ranged between ~400-1900μm.

For stimulation at each region, EMG signals (Figure 4.4) were amplified (gain 0.2-5k) according to response size on a capture screen and digitised at a 5kHz sampling rate, alongside stimulus and task markers using a custom-written EMG capture program. Signals were band-pass filtered at 30Hz-2kHz.

4.3.6 Histology

In order to identify the subdivisions (old vs. new) of M1 targeted by the electrode in this experiment, histology was carried out. This involved slicing the primary motor cortex of monkey Uw into 50µm sections before mounting them on slides. A Cresyl violet stain was then used on all slices to allow easier identification of white and grey matter.

In order to see where on the bank or sulcus the M1 sites were located, a representation of all penetrations was made and overlain onto the outline of motor cortex taken from a histological slice (Figure 4.5).

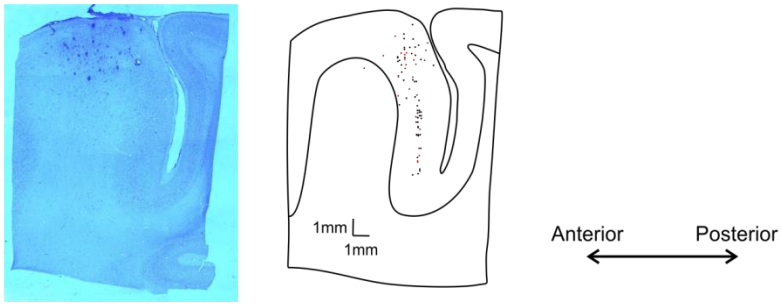

Figure 4.5: A representative slice from the centre of the penetration zone in M1 (left) and an outline of this slice with penetration points overlain (right).

4.3.7 Analysis

Once all required sites had been recorded, the analysis was similar to that carried out during the experiment itself by a custom-written MatLab program.

For each site, taking one muscle at a time, a window of EMG starting 40ms before and ending 60ms after each stimulus pulse was read in, then a mean trace created by averaging the windows taken across stimuli. The mean and standard deviation of the mean trace within the time period 40ms to 1ms

before the time of the pulse was calculated. The program then searched for any points of the mean trace which exceeded three standard deviations of the baseline above or below the mean of the baseline, during the period 5-50ms after the stimulus pulse. If a response within these limits was found, the section of EMG falling between the first and last points of the mean response was taken following each stimulus pulse. A window of the same length was taken preceding the stimulus pulse, and the mean taken for each window. This resulted in the mean of the response period and the mean of the baseline period for each stimulus. In order to test whether there were any significant differences between these groups in the form of a significant response to stimulation, a paired *t*-test was carried out between the two groups. If there were a difference significant at the level of $P<0.05$, the mean across the response means minus the mean across the baseline means was taken, resulting in one value for that muscle for that intensity at that site. This process was repeated for each muscle for each intensity and site within old M1, new M1 and RF respectively, resulting in a matrix of *muscles x sites* per region. If a muscle had no significant response for a particular site, it was represented by a zero in the matrix.

Normalisation Two different normalisation techniques were used for the PCA data recorded here; each was carried out individually for each muscle. The first was to Z-score normalise, which involves transforming each value in mV for that muscle into the number of standard deviations it is away from the mean, assuming the data is from a normal distribution in which the mean is zero and standard deviation is one:

$$Normalised(d_i) = \frac{d_i - \bar{d}}{\sqrt{\frac{1}{(n-1)}\sum_{i=1}^{n}(d_i - \bar{d})^2}} \quad (1)$$

Where d_i represents the ith data point (i.e. height of the muscle activation at that point) and n represents the length of the data.

The second normalisation method involved concatenating many EMG recordings of the macaques carrying out the task described in Figure 4.3 without stimulation and finding the 97th percentile value of the cumulative distribution for each muscle. Often the maximum (100%) value of voluntary contraction is used as a value by which to normalise, but in order to avoid normalising by any unexpected short-lived but high amplitude recording artefacts, the 97% maximal contraction (MC) value was used here instead. In order to normalise, every value in mV for each muscle was divided by its respective 97% contraction value. PCA was then carried out separately on the data normalised by these two methods. Independent component analysis (ICA) was also carried out on data normalised by 97% value. For both PCA and ICA the cumulative percentages of variance explained (PVE) for each component were calculated, plotted and compared. This provided a method of assessing the level of fractionation of the movement produced by each area.

ICA ICA extracts a set of components (C), each of which is a vector of coefficients for each muscle. This represents how much each muscle contributes to that component. It also extracts a matrix of coefficients, each representing how much each component contributes to each data value (M). So to find how much activity in a particular data value is accounted for by a particular component (CM), C is multiplied by M. However in order to result in CM, C and M could both be either negative or positive. In this experiment it was assumed that M is a matrix of positive values, meaning that the C reflects the actual amount each muscle was either suppressed or facilitated by this component. However if M is actually negative, then C should be inverted. This would flip whether each muscle is suppressed or facilitated in each component. Here, the components are plotted in Figures 4.12, 4.13 and 4.14. M was actually found to be a mixture of negative and positive values, therefore it is not known whether the polarity of the coefficients represented by each component truly reflects whether each muscle was suppressed or facilitated. Hence we can only conclude that these muscles were dominant in the components, but not whether they are facilitated or suppressed.

The stereotaxic coordinates of the sites ranged from ~21-35mm lateral and 1.7-15.6mm AP for M1, and 4.9-6.6mm lateral and ~4-17mm AP for the RF. However, most RF sites were in the left hemisphere, with a mean±standard deviation of 0.7±1.3mm left (lateral). RF sites were spread out more evenly across the AP extent explored, with mean±standard deviation of ~10±3mm.

4.4 Results

The number of sites found in each region and the average stimulation intensity used across these sites is shown in Table 4.1.

Table 4.1: Sites found and average intensity used in each region for each animal.

Region	No. of sites found at threshold stimulation intensity	Average threshold intensity (μA)	Species	Animal
RF	16	42	Macaque	Sa
Old M1	22	33	Macaque	Uw
New M1	25	30	Macaque	Uw

4.4.1 Output divergence

Reticular formation RF sites projected equally as often to one, three and four muscles, with slightly fewer sites projecting to two muscles, and fewer still to eight muscles (Figure 4.6). Every RF site activated flexors (Figure 4.7), particularly elbow flexors (Figure 4.8). No extensors were activated by RF stimulation. A few sites activated intrinsic hand muscles, though flexor muscles located in the forearm and upper arm were the most active. No shoulder muscles were recorded from the monkey used for this region, so no conclusions as to the output of the RF to shoulder muscles can be made.

Old M1 Almost 60% of sites located in old M1 activated one muscle, though up to five different muscles could be activated by this area (Figure 4.6). Both flexors and extensors were activated, though flexors more commonly, particularly those located in the forearm for finger movement, and those in the upper arm for elbow flexion. Stimulation of old M1 activated muscles located in

the forearm, upper arm and most commonly shoulder (the posterior deltoid, Figures 4.7 and 4.8). Only one site activated an intrinsic hand muscle, ADM.

New M1 New M1 also projected most commonly to one muscle, however less commonly than old M1, and also almost as frequently projected to two muscles. The highest number of muscles activated by any site in this area was six. New M1 was the only area to activate more extensors than flexors; it also most frequently activated forearm muscles. The only arm rotator recorded in this animal, latissimus dorsi, was also never activated. New M1 activated ECU most commonly and shoulder muscles the least. Intrinsic hand muscles were activated to a similar extent as the RF, with one fewer site activating the APB muscle; though as these were activated across more sites than in the RF, the overall proportion of sites activating intrinsic hand muscles is larger for new M1.

Some suppressive effects were observed at sites where facilitatory effects were elicited; when found, these were also significance tested and included for analysis.

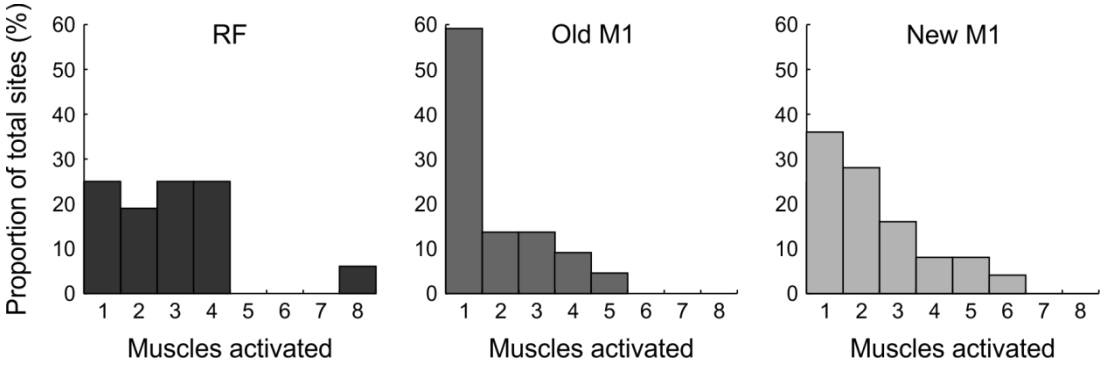

Figure 4.6: Output divergence of the RF and old and new M1.

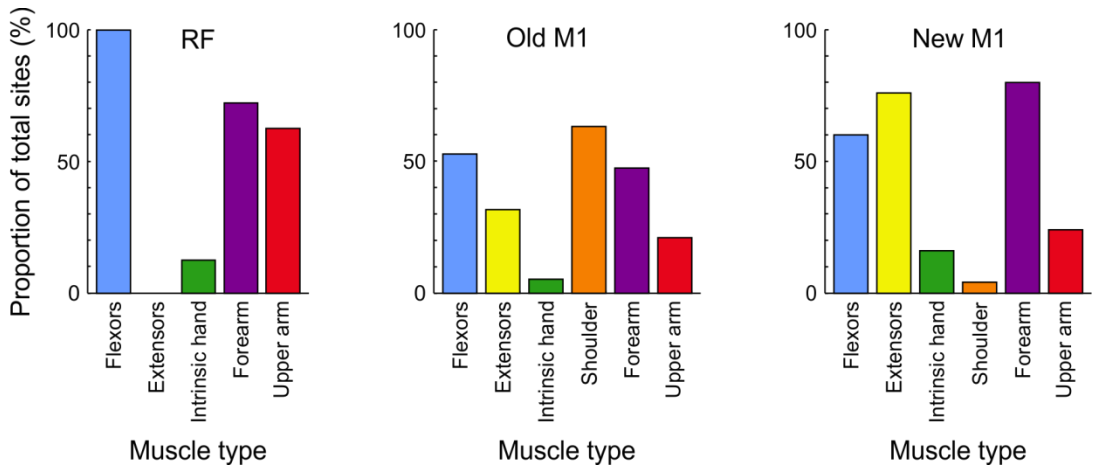

Figure 4.7: The percentage of sites which activated different types of muscle. Flexors and extensors include those in the forearm and upper arm.

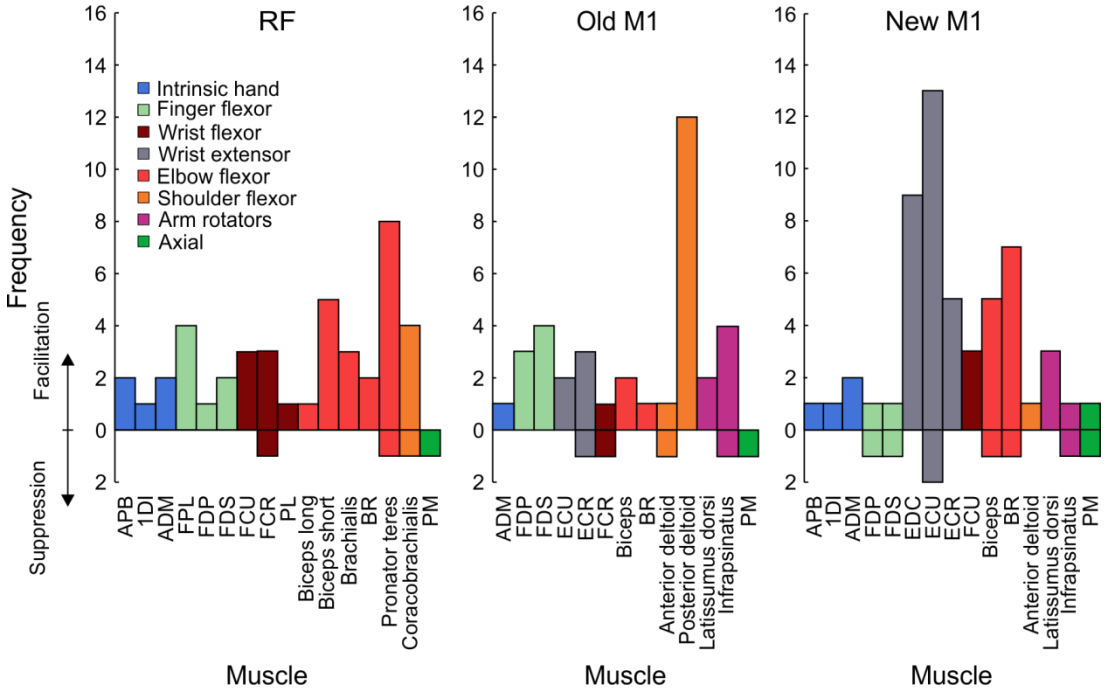

Figure 4.8: Frequency of activation and suppression of different muscles by the RF, old and new M1. Key to muscle type is located within RF histogram.

4.4.2 Muscle co-activations

Reticular formation Nearly half (44%) of sites projecting to forearm muscles also activated upper arm muscles (Figure 4.9, also see Figure 4.10 for examples of raw traces). Of all the muscles activated by the RF, three were intrinsic hand muscles (Figure 4.8). These were activated by two sites, which also activated muscles located in the forearm and upper arm.

Old M1 The highest level of co-activation was between the shoulder and forearm muscles, whereby of the 13 sites activating shoulder muscles, five also activated forearm muscles. Of the ten old M1 sites activating flexors, over half activated flexors alone and roughly a quarter co-activated extensors, leaving a few sites with extensor activation alone (Figure 4.9). There was a low level of co-activation between upper arm and shoulder, as well as between the upper arm and forearm muscles (raw traces shown in figure 4.10). Only one old M1 site activated an intrinsic hand muscle, and this was co-activated with both flexors and extensors of the forearm, but not any upper arm or shoulder muscles.

New M1 There was a generally low level of co-activation of muscles in response to new M1 stimulation. The highest degree (48%) was between flexor and extensor muscles (example raw trace seen in Figure 4.10). New M1 was the only area where a site activated an intrinsic hand muscle (ADM) alone, though the other three sites activating intrinsic hand muscles co-activated forearm muscles. Other than this, the only other co-activation seen was between forearm and upper arm muscles, and this was to a lesser degree than in old M1 and the RF.

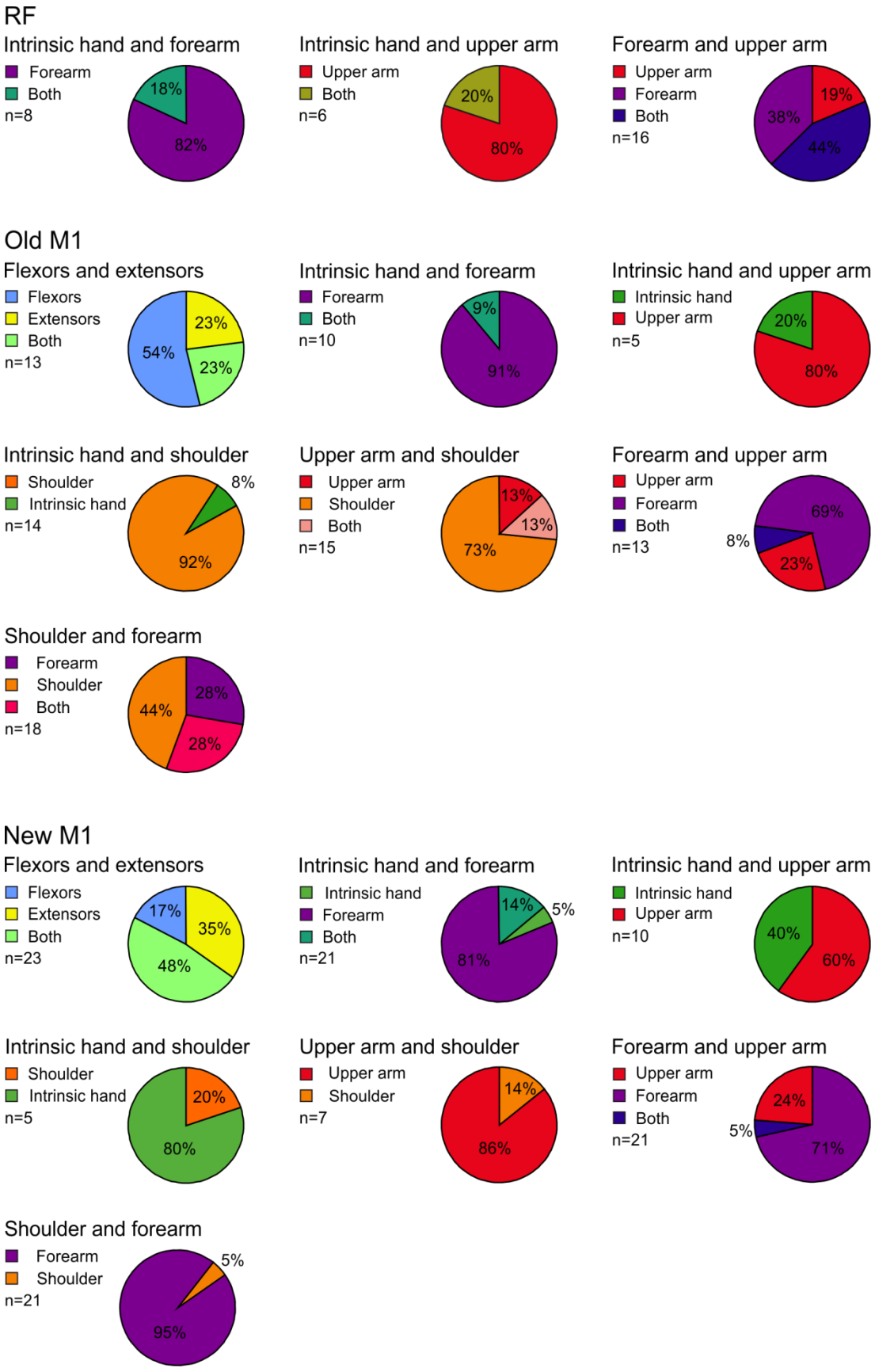

Figure 4.9: Pie charts showing the percentages of sites which activated different types of muscle alone or co-activated with another muscle type for each area. Representing muscles activated by sites stimulated at threshold intensity only. Each pie chart reflects

the percentage of each muscle type from the total number of both types examined per chart. N indicates the number of total sites included in each pie chart.

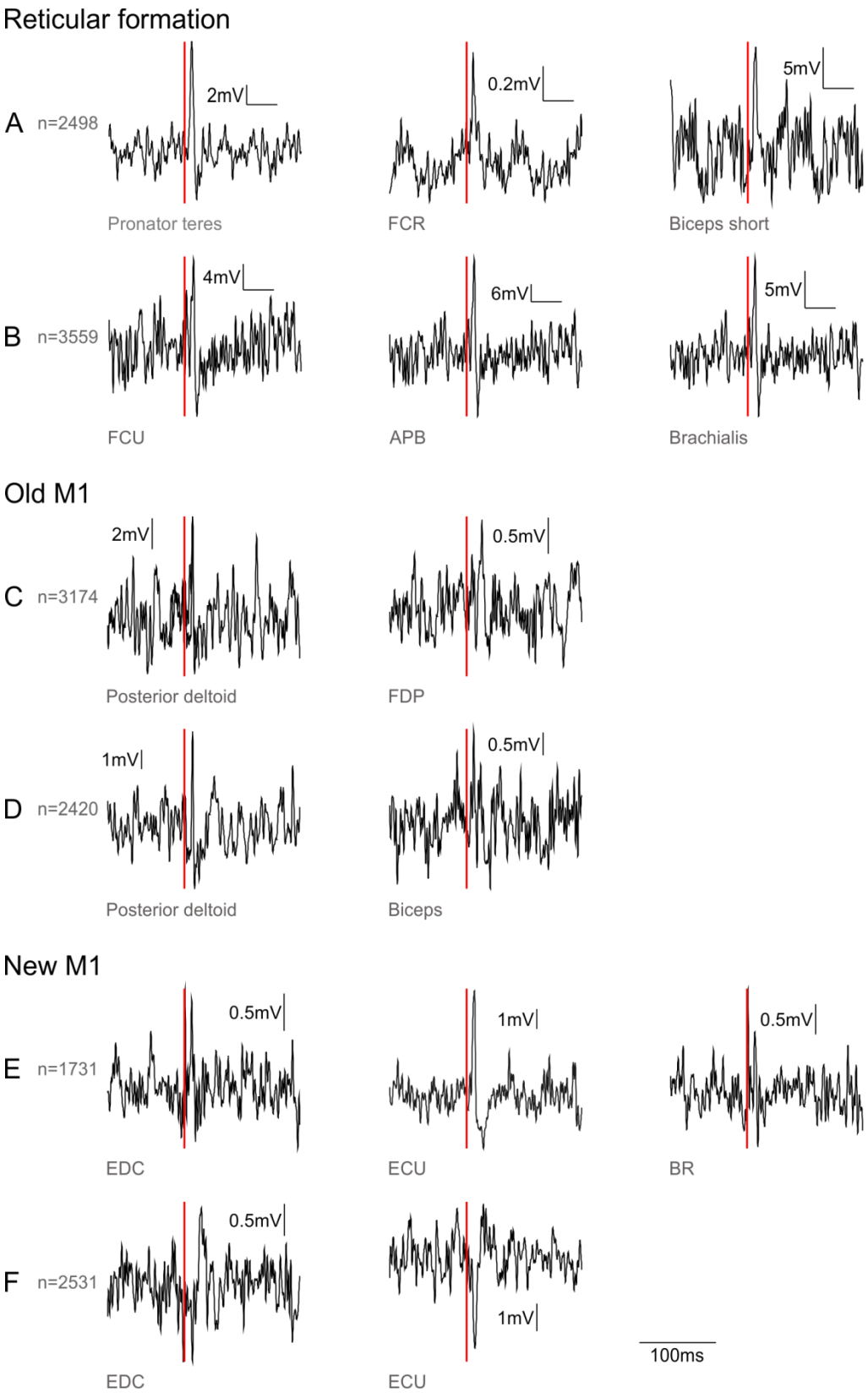

Figure 4.10: Example raw traces of stimulusTA responses for each region. Examples include co-activation of lower and upper arm muscles (RF), shoulder and forearm or

shoulder and upper arm (old M1) and finger and wrist extensors (new M1). Vertical scale for each trace indicated individually. Horizontal scale for each trace is the same, see scale bar in bottom right corner. All traces were low-pass filtered at 380Hz. Red bars indicate timing of stimulus pulse. Numbers of stimulus pulses averaged over for each trace indicated at the left of each example.

4.4.3 Fractionation

Two matrix decomposition algorithms, PCA and ICA, were used on the data recorded in this chapter. Additionally, as described in Section 4.3.6, two different normalisation techniques were used. The first was to Z-score normalise, the second to normalise each muscle by the 97th percentile value of its cumulative distribution plot of EMG recorded during task performance for each monkey. When normalising by Z-score, the first principal component (PC) for the RF, old M1 and new M1 explained 27.5%, 22.1% and 20.4% of the variance in the EMG respectively (Figure 4.11). It took the RF nine PCs, old M1 nine PCs and new M1 11 PCs to explain 95% of the variance when Z-score normalised.

When normalising by MVC, the first PC for RF, old M1 and new M1 explained 32.1%, 31.3% and 33.5% of the variance respectively. It took the RF eight PCs, old M1 eight PCs and new M1 11 PCs to explain 95% of the variance when normalised by 97% MVC.

The first independent component (IC, as extracted by ICA) explained 26.6%, 39.8% and 22.8% and of the variance respectively for the RF, old M1 and new M1. For the RF, 10 ICs were required to explain 95% of the variance; for old M1 10 ICs were required and for new M1 11 ICs were required.

Therefore there were not large differences between the PVE by the first PC for each stimulated site. However, across both versions of PCA as well as ICA it took new M1 more components than both the RF and old M1 to explain 95% of the variance, suggesting that new M1 is more fractionated than these other regions. In comparing the ICA plots in Figure 4.11C, the curve is much more gradual for new M1 than the RF or old M1, meaning that many ICs explain a more equal

percentage of the variance. This can also be seen from contrasting the percentages for each area in Figures 4.12, 4.13 and 4.14.

There is no consistent pattern across the three cumulative PVE plots in Figure 4.11 as to the order of fractionation of the three regions. However when looking at plots A and C, new M1 has the most fractionated pattern. The RF and old M1 might have a similar level of fractionation.

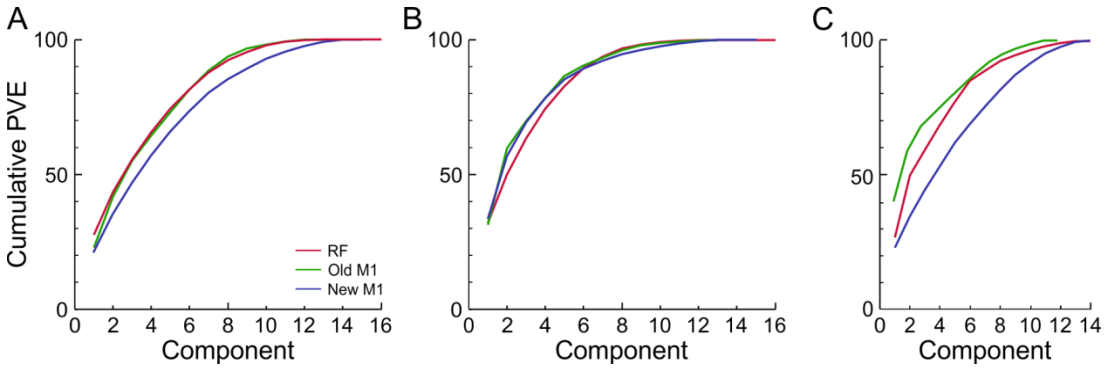

Figure 4.11: Cumulative PVE by each component extracted by PCA on Z-score normalised data (A); PCA on MVC normalised data (B), and ICA on MVC normalised data (C).

4.4.4. Synergies extracted by ICA

ICs can be thought of as synergies, each being composed of an activation coefficient for each muscle, which can be positive or negative, indicating activation or inhibition respectively. However, as discussed earlier, the sign of the coefficient for each muscle is not reliably represented by the components extracted, therefore no conclusions as to the mode of action (facilitation or suppression) of each muscle in each component plotted below can be made. The synergies described below are the first nine to ten ICs shown in Figures 4.12-4.14; only muscles which had a coefficient of >0.05 or <-0.05 were included, to clarify the key muscles within each synergy. This threshold was chosen as, when plotting each synergy, there seemed to be a clear number of muscles with activation above or below these values. Many muscles excluded in this way had a very small coefficient, indicating a very low contribution to the synergy.

Reticular formation Two main synergies explained a total of ~50% of the variance in the EMG responses evoked by RF stimulation. Thereafter, four more synergies each explained an additional 8-9.6% of the variance. Most synergies were composed of a mixture of muscles acting on different joints, commonly including intrinsic hand, wrist flexors, extrinsic finger flexors, elbow flexors and axial muscles. Several muscles of the same type were often included, such as wrist and shoulder flexors. Often two or three intrinsic hand muscles were involved in RF synergies (Figure 4.12).

Old M1 Two key synergies also dominated the responses from old M1, together explaining 58.8% of the variance. The first synergy had strong involvement of ECU, infraspinatus and FDS, and lesser involvement of ADM, FDP, ECR, biceps and PM muscles. The second synergy had predominant involvement of ADM, FCR, ECR and latissimus dorsi, and lesser involvement of FDP, BR, posterior deltoid and infraspinatus (Figure 4.13).

New M1 14 synergies or ICs were extracted from the new M1 responses. Of these, one key synergy explained 22.8% of the variance, after which the remaining 13 components explained incrementally less of the variance. Of the ten components plotted below, every new M1 synergy involved intrinsic hand muscles, with 4/10 containing three intrinsic hand muscles, 5/10 involving two and one involving one intrinsic hand muscle. The top three synergies explaining most of the variance also contained fewer muscles than those of the RF and old M1. Indeed, the first synergy was composed of only three muscles, two intrinsic hand muscles and a wrist extensor (Figure 4.14).

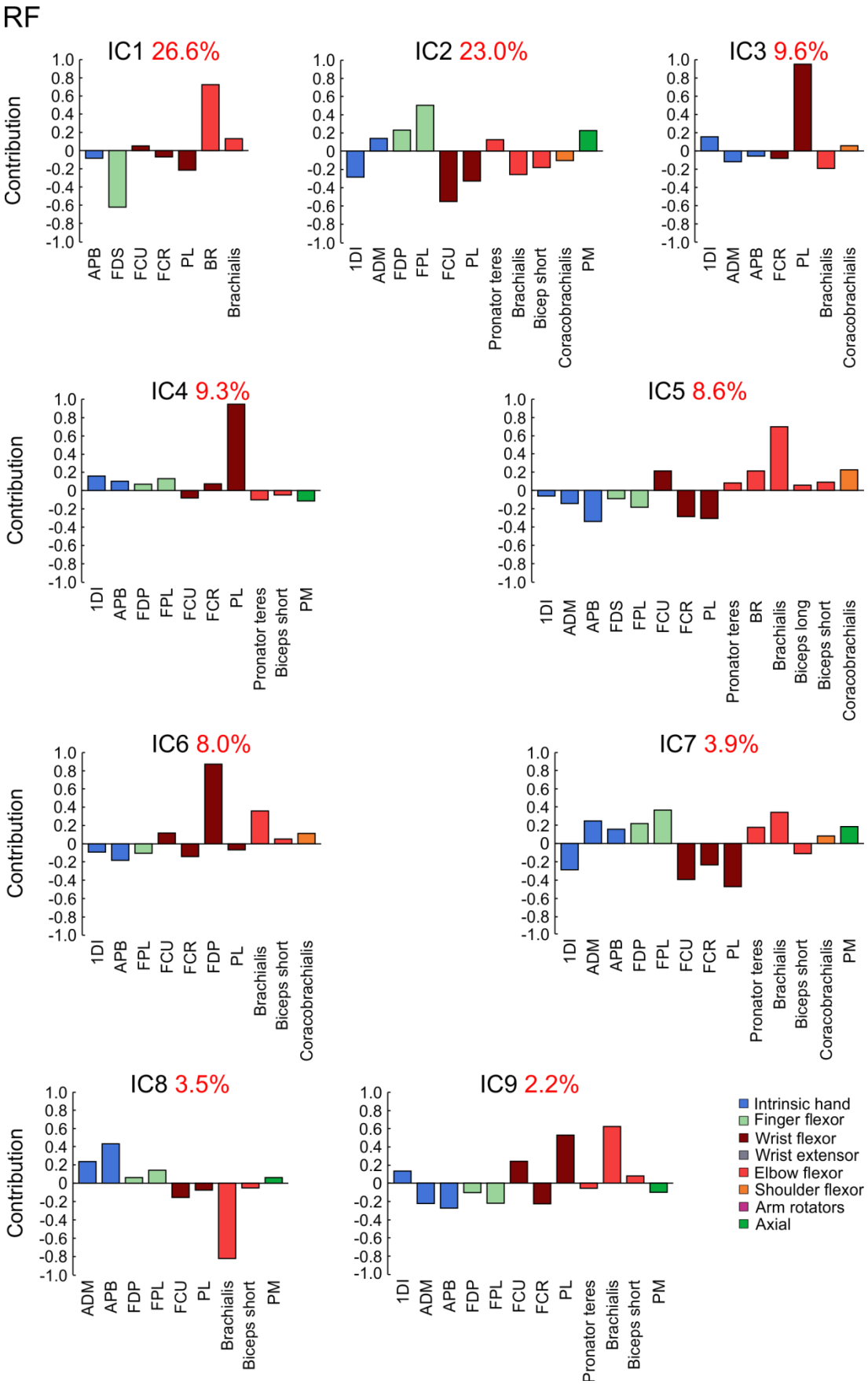

Figure 4.12: First nine ICs of the RF data. Key is in the bottom right corner. Red percentages represent the PVE by each component.

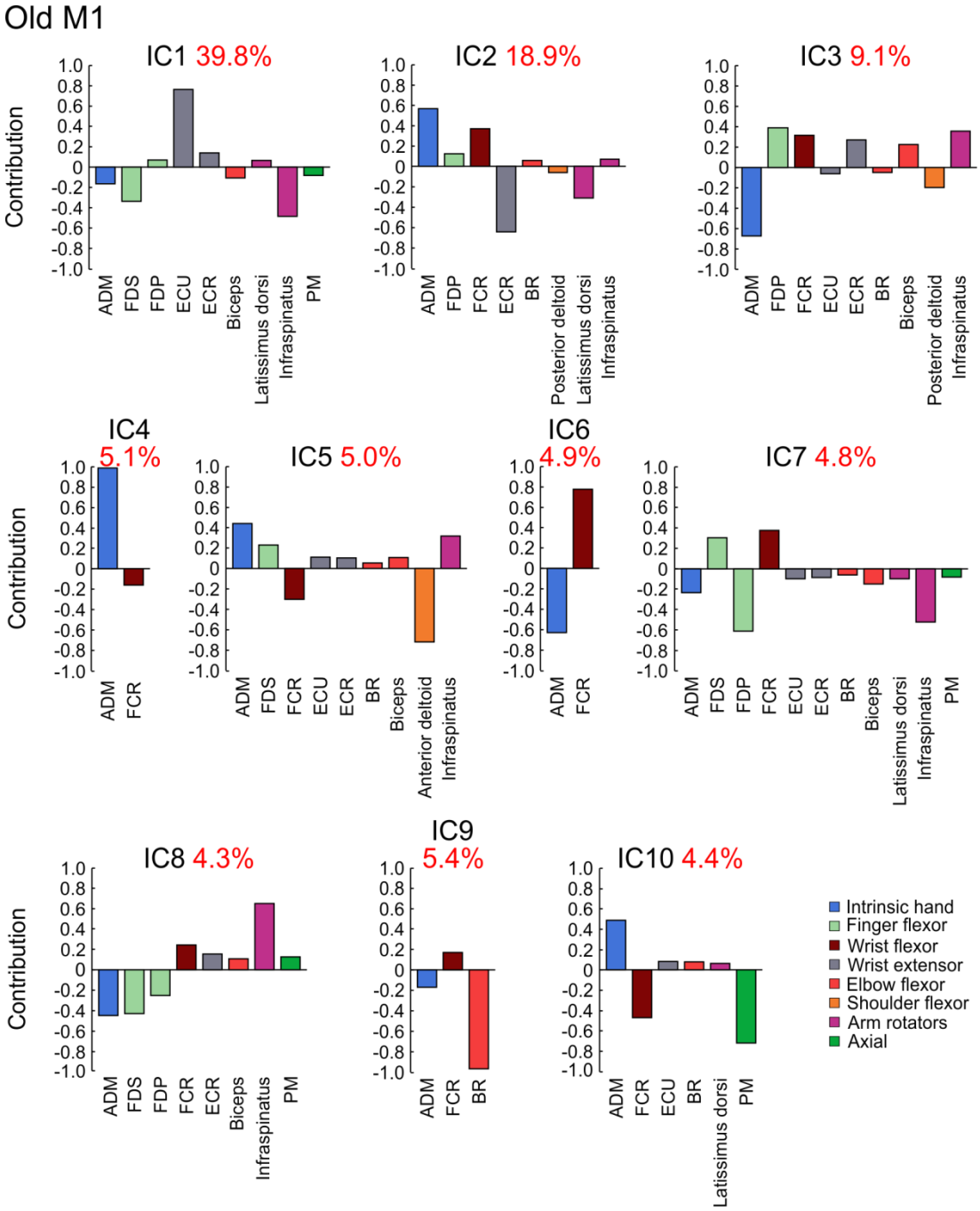

Figure 4.13: First ten ICs of the old M1 data. Key is in the bottom right corner. Red percentages represent the PVE by each component.

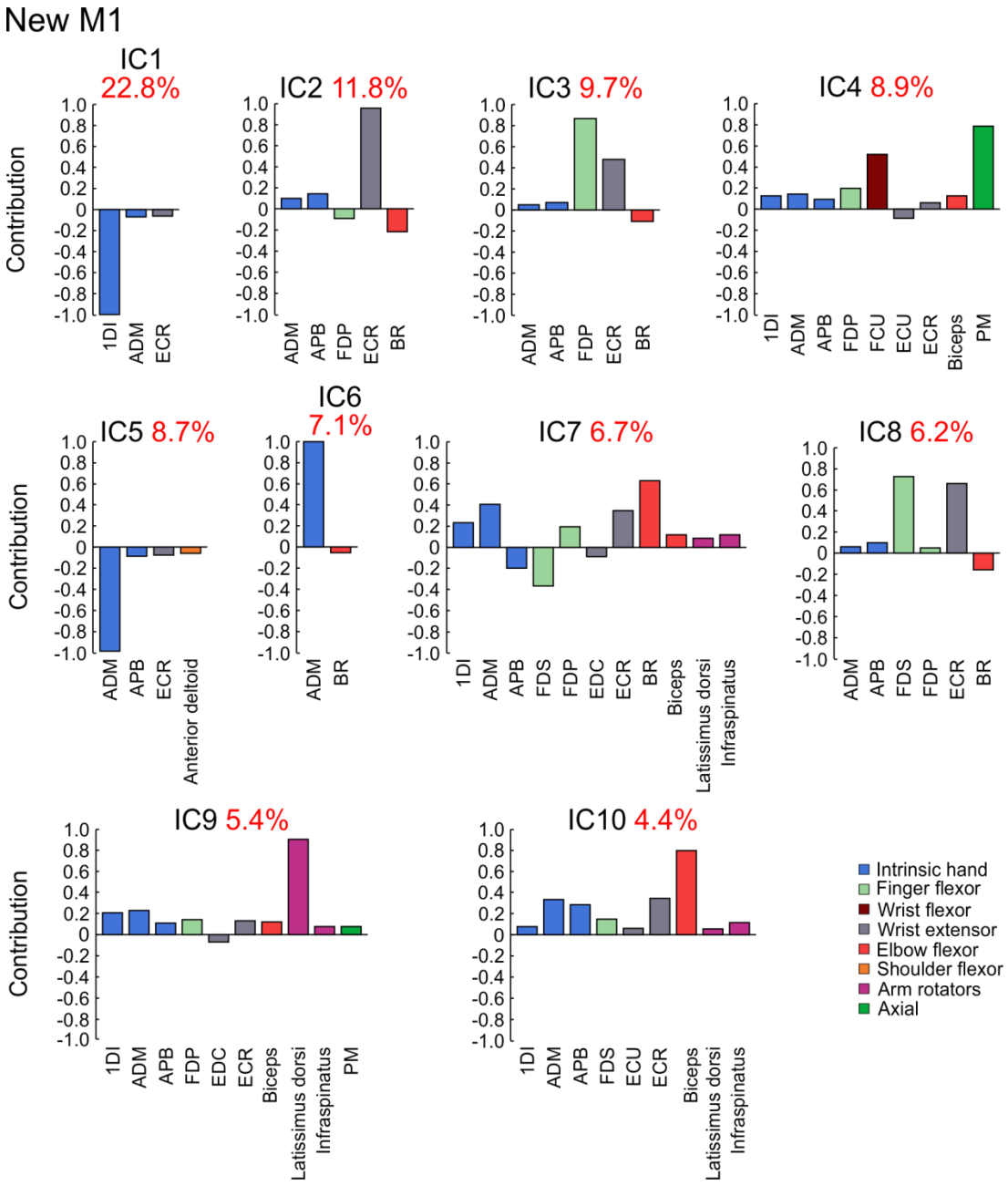

Figure 4.14: First ten ICs of the new M1 data. Key is in the bottom right corner. Red percentages represent the PVE by each component.

4.5 Discussion

4.5.1 Output divergence

In trying to delineate the output of a focal (sub)cortical region with single pulse stimulation, using threshold stimulation might have the advantage of limiting current spread as much as possible. However it also has the inherent problem of being biased towards target cells such as motoneurons with a higher level of excitability. Hence, any motoneurons projected to by the target cells with a

higher activation threshold might not be activated, consequently leading to underestimations of the output divergence of the region of interest. Measuring the number of muscles activated by a region might also be limited by the number of muscles recorded from. In this experiment, 21 muscles were recorded from in response to M1 stimulation, and 18 in response to RF stimulation. Therefore at best we can conclude that the sites stimulated ultimately activate the muscles we show responses for, not excluding the possibility that a higher number might be activated in reality.

The threshold stimulation intensities used ranged from 2-200μA for the RF, with an average of 42μA±43μA (mean±standard deviation, see Table 4.1). For old M1, threshold intensities ranged from 10-50μA with an average of 33μA±12μA (mean±standard deviation, see Table 4.1). For new M1, threshold intensities ranged from 5-50μA with an average of 30μA±12μA (mean±standard deviation, see Table 4.1).

Reticular formation Tracer findings from the cat have shown single RST axons to project widely throughout the spinal cord (Matsuyama *et al.*, 1997), and although no such evidence has yet been provided for the macaque, a primate stimulusTA study has revealed bilateral effects (62% of sites) of the RST on upper limb muscles (Davidson and Buford, 2006). It might therefore be predicted that individual RST cells activate multiple muscles most commonly. Here a roughly equal number of sites were found to elicit responses in one, two, three and four different muscles, with 75% therefore projecting to >1 muscle.

Several previous studies have shown the RF to activate ipsilateral flexors, with suppression of ipsilateral extensors (e.g. Davidson and Buford, 2006). The results presented here provide strong support of this, with all stimulated RF sites activating ipsilateral flexors, and no sites activating extensors. Flexors activated included those located in the forearm for finger and wrist flexion, as well as those in the upper arm for elbow and shoulder flexion. As previous work has found extensor activation in response to stimulation of the contralateral side of the RF, the lack of extensor responses seen here may have been due to

the fact that all but three RF sites were located on the left side. As EMG responses from only the left arm were recorded, no contralateral effects could have been found here.

Additionally, some intrinsic hand muscles were activated by RF stimulation in the present experiment. It has recently been shown that RF cells project to motoneurons of intrinsic hand muscles (Riddle *et al.*, 2009), therefore the evidence here supports the recently held view that the RST does have some control of hand function. Although, it is not yet known to what extent the RF has a role in controlling fine finger movements, an area which future research will need to address. No shoulder muscles were recorded from in the macaque used for RF stimulation in this experiment, so no evidence for the shoulder adduction and elbow flexion synergy seen in motor stroke patients (Dewald *et al.*, 1995) can be found here.

Old M1 Due to the lack of previous research specifically into old M1, it is difficult to make predictions about its level of output divergence. However, as it has predominantly di- and polysynaptic connections to motoneurons (Rathelot and Strick, 2009), stimulation of old M1 might be expected to activate several muscles at once. However, as very few studies have investigated the properties of old M1 specifically, its level of branching and divergence of output is not known. Although, old M1 is a source of corticoreticular projections; therefore stimulation of old M1 might activate muscles via the RF. As the RF is thought to project divergently, stimulation of old M1 might be expected to activate several different muscles indirectly via its corticoreticular connections (Keizer and Kuypers, 1989). One previous study carried out stimulusTA throughout M1, though they made no distinctions between the subdivisions in their analysis. They found that any one site activated at most 17/24 upper limb muscles (Park *et al.*, 2004). It was most common (71% of sites) to activate >2 muscles, with 15% of sites facilitating only one muscle. Sixty per cent of facilitatory effects were in distal muscles (Park *et al.*, 2004). In the current experiment it was most common by far for old M1 sites to activate only one muscle, though as fewer muscles were recorded from in the current study (18 for the monkey M1 was

stimulated in), their results might be a more accurate reflection of the data. However they did not use threshold stimulation intensities specific to each site, but instead a fixed intensity of 15μA. This might be too weak to activate some motoneurons, therefore underestimating the extent of projections to the associated muscles. On the other hand 15μA might be very strong for some motoneurons, and may therefore preferentially activate the muscles they project to. Overall, using a fixed intensity would result in different results from those elicited by threshold intensity here, again making comparisons difficult.

New M1 Due to its high proportion of monosynaptic corticomotoneuronal (CM) connections to motoneurons in the ventral horn, the caudal part of M1, termed 'new M1' has been suggested to subserve highly skilled movements involving few muscles (Rathelot and Strick, 2009). Because of this fine level of control, any sites within new M1 would perhaps be expected to activate a small number of muscles. However, given the wide branching of most monosynaptic CST axons to multiple motoneuron pools at one or more spinal level (Shinoda *et al.*, 1979), activation of at least two muscles per site would be expected. Indeed, in this experiment only 35% of sites activated only one muscle, with a maximum of six muscles activated by any one site. This is in agreement with a number of earlier spikeTA studies which found an average of two to five muscles activated by CM cells; estimates increasing slightly with the number of muscles recorded (Fetz and Cheney, 1980; Kasser and Cheney, 1985; Buys *et al.*, 1986). As the number of muscles activated by single pulse stimulation used in stimulusTA has been found to be similar to the number responding in spikeTA (Cheney and Fetz, 1985) these results could be considered comparable. However, a spikeTA study which recorded responses in a much larger number of muscles (22-24) in the arm and hand found that the majority of CM cells (71.4%) had a facilitatory effect in two muscles on average (McKiernan *et al.*, 1998). This could suggest that CM cells in new M1 most commonly project to two to three muscles, with cells occasionally activating one muscle or up to five to six.

The majority (72.2%) of responses elicited by CM cells have previously been shown to be located in the distal region of the arm (McKiernan *et al.*, 1998), with 44.7% of cells activating only distally located muscles. Furthermore, the magnitude of spikeTA responses increased from proximal to distal muscles, which was suggested to be due to CM cells having more frequent and stronger connections onto distal motoneurons (Fritz *et al.*, 1985). The majority of effects were located in the forearm and acted on the wrist and digits, which is congruent with the current results. Additionally, some of the forearm muscles most commonly activated in the study by McKiernan *et al.* (1998, e.g. EDC, ECR, ECU) were also some of the most frequently activated here. However, the second most common type of muscles activated following those located in the forearm was not the same between studies. The possibility of the results of both experiments being skewed towards forearm muscles must be acknowledged due to a higher proportion of forearm than other types of muscles being measured. This was accounted for by McKiernan *et al*., (1998) who normalised responses by dividing the number of effects found for a type of muscle by the number of types of that muscle recorded. The number of effects was then highest on average in forearm (wrist and digit) muscles, followed by intrinsic hand.

Facilitatory effects from CM cells have also been found to be stronger and more widespread in extensors than flexors in the forelimb (Fetz and Cheney, 1980). This was supported by later work by Cheney's group, which found patterns of extensor activation and reciprocal flexor inhibition from CM cells, as well as more common pure suppressive effects in flexor muscles (Cheney *et al.*, 1985; Kasser and Cheney, 1985). In agreement with this, here stimulation of new M1 activated most commonly forearm extensors, which was more frequently than in old M1. Suppression of flexor muscles by new M1 was also more commonly seen than suppression of extensors. Intrinsic hand muscles were activated by both new and old M1 sites, though more often in new M1.

Therefore overall, the region most commonly activating only one muscle was old M1, followed by new M1 then the RF. This is perhaps surprising given the

assumption that new M1 has a role in controlling fine, fractionated movements, involving few muscles, due to its CM connections. However, as discussed previously, it is difficult to say that this is an accurate reflection of the projection of these areas, due to limitations of the techniques used. Single pulse stimulation delivered at threshold was used in this experiment, which although is beneficial in activating the smallest neural region possible, would be biased towards ultimately activating the most excitable motoneurons. The activation threshold of some less excitable motoneurons might have been higher; therefore the level of output divergence of any of the regions explored might be underestimated.

Furthermore, when looking at the output of old or new M1 stimulation, the ability to say via which pathways and relays these muscles are activated is limited. Primary motor cortex projects to brainstem areas, including the RF, as well as to the spinal cord. Evidence has shown that projections from new M1 predominantly terminate directly onto motoneurons, whereas old M1 has corticoreticular projections (Keizer and Kuypers, 1989). In the spinal cord, connections from either area could be made with propriospinal or other types of interneurons; potential differences between projections from old and new M1 to segmental or propriospinal interneurons are not yet known. Therefore although we can conclude to some extent about the likelihood of termination, the muscles recorded here could have been activated by any of these pathways.

4.5.2 Co-activation patterns

RF A high degree of co-activation of the RST might be expected, due to its bilateral projections, which may be to multiple spinal segments in primates as in cats (Matsuyama *et al.*, 1997). The RF had a higher degree of co-activation than old and new M1 in three comparison co-activation pairs (intrinsic hand and forearm, intrinsic hand and upper arm, and forearm and upper arm), with the highest amount of co-activation between forearm and upper arm muscles. As all RF sites activated flexors and none activated extensors, the co-activation of these types of muscle and any agonist/antagonist relationships could not be examined, which would be potentially useful to compare to the

agonist/antagonist co-activations found in stroke subjects. Additionally, due to lack of recordings in shoulder muscles, no evidence for the RST control of the stroke-like elbow flexion, shoulder adduction synergy could be found.

New M1 Due to its known role in the ability of higher monkeys and apes to control individual fingers, new M1 might be expected to have a low level of co-activation. Although, given the suggestion that new M1 sites activate two to three muscles most commonly, co-activations are possible. However it would be expected that these are functionally synergistic groups of muscles, rather than diverse groups. In fact, a generally low level of co- activation was seen, with all co-activation being between contiguous joints (intrinsic hand and forearm, forearm and upper arm) which might be functionally co-activated during the reaching task used in the experiment.

Previous research has found infrequent co-facilitation of flexors and extensors (Kasser and Cheney, 1985; McKiernan *et al.*, 1998), in stark contrast to the present findings in which almost half of all new M1 sites co-activated flexors and extensors. However, here flexor and extensor co-activation patterns within individual joints were not examined due to lack of many pairs of flexors and extensors recorded. Therefore the co-activation seen was between, for example, digit extensors and elbow flexors. This particular synergy might be functionally relevant to behaviours such as lifting a piece of food to the mouth (using the elbow flexors) and releasing it (using the digit extensors). Similar movement synergies have been elicited in response to long trains of stimulation (200Hz, 500ms train duration) at particular sites of M1, regardless of initial hand position (Graziano *et al.*, 2002; Griffin *et al.*, 2014a; Griffin *et al.*, 2014b). This was suggested to be the result of the stimulation 'hijacking' neural circuitry and replacing the naturally occurring movements with those resulting from stimulus-driven activation (Griffin *et al.*, 2014a). The fact that these functional synergies were elicited from the same site lends support for the argument that functional 'clusters' of synergistic muscles are located in M1 (Cheney and Fetz, 1985). However due to the long trains used, the authors suggested the

likelihood of current spread to premotor areas as well as corticoreticular and corticorubrospinal connections (Griffin *et al.*, 2014a).

Old M1 Again, due to a lack of research into old M1 specifically, making predictions about its co-activation patterns is not easy, especially when predicting comparisons between co-activations produced by the RF and old M1. Though it might be expected that old M1 has more divergent outputs than new M1; in fact, this was generally the case. Old M1 also co-activated muscles at non-contiguous joints (forearm and shoulder muscles). This is in-keeping with previous work which has shown that M1 most commonly co-activates (42% of sites) proximal and distal muscles (Park *et al.*, 2004). However as mentioned previously, although thoroughly mapping the extent of M1, this study made no distinctions between the output of old and new M1 regions, making comparisons with the present work difficult.

There was an interesting gradient of the degree of co-activation of some muscle types (hand and forearm as well as forearm and upper arm) from the RF to old M1 to new M1. This might be explained by a gradient of fractionation from the RF as least fractionated to new M1 as most fractionated, if previous findings about the level of RF output divergence are applied to macaques, and the divergence of new M1 is assumed to be lower than that of old M1. However our ICA and PCA findings on the comparable levels of fractionation of each area do not fully support this.

4.5.3 Normalisation of EMG

EMG works to measure action potentials from motor units in the vicinity of the electrodes used. Consequently any signals might be affected by factors connected to electrode placement, such as the types and diameters of fibres in the vicinity. Attempts to diminish these factors are made by inserting the electrode into the belly of the muscle, therefore taking a representative signal. However with no reference value with which to compare the voltage of muscles, the unit is not of much value. Additionally, using the measured amplitude of muscles in mV would bias recordings towards larger muscles which are more

likely to have a larger magnitude signal than smaller muscles, even if the smaller muscles have more of a key role in the movement recorded. Therefore in order to be able to make fair comparisons between muscles, EMG data must be converted into a standardised scale which is relative to a repeatable unit (Halaki and Ginn, 2012). This is often done by normalising data to a proportion of MVC, though it is also possible to Z-score normalise. As it was not known which technique is best for use on data required for PCA, both normalisation techniques were implemented separately, and PCA carried out on both versions of the data.

Both normalisation techniques alter the variance and consequently the covariance matrix of the data, and as PCA is carried out on the covariance matrix, the output of PCA would be expected to be different. Z-score normalising might be argued as being less accurate as it rescales all muscles to a similar magnitude, therefore muscles that have very small activation and so might be mainly noise would be inflated to the amplitude of large muscles with key involvement in the recorded EMG. This would result in more muscles having a similar involvement in the movement, which would falsely increase the fractionation assessed by PCA. Conversely, normalising to a proportion of MVC retains the relative scaling between different muscles, and muscles which are not active very often during the recording get scaled down. Indeed, in the current experiment the PCA plots from Z-score normalised data were more fractionated than those from MVC-normalised data, which were more similar to the plots produced from ICA.

Therefore it is argued that normalising each muscle to the 97^{th} percentile value of its cumulative distribution plot is a more accurate way to normalise than by Z-score standardisation.

4.5.4 Fractionation

The fractionation of the three areas stimulated can be assessed by plotting the cumulative PVE by the components underlying the data, as extracted by PCA and ICA.

As would probably be expected, new M1 looks like the most fractionated pathway of the three studied here. For PCA normalised by both methods and ICA, new M1 required more components than both other areas to account for 95% of the variance. Additionally, the first IC for new M1 explains less of the variance than for old M1 and the RF, and each subsequent component explains gradually less of the variance than the former, without the larger jumps found for the other two regions.

The fractionation of old M1 and RF seems roughly similar; they have similar patterns of variance explained, and for PCA and ICA the same number of components were required to explain 95% of the variance for both areas. However If ICA is believed to extract components more accurately reflective of the data, as claimed by previous research (Tresch et al., 2006), it could be suggested that the RST is slightly more fractionated than old M1, as the first component extracted by ICA for the RF explains >10% less of the variance than the first component for old M1. Therefore although it has long been thought that the RF controls gross movements, here results suggest that the RST may be able to produce quite well-fractionated movement. As it is an evolutionarily earlier pathway present in older species unable to control their digits independently, the very high degree of fractionation of finger muscles possible in new M1 might not be expected from the RST. This might explain the difference in fractionation between the RF and new M1.

One previous study looking at fractionation of human movements identified three PCs which explained ~80% of the variance across seven muscles used in different grasps or to spell out different letters (Weiss and Flanders, 2004). These components might be a result of combined output from both old and new M1 and the RF, but might be expected to have a higher level of fractionation imposed by new M1. Here, three principal components explained 55.4% (Z-score normalised) or 63.5% (MVC normalised) of variance in the RF, 54.5% (Z-score normalised) or 69.7% (MVC normalised) of variance in old M1 and 46.0% (Z-score normalised) or 69.2% (MVC normalised) in new M1. However, in the

current experiment 18 muscles were recorded from for RF and 21 muscles for M1, which might have increased the variance of the EMG and therefore the number of components required to explain all of the variance.

Another study examining principal components extracted from human hand movements found that from eight muscles, four components were required to explain the majority of the variance (Klein Breteler *et al.*, 2007). This result might be in-keeping with that of Weiss and Flanders (Weiss and Flanders, 2004) but again with added variance contributed by an extra muscle. Therefore due to different numbers of muscles included in the present and these previous studies, comparisons are difficult to make.

However a macaque study which recorded from 15-19 forearm muscles found that three synergies could explain 81% of the variance in the EMG data (Overduin *et al.*, 2008) this is consistent with previous reports, though these components were extracted using non-negative matrix factorisation, an alternative technique to PCA, therefore again the results are not completely comparable.

4.6 Conclusions

This is the first experiment which has assessed the fractionation patterns and synergies of old M1, new M1 and the RF and compared these factors between these regions. It is also the first experiment to assess the co-activation patterns and level of output divergence of old M1 specifically.

In conclusion, firstly support was found for previous findings about particular characteristics of old/new M1 and the RF, including that the RF facilitated mainly ipsilateral flexor muscles, with no ipsilateral extensor activation. Additionally, new M1 was commonly found to activate forearm extensor muscles, lending support to findings from earlier work.

Novel findings included co-activation patterns of different types of muscles by all three areas stimulated. It could be suggested that old M1 more commonly co-

activates muscles than new M1, as three of the pairs of muscle type examined were co-activated more often in old M1 than in new M1. Additionally, all of the old M1 sites which activated intrinsic hand muscles coactivated forearm muscles, whereas some did not in new M1. This may suggest that new M1 has the ability to control individual fingers independently, perhaps due to its direct CM connections. However this needs to be clarified in future work.

It is possible that as responses to single-pulse threshold stimulation were examined here, the results were biased towards muscles with more excitable motoneurons, or motoneurons with monosynaptic connections from target regions.

Fractionation is suggested to be higher in new M1 than old M1 and the RF, which had roughly similar levels of fractionation, though it is suggested that the RF might produce slightly more fractionated movement than old M1.

5 Natural muscle synergies

In this brief chapter I will discuss how natural muscle activity was recorded from 18 muscles in one monkey across several days. As well as being the first experiment to record truly natural data from primates in their 'home' environment, this chapter examines the fractionation and synergies underlying everyday movement.

All data presented in this chapter was collected by me. Surgical techniques were carried out with the help of Stuart Baker.

5.1 Abstract

Introduction and aims: Limited data to date has been gathered on natural, everyday movements from a range of muscles. Recording these data would allow us to assess the level of fractionation and muscle synergies underlying natural movement. Therefore the aim of this chapter was to record electromyography (EMG) from one macaque monkey over several hours in its home environment, in order to explore these characteristics.

Methods: In between chronic recording sessions (the subject of Chapter 4), one macaque was fitted with a datalogging hat, containing an SD card, battery and circuit board incorporating amplifiers, A/D convertors and a microcontroller. This hat plugged into the monkey's existing EMG connectors and recorded natural muscle activity to the SD card. The hat was usually fitted at the end of chronic recording sessions, so that EMG activity from the rest of that day, night and the following morning were recorded, as well as at the weekend. The recorded activity for all sessions was concatenated and principal component analysis (PCA) and independent component analysis (ICA) carried out on the resulting data. The number of components required to explain the variance of this EMG was used as a measure of the level of fractionation in the recordings. ICA also enabled the extraction of muscle synergies.

Results and conclusions: Around ten components from both PCA and ICA were required to explain >95% of the variance in the EMG data, with the first

component explaining about 30%. However three to four key synergies explained ~80% of the variance. This was strikingly similar to the findings of previous research on naturalistic movement, perhaps indicating that it is an accurate reflection of the underlying control of movement. Synergies included a range of muscles, including intrinsic hand muscles and the one trunk muscle recorded.

5.2 Introduction and background

5.2.1 Recording natural movement

Very few previous studies have attempted to record natural muscle activity, and those which have were based in a laboratory rather than the subject's natural setting. Some studies have recorded muscle activity from leg muscles in frogs during swimming, jumping and walking in a laboratory in order to examine the muscle synergies involved in these movements (d'Avella and Bizzi, 2005). Other experiments have involved macaque subjects performing 'naturalistic' grasps of everyday objects or carrying out every day-type movements (Brochier *et al.*, 2004). One such experiment involved macaques grasping and lifting 13-25 different sized cubes, cylinders and spheres (Overduin *et al.*, 2008) with the aim of finding natural hand synergies. To date, this is the most naturalistic EMG data gathered from macaques. Most experiments on humans aiming to record natural EMG required subjects to carry out grasps of everyday items, or perform sign language (Weiss and Flanders, 2004; Klein Breteler *et al.*, 2007; Ajiboye and Weir, 2009).

However, one group managed to record much more naturalistic movement in humans going about their daily lives (Ingram *et al.*, 2008; Howard *et al.*, 2009). In these experiments, subjects wore arm joint sensors which measured the position of their arms and hands during everyday tasks such as having lunch, reading and cooking. Measurements of hand joint positions were also made using a fabric glove embedded with sensors (CyberGlove), fed to a laptop via cables secured to the arms, and carried in a backpack alongside a 12V battery, which subjects had to wear for the duration of recording time. However,

recordings in this study were restricted to two hours per session due to limitations of the power supply.

5.2.2 Natural muscle synergies

In an experiment mentioned earlier, Overduin *et al.* (2008) found that in naturalistic hand movements, three synergies which were well conserved across two animals accounted for 81% of the variance in the activity of 15-19 muscles, with extra synergies explaining very small incremental increases thereafter. The first of these synergies included proximal, wrist and extrinsic hand flexors, intrinsic thumb abductors as well as muscles of the little finger, and was related to reaching movements. The second was comprised of wrist and extrinsic hand muscles. The third synergy reflected the transport-related phase of movement and involved tonic proximal activation during wrist followed by extrinsic hand extensor activity and proximal muscle activity. Naturally-occurring synergies have been found to be flexibly combined across different types of movement (d'Avella and Bizzi, 2005). Another experiment aiming to extract the synergies from naturalistic hand movements (this time in humans) found that again, three components accounted for around 80% of the variance from seven muscles (Weiss and Flanders, 2004). Four components explained about 80% the variance from eight muscles in an experiment with similar methods (Klein Breteler *et al.*, 2007). Therefore although the number of muscles recorded by these three studies varied, they all extracted three to four key synergies which explained a very similar amount of variance; it is possible that this is a general feature of natural movements.

The experiment presented here sought to record EMG activity from 18 muscles in the hand, arm, shoulder and back of one macaque while she went about her usual behaviour in the home cage. As in previous Chapters, PCA was carried out on the recordings to give a measure of the level of fractionation in the movements. It was hypothesised that if the variance in the muscle activity of the recordings could be explained by only a few components, the movement would not be very fractionated and therefore controlled to a larger extent by less-fractionated motor pathways. However if many components were required to

explain most of the variance, then the movements would be more highly fractionated, perhaps with more control from the highly fractionated corticospinal tract (CST). In healthy macaques the CST has dominance in the control of movement over other pathways. As the CST is suggested as being the pathway enabling the ability to make fine movements using few muscles, such as those of the fingers, the movements were expected to be quite well fractionated and therefore expected to be explained by many components.

The natural data were found to be quite well fractionated, though three key synergies explained the majority of the variance.

As in previous Chapters, two methods of normalisation were used here before carrying out PCA. In this Chapter, the issue of how these normalisation techniques affect the data and therefore the level of fractionation extracted by PCA is explored in more depth.

5.3 Methods

One female rhesus macaque (*Macaca mulatta,* Uw, weight 5.5kg) was used in this experiment. All procedures adhered to the UK Animals (Scientific Procedures) Act (ASPA, 1986, amended 2012) and at all times efforts were made to follow the recommended '3Rs' of reduction in number of animals used, replacement of animals where possible, and refinement of techniques. The experiment had the approval of the Animal Welfare and Ethical Review Board of Newcastle University.

5.3.1 Surgery

For the experiment presented in this Chapter, it was necessary to surgically implant a headpiece and EMG wires as described in Chapter 4. The headpiece provided a stable structure upon which to secure the datalogging hat (described below). EMG wires were implanted in 18 muscles on the right arm, including first dorsal interosseous (1DI), adductor digiti minimi (ADM), abductor pollicis brevis (APB), anterior deltoid, biceps long , brachioradialis (BR), extensor carpi radialis (ECR), extensor carpi ulnaris (ECU), extensor digitorum communis

(EDC), flexor carpi radialis (FCR), flexor carpi ulnaris (FCU), flexor digitorum profundus (FDP) flexor digitorum superficialis (FDS), infraspinatus, latissimus dorsi, pectoralis major (PM), posterior deltoid and triceps.

5.3.2 Recording

A newly designed datalogging hat was developed and built by our laboratory engineers from acetyl (Figure 5.1). This consisted of a base, custom-made to fit the head bolts of the monkey, a compartment section to house the components, and a lid. The components comprised a printed circuit board which plugged into the EMG connectors on the monkey's headpiece in order to pre-amplify and record signals, as well as a 3.6V battery. Signals were recorded at 1024 samples/second/channel, 200x gain and stored on an SD card.

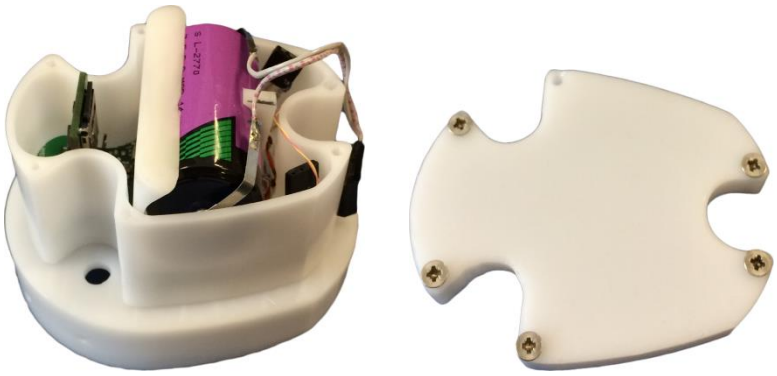

Figure 5.1: The base and compartment section of the datalogging hat (left) and lid (right).

The hat could be fixed onto the bolts of a headpiece in an awake animal in several steps (Figure 5.2); this process was complicated by the need for the monkey to be kept still while the connectors were plugged in, and the circuit switched on. In order to do this, firstly the base of the hat would be slotted over the headbolts, and secured with nuts. The monkey would then be head-fixed (method described in Chapter 4) over the base, allowing the compartment section of the hat to be screwed into position on the base. The connectors within this section would then be connected to the EMG sockets on the headpiece, the battery slotted into its cradle and connected to the chip. The lid of the hat would then be screwed on, allowing the monkey to be unhead-fixed and sent to her home cage. Recording sessions were repeated over several weekdays and weekends to collect the widest possible range of movement from

the animal. Due to technical difficulties in developing the datalogging hat, data could only be collected from one animal for this chapter.

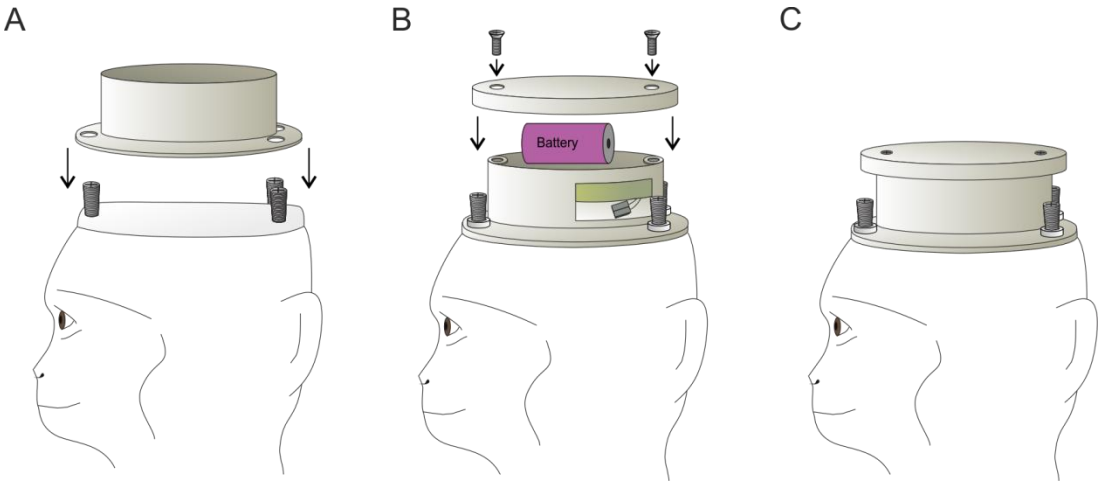

Figure 5.2: How the hat was fitted to the monkey's head. First the base of the hat was fitted over the head bolts (A), after which the monkey was head-fixed and the connectors and battery fitted (B). Finally the lid could be screwed into place, and the monkey unhead-fixed (C).

5.3.3 Analysis

EMG data were full-wave rectified, low-pass filtered (10Hz cut off) and then downsampled to 20Hz. For each recording session, only data recorded from daylight hours (07:30-19:30) were used. Any time periods during which no muscles were active were also removed. The threshold for this was determined by eye, whereby the complete trace for each muscle was overlain and inspected for time periods at which there was no muscle activity (Figure 5.3A). Then a y-axis point was manually chosen, below which all muscles were inactive (Figure 5.3B, indicated by arrow). A custom script then removed all time points at which all muscles were below this threshold, leaving the remaining data (Figure 5.3C). After removing night time data and time points at which all muscles were inactive, around 9hrs of EMG data were remaining and used for analysis.

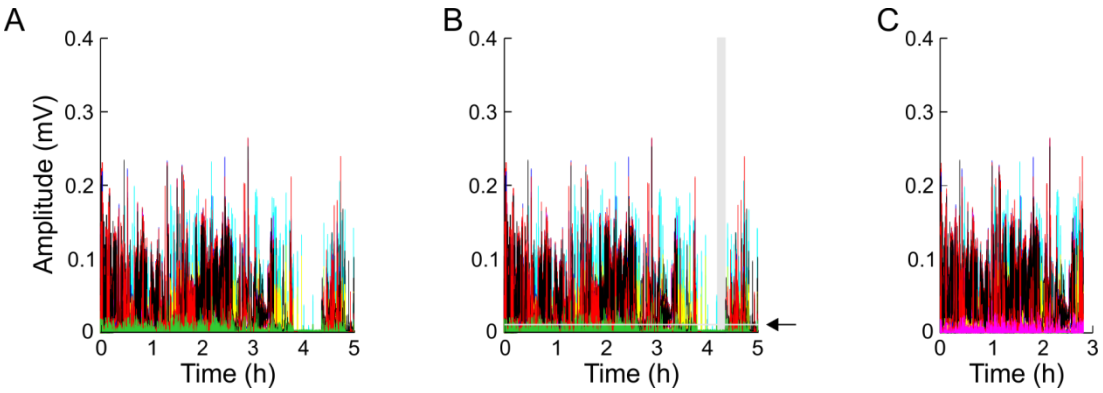

Figure 5.3: Natural data from one recording file, with each muscle overlain (A). The same data with the threshold line (indicated in grey and by arrow) and a grey box to represent a section of data in which all muscles were below threshold (B). The data with all inactive periods removed (C).

Following this all recording sessions were concatenated, then the raw EMG amplitude was normalised by one of two different methods (see below). PCA and ICA (described in detail in Chapter 4) were carried out on the resulting matrix of *muscles x time*. These matrix decomposition algorithms reduce the data into a number of underlying components, each of which explains a percentage of the total variance in the data (percentage of variance explained, PVE). The cumulative sum of the PVE by each component was then calculated and plotted, giving a visual representation of the pattern of fractionation of the data. As explained earlier, if a movement has a high degree of fractionation, many components are required to explain most of the variance.

Normalisation As in Chapter 4, two different types of normalisation of the EMG data were carried out separately before each resultant set of data was run through PCA. The first was Z-score normalisation of each muscle, and the second was normalisation of each muscle by the 97th percentile value of a cumulative distribution plot of all data for that muscle (Figure 5.4). This second form of normalisation can be considered similar to normalising by the maximum voluntary contraction (MVC) voltage, which is commonly done with EMG data. However, here the 97th percentile value of maximum was used, in order to avoid normalising by any large artefacts which may have occurred during recording. In order to perform this normalisation, the value for each time point was divided by its 97% MVC value. Z-score normalisation centres the

data for each muscle around a mean of zero with a standard deviation of 1, then converts each value in mV into a Z-score, which is the number of standard deviations each value is away from the mean:

$$Normalised(d_i) = \frac{d_i - \bar{d}}{\sqrt{\frac{1}{(n-1)}\sum_{i=1}^{n}(d_i - \bar{d})^2}} \quad (1)$$

Where d_i represents the i^{th} data point (i.e. normalised height of the muscle activation at that point) and n represents the length of the data.

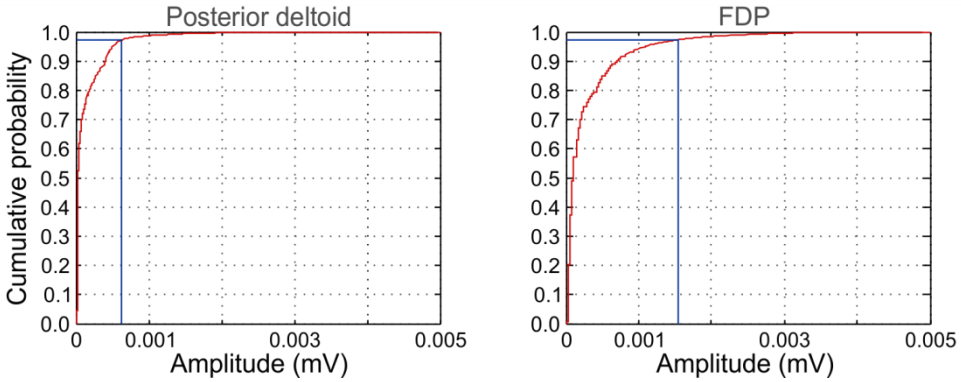

Figure 5.4: Cumulative probability density plots of activity of the posterior deltoid and FDP muscles. Blue lines represent how the 97th percentile value of MVC was read off for each muscle. Every data point for these muscles was then divided by this value in order to normalise.

Figure 5.5 shows how the amplitudes of two muscles are scaled relative to one another initially in mV after recording, then after normalisation by the two methods described above.

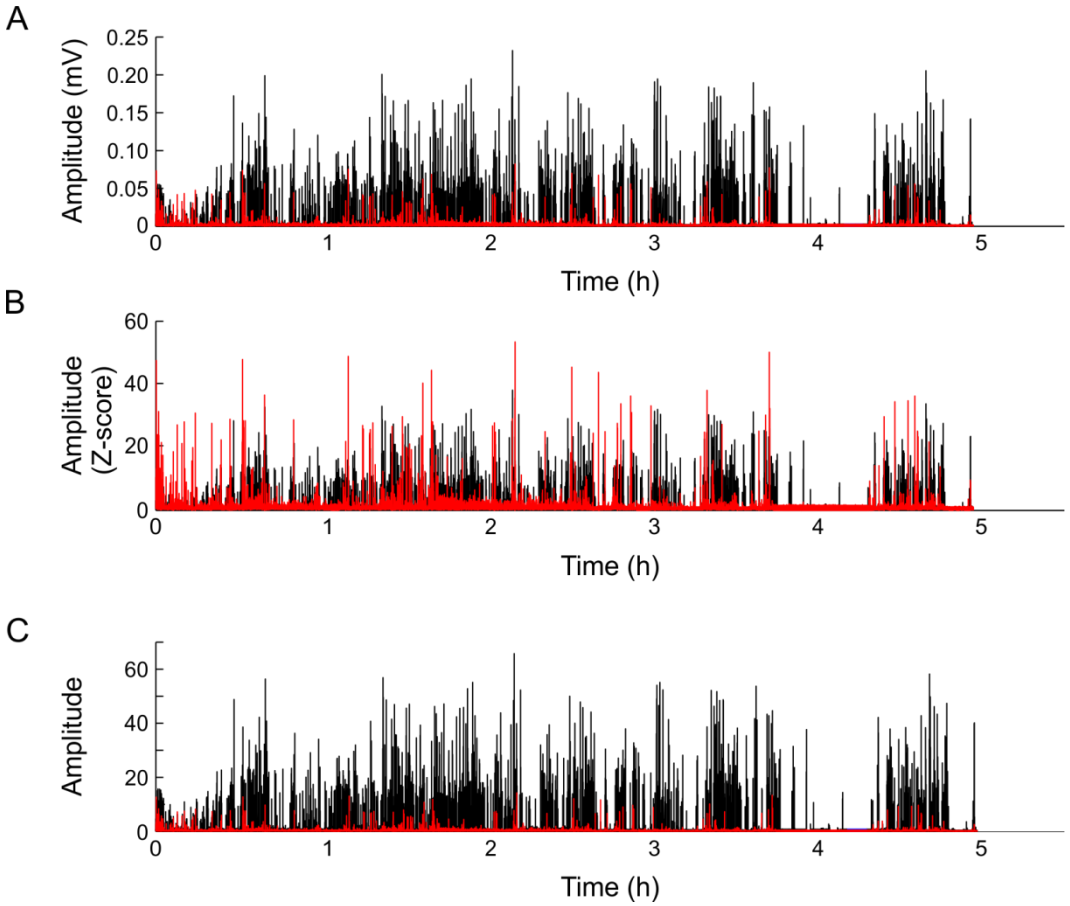

Figure 5.5: Raw data traces for two muscles overlain (infraspinatus in red and ADM in black). Data for both muscles before normalisation, in mV (A); data for both muscles, each Z-score normalised (B); and data for both muscles, each normalised to its 97th percentile value of MVC (C).

Figure 5.6 also shows how the different normalisation methods alter the proportion of the total variance of the data explained by each muscle. This was calculated by summing the variance for the dataset, then expressing the variance of each muscle as a percentage of the sum.

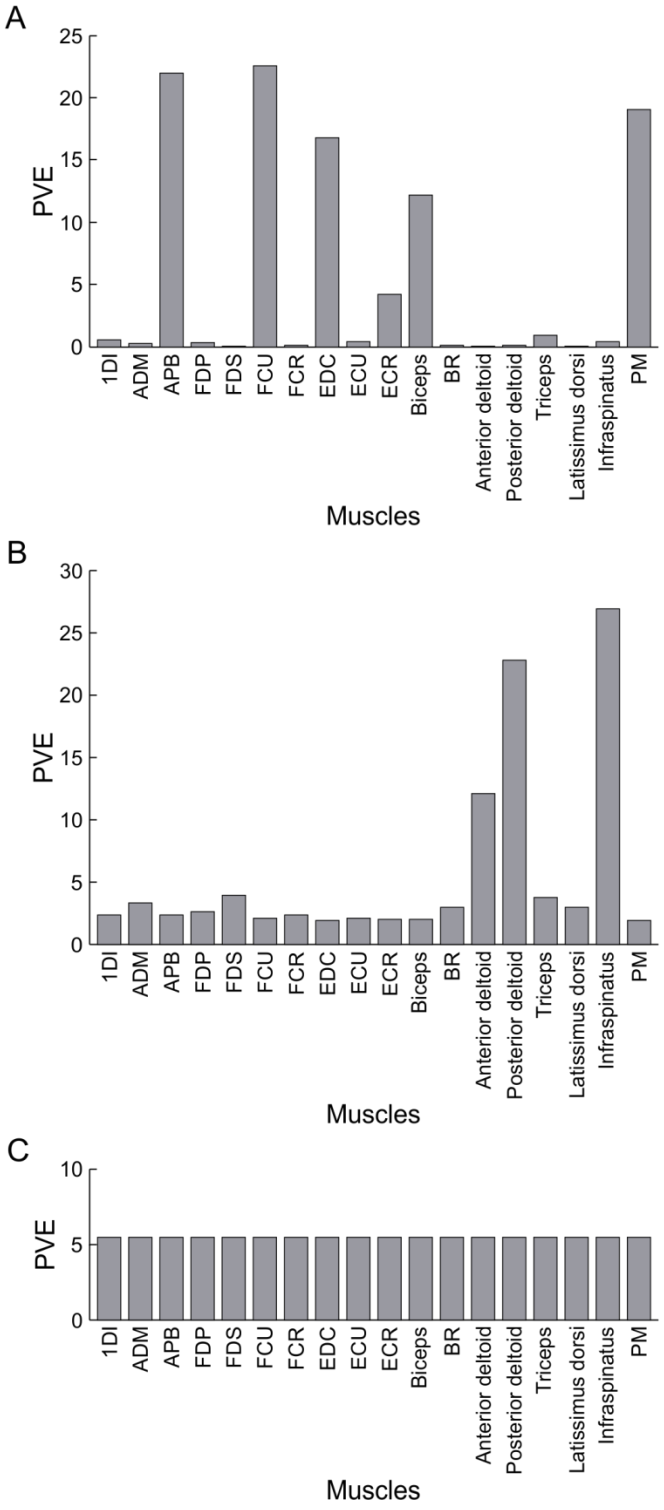

Figure 5.6: The PVE of the EMG data explained by each muscle before normalisation (A), after normalisation of each muscle to its 97th percentile of MVC value (B) and after Z-score normalisation of each muscle (C).

It is clear from Figure 5.6 that both normalisation techniques alter the variance of the data for each muscle, and in different ways. As PCA is carried out on the covariance matrix of the data for each muscle, changing the variance of the data

will affect the covariance matrix and therefore the components that PCA extracts. By its very nature, Z-score normalisation rescales the data of each muscle to have unit variance (Figure 5.6C); therefore PCA is more likely to extract a more fractionated pattern of PVE from Z-score normalised data.

Normalising by 97% MVC does not inflate the magnitude and variance of muscles which are rarely used, like Z-score normalising. However, normalising by MVC is not without problems either. Some muscles vary a lot in the amount of time spent at different contraction strengths, possibly including the shoulder muscles (as in Figure 5.6). For example, shoulder muscles might be activated to half their maximum when the animal is sitting and foraging, less than half their maximum when the animal is resting, and close to maximum when the animal is climbing. Normalising this type of muscle by MVC would retain the relative amount of time spent at different contraction strengths, resulting in that muscle having higher variance than a small muscle which spends most of the time at the same contraction strength or in narrower range of contraction strengths due to fewer motor units to recruit, such as an intrinsic hand muscle. This type of muscle might be more likely to contract at a smaller percentage of maximum for most of the time, as most grasps and hand movements do not require high degrees of contraction. Therefore although some smaller muscles might be important to the movement recorded, they might be outweighed by larger, possibly postural muscles.

Therefore any method of normalising and rescaling the magnitude of muscles might be problematic. Indeed, retaining any magnitude scaling affects the variance of the data, which will bias the PCA towards muscles with more variance. For instance, a postural muscle which is active for most of the time but to a similar degree would have low variance and therefore not contribute as much in PCA. This might result in PCA extracting components which do not accurately reflect the actual fractionation of the movements. One way of avoiding this problem might be to express the data simply as active or not. This would result in components which reflect which muscles contribute towards the movement recorded.

Binary transformation of data In order to remove all magnitude scaling, the EMG trace for each muscle was converted to a [0,1] binary format, whereby ones represented activation of the muscle at that time point, and zeros represented inactivation. Muscles were determined as being active at each time point by whether they exceeded a particular percentage of MVC. Six different percentages of MVC were used (2%, 5%, 10%, 20%, 50% and 75%). This meant that muscles which were rarely used were mostly replaced by zeros, and muscles which were used a lot mostly replaced by 1s. Unlike Z-score normalising, this has the benefit of reducing the variance of muscles which are rarely used. PCA and ICA were carried out on this binary-transformed data, in order to see whether fractionation is affected by focusing on different muscle contraction strengths. Like the non-binary transformed data used in PCA and ICA, any time points at which all muscles were zero (i.e. inactive) should be removed. Otherwise the first component extracted by PCA or ICA on this data would be due to the difference in active versus non-active data. There were no time points at which all muscles were inactive for all thresholds except 75%, therefore these points were removed, and PCA repeated.

5.4 Results

5.4.1 Raw recordings

Data were recorded over one weekend (Figure 5.7), plus two weekday sessions in the evening, resulting in a total of 30hrs recorded. Data from both the weekend and weekdays were included in order to capture the widest possible range of movement from the animal, which would differ to some extent between these periods. For example, during the week, the animal would be taken into the laboratory and required to perform a task for food rewards, after which it would return to its cage full. Therefore relieved of the need to forage, the animal might spend more time playing with the enrichment toys and swinging in the cage. Conversely, at the weekend the animal would probably spend a lot of the day foraging for food in the sawdust on the cage floor. In Figure 5.7, shaded areas represent daytime hours used for PCA and ICA. In the first night shown (a Friday night), the animal shows clear reductions in EMG

activity in some muscles, though the second night shows much more activity. It is possible that some factor prevented the animal from sleeping properly during that period.

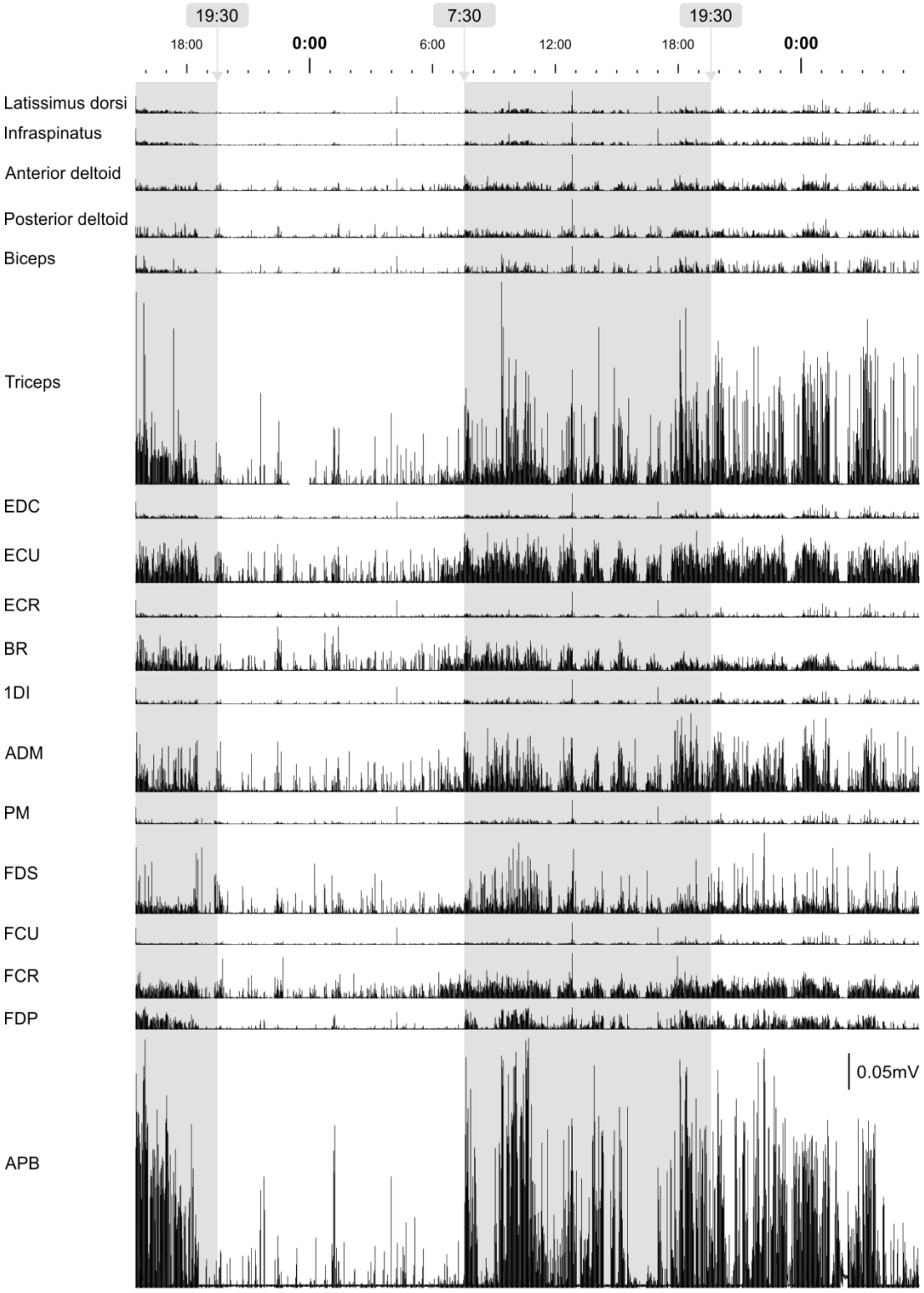

Figure 5.7: An example of one recording session of natural EMG from all 18 muscles implanted. Sections shaded in grey represent the daytime hours used for PCA and ICA.

5.4.2 Fractionation

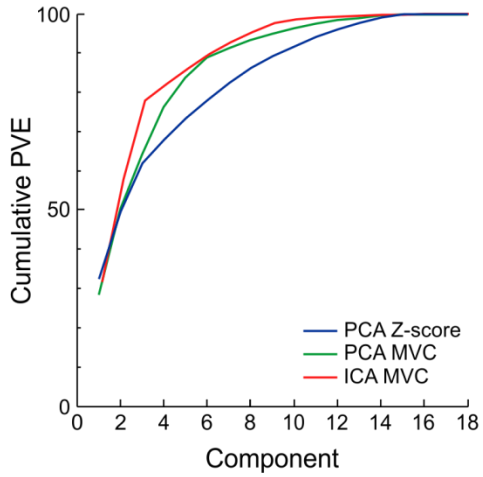

Figure 5.8: Cumulative PVE by each component calculated by PCA and ICA of all data. PCA was carried out on data either Z-score normalised (blue curve) or normalisated to the 97th percentile value of cumulative distribution plots for each muscle (green curve). ICA was also carried out on data normalised to the same 97th percentile values (red curve, key in bottom left hand corner).

PCA was carried out on data normalised by Z-score and by 97th percentile value of MVC (Figure 5.4) as discussed above. Independent component analysis (Figure 5.8) was then carried out on the data normalised to MVC.

The PVE by the first component from PCA normalised by both techniques looked quite similar, with the first component explaining 32.3% of the variance for Z-score normalised data and the first component explaining 28.3% of the variance for MVC normalised data (Figure 5.8). However overall, Z-score normalising produced a more fractionated pattern of variance explained than the other normalisation technique, with each component subsequent to component one explaining slightly less of the variance than in MVC normalisation. PCA on MVC normalised data required four to five components to explain 76-84% of the variance, whereas PCA on Z-score normalised data required six to seven components to explain 78-82%.

ICA produced a very similar pattern of cumulative PVE to the pattern produced by PCA carried out on data normalised in the same way (to 97% MVC). ICA required three to four components to explain 78-82% of the variance.

5.4.3 Fractionation at different contraction strengths

The data were then converted to a binary format, where the threshold for assigning a 0 or 1 was based on whether each value exceeded a particular percentage of MVC for each muscle. When the threshold was 2% MVC, the first component extracted by PCA explained 32.2% of the variance, and five to six components were required to explain ~80% of the variance (Figure 5.9). At such a low threshold, there was quite a large difference in the number of 1s and 0s assigned to each muscle. The 1s and 0s were also very inconsistent across muscles, i.e. did not occur at the same times across muscles. One muscle, FCR, had a much higher proportion of 0s than the other muscles, and it also had a much higher variance. For this reason it explains more of the total variance than the other muscles. Each muscle had a very different variance, resulting in the PVE for each muscle being quite different for this threshold (bar charts below each PCA cumulative PVE plot, Figure 5.9). When the threshold was set to 75%, the variance of each muscle was very similar, due to all muscles having a very similar number of 0s and 1s, being 0 most of the time. This would explain why the PVE for each muscle is very similar.

As mentioned in the Methods, for the 75% threshold, any data points at which all muscles were inactive (represented by a zero) were removed. However this resulted in exactly the same pattern of PVE as found by PCA carried out on this data before any data points were removed (Figure 5.9).

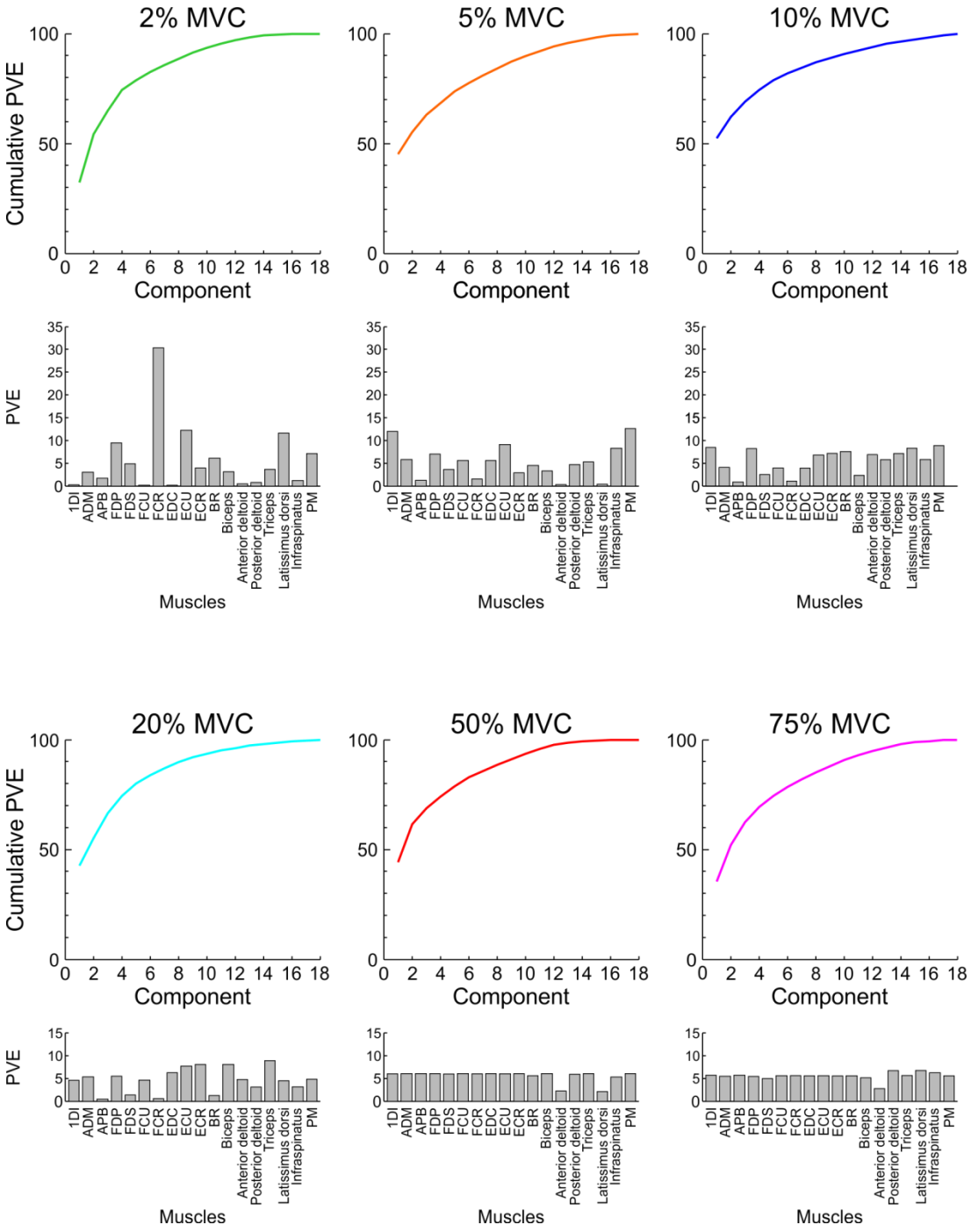

Figure 5.9: Plots of the cumulative PVE for each component when PCA is carried out on data converted to a [0,1] binary format, with the threshold for activation set as a particular percentage of MVC, shown by plot titles. Below each plot is its respective bar chart, showing the PVE of the total data by each muscle after transformation of the data to a binary format.

The highest level of fractionation was seen when the threshold was set at 5%, followed by 75%, 10%, 20%, 2% then 50% (Figure 5.10).

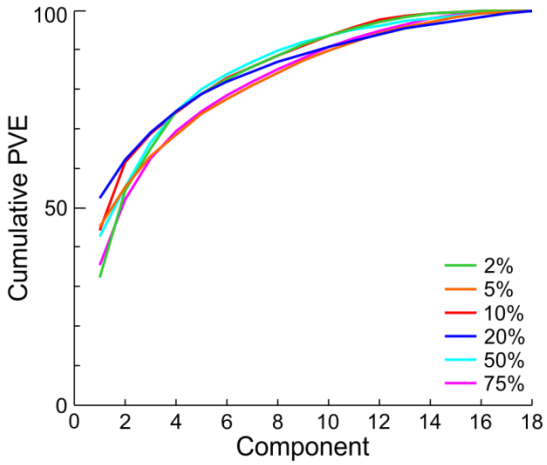

Figure 5.10: The cumulative PVEs for each contraction strength as in Figure 5.9 overlain. Colours correspond to those in Figure 5.9, key in bottom left hand corner.

As the threshold was increased to 5% and 10% MVC, the first component explained slightly more of the variance (45% and 52% respectively) and a few more components were required to explain ~80% of the variance (seven and six respectively). However at thresholds of 20%, 50% and 75% the first component explained slightly less of the variance (43%, 44% and 35% respectively) and the number of components required to explain ~80% of the variance was five, six and seven respectively. Therefore PCA carried out on binary-transformed data at any threshold generally required more components than MVC-normalised data or ICA to explain ~80% of the variance.

5.4.4 Synergies extracted from ICA

Figure 5.11 shows the first 12 independent components extracted by ICA, which can also be considered synergies. These are composed of coefficients which represent the involvement of each muscle in that component. Only muscles with a coefficient of >0.05 or <-0.05 in each component are shown in Figure 5.11. Muscles commonly found above these levels in most components include PM, EDC, FCU and ECR. Synergies often included intrinsic hand muscles, and also coactivation of flexors and extensors. As discussed in Chapter 4, ICA extracts a set of components (C), each of which is a vector of coefficients for each muscle. This represents how much each muscle contributes to that component. It also extracts a matrix of coefficients, each representing how much each component contributes to each data value (M). So in order to find how much activity in a

particular data value is accounted for by a particular component (CM), C is multiplied by M. However in order to result in CM, C and M could both be either negative or positive. In this experiment it was assumed that M is a matrix of positive values, meaning that the C reflects the actual amount each muscle was either suppressed or facilitated by this component. However if M is negative, then C should be inverted. This would flip whether each muscle is suppressed or facilitated in each component. M was actually found to be a mixture of negative and positive values, therefore it is not known whether the polarity of the coefficients represented by each component truly reflects whether each muscle was suppressed or facilitated. Hence we can only conclude that these muscles were dominant in the components, but not whether they are facilitated or suppressed.

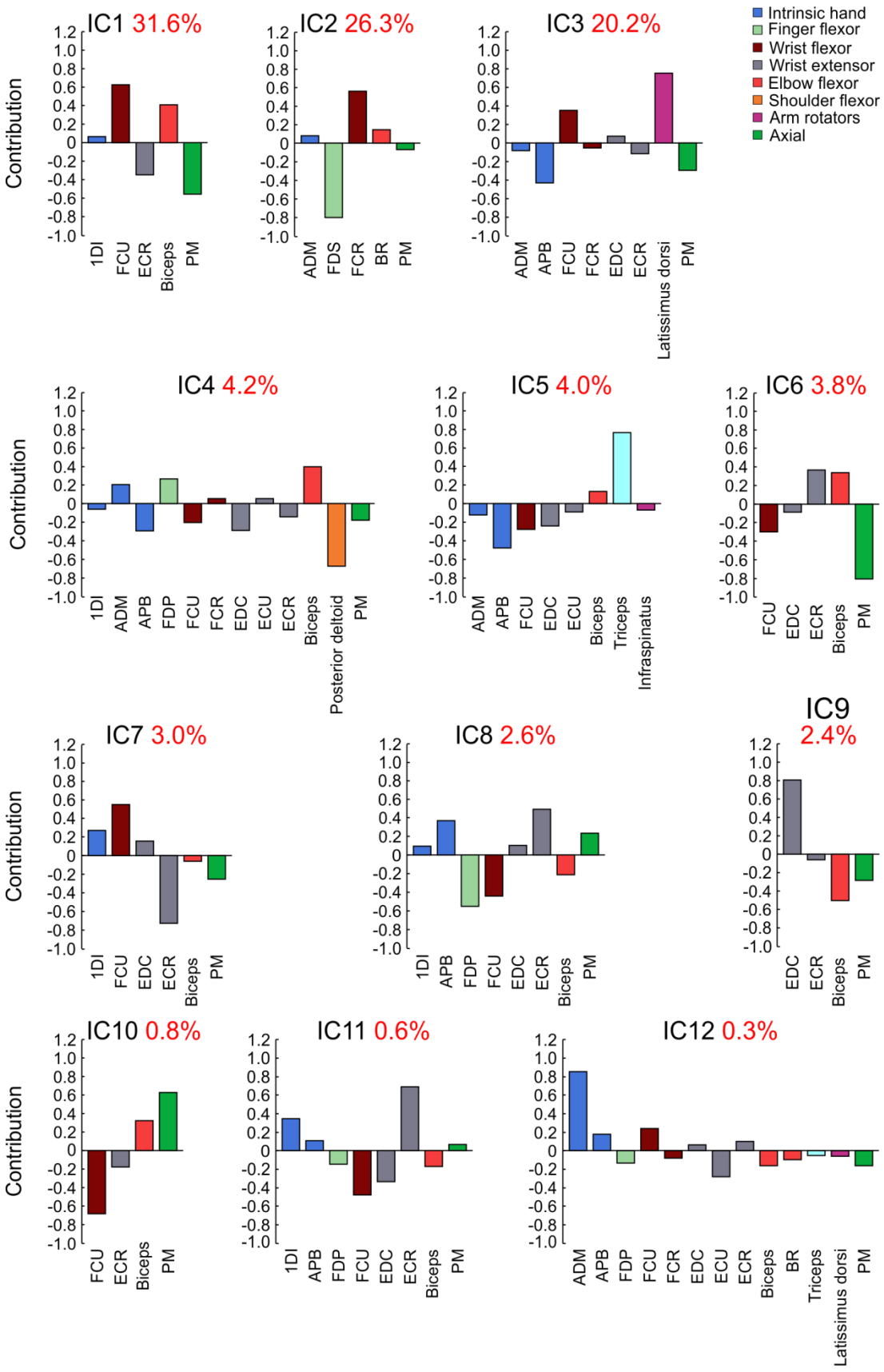

Figure 5.11: First 12 ICs. Key is in the top right corner. Red percentages represent the PVE by each component.

5.5 Discussion

5.5.1 Normalisation

As discussed in Chapter 4, normalisation of EMG signals must be carried out before any comparisons between muscles or subjects can be made. Here, as in previous chapters, both Z-score normalisation and normalising by 97% MVC were used. As PCA is carried out on the covariance matrix of all muscles, altering the variance of muscles is an important factor which is likely to affect the components extracted. Z-score normalisation transforms the data so that the variance of each muscle is the same, so even if some muscles are rarely used, their amplitude will still be scaled up. This would increase fractionation, as every muscle would contribute, even if some are not used. Indeed, in the current study the level of fractionation from Z-score normalised data was higher than for MVC normalised data, and ICA. Z-scoring is therefore argued to rescale the muscles in a way less reflective of the relative contribution each makes to a given movement. As, for reasons discussed, no value can be placed on the relative maximum activation in mV of each muscle, the property of EMG to focus on is the amount of contraction relative to the maximum. As this is exploited in normalising to MVC, this could be considered an appropriate method. Though there are also problems with normalising by MVC, such as more heavily weighting muscles which act nearer to their MVC more of the time. However overall it is argued to be the preferable technique when preparing data for PCA.

On the other hand, ICA does not use covariance as it aims to produce ICs. However the ordering of ICs depends on the PVE by each IC. As normalisation does affect the variance of each muscle, the ordering of ICs would therefore be affected by the normalisation.

5.5.2 Fractionation

Here, it is shown that the PVE of the first component extracted by PCA carried out on data normalised by both techniques is very similar. However, as discussed, the overall pattern of fractionation for Z-score normalisation is higher than after normalisation by 97% MVC. In Chapter 4 it was shown that the

first component for the RF, old and new subregions of the primary motor area (M1) always explained slightly less of the variance when carried out on Z-score compared to MVC-normalised data.

Around ten components are required to explain >95% of the variance in both PCA and ICA. This therefore reduced the degrees of freedom of 18 muscles down to about 10 different synergies combining the muscles in different groupings and with differing levels of activation. However from these synergies as extracted by ICA, three explained considerably more of the variance than subsequent ones (78% in total). About four synergies identified by MVC-normalised PCA explained 76% of the variance. This is strikingly similar to findings from previous studies, which, despite each using a different number of muscles, each extracted three key synergies explaining ~80% of the variance (Weiss and Flanders, 2004; Overduin *et al.*, 2008). On top of the three to four dominant synergies, several smaller synergies were also extracted. These might reflect the higher level of fractionation imposed upon the basic movement ability, resulting from monosynaptic projections to motoneurons from new M1.

It has previously been argued that muscle synergies are a reflection of task constraints rather than actual neural properties (Tresch and Jarc, 2009). However, the fact that a similar number of key synergies as found in previous 'naturalistic' task-based experiments were identified here from natural data, again lends strength to the suggestion that these synergies do underlie movement.

The pattern of variance explained by 97% MVC-normalised PCA and ICA was very similar here. This might be expected, as although the limitations inherent in PCA require all components to be orthogonal, it should extract the orthogonal decomposition of the components extracted by ICA. The fact that both techniques have extracted a similar number of dominant synergies perhaps suggests that this is an accurate reflection of the data.

Comparison with Chapter 4 data In Chapter 4, three to four synergies explained 64-75% of the variance in the RF, 69-78% in old M1 and 69-78% in new M1 (in MVC-normalised PCA). This is similar to the findings in this Chapter, however here three clear key synergies dominated ICA, which was not the case in the previous Chapter. It is not possible to draw any conclusions as to how the regions studied in Chapter 4 contribute to the natural data recorded here. However it would be very interesting to explore whether brainstem pathways control the dominant synergies found here, and whether the smaller, more fractionated synergies result from corticomotoneuronal connections from new M1.

Fractionation of the data at different contraction strengths It is likely that different muscles use a particular range of MVC most of the time. For example, intrinsic hand muscles are able to produce a stronger MVC than is used in most finger movements, which instead might use a small range of up to maybe 30% of MVC most of the time. On the other hand, larger muscles not used in fine movements, such as the biceps, might spend more time at a different range of contraction strengths. Therefore expressing all muscles relative to their MVC might be unfairly weighting muscles which operate near to their MVC more of the time. In order to circumvent this issue, a binary transformation of the data was carried out. This allowed the comparison of the level of fractionation of the data at different fractionation strengths.

The highest level of fractionation was seen when the threshold was set at 5%, and the lowest at 50%. When the threshold was set at 50%, all but two muscles had very similar numbers of 0s and 1s, which would increase fractionation as many muscle are weighted similarly. When the threshold was set at 5%, there was a wider range of different variances across muscles. Because of the wider range of variances, fractionation was higher. Four muscles had the highest variance and the highest PVE, with the highest number of data points replaced with 0s. This means that they had less activation over 5% MVC than other muscles. These four muscles were ECU, infraspinatus, 1DI and PM, which are all quite different, so it is difficult to explain why they have less activation over 5%

of MVC than other muscles. It is especially surprising that ECU has a higher variance than the other forearm extensors or flexors. 1DI might be expected to have less activation over 5% MVC than other muscles as it is probably activated to a small percentage of its MVC most of the time, though for this reason the other intrinsic hand muscles (ADM and APB) would also be expected to have less activation over 5% MVC, which was not the case. At 2% threshold, the range of variances was wider than at 5% but had a lower level of fractionation. This was probably due to one dominant muscle (FCR), which had a much higher activation coefficient in the first component than the other muscles. This would have therefore increased variance but decreased fractionation.

It might be assumed that using a high MVC threshold such as 75% might result in a low level of fractionation due to retaining the strongest periods of contraction for the animal, which might be during the grossest movements. However, the level of fractionation at this threshold was the second highest of all used. At these strengths some larger muscles might be more likely to be active and possibly at the same time. Smaller muscles are less likely to be active, especially not at the same time as the larger muscles. This might mean that only larger muscles would be likely to co-vary together, resulting in a higher level of fractionation; co-activation of many muscles at this strength is probably unlikely. When looking at the proportion of 1s and 0s for each muscle at this threshold, most muscles had similar numbers of each, with many more 0s than 1s. One exception was anterior deltoid, which had many more 1s than 0s. Therefore, the high level of fractionation is probably also due to the similarity of variance across muscles.

It is interesting that fractionation at a 50% threshold is not almost as fractionated as at 75% as the PVE across muscles at 50% is almost as equal as at 75%. It is possible that muscles were more often co-activated at the same times when a 50% threshold was used, decreasing fractionation.

Synergies One dominant IC explained almost a third of the variance in the EMG and has involvement of 1DI, FCU, bicep, ECR and PM muscles. The PM

muscle was present in every synergy; it is possible it is activated with movement of upper limb muscles as a postural response to stabilise the body.

Previous research has found synergies involving co-activation of all muscles, or reciprocal activation of muscles such as extrinsic hand flexors (FDS) and extensors (EDC) or thumb (APB and flexor pollicis brevis) and index finger (1DI) muscles (Weiss and Flanders, 2004). These synergies are different from those identified here, though the previous study only recorded muscles involved in hand and finger movement, whereas a wider range of movement was sampled here.

5.6 Conclusions

Normalising EMG data to a percentage of MVC is suggested to be a more accurate method than Z-score normalising when carrying out PCA. However the inherent problems in MVC normalising must also be acknowledged. In order to circumvent any normalisation-induced skewing of the level of fractionation extracted from the data recorded here, it was transformed into a binary format. This allowed comparisons of the fractionation at different contraction strengths to be made. The highest level of fractionation was seen at a threshold of 5% MVC, as the range of variances across muscles at this threshold was wider. At this contraction strength, four muscles had a much different variance to that of the remaining muscles. The level of fractionation at a 75% threshold was very similar to that of 5%, but for a different reason; probably due to all muscles having a similar amount of variance.

Natural movements from 18 muscles recorded in one macaque over >30 hours were found by both PCA and ICA to be explained by three to four key synergies, similar to that found in previous studies. This may suggest that these synergies accurately reflect the underlying control structures of the movement recorded. However, future work is required to clarify the origins of the different synergies, and the relative contributions from different movement pathways.

6 Reticulospinal output in four limbs of the baboon

In this chapter I will detail an acute experiment carried out on two baboons in Kenya, in which the EMG responses in all four limbs evoked by RF stimulation were recorded. This aimed to identify the output divergence of the RF to multiple limbs, and whether reticular synergies involving multiple limbs exist.

The experiment presented in this chapter was carried out at the Institute for Primate Research (IPR) in Karen, Nairobi, Kenya. All data presented were collected by Stuart Baker and me. Surgical techniques were also carried out with the help of Stuart Baker.

6.1 Abstract

Background and aims: Although the reticular formation (RF) does have a role in locomotion and standing posture, very little is known about the branching patterns of reticulospinal (RST) connections to lower limb motoneurons in primates. No previous work has looked at the foot and leg synergies that may be produced by the RST, or investigated the existence of synergies involving both upper and lower limbs. These were the aims of the current experiment.

Methods: Responses to RF stimulation were measured in 112 muscles across all four limbs in two decerebrated male baboons. Penetrations by a stimulating electrode were made throughout the RF, and stimulus threshold intensities for resulting muscle responses were identified at each site. Both principal component analysis (PCA) and independent component analysis (ICA) were then carried out on the average significant responses across stimuli for each muscle at each site as a method of assessing the fractionation of the RF system. It was also calculated what proportion of stimulated sites evoked responses in bilateral muscles, muscles located in the upper and lower limb, and proximal as well as distal locations along the arm and leg. Muscle co-activations were also examined.

Results and conclusions: Output divergence ranged from 1-43 different muscles per site, with one muscle being the most common level of divergence at

threshold. However this was believed to be the consequence of several factors limiting the output observed. Threshold stimulation activated mainly arm and some axial muscles, whereas higher intensities at one or three shocks additionally elicited leg and foot muscles. Bilateral effects were observed, in line with the existing finding that RF cells terminate on both sides of the spinal cord. Surprisingly though, distal effects were more than twice as common as proximal responses. PCA and ICA also revealed the RF to be more highly fractionated than predicted, with the first component explaining 27% and 11% of the variance in the electromyography (EMG) recordings respectively. This is likely to reflect how commonly sites activated only one muscle.

6.2 Introduction

Recent evidence has shown to some extent the role of the RST in the control of upper limb movement (Buford and Davidson, 2004; Davidson *et al.*, 2007; Riddle *et al.*, 2009; Riddle and Baker, 2010), which is discussed in previous Chapters. However there has as yet been little research into its involvement in the motor control of lower limbs.

6.2.1 Reticular control of lower limb muscles

The projection of the RST onto leg and foot motoneurons in humans has yet to be explored, though this is to a considerable extent due to the limited range of non-invasive techniques available to probe the RST. One useful technique is the use of a startling stimulus, which activates the pontine reticular nucleus and therefore the RST (Yeomans and Frankland, 1995); consequently any muscles activated by startle can be argued to have input from the RF. Indeed, in Chapter 2 results are presented in support of the role of the RST in startle-elicited muscle responses. To date only a handful of startle experiments have found evidence for RST inputs to lower limb motoneurons, by eliciting responses in muscles such as soleus and tibialis anterior (Brown *et al.*, 1991a; Ilic *et al.*, 2011; Nonnekes *et al.*, 2013). In primates, RST projections to lumbar cord motoneurons have been shown (Shapovalov, 1972). Additionally, cells originating in the pontomedullary reticular formation have been found to facilitate or suppress bilateral muscles in both fore- and hindlimbs (Drew,

1991). There are two functions in which the feet and legs are key across humans and primates: locomotion and posture, therefore studies into these functions can be drawn upon for information on the extent of leg and foot control by the RST.

Evidence from locomotion Evidence for the control of whole-body or hindlimb muscles by the RST includes work in the lamprey, bird, cat and monkey. In the lamprey, reticulospinal neurons have been shown to relay inputs received from the vestibular system regarding deviations in posture to the spinal cord (Vilensky, 1987; Deliagina *et al.*, 2008). Locomotion can be initiated by stimulation of the gigantocellular and parvocellular reticular nuclei in birds (Steeves *et al.*, 1987), and discharge of medullary reticulospinal neurons has been found during cat locomotion, with firing of a third of recorded cells being correlated to one or more muscles, which included both flexors and extensors and could be bilateral (Shimamura *et al.*, 1982; Shimamura and Kogure, 1983; Drew *et al.*, 1986; Perreault *et al.*, 1993; Perreault *et al.*, 1994). The RF projects to the lumbosacral segments of the spinal cord in cats (Eidelberg *et al.*, 1986), with more than 60% of these axons also projecting collaterals to the cervical segments, meaning that some reticular cells have connections to muscles in upper and lower limbs (Peterson *et al.*, 1975; Hayes and Rustioni, 1981). Functional magnetic resonance imaging (fMRI) studies in humans have also shown that when walking or running is imagined, activation is seen in the interfastigial cerebellum and midbrain tegmentum as well as their target output regions in the pontine reticular formation (Jahn *et al.*, 2008). These networks were part of a network considered similar to the supraspinal locomotor network present in cats. As it has been shown that motor imagery and motor actions are controlled by the same neural areas, it is possible that these areas, including the pontine RF, are also involved in human locomotor activity.

Evidence from posture Further evidence for the RST control of legs comes from work on posture in cats; cells in the PMRF have shown changes in firing rate after posture has been perturbed, with >80% of recorded cells responding

to perturbations in more than one limb and some responding to all four limbs (Stapley and Drew, 2009). Neurons in this area have also been found to modulate firing rate during alterations in posture made during walking when objects are placed in the path of a cat (Prentice and Drew, 2001), with 25% of cells responding when each of four limbs was negotiated over the obstacle.

6.2.2 Lower limb function post-stroke

It has been suggested that stroke patients rely on the RST for arm and perhaps function after the corticospinal tract (CST) is damaged. Evidence for this includes the finding that excitatory post-synaptic potentials elicited by medial longitudinal fasciculus stimulation in motoneurons of flexor muscles selectively increase following CST lesion, which is strikingly similar to the flexor overactivation seen in stroke patients. Therefore it is also possible that the RST underlies lower limb control after stroke. Post-stroke lower limb impairments include bilateral weakness of the knee extensors (Bohannon, 2007; Chow and Stokic, 2011; Madhavan *et al.*, 2011) and ankle plantar flexors (however the second finding may be due to reduced loading on the affected leg post-stroke, Pandian and Arya, 2013). Additionally the Brunnstrom recovery stages for stroke classify lower stages of recovery as having hip, knee and ankle flexion, whereas extension is expected to be possible in more advanced stages of recovery (Pandian and Arya, 2013).

Therefore, the RST has a known involvement in control of leg functions, and is known to synapse with leg and foot motoneurons. However it is not known exactly to which muscles and in what synergies the RST projects. This is the aim of the current experiment. It is difficult to predict what synergies might be found due to the lack of previous work in this area, though it is expected that the RST will have leg synergies. Based on the work carried out in cats and the fact that baboons are also quadrupedal it is possible that there are also some synergies involving both upper and lower limbs.

The current experiment uses baboons as an animal model due in part to their size, being approximately five times the size of the macaques usually used; this

makes it much easier to identify and implant all 112 pairs of electrodes required here. Additionally, baboons are phylogenetically more closely related to humans than macaques, potentially meaning that the muscle synergies found here are closer to what might be expected to be found in humans.

6.2.3 Stimulation techniques

As in previous Chapters, this experiment used a technique which involves taking a window of EMG for each muscle surrounding each stimulus pulse and averaging it, to find the overall response of each muscle to stimulation of a particular area. This technique is called stimulus triggered-averaging, or stimulusTA. StimulusTA usually uses single pulses of stimulation at low frequencies (such as 7Hz used here). Another method mentioned in this Chapter as used by previous studies is spike triggered averaging (spikeTA); similarly to stimulusTA this technique averages windows of EMG, but surrounding spontaneously occurring action potentials or 'spikes' rather than stimulus pulses. This allows the delineation of muscles naturally activated by the cell producing the spikes. However, in order to carry out spikeTA, background activity is required; such activity was very limited in the current experiment. Although the animals had very little anaesthesia post-decerebration, their movements were still limited to periodic waves of activity travelling down the body. Additionally, finding individual cells required for spikeTA takes much longer than stimulusTA. The experiment carried out here took >48hrs from initial sedation, and maintaining stability of an animal in a surgical setting for this period of time is already challenging. StimulusTA is much easier and quicker, allowing the rapid collection of a large dataset.

6.3 Methods

Two male baboons (*Papio anubis*, weight 23.5kg) were sedated using a mixture of ketamine (10mg/kg) and xylazine (0.5mg/kg) and ventilated using halothane (0.5% in 50% O_2). Surgical preparation was then carried out, involving shaving the entire animal and urinary catheterisation. The animal was then maintained on terminal anaesthesia with ketamine (10mls/hr). Methyprednisolone (6-

10mls/hr) was given to minimise brain oedema and Hartmann's (60-200mls/hr) was administered to replace body fluids lost during surgery. Throughout the experiments, pulse rate and 0_2 saturation were measured by pulse oximetry, a capnograph was used to measure end-tidal CO_2 and carotid blood pressure was monitored. A tracheotomy also was performed to allow artificial ventilation. Temperature was maintained using hot water bottles and an over-body warm air blanket (Bair Hugger, 3M, St. Paul, MN, USA), and was measuring using a nasal thermometer.

Decerebration was carried out by ligating the sagittal sinus and external carotids, then removing all of the neuraxis rostral to the superior colliculus. This allowed anaesthesia to be stopped completely, therefore preventing the inhibition of neurons usually caused by general anaesthetic agents (Komai and McDowell, 2001).

6.3.1 Electromyography

Electrodes made from either 150μm diameter 7-stranded stainless steel Teflon-insulated wire (AISI316, Advent Research Materials, Oxford, UK) or 175μm diameter 7-stranded stainless steel nylon-insulated pike fishing wire (Drennan International, UK) were implanted in 112 muscles in each animal (across all four limbs and the trunk, 56 on each side of the body). For a full list of implanted muscles, see Appendix B.

When discussing proximal and distal muscles in this Chapter, proximal in the upper limb refers to muscles located above the elbow and including the shoulder, and distal refers to any muscles below the elbow. Proximal upper arm muscles include those acting on the arm but located on the back. Axial muscles are those located on the trunk and acting on the trunk only.

Superficial muscles were implanted percutaneously using 23 gauge needles as introducers, whereas those which were more difficult to locate were accessed via dissection and then implanted using the same needle method. Signals were

amplified using custom-built amplifiers, digitised at 5kHz by an Intan recording system (Intan technologies, LA, CA, USA) and band-pass filtered at 30Hz-2.5kHz.

6.3.2 Stimulation

Stainless steel electrodes (300μm diameter shaft, 3μm diameter tip, 0.1 MΩ impedance: MicroProbes, Gaithersburg, MA, USA) were used to make penetrations into the RF. The RF was initially located by observing neural landmarks easily seen post-decerebration such as the cerebellar vermis and inferior colliculi, then tested for muscle responses to a train of stimuli (trains of 13 pulses of ICMS). Once a site in the RF was found, single-pulse stimulation (7Hz) was delivered to elicit responses in the muscles recorded. Over around 90 seconds, ~500-630 stimuli were delivered per intensity (initially some human error in duration of stimulation given). A starting stimulation intensity of 50μA was used, and then a custom-written program (MatLab, Mathworks Inc., Natick, MA, USA) run to check if any significant responses were present. This program averaged windows of EMG for each muscle from 100ms before to 200ms after each stimulus pulse. The 99ms period before stimulus onset was referred to as the baseline period. Responses were defined as any period during which the EMG from 5-50ms after the stimulus pulse exceeded three standard deviations above or below the mean of the baseline. In order to find whether each response was significant, a paired *t*-test was carried out between the mean of the response and the mean of the baseline period for each stimulus. If any significant responses (at the $P<0.05$ level) were seen at this intensity, a lower intensity was tested. This process was repeated until the threshold intensity was found, defined as the lowest intensity at which ≥1 muscles responded when the intensity 10% below had no significant response. Only sites with thresholds below 50μA were used. At each site, responses at 130% of threshold intensity were also recorded. Additionally, at many sites responses to short trains of 3 shocks at both threshold and 130% threshold intensity, as well as trains of 13 shocks at both threshold and 130% threshold intensity were recorded. This process was repeated until adequate coverage of the RF was achieved. In each animal 11 anterior-posterior (AP) electrode penetrations were made at two different medio-lateral locations, with recordings at three to four depths per

penetration. These tracks were located 2-12mm caudal to and at 2mm and 4mm lateral to obex, on the right side of the RF.

6.3.3 Analysis

Between the two animals used, 67 penetration sites within the RF were stimulated; in 51 of these sites the stimulation threshold was found, defined as the lowest intensity eliciting responses where the intensity 10% below did not. Before any analysis took place, removal of 50Hz mains noise was carried out on all raw EMG traces. This involved subtracting an average of the noise which was built up using a sliding window of the EMG. The data were offset removed and rectified. Cross-talk analysis was not carried out for two reasons: to carry out such an analysis as described by Kilner *et al.* (2002) correlations are calculated between muscles from behavioural EMG recordings. It was not possible to record any awake behaving data in the animals used here, and stimulus-evoked responses would be highly correlated between some channels, reflecting the synergies this experiment aimed to find. Secondly, intramuscular EMG was recorded here, which is less likely than surface EMG to be susceptible to cross-talk between electrodes.

For every site showing a response (for any stimulation intensity, therefore there could be multiple traces recorded for each site) at the time of recording, a very similar analysis to that run during time of recording was carried out. For each muscle and each site, this involved calculating the mean of the baseline period 99ms before stimulus onset. Any sections of EMG between 5 and 50ms after each stimulus which exceeded three standard deviations above or below the mean baseline were considered potential responses. In order to find whether these responses were significant, paired t-tests were carried out on the mean of each response and the mean of the baseline area for each response. A significance level of $P<0.001$ was approximated as a Bonferroni-corrected value, to correct for the hypothetical multiple comparisons carried out when choosing the response window three standard deviations above or below the mean baseline as opposed to any other window in the period following the stimulus pulse. If the muscle had a significant response, the size of the response was

quantified by subtracting the mean of the area (integral) of the baseline from the mean of the area (integral) of the response. If a response were a suppression followed by a facilitation or vice-versa, the first response was taken. After all computer-generated responses were found, each was examined by eye to check it looked like a convincing response. Following this, as a more objective test, all onset latencies for anatomically grouped muscles (e.g. all forearm flexors, all back muscles, all hand muscles, and so forth) were compared to find a general onset latency for each group; then any outliers, defined as those >3 standard deviations below the mean of the group were removed. Again, these responses were checked by eye. Outliers smaller than three standard deviations below the mean were considered too early to be true responses. This resulted in a matrix of response values for each muscle, for each site. Any muscles which did not respond for a particular site were assigned zeros. Any muscles which never responded were removed from the matrix, which was Z-score normalised. As discussed in other Chapters, normalisation by maximum voluntary contraction (MVC) is perhaps a more valid method of standardising the data than by Z-score. However, in order for this to be done, it is necessary to record awake, behaving EMG from which the level of maximum voluntary contraction for each muscle can be taken, which was not possible for the baboons used in this experiment. PCA was then carried out, which reduced the data into a group of core components. Every component had a respective vector of coefficients or eigenvalues, each of which defined the extent to which each muscle was involved in that component. These are found by taking the dot product of each component with every set of observations for all muscles and calculating the variance of the resulting vector. These variances were then each divided by the sum of all variances and multiplied by 100 to find the percentage of variance explained (PVE).

Independent component analysis (ICA) was also carried out as a second measure in order to ensure the accurate level of fraction was calculated. The same method as described above for PCA was used to extract the eigenvalues and PVE for the component matrix calculated by ICA.

PCA and ICA were each carried out on matrices of muscle responses for all stimulation intensities as they both require at least an equal number of observations and signals, and here fewer threshold intensity sites were gathered than number of muscles recorded from.

ICA As mentioned in Chapters 4 and 5, ICA extracts a set of components (C), each of which is a vector of coefficients for each muscle. This represents how much each muscle contributes to that component. It also extracts a matrix of coefficients, each representing how much each component contributes to each data value (M). Therefore to find how much activity in a particular data value is accounted for by a particular component (CM), C is multiplied by M. However in order to result in CM, C and M could both be either negative or positive. In this experiment it was assumed that M is a matrix of positive values, meaning that the C reflects the actual amount each muscle was either suppressed or facilitated by this component. However if M is actually negative, then C should be inverted. This would flip whether each muscle is suppressed or facilitated in each component. M was actually found to be a mixture of negative and positive values, therefore it is not known whether the polarity of the coefficients represented by each component truly reflects whether each muscle was suppressed or facilitated. Hence we can only conclude that these muscles were dominant in the components, but not whether they are facilitated or suppressed.

6.4 Results

In total across the two baboons, 67 sites were found, with 51 of these at threshold intensity. The mean threshold intensity for the 51 sites for which threshold was found was 27±13μA (mean±standard deviation). The number of sites found in each baboon and the average threshold stimulation intensity found across these sites for each baboon are shown in Table 6.1.

Table 6.1: Sites found and average stimulation intensity used in each animal.

Region	No. of sites found at threshold stimulation intensity	Average threshold intensity (μA)	Species	Animal
RF	27	27	Baboon	Embe
RF	24	29	Baboon	Fundi

6.4.1 Cross-talk

When recording EMG there is the risk of picking up muscle activity not only from the target muscle but also from neighbouring muscles; this is a particular problem when recording from smaller muscles which are in close proximity to other muscles, such as those in the hand or forearm. In the current work, this risk is unlikely due to the use of closely apposed intramuscular electrodes as opposed to surface EMG patches.

However in order to show that cross-talk was not a major factor in the recordings made here, the presence or absence of responses in two closely anatomically-located muscles were compared. This was done for the 1DI muscle and the 2DI at one example site; stimulation by 3 shocks at 130% threshold activated the 1DI muscle but no other intrinsic hand muscles (Figure 6.1). As all muscles had at least a similar amount of spatial separation as this pair (1DI and 2DI), it is unlikely that cross-talk occurred in any muscles recorded here.

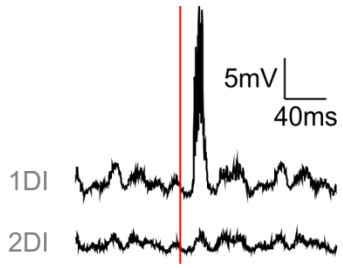

Figure 6.1: Example responses from the 1DI (top) and 2DI (bottom) muscles to evidence lack of cross-talk. From stimulation of one site by 3 shock 130% threshold stimulation. Stimulus timing is indicated by the red line.

6.4.2 Response divergence

It was most common to see responses in one muscle in response to threshold stimulation, 130% threshold stimulation, and across all intensities and number of shocks (Figure 6.2). Three shocks at 130% threshold intensity elicited responses in the most widespread number of muscles. As many as 11 muscles were activated by threshold stimulation of sites, with up to 43 being activated across all stimulation intensities (Figure 6.2).

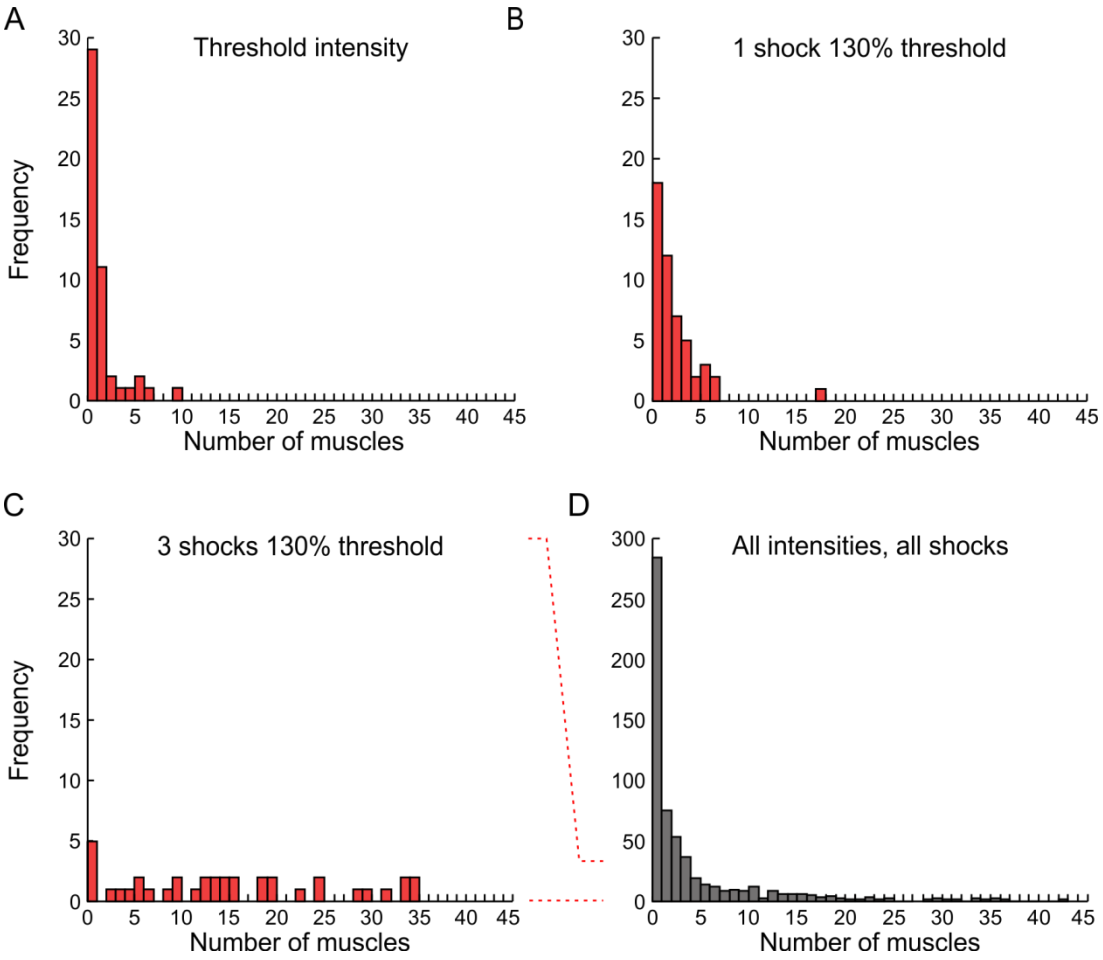

Figure 6.2: Histogram of number of muscles activated by threshold stimulation (A), for single shocks at 130% threshold intensity (B), for 3 shocks at 130% threshold intensity (C) and across all intensities, with either a single shock, 3 or 13 shocks, therefore including multiple intensities per site (D). Dotted red lines next to D indicate relative height of A, B and C to D.

Sites stimulated at threshold intensity most commonly activated upper limb muscles, followed by those located axially (Figure 6.3). Around a quarter of these sites activated bilateral muscles. Distal muscles were more commonly

activated than proximal muscle. When single shocks at 130% threshold were used, lower limb muscles were activated, alongside a higher percentage of activation of all other types of muscle (bilaterally located, upper limb, axial, proximal and distal, Figure 6.4). When trains of three shocks at 130% threshold were delivered, almost every site elicited responses in bilaterally located muscles and upper limb, axial, proximal and distal muscles. Lower limb muscles were still activated by the fewest sites (Figure 6.5).

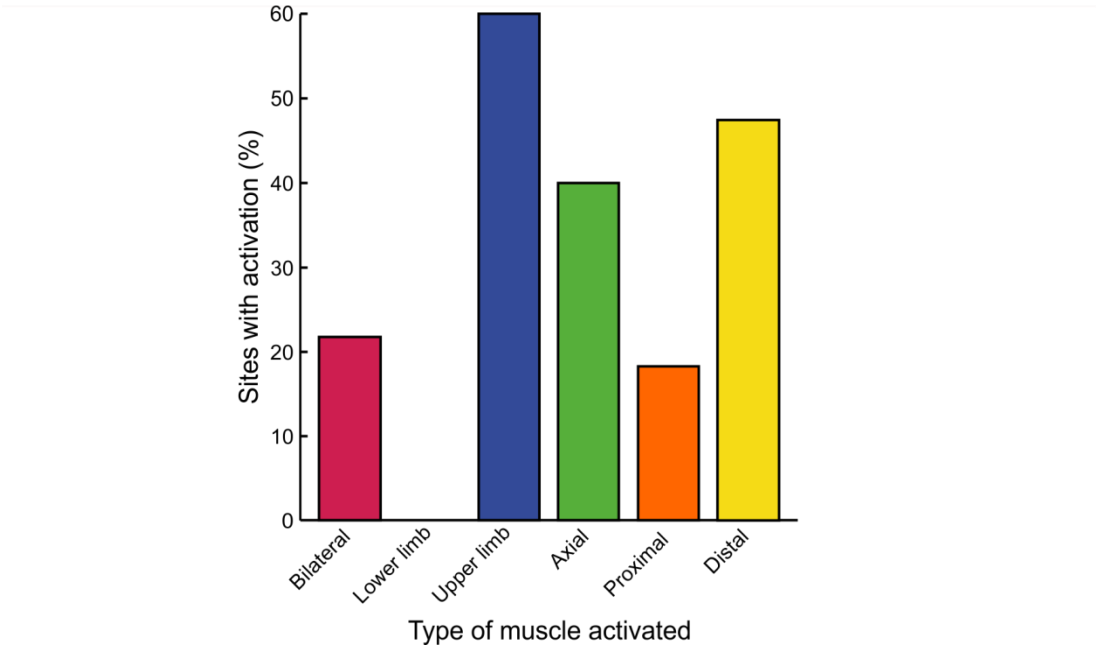

Figure 6.3: Percentage of sites which activated different categories of muscle when stimulated at threshold intensity. Distal and proximal refer to muscles in the arm and trunk, not the leg and foot. Lower limb refers to all muscles in the leg and foot.

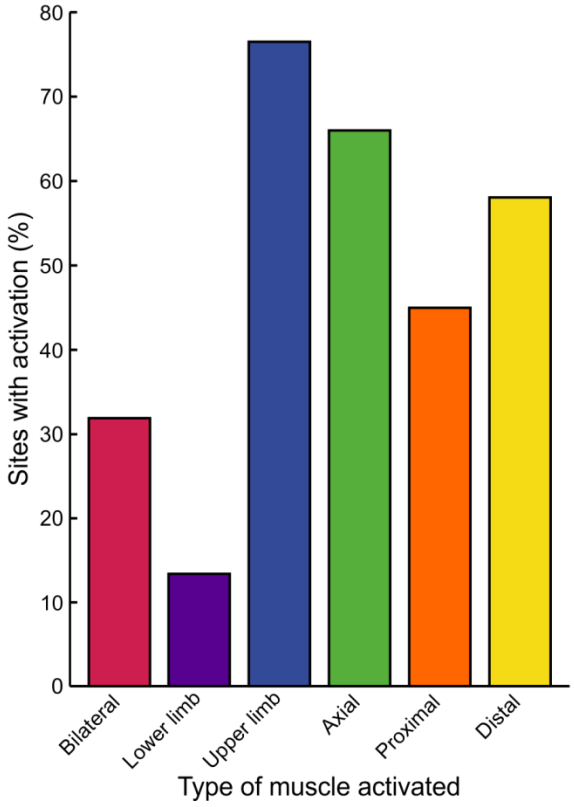

Figure 6.4: Percentage of sites which activated different categories of muscle when stimulated by single shocks at 130% threshold intensity. Distal and proximal refer to muscles in the arm and trunk, not the leg and foot. Lower limb refers to all muscles in the leg and foot.

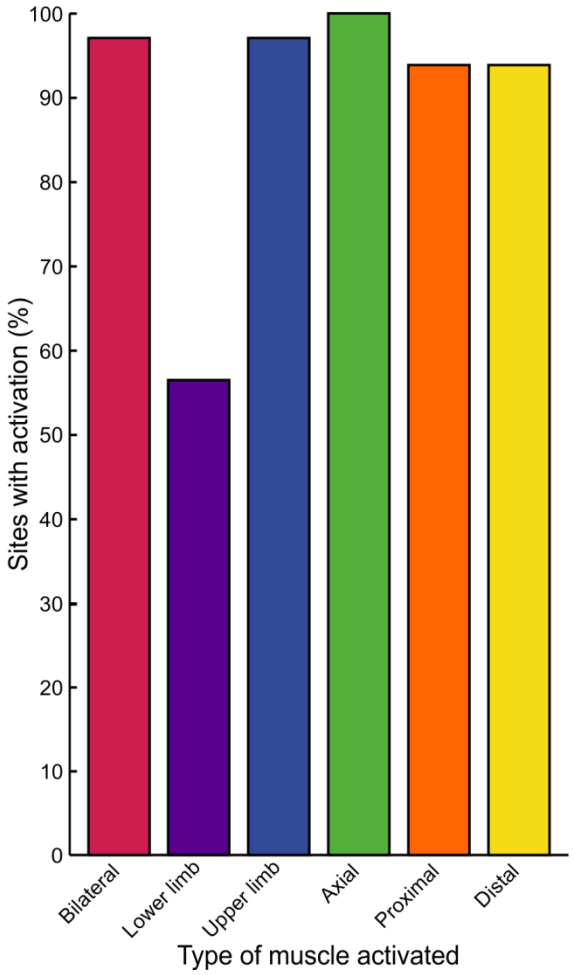

Figure 6.5: Percentage of sites which activated different categories of muscle when stimulated by trains of 3 shocks at 130% threshold intensity. Distal and proximal refer to muscles in the arm and trunk, not the leg and foot. Lower limb refers to all muscles in the leg and foot.

Responses in the arm, hand, trunk, leg and foot were elicited, though these differed according to type of stimulus (single shock at threshold, single shock at 130% of threshold, 3 shocks at 130% of threshold; Figures 6.6, 6.7 and 6.8).

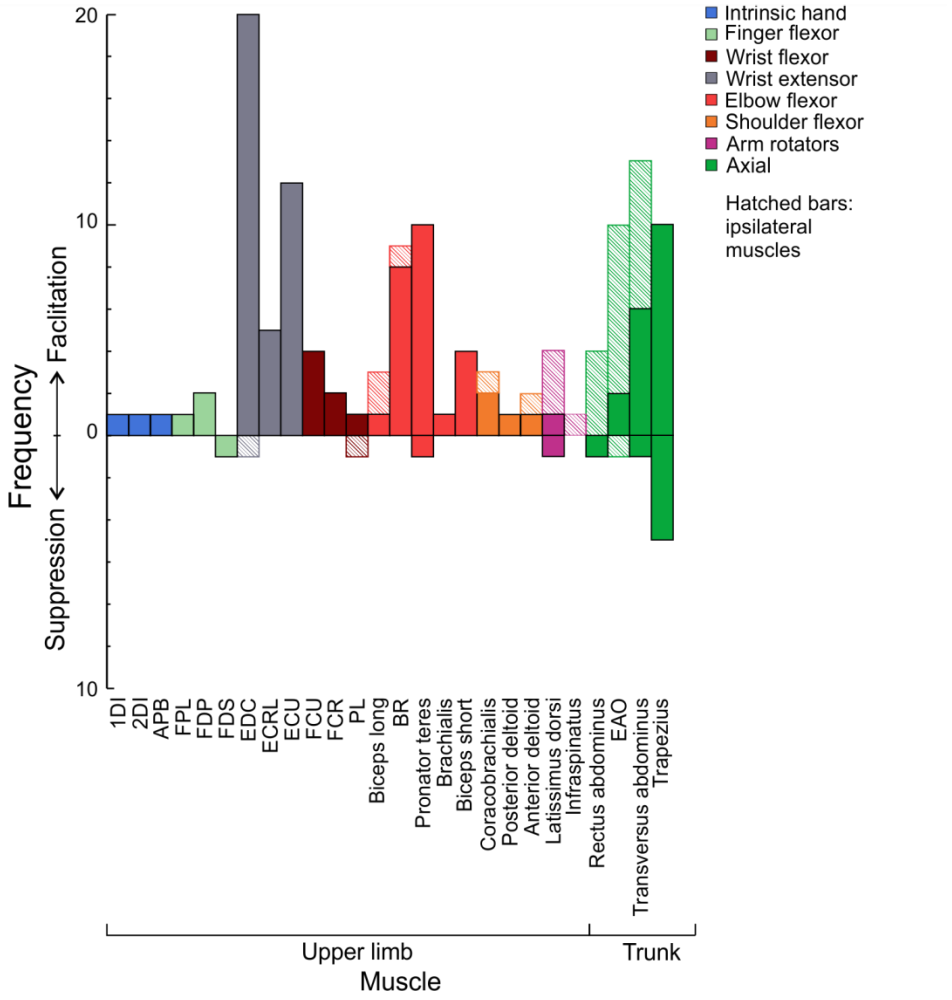

Figure 6.6: Histogram of muscles activated across two baboons by sites stimulated with single shocks at threshold intensity. The key to the action of each muscle is given in the top right panel.

As seen from Figure 6.6, threshold stimulation of RF sites elicited responses most commonly in the EDC muscle, followed by ECU, pronator teres and trapezius. Responses were most often in the contralateral muscles, and facilitatory effects were much more prevalent than suppressive ones. No lower limb muscles were activated by threshold stimulation.

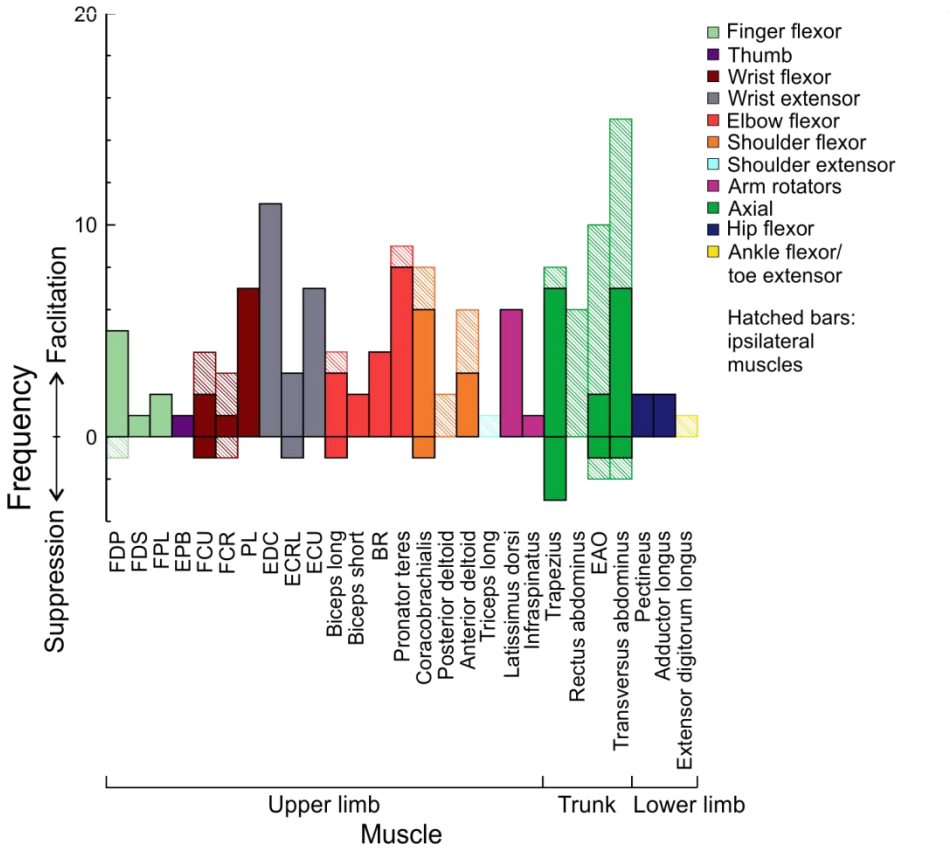

Figure 6.7: Histogram of muscles activated across two baboons by sites stimulated with single shocks at 130% threshold intensity. The key to the action of each muscle is given in the top right panel.

Figure 6.7 shows that when 130% threshold intensity was used, lower limb and foot muscles were activated, though no responses in intrinsic hand muscles were found.

When the RF was stimulated with 3 shocks at 130% threshold intensity, more muscles of each type were activated than by the stimulation types used for Figures 6.6 and 6.7 (Figure 6.8). This was the only type of stimulation to activate knee flexors.

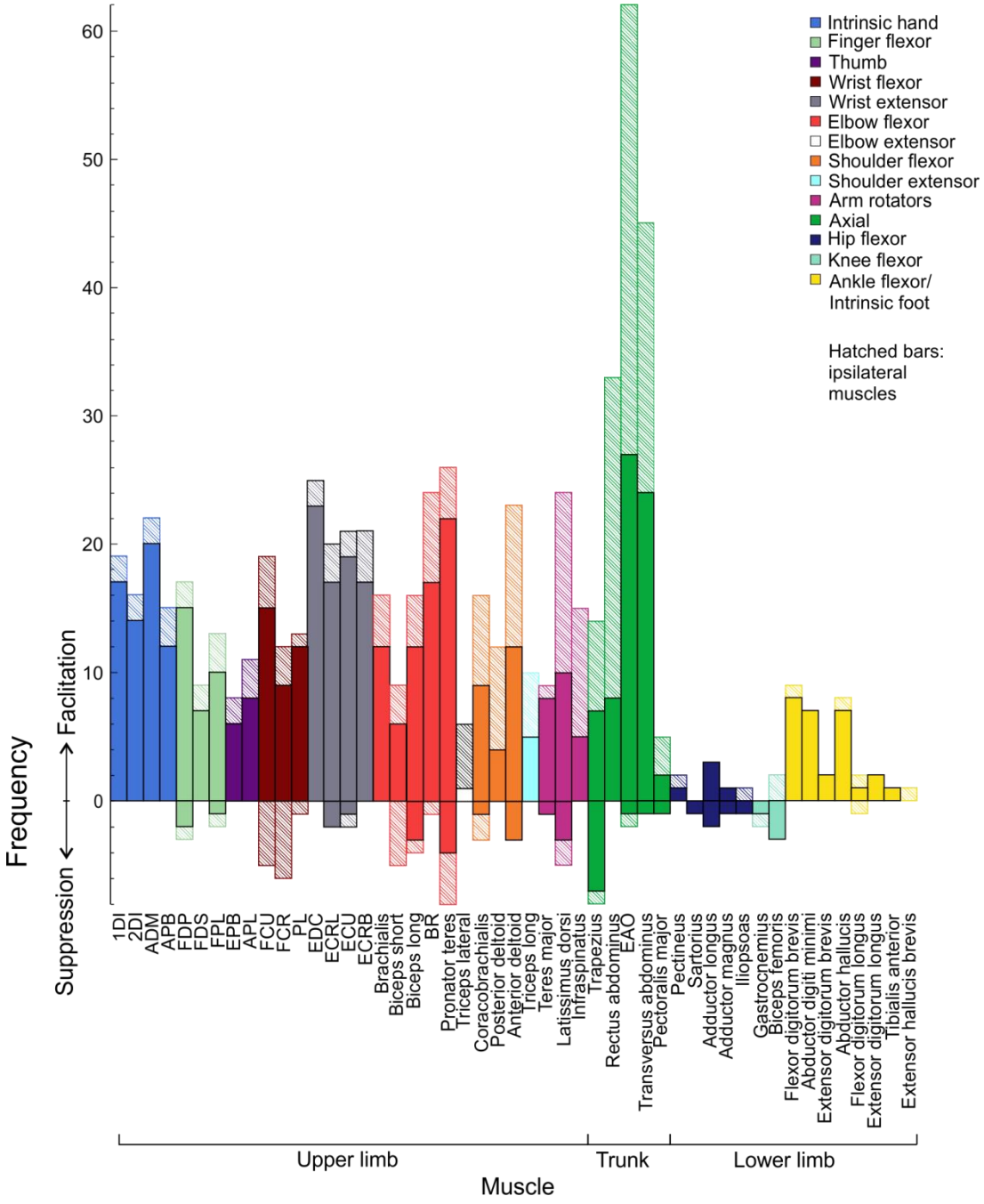

Figure 6.8: Histogram of muscles activated across two baboons by sites stimulated by trains of 3 shocks at 130% threshold intensity. The key to the action of each muscle is given in the top right panel.

6.4.3 Fractionation

The level of fractionation of the RF was assessed by carrying out PCA and ICA on the data (all intensities, for one, three and 13 shocks) separately for each animal and the cumulative PVE calculated for each algorithm. For PCA the mean of the cumulative PVE across animals was plotted (Figure 6.9). As ICA results in a different number of components for each animal, the cumulative PVE for one

baboon was plotted (Figure 6.9). Both algorithms resulted in a fairly fractionated pattern of variance explained though in ICA the first independent component (IC) explained less variance than the first PCA component. The plot of variance explained by ICA has a steep gradient until it reaches 70% of variance explained, after which the gradient is smaller as the components gradually sum to 100% variance explained. The variance explained by ICA reaches 95% after 42 components, whereas the variance calculated from PCA reaches 95% after 25 components. Therefore ICA shows the EMG data to be more fractionated than shown by PCA.

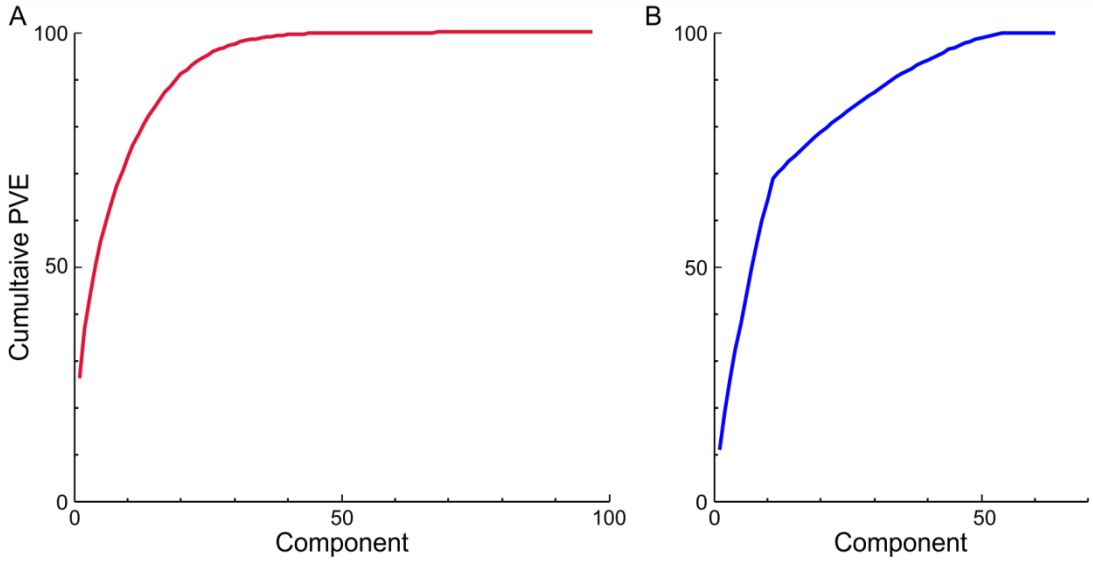

Figure 6.9: The cumulative PVE explained by each component as found by PCA (A) and ICA (B) carried out on all sites at all intensities, with 1, 3 or 13 shocks. PCA was carried out on both baboons and the average cumulative PVE for each component taken across them and plotted. The cumulative PVE found by ICA from one baboon (Embe) is plotted here.

The activation coefficients for each muscle for the first nine components (considered as synergies) from ICA were then examined to find what muscles were dominant and which not represented (Figure 6.10). Due to the large number of muscles recorded, only muscles with a coefficient of >0.1 or <-0.1 were plotted. These muscles had clear contributions above that of most other muscles which were excluded from the Figure.

Upper body muscles were most common in these synergies, though some lower limb muscles were also present. The synergies were dominated by a small group of muscles consisting of 1DI, APB, FPL, AL, posterior deltoid, PM and EAO, with a limited range of other muscles contributing to most synergies, including infraspinatus and ECRB. Only two lower limb muscles (biceps femoris and extensor digitorum brevis) contributed to these synergies. As discussed in the Methods section, the sign (positive or negative) of the coefficients was not considered a reliable reflection of whether muscles were facilitated or suppressed in each component. Therefore we can only conclude that the muscles represented in Figure 6.10 were dominant in each component, and not whether they were facilitated or suppressed.

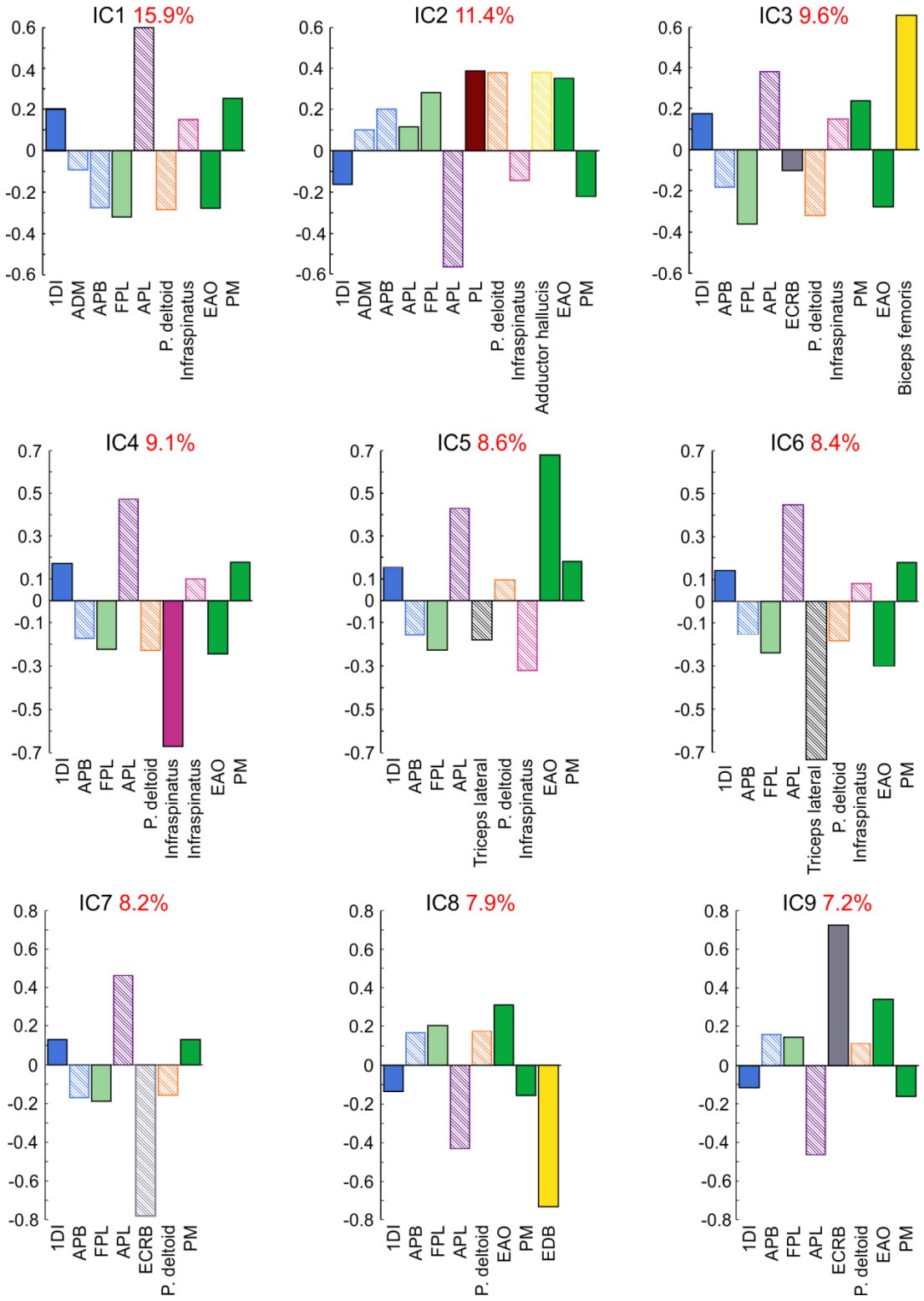

Figure 6.10: First nine ICs for one baboon. Y-axis represents the activation coefficient of each muscle within each synergy. Red percentages reflect the PVE by each component.

6.4.4 Co-activations

Co-activations of muscles were also examined, defined as all the muscles activated by stimulation of one site. These included bilaterally located muscles, both suppressive and facilitatory effects, coactivation of flexors and extensors, as well as of both distal and proximal muscles (Figure 6.11).

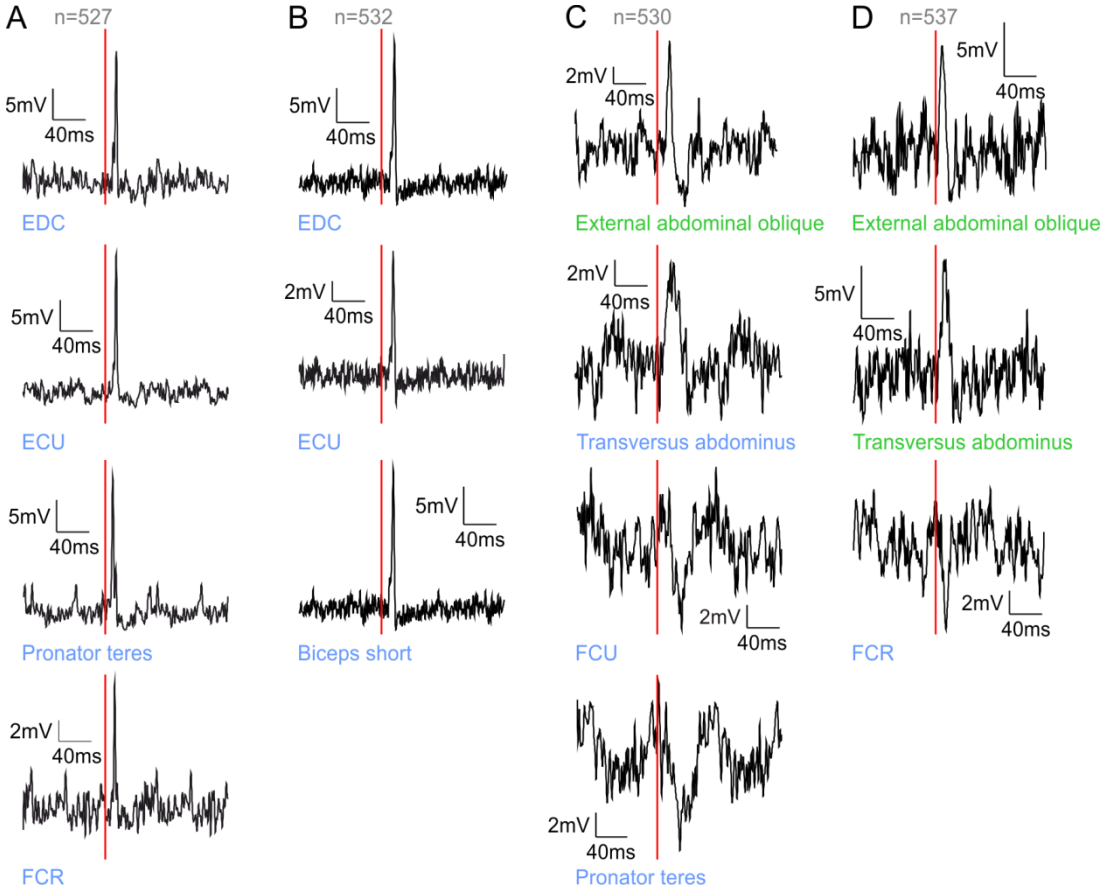

Figure 6.11: Example traces of co-activations resulting from stimulation of different sites within the RF. Each set of traces was elicited from one site at threshold stimulation intensity. Co-activations included flexors and extensors (A), proximal and distal muscles (B), suppressive and facilitatory effects (C) and bilaterally located muscles (D). Traces are averages across stimuli (number of stimuli indicated for each synergy), low-pass filtered at 400Hz. Contralateral muscles are labelled in blue; ipsilateral muscles are labelled in green. Stimulus times are indicated by red lines.

There was some degree of co-activation between arm and axial muscles, and a similar degree between axial and distal muscles (Figure 6.12). Co-activation of axial and proximal muscles was not common, with only 6% of sites activating both. More than a quarter of all sites co-activated distal and proximal muscles. Contralateral muscles were activated by more than half of sites, with 25% of

sites activating bilaterally located muscles. The highest type of co-activation was between contralateral flexors and extensors; ipsilateral flexors were not activated by any sites. Flexors were never activated bilaterally, and were most commonly activated on the contralateral side of the body. There was a small degree of co-activation of axial muscles and contralateral flexors, as well as axial muscles and contralateral extensors.

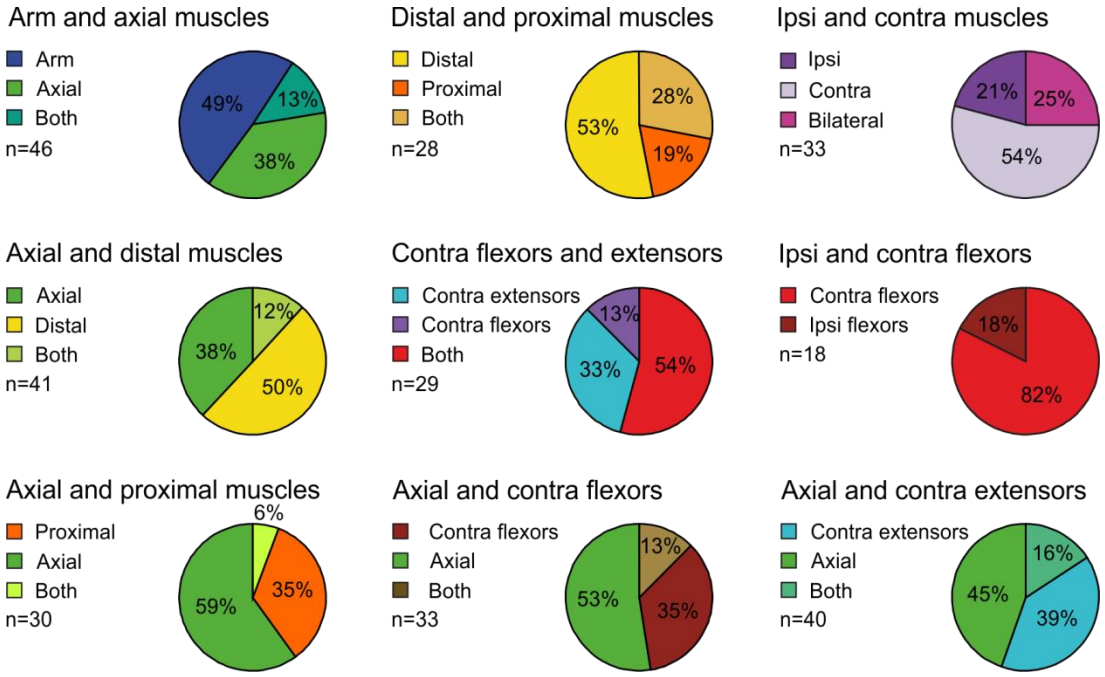

Figure 6.12: Pie charts showing the percentages of sites which activated different types of muscle alone or co-activated with another muscle type. Representing muscles activated by sites stimulated at threshold intensity only. Each pie chart reflects the percentage of each muscle type from the total number of both types examined per chart. N indicates the number of total sites included in each pie chart.

6.5 Discussion

6.5.1 Output divergence

Previous studies have shown that single cat RF axons have branching projections to several spinal segments (Matsuyama *et al.*, 1997), therefore it is surprising to find that in the present experiment, RF sites most commonly elicited responses in only one muscle from the 112 recorded. There are several possible explanations for this, including that it is an accurate reflection of the output divergence of the RST. However given previous findings, this is unlikely. Instead, the low number of muscles activated may have been due to using

threshold stimulation. Benefits of stimulating at threshold intensity include the low levels of current spread, which is ideal for finding the output of the smallest target area possible; single pulse stimulation has been found to activate corticomotoneuronal cells both directly and indirectly, with muscles activated being very similar to those responding in spikeTA (Cheney and Fetz, 1985). However this level of intensity would also be fairly weak, and therefore might only activate the most excitable motoneurons, or may excite more motoneurons but below the level of detection used in the analysis.

Although, significant similarities have been found between spikeTA and stimulusTA responses in the RF, which have been argued to show that single pulse stimulation excites RF cells directly and accurately reflects RST output (Davidson *et al.*, 2007). However this similarity was found in awake, behaving macaques and the accuracy of output effects from single pulse stimulation in decerebrated animals is unknown.

Therefore it is still possible that the number of muscles activated by the sites stimulated at threshold intensity in this experiment is underestimated. This issue is difficult to resolve; using higher intensities than threshold (such as 130% threshold as also used here) have the benefit of stimulating RF cells enough to potentially activate a higher number of the motoneurons projected to by a particular cell, therefore revealing its output more accurately. However, it is then difficult to conclude whether the responding muscles are not actually activated via current spread in the RF. Current spread of single pulse stimulation in the cortex has been found to be quite low, with currents of 10μA limited to the immediate 88μm radial vicinity of the electrode tip (Stoney *et al.*, 1968). So it is possible that current spread in the RF might also be limited.

Potential explanations One explanation of the low output divergence found is that it might be the result of the periodic waves of muscle contraction that both baboons exhibited during this experiment, which seemed to occur mainly in muscles acting on the shoulder and hip. It is possible that only some of the muscles recorded were contracted in these waves, consequently increasing the

excitability of their motoneurons selectively. If the stimulus occurred on top of this excitation, the motoneurons would rapidly be pushed above threshold, resulting in a response in these muscles and not others. This factor may therefore have affected the number of responding muscles seen.

Another explanation might be that primary motor cortex has the ability to gate RST output (Schepens and Drew, 2006), potentially via the common interneurons onto which both of these pathways terminate (Riddle and Baker, 2010). It is possible that decerebration disturbs this gating so that only the strongest responses are seen.

One previous study found that, although the same number of muscles was not recorded for every site stimulated, on average 38% of the (≤9) muscles had a suppressive or facilitatory effect per site (Davidson and Buford, 2004). If this percentage were applied to the current experiment, an average of 43 muscles would be expected to respond per site. This is a very high degree of co-activation, so it is unlikely that the estimates from previous experiments which have recorded far fewer muscles can be compared to those found here.

Lower limb responses Another unanticipated finding here was the lack of any lower limb responses to threshold stimulation. Herbert *et al.* (2010) found no evidence of somatotopy within the RF, therefore it is surprising that repeated penetrations throughout the RF did not elicit lower limb effects at any site. However the fact that leg and foot muscles were activated by 130% three shock stimulation to the RF means that the RF does have connections to these muscles. Explanations for this disparity include the possibility that motoneurons for upper limb muscles receive more RST monosynaptic connections than lower limb muscles, therefore their effects would be seen more readily by single pulse stimulation. This would also explain why responses in lower limb muscles are only seen after trains of three shocks, as trains of stimuli are more likely to elicit responses polysynaptically (Herbert *et al.*, 2010). Stimulus trains have also been suggested to activate alternative pathways to single pulse stimulation (Herbert *et al.*, 2010), a thought prompted

by the finding that typical inhibitory RF synergies (e.g. suppression of ipsilateral extensors and contralateral flexors) can be facilitated when stimulus trains are used. Hence the lower limb activation found in response to stimulus trains may have been via pathways not activated by single pulses. Alternatively it is possible that in intact animals, upper limb muscles are more subject to inhibitory control by the corticospinal tract than lower limb muscles, and that severing this pathway in decerebration removes this inhibition, raising the excitability of the upper limb muscles above that of the lower limb muscles.

If it is to be believed that threshold single pulse stimulation here was too weak to activate all the motoneurons projected to by RF cells, an alternative would be to focus on the responses to 3 shocks. Stimulating sites with trains of 3 shocks at 130% threshold intensity elicited a wider number of muscle responses than single shocks at threshold stimulation. However as trains of stimuli have previously been found to activate more muscles than single shocks (Herbert *et al.*, 2010), suggested to be due to polysynaptic activation (Cheney and Fetz, 1985), it is still difficult to make conclusions about the true level of output divergence of the RST using this stimulation technique. Alternatively, responses to 130% threshold stimulation could be the focus. However although this intensity produced leg effects, therefore representing RF projections to lower limb muscles, it did not activate intrinsic hand muscles which were activated by threshold intensity; reasons for this are unknown.

Earlier findings show that most RST cells in the cat project to both the cervical and lumbar segments of the cord (Peterson *et al.*, 1975), and that at least 20%, (Matsuyama *et al.*, 1997) if not the majority of axons project to both sides of the spinal cord. A primate tracer study found RF projections to bilateral motoneurons, though only the division of cells projecting contralaterally or ipsilaterally were discussed, not individual cells which were bilaterally branching (Sakai *et al.*, 2009). Overall it seems hard to believe that the present results would underestimate divergence so dramatically. Primates are able to use their hands in a more developed manner than cats which is only possible with the ability to co-activate smaller groups of muscles, so it is possible that

the primate RST is actually not as branched in the cat. However, research in the macaque has also found high levels of bilateral effects from single-pulse stimulation (62% of sites, Davidson and Buford, 2006), though it is still possible there are differences between the baboon and the macaque. Although, the RST has been argued as being conserved across different species (Voogd 1998, cited in Sakai 2009).

6.5.2 Fractionation

Fractionation is a term used to describe how independently the motor system can activate different muscles at different times and with different levels of force. If a cell or area from a motor pathway projects to the motoneurons of many different muscles in the same or different limbs, it would be most likely to produce gross movement involving multiple muscles and would therefore have a low level of fractionation. Conversely, if a neuron in a pathway projected to the motoneurons of a small number of muscles, it would be able to produce more precise movements involving those muscles only, making it a highly fractionated pathway. Another way of looking at this is in terms of muscle synergies. It is thought that in order to reduce the number of degrees of freedom of the motor system, motor output regions contain cells which ultimately project to muscles belonging to a synergistic group. These synergies are then flexibly combined to produce more complicated movements. A more fractionated pathway would be suggested to have more synergies, each possibly containing fewer muscles. Studies have demonstrated the limited ability to produce fine finger movements post CST lesion, suggesting that this is due to the fine motor control imposed by the CST upon grosser pre-existing systems (Lawrence and Kuypers, 1968). This might suggest that the most fractionated pathway in the primate and human motor systems is the CST. The level of fractionation of the RST is assumed to be lower than that of the CST due to its more divergent projections.

This was assessed using two different matrix factorisation algorithms, PCA and ICA, which were used here to reduce the dataset down into its underlying synergies. It was thought that a very fractionated pathway would have many

synergies underlying the data, whereas low fractionation would be characterised by few synergies. Both algorithms found the RF to be surprisingly highly fractionated, especially so in ICA. In light of the findings of Tresch *et al.*, (2006) who compared different matrix factorisation techniques, the results from ICA might be considered more reliable, as it was found to extract predetermined synergies from artificial data more accurately than PCA. However it is likely that the high level of fractionation found here reflects the finding that most stimulated sites elicited responses in only one muscle. In order to further investigate this, it would be ideal to carry out PCA and ICA on responses to trains of 3 shocks at 130% threshold intensity, as the output responses to this type of stimulation were more divergent. Unfortunately, an insufficient number of sites were recorded to carry out these analyses with this type of stimulation.

The true level of fractionation of the RST is difficult to assess accurately, given the lack of results from a comparable EMG dataset elicited from other brain regions (such as M1) in the baboon. The level of fractionation could be compared to that found for macaques in Chapter 4. However as the two Chapters recorded from different number of muscles, in order to make comparisons, the number of muscles must be divided by the number of components required to explain 95% of the variance. For any of the 42 components extracted from ICA here, 2.7 muscles were recorded, and for any of the 25 principal components, 4.5 muscles were recorded. In Chapter 4 for new M1, 1.6 muscles were recorded for every (independent or principal) component. For old M1, 1.8 (ICA) or 2 (PCA) muscles were recorded for every component extracted. Hence, as more muscles were required for every component extracted, responses elicited by the RF here could be argued to be less fractionated than those produced by old or new M1 in macaques. However, the present findings and those of previous chapters are not completely comparable, due to the lack of spontaneous activity in the baboons used in this chapter.

6.5.3 Synergies

Comparison with previously found RST synergies A key characteristic of RF output identified by several previous studies is that of ipsilateral flexor facilitation and reciprocal extensor suppression, as well as contralateral flexor suppression and reciprocal extensor facilitation. These facilitatory effects have been shown in the cat (Drew and Rossignol, 1990b, Drew and Rossignol, 1990a), and both facilitatory and suppressive effects found in the macaque (Davidson and Buford, 2004; Davidson and Buford, 2006; Davidson *et al.*, 2007). In the present investigation, threshold stimulation most commonly produced contralateral extensor facilitation, in support of previous findings. The second most common finding here was of contralateral flexor facilitation, which has been reported by only one previous study in the FCR muscle in response to single pulse ICMS, and was outweighed heavily by suppressive effects (Herbert *et al.*, 2010). Though suppressive effects were rarely seen in the present work (due to lack of background activity), one site suppressed an ipsilateral flexor, another site suppressed two contralateral flexors, and another site suppressed an ipsilateral extensor. These results are mainly congruous with the existing literature, apart from the ipsilateral flexor suppression.

A previous study using stimulusTA in the (macaque) RF found axial muscle activation most commonly, followed by extensors then flexors (Herbert *et al.*, 2010). Here the most commonly activated muscle type by threshold single-pulse stimulation was extensors, followed by axial muscles then flexors. These differences might be attributable to the differences in conscious state between the decerebrated baboon used here and the awake, behaving macaques used in the previous experiment.

Laterality of responses Contralateral muscles were activated alone by just over half of all sites, with around a quarter activating ipsilateral sites and the remaining quarter activating both bilaterally located muscles. This supports the previous finding that RF neurons terminate on bilateral sides of the spinal cord (Davidson and Buford, 2006). However the prevalence of bilateral responses here (24% of total sites) was lower than that previously found in the macaque

(62% of sites, Davidson and Buford, 2006), but consistent with tracer findings from the cat that RF neurons terminate mainly ipsilaterally and about 20% of the time bilaterally (Matsuyama *et al.*, 1997). This is still consistent with the idea that stimulusTA effects are fairly representative of spikeTA outputs, as both monosynaptic and disynaptic connections (via interneurons) from RF to bilateral motoneurons have been found in cat (Jankowska *et al.*, 2003).

Inhibitory effects Trains of stimuli are more likely to facilitate muscles suppressed by stimulusTA, though here there were more suppressive effects elicited by trains than single pulses (Herbert *et al.*, 2010). However, the suppressive effects shown here cannot be compared to those shown by Herbert and colleagues as they used awake behaving animals, whereas the present experiment used decerebrated animals. Due to a relative lack of background activation, suppressive effects would be harder to detect in decerebrated animals, so those found here cannot be considered representative of the inhibitory connections controlled by the RF.

Comparison of stroke patient synergies with RST synergies Some key synergies in patients after stroke have been noted. One of these is the tonic activation of flexor muscles alongside extensor weakness in the impaired (contralateral) hand and arm (Kamper *et al.*, 2003). This may be related to CST damage revealing the ipsilaterally descending RST effects of flexor facilitation and extensor suppression. Alternatively it is possible that the RST from the side contralateral to injury would still have flexor suppressive and extensor facilitative effects on motoneurons of the injured arm, which would potentially work with and balance out the ipsilateral RST effects. However this depends on the strength of corticoreticular connections, and whether they have an ipsilateral or contralateral bias; no currently published work can elucidate this finding.

Another synergy is the co-activation of agonist/antagonist muscles including flexors and extensors (Dewald *et al.*, 1995). Here more than half of all sites which produced responses in a (contralateral) flexor or extensor activated both

at the same site, suggesting that this stroke synergy might be related to RST control.

Another key maladaptive synergy exhibited by stroke patients is shoulder abduction and elbow flexion. Here amongst threshold sites only three activated shoulder muscles (posterior or anterior deltoid), though all three of these sites also involved an elbow flexor. However the trapezius and elbow flexor co-activation noted in stroke subjects was not clear in the results here, with trapezius often being activated alone, alongside other axial muscles, or with EDC.

Overall the present results do show some support for the possible RST control of some synergies observed in stroke patients.

Intrinsic finger muscle synergies Recent work has highlighted the role of the RST in finger control. This includes the finding of RF cell input to intrinsic hand motoneurons (Riddle *et al.*, 2009), as well as modulation of RF cells in response to finger movements (Soteropoulos *et al.*, 2012). Additionally, a slightly higher incidence of excitatory post-synaptic potentials (EPSPs) has been found in distal than in proximal muscles after medial longitudinal fasciculus (MLF) stimulation (Riddle *et al.*, 2009). The current experiment has further supported this work by showing that intrinsic hand muscles including 1DI, 2DI and APB are activated by RF single pulse stimulation. One site co-activated 1DI, 2DI and APB alone with no other muscles. No sites activated finger muscles alone, in accordance with the previous suggestions that RF does not have that degree of hand fractionation. This indicates that the RST may be able to control synergistic movements involving multiple fingers such as whole-hand grasps, such as described in the CST-lesioned macaques studied by Lawrence and Kuypers (1968).

6.5.4 Possibility of activation of corticospinal tract by stimulation of the reticulospinal tract

The CST sends collaterals to the RF (Keizer and Kuypers, 1989; Kably and Drew, 1998), so it could be possible that stimulation of the RF also activates the CST, therefore some of the muscle responses observed here maybe have been activated via the CST instead of or as well as the RST. However, one study found that responses of motoneurons to RF stimulation were similar to those elicited in monkeys with chronic CST lesions, suggesting that RF stimulation effects are not due to activation of collaterals from the CST (Shapovalov, 1972). Though when decerebrating the baboons in the current experiment, an acute M1 lesion was made, different from the chronic lesion made by Shapovalov. This distinction is important as in chronically-lesioned animals the CST fibres would have degenerated, whereas after an acute lesion they would still be functional and conductive. Therefore we cannot rule out the possibility of CST activation via RF stimulation in the current experiment.

6.6 Conclusions

This experiment has provided further information on the output divergence of the RF. It has shown that RF sites stimulated at threshold mainly activate muscles located in the arm, followed by axial muscles; sometimes co-activation of these types of muscles were seen. Distal muscles of the arm were the most commonly activated sub-group of muscles, in particular contralateral extensors. The most highly occurring co-activation of muscle subgroups was between contralateral flexors and extensors. Sites most commonly activated only one muscle; however it is unclear whether this accurately reflects the RST output divergence. Fractionation of the RF was quite high, though this fractionation was thought to be the result of most sites activating only one muscle. Due to the uncertainty of the present findings concerning divergence, making any conclusions as to the level of fractionation is difficult.

A recent increase in research carried out on the RF is motivated to a large extent by the possibility that after CST damage post-stroke, the remaining

movement ability is controlled by the undamaged RST. Therefore any similarities between the motor synergies exhibited by stroke subjects and output characteristics of the RF could be seen as evidence to support this view. Supporting results found here include synergies which reflect the common agonist/antagonist co-activation of contralateral flexors and extensors found in stroke patients, as well as the shoulder abduction/elbow flexion synergy.

In conclusion, this work has been the first to examine the muscle output patterns from the baboon RF in all four limbs and the trunk, which may be of importance in informing future research into the role of the RST in post-stroke movement and its potential in recovery.

7 General discussion

7.1 Context

Stroke affects roughly 150,000 new patients every year in the UK alone and often results in limitations of hand function. Since impaired hand function can significantly reduce quality of life, efforts to help restore this function are important. Impairments often result from damage to the major pathway involved in movement control, the corticospinal tract (CST). It has been suggested that residual hand and arm motor capacity post-stroke is at least in part driven by one of the brainstem motor pathways, the reticulospinal tract (RST), which originates in the reticular formation (RF). One way of potentially improving motor outcome in stroke patients is to manipulate the RST in order to strengthen weak but potentially useful connections and weaken maladaptive ones. However, such efforts require more knowledge of the muscles activated by the RST and the co-activation patterns or synergies in which activation occurs.

In addition, a non-invasive method of probing the RST in humans would be very useful. Most previous work on the RST employed invasive approaches in animals, and it is not known to what extent the characteristics of the RST found in other species are conserved in humans. One non-invasive method involves auditory startle in a paradigm known as StartReact. Although the RST has been suggested to underlie the StartReact effect, it is not known whether this pathway is responsible for ultimately activating motoneurons of the muscles involved in the startle response.

In this thesis, we aimed to clarify the role of the RST in the StartReact effect. We also aimed to delineate the range of muscles activated by the RST, the combinations and functional synergies of this activation, and the level of fractionation of resulting movements. These factors were also assessed in

movement evoked by stimulation of two subdivisions of primary motor cortex (old and new M1) to allow comparison to the RST. Furthermore, we probed these characteristics of the RST in muscles of all four limbs and the trunk in baboons, thus permitting assessment of output divergence to the lower limb and the extent of bilateral co-activation; no previously reported experiment had collected such an anatomically widespread EMG dataset.

A final aim was to record truly natural EMG data from monkeys in their home cage environment to assess the level of fractionation and synergies underlying natural movement.

7.2 Summary

While several previous studies used the StartReact effect, the pathways involved had not been fully identified. We found that movements elicited by a startling auditory cue had a significantly lower level of fractionation to those elicited by quiet cues, suggesting that the RST has a role in the control of startle-induced movements. It is hypothesised that these movements are the result of the CST providing an initial, preparatory level of excitation to motoneurons of muscles involved in the forthcoming movement. Upon exposure to a startling stimulus the RST might act to increase this existing level of excitation above threshold, releasing the movement. Alternatively, the motor cortex may send a copy of the motor program for the prepared movement to the RF, which is released by startle-induced RF excitation.

We also investigated two factors relevant to using StartReact to probe the RST: firstly, the validity of a previously used marker for startle, sternocleidomastoid (SCM) muscle activation, and secondly, how many trials are required before habituation of the StartReact effect occurs. Our main argument against the validity of using SCM as a marker for startle was the finding that SCM was also activated by quiet-cued trials. We re-evaluated the conclusions of some previous work which based their conclusions that individual finger movements are not susceptible to startle on the assumed validity of the SCM marker. Instead, here it is argued that individual finger movements might be affected by

startle. Earlier research on habituation of the StartReact effect had focussed on habituation in the SCM muscle, neglecting limb muscles. These studies also used a low ratio of startling: non-startling trials, and were often carried out in non-reaction-time (RT) paradigms, making their results inapplicable to RT tasks. We found that the StartReact effect did not habituate over 160 trials, when presented in a ratio of 1:1 during a RT paradigm. These findings might prove useful when using the StartReact technique in probing the RST in humans if, for example, an experiment required many trials.

Characteristics of the RF, old and new M1 were investigated using stimulus triggered-averaging in macaques. Output divergence of the RF was probably higher than for old and new M1. However, methodological limitations may have led to underestimations in the level of output divergence of each area and may have biased results towards muscles with the most excitable motoneurons. The extent of the underestimation is unknown, and resolving this might prove difficult. One approach would be to examine spike-triggered average responses in muscles for each of these regions, though it would be very time consuming and challenging to gather a large dataset of this type. The RF activated ipsilateral flexors at all sites, providing support of previous findings. It also co-activated muscles more commonly than old or new M1. Fractionation was roughly the same in movements produced by stimulation of old M1 and the RF, though possibly slightly higher in the RF and highest overall in those produced by new M1. This finding also supports the notion that the RST underlies less fractionated startle-induced movements.

The number of synergies produced by the RF, old and new M1 was quite different, as were the number and type of muscles involved in each synergy. For example, old and new M1 each produced some synergies consisting of only two or three muscles, whereas RF synergies were composed of seven to fourteen muscles each. It is interesting that multiple separate motor control systems with slightly different characteristics have evolved alongside each other, rather than one existing adapting new projections to allow more fractionated

movement. This suggests that retaining this separation is useful, perhaps allowing more flexible combination of synergies controlled by each pathway.

We present data from a macaque carrying out natural behaviour in its home cage, and assess and compare the level of fractionation and synergies produced by the RF as well as old and new M1. This contrasts with previously reported studies using pseudo-natural behaviour during a behavioural task. Three to four key synergies were found to underlie the data, which is strikingly similar to that found in other studies into natural movement. Although previous studies had not used truly natural movement, the consistency of the number of underlying synergies suggests that this finding is a robust and accurate reflection of the data. Since these synergies explain much of the data they may originate from an area of low fractionation such as the RST. Smaller synergies were also found in addition to these dominant synergies; these might reflect the more fractionated contribution to natural movement by monosynaptic projections to motoneurons from the primary motor area. However, these explanations remain conjectures and the contribution of the CST and RST to natural movement requires further investigation.

We present the first experiment to record from a very large number of muscles across all four limbs of a baboon. Stimulation of the baboon RF most commonly activated one muscle though this might be due to limitations of the stimulation technique used. Bilateral responses were seen, showing that the baboon RF has projections to both sides of the spinal cord, either directly or via excitatory interneurons. Surprisingly, in light of the long-held belief that the predominant role of the RST is in control of axial muscles, responses in distal muscles were more common than those in proximal muscles. Leg and foot responses were elicited by higher stimulation intensities or trains of pulses but not with threshold stimulation. One potential explanation is that upper limb muscles may receive more monosynaptic RST connections than lower limb muscles, therefore biasing the results towards upper limb muscles.

7.3 Future research

Future research could employ the StartReact technique to characterise the output divergence, level of fractionation and synergies produced by the RF in human subjects. Animal studies should elucidate to what extent the RF, old and new M1 each contribute to natural movement. Additionally, further clarification of the role of the RF, old and new M1 in the control of fine, fractionated finger movements is required. This could be achieved by measuring the extent to which fine finger movements remain possible after selective lesions of each area.

It would also be interesting to consider whether the synergies and projection patterns produced by these pathways alter following a lesion. Previous work found that the magnitude of excitatory post-synaptic potentials in motoneurons of particular muscles increases after CST lesion, showing that connections might strengthen, though this does not necessarily imply that synergies also change. There are some synergies exhibited by stroke subjects but not healthy humans, which could either be normally produced by the RST and exposed by CST damage, or result from stroke-induced adaptive changes to normal synergies. It would be valuable to explore this further, which could be done by examining the differences in ICA-extracted synergies on the stimulus-triggered average responses as carried out here, before and after CST lesion.

Eventually, experimental techniques to manipulate the characteristics of movements produced by the RST need to be investigated further prior to potential translation of such techniques to aid motor recovery post-stroke. It is hoped that the characteristics defined here will ultimately contribute to achieving this goal.

A Details of macaques used

A.1 General details

Name	Data gathered	Chapter(s)	Species	Date of birth	Sex	Weight
Sally	Chronic	4	*Macaca mulatta*	10/6/2008	F	5.5kg
Uwee	Natural and chronic	4 and 5	*Macaca mulatta*	29/5/2010	F	5.5kg

A.2 Muscles recorded

Macaque	Muscles	Macaque	Muscles
Sally	1DI ADM APB Anterior deltoid Biceps long Biceps short Brachialis BR Coracobrachialis ED2,3 ED4,5 EDC FCR FCU FDL FDP Latissimus dorsi PL PM Posterior deltoid Pronator teres	Uwee	1DI ADM APB Anterior deltoid Biceps long BR ECR ECU EDC FCR FCU FDP FDS Infraspinatus Latissimus dorsi PM Posterior deltoid Triceps

B Details of baboons used

B.1 General details

Name	Chapter	Species	Date of birth	Sex	Weight
Embe	6	*Pan anubis*	Unknown – wild caught	M	23.5kg
Fundi	6	*Pan anubis*	Unknown – wild caught	M	23.5kg

B.2 Muscles recorded

Muscles: upper limb	Muscles: trunk	Muscles: lower limb
1DI	EAO	Abductor digiti minimi
2DI	Rectus abdominis	Abductor hallucis
ADM	Transversus abdominis	Adductor longus
APB		Adductor magnus
AbPL		Biceps femoris
Anterior deltoid		Extensor digitorum brevis
Biceps short		Extensor digitorum longus
Biceps long		Extensor hallucis
BR		Flexor digitorum brevis
Brachialis		Flexor digitorum longus
Coracobrachialis		Flexor hallucis brevis
ECRB		Gastrocnemius
ECRL		Gracilis
ECU		Iliopsoas
EDC		Pectineus
EPB		Rectus femoris
FCR		Sartorius
FCU		Semimembranosus
FDP		Soleus
FDS		Tibialis anterior
FPL		Tractus iliotibialis
Infraspinatus		Vastus medialis
Latissimus dorsi		
PL		
PM		
Posterior deltoid		
Pronator teres		
Trapezius		
Teres major		
Triceps lateral		
Triceps long		

References

Abel K, Waikar M, Pedro B, Hemsley D and Geyer M (1998) Repeated testing of prepulse inhibition and habituation of the startle reflex: a study in healthy human controls. *J Psychopharmacol* **12**, 330-337.

Adamson J, Beswick A and Ebrahim S (2004) Is stroke the most common cause of disability? *J Stroke Cerebrovasc Dis* **13**, 171-177.

Ajiboye AB and Weir RF (2009) Muscle synergies as a predictive framework for the EMG patterns of new hand postures. *J Neural Eng* **6**, 036004.

Andersen P, Hagan PJ, Phillips CG and Powell TP (1975) Mapping by microstimulation of overlapping projections from area 4 to motor units of the baboon's hand. *Proc R Soc Lond B Biol Sc* **188**, 31-36.

Anderson KD (2004) Targeting recovery: priorities of the spinal cord-injured population. *J Neurotrauma* **21**, 1371-1383.

Armand J, Olivier E, Edgley SA and Lemon RN (1997) Postnatal development of corticospinal projections from motor cortex to the cervical enlargement in the macaque monkey. *J Neurosc* **17**, 251-266.

Asanuma H, Arnold A and Zarzecki P (1976) Further study on the excitation of pyramidal tract cells by intracortical microstimulation. *Exp Brain Res* **26**, 443-461.

Association S (2012) Webster factsheet: What is a stroke? Available at: http://www.stroke.org.uk/factsheet/what-is-a-stroke (Accessed: 21/08/2014).

Baker SN, Olivier E and Lemon RN (1998) An investigation of the intrinsic circuitry of the motor cortex of the monkey using intra-cortical microstimulation. *Exp Brain Res* **123**, 397-411.

Bannatyne BA, Edgley SA, Hammar I, Jankowska E and Maxwell DJ (2003) Networks of inhibitory and excitatory commissural interneurons mediating crossed reticulospinal actions. *Eur J Neurosci* **18**, 2273-2284.

Bell AJ and Sejnowski TJ (1995) An information-maximization approach to blind separation and blind deconvolution. *Neural Comput* **7**, 1129-1159.

Bennett KM and Lemon RN (1996) Corticomotoneuronal contribution to the fractionation of muscle activity during precision grip in the monkey. *J Neurophysiol* **75**, 1826-1842.

Bizzi E, D'Avella A, Saltiel P and Tresch M (2002) Modular organization of spinal motor systems. *Neuroscientist* **8**, 437-442.

Bohannon RW (2007) Muscle strength and muscle training after stroke. *J Rehabil Med* **39**, 14-20.

Bortoff GA and Strick PL (1993) Corticospinal terminations in two new-world primates: further evidence that corticomotoneuronal connections provide part of the neural substrate for manual dexterity. *J Neurosci* **13**, 5105-5118.

Bourbonnais D, Vanden Noven S, Carey KM and Rymer WZ (1989) Abnormal spatial patterns of elbow muscle activation in hemiparetic human subjects. *Brain* **112**, 85-102.

Brocard F and Dubuc R (2003) Differential contribution of reticulospinal cells to the control of locomotion induced by the mesencephalic locomotor region. *J Neurophysiol* **90**, 1714-1727.

Brochier T, Spinks RL, Umilta MA and Lemon RN (2004) Patterns of muscle activity underlying object-specific grasp by the macaque monkey. *J Neurophysiol* **92**, 1770-1782.

Brown P, Day BL, Rothwell JC, Thompson PD and Marsden CD (1991a) The effect of posture on the normal and pathological auditory startle reflex. *J Neurol Neurosurg Psychiatry* **54**, 892-897.

Brown P, Rothwell JC, Thompson PD, Britton TC, Day BL and Marsden CD (1991b) New observations on the normal auditory startle reflex in man. *Brain* **114**, 1891-1902.

Buford JA and Davidson AG (2004) Movement-related and preparatory activity in the reticulospinal system of the monkey. *Exp Brain Res* **159**, 284-300.

Buys EJ, Lemon RN, Mantel GW and Muir RB (1986) Selective facilitation of different hand muscles by single corticospinal neurones in the conscious monkey. *J Physiol* **381**, 529-549.

Caeser M, Ostwald J and Pilz PK (1989) Startle responses measured in muscles innervated by facial and trigeminal nerves show common modulation. *Behav Neurosci* **103**, 1075-1081.

Canedo A (1997) Primary motor cortex influences on the descending and ascending systems. *Prog Neurobiol* **51**, 287-335.

Canedo A and Lamas JA (1993) Pyramidal and corticospinal synaptic effects over reticulospinal neurones in the cat. *J Physiol* **463**, 475-489.

Capaday C, Ethier C, Van Vreeswijk C and Darling WG (2013) On the functional organization and operational principles of the motor cortex. *Front Neural Circuits* **7**, 66.

Carlsen AN, Chua R, Inglis JT, Sanderson DJ and Franks IM (2003) Startle response is dishabituated during a reaction time task. *Exp Brain Res* **152**, 510-518.

Carlsen AN, Chua R, Inglis JT, Sanderson DJ and Franks IM (2004a) Can prepared responses be stored subcortically? *Exp Brain Res* **159**, 301-309.

Carlsen AN, Chua R, Inglis JT, Sanderson DJ and Franks IM (2004b) Prepared movements are elicited early by startle. *J Mot Behav* **36**, 253-264.

Carlsen AN, Chua R, Inglis JT, Sanderson DJ and Franks IM (2009) Differential effects of startle on reaction time for finger and arm movements. *J Neurophysiol* **101**, 306-314.

Carlsen AN, Dakin CJ, Chua R and Franks IM (2007) Startle produces early response latencies that are distinct from stimulus intensity effects. *Exp Brain Res* **176**, 199-205.

Carlsen AN, Lam MY, Maslovat D and Chua R (2011a) Reaction time effects due to imperative stimulus modality are absent when a startle elicits a pre-programmed action. *Neurosci Lett* **500**,177-181.

Carlsen AN, Maslovat D, Lam MY, Chua R and Franks IM (2011b) Considerations for the use of a startling acoustic stimulus in studies of motor preparation in humans. *Neurosci Biobehav Rev* **35**, 366-376.

Castellini C and van der Smagt P (2013) Evidence of muscle synergies during human grasping. *Biol Cybern* **107**, 233-245.

Cerri G, Shimazu H, Maier MA and Lemon RN (2003) Facilitation from ventral premotor cortex of primary motor cortex outputs to macaque hand muscles. *J Neurophysiol* **90**, 832-842.

Chen R and Hallett M (1999) The time course of changes in motor cortex excitability associated with voluntary movement. *Can J Neurol Sci* **26**, 163-169.

Chen R, Yaseen Z, Cohen LG and Hallett M (1998) Time course of corticospinal excitability in reaction time and self-paced movements. *Ann Neurol* **4**, 317-325.

Cheney PD and Fetz EE (1985) Comparable patterns of muscle facilitation evoked by individual corticomotoneuronal (CM) cells and by single intracortical microstimuli in primates: evidence for functional groups of CM cells. *J Neurophysiol* **53**, 786-804.

Cheney PD, Fetz EE and Palmer SS (1985) Patterns of facilitation and suppression of antagonist forelimb muscles from motor cortex sites in the awake monkey. *J Neurophysiol* **53**, 805-820.

Cheung VC, d'Avella A, Tresch MC and Bizzi E (2005) Central and sensory contributions to the activation and organization of muscle synergies during natural motor behaviors. *J Neurosci* **25**, 6419-6434.

Cheung VC, Piron L, Agostini M, Silvoni S, Turolla A and Bizzi E (2009) Stability of muscle synergies for voluntary actions after cortical stroke in humans. *Proc Natl Acad Sci U S A* **106**, 19563-19568.

Cheung VC, Turolla A, Agostini M, Silvoni S, Bennis C, Kasi P, Paganoni S, Bonato P and Bizzi E (2012) Muscle synergy patterns as physiological markers of motor cortical damage. *Proc Natl Acad Sci U S A* **109**, 14652-14656.

Chouinard PA and Paus T (2006) The primary motor and premotor areas of the human cerebral cortex. *Neuroscientist* **12**, 143-152.

Chow JW and Stokic DS (2011) Force control of quadriceps muscle is bilaterally impaired in subacute stroke. *J Appl Physiol* **111**, 1290-1295.

Clough JF, Kernell D and Phillips CG (1968) The distribution of monosynaptic excitation from the pyramidal tract and from primary spindle afferents to motoneurones of the baboon's hand and forearm. *J Physiol* **198**, 145-166.

Cox LA, Comuzzie AG, Havill LM, Karere GM, Spradling KD, Mahaney MC, Nathanielsz PW, Nicolella DP, Shade RE, Voruganti S and VandeBerg JL (2013) Baboons as a model to study genetics and epigenetics of human disease. *Ilar j* **54**, 106-121.

Cruz TH and Dhaher YY (2009) Impaired lower limb muscle synergies post-stroke. *Conf Proc IEEE Eng Med Biol Soc* **2009**, 3956-3959.

d'Avella A and Bizzi E (2005) Shared and specific muscle synergies in natural motor behaviors. *Proc Natl Acad Sci U S A* **102**, 3076-3081.

d'Avella A, Portone A, Fernandez L and Lacquaniti F (2006) Control of fast-reaching movements by muscle synergy combinations. *J Neurosci* **26**, 7791-7810.

d'Avella A, Saltiel P and Bizzi E (2003) Combinations of muscle synergies in the construction of a natural motor behavior. *Nat Neurosci* **6**, 300-308.

Darbutas T, Juodzbaliene V, Skurvydas A and Krisciunas A (2013) Dependence of reaction time and movement speed on task complexity and age. *Medicina (Kaunas)* **49**, 18-22.

Darling WG, Pizzimenti MA and Morecraft RJ (2011) Functional recovery following motor cortex lesions in non-human primates: experimental implications for human stroke patients. *J Integr Neurosci* **10,** 353-384.

Davidoff RA (1990) The pyramidal tract. *Neurology* **40**, 332-339.

Davidson AG and Buford JA (2004) Motor outputs from the primate reticular formation to shoulder muscles as revealed by stimulus-triggered averaging. *J Neurophysiol* **92**, 83-95.

Davidson AG and Buford JA (2006) Bilateral actions of the reticulospinal tract on arm and shoulder muscles in the monkey: stimulus triggered averaging. *Exp Brain Res* **173**, 25-39.

Davidson AG, Schieber MH and Buford JA (2007) Bilateral spike-triggered average effects in arm and shoulder muscles from the monkey pontomedullary reticular formation. *J Neurosci* **27**, 8053-8058.

Davis M, Gendelman DS, Tischler MD and Gendelman PM (1982) A primary acoustic startle circuit: lesion and stimulation studies. *J Neurosci* **2**, 791-805.

Deliagina TG, Beloozerova IN, Zelenin PV and Orlovsky GN (2008) Spinal and supraspinal postural networks. *Brain Res Rev* **57**, 212-221.

Dettmers C, Teske U, Hamzei F, Uswatte G, Taub E and Weiller C (2005) Distributed form of constraint-induced movement therapy improves functional outcome and quality of life after stroke. *Arch Phys Med Rehab* **86**, 204-209.

Dewald JP, Pope PS, Given JD, Buchanan TS and Rymer WZ (1995) Abnormal muscle coactivation patterns during isometric torque generation at the elbow and shoulder in hemiparetic subjects. *Brain* **118**, 495-510.

Dewald JP, Sheshadri V, Dawson ML and Beer RF (2001) Upper-limb discoordination in hemiparetic stroke: implications for neurorehabilitation. *Top Stroke Rehabi* **8**, 1-12.

Donoghue JP, Leibovic S and Sanes JN (1992) Organization of the forelimb area in squirrel monkey motor cortex: representation of digit, wrist, and elbow muscles. *Exp Brain Re*s **89**, 1-19.

Drew T (1991) bFunctional organization within the medullary reticular formation of the intact unanesthetized cat. III. Microstimulation during locomotion. *J Neurophysio* **66**, 919-938.

Drew T, Dubuc R and Rossignol S (1986) Discharge patterns of reticulospinal and other reticular neurons in chronic, unrestrained cats walking on a treadmill. *J Neurophysiol* **55**, 375-401.

Dum RP and Strick PL (1991) The origin of corticospinal projections from the premotor areas in the frontal lobe. *J Neurosci* **11**, 667-689.

Eidelberg E, Nguyen LH and Deza LD (1986) Recovery of locomotor function after hemisection of the spinal cord in cats. *Brain Res Bull* **16**, 507-515.

Elston GN, Benavides-Piccione R and DeFelipe J (2001) The pyramidal cell in cognition: a comparative study in human and monkey. *J Neurosci* **21**, 163.

Ethier C, Brizzi L, Giguere D and Capaday C (2007) Corticospinal control of antagonistic muscles in the cat. *Eur J Neurosci* **26**, 1632-1641.

Eyre JA, Miller S, Clowry GJ, Conway EA and Watts C (2000) Functional corticospinal projections are established prenatally in the human foetus permitting involvement in the development of spinal motor centres. *Brain* **123**, 51-64.

Fetz EE and Cheney PD (1980) Postspike facilitation of forelimb muscle activity by primate corticomotoneuronal cells. *J Neurophysiol* **44**, 751-772.

Frings M, Awad N, Jentzen W, Dimitrova A, Kolb FP, Diener HC, Timmann D and Maschke M (2006) Involvement of the human cerebellum in short-term and long-term habituation of the acoustic startle response: A serial PET study. *Clin Neurophysiol* **117**, 1290-1300.

Fritz N, Illert M, Kolb F, Lemon R, Muir R, van der Burg J, Wiedemann E and Yamaguchi T (1985) The cortico-motoneuronal input to hand and forearm motoneurones in the anaesthetized monkey (Abstract). *J Physiol*, 366.

Galea MP, Hammar I, Nilsson E and Jankowska E (2010) Bilateral postsynaptic actions of pyramidal tract and reticulospinal neurons on feline erector spinae motoneurons. *J Neurosci* **30**, 858-869.

Glees P and Cole J (1950) Recovery of skilled motor functions after small repeated lesions of motor cortex in macaque. *J Neurophysiol* **13**, 137-148.

Graziano MS, Taylor CS and Moore T (2002) Complex movements evoked by microstimulation of precentral cortex. *Neuron* **34**, 841-851.

Griffin DM, Hudson HM, Belhaj-Saif A and Cheney PD (2014a) EMG activation patterns associated with high frequency, long-duration intracortical microstimulation of primary motor cortex. *J Neurosci* **34**, 1647-1656.

Griffin DM, Hudson HM, Belhaj-Saif A and Cheney PD (2014b) Hijacking cortical motor output with repetitive microstimulation. *J Neurosci* **31**, 13088-13096.

Grillner S, Hongo T and Lund S (1968) The origin of descending fibres monosynaptically activating spinoreticular neurones. *Brain Res* **10**, 259-262.

Groves PM, Wilson CJ and Boyle RD (1974) Brain stem pathways, cortical modulation, and habituation of the acoustic startle response. *Behav Biol* **10**, 391-418.

Halaki M and Ginn K (2012) Normalization of EMG signals: to normalize or not to normalize and what to normalize to? In Naik, G. R. (ed.) *Computational Intelligence in Electromyography Analysis- A Perspective on Current Applications and Future Challenges*. InTech.

Hallett M (2001) Plasticity of the human motor cortex and recovery from stroke. *Brain Res Brain Res Rev* **36**, 169-174.

Hammond GR (1973) Lesions of pontine and medullary reticular formation and prestimulus inhibition of the acoustic startle reaction in rats. *Physiol Behav* **10**, 239-243.

Hart CB and Giszter SF (2004) Modular premotor drives and unit bursts as primitives for frog motor behaviors. *J Neurosci* **24**, 5269-5282.

Hayes NL and Rustioni A (1981) Descending projections from brainstem and sensorimotor cortex to spinal enlargements in the cat. Single and double retrograde tracer studies. *Exp Brain Res* **41**, 89-107.

Heffner R and Masterton B (1975) Variation in form of the pyramidal tract and its relationship to digital dexterity. *Brain Behav Evol* **12**, 161-200.

Herbert WJ, Davidson AG and Buford JA (2010) Measuring the motor output of the pontomedullary reticular formation in the monkey: do stimulus-triggered averaging and stimulus trains produce comparable results in the upper limbs? *Exp Brain Res* **203**, 271-283.

Herculano-Houzel S, Collins CE, Wong P and Kaas JH (2007) Cellular scaling rules for primate brains. *Proc Natl Acad Sci U S A* **104**, 3562-3567.

Hlustik P, Solodkin A, Gullapalli RP, Noll DC and Small SL (2001) Somatotopy in human primary motor and somatosensory hand representations revisited. *Cereb Cortex* **11**, 312-321.

Holdefer RN and Miller LE (2002) Primary motor cortical neurons encode functional muscle synergies. *Exp Brain Res* **146**, 233-243.

Holstege G and Kuypers HG 57 (1982) The antomy of brain stem pathways to the spinal cord in cat. A labeled amino acid tracing study. *Prog Brain Res* **57**, 145-175.

Honeycutt CF, Kharouta M and Perreault EJ (2013) Evidence for reticulospinal contributions to coordinated finger movements in humans. *J Neurophysiol* **110**, 1476-83.

Howard IS, Ingram JN, Kording KP and Wolpert DM (2009) Statistics of natural movements are reflected in motor errors. *J Neurophysiol* **102**, 1902-1910.

Huntley GW and Jones EG (1991) Relationship of intrinsic connections to forelimb movement representations in monkey motor cortex: a correlative anatomic and physiological study. *J Neurophysiol* **66**, 390-413.

Hyvarinen A and Oja E (2000) Independent component analysis: algorithms and applications. *Neural Netw* **13**, 411-430.

Ilic TV, Potter-Nerger M, Holler I, Siebner HR, Ilic NV, Deuschl G and Volkmann J (2011) Startle stimuli exert opposite effects on human cortical and spinal motor system excitability in leg muscles. *Physiol Res* **60**, S101-106.

Ingram JN, Kording KP, Howard IS and Wolpert DM (2008) The statistics of natural hand movements. *Exp Brain Res* **188**, 223-236.

Isa T, Ohki Y, Seki K and Alstermark B (2006) Properties of propriospinal neurons in the C3-C4 segments mediating disynaptic pyramidal excitation to forelimb motoneurons in the macaque monkey. *J Neurophysiol* **95**, 3674-3685.

Ivanenko YP, Poppele RE and Lacquaniti F (2004) Five basic muscle activation patterns account for muscle activity during human locomotion. *J Physiol* **556**, 267-282.

Jahn K, Deutschlander A, Stephan T, Kalla R, Wiesmann M, Strupp M and Brandt T (2008) Imaging human supraspinal locomotor centers in brainstem and cerebellum. *Neuroimage* **39**, 786-792.

Jaiser SR, Barnes JD, Baker SN and Baker MR (2014) A multiple regression model of normal central and peripheral motor conduction times. *Muscle Nerve*. DOI: 10.1002/mus.24427.

Jankowska E, Hammar I, Slawinska U, Maleszak K and Edgley SA (2003) Neuronal basis of crossed actions from the reticular formation on feline hindlimb motoneurons. *J Neurosci* **23**, 1867-1878.

Jankowska E, Padel Y and Tanaka R (1975) The mode of activation of pyramidal tract cells by intracortical stimuli. *J Physiol* **249**, 617-636.

Jankowska E, Padel Y and Tanaka R (1976)Disynaptic inhibition of spinal motoneurones from the motor cortex in the monkey. *J Physiol* **258**, 467-487.

Kably B and Drew T (1998) Corticoreticular pathways in the cat. I. Projection patterns and collaterization. *J Neurophysiol* **80**, 389-405.

Kamper DG, Harvey RL, Suresh S and Rymer WZ (2003) Relative contributions of neural mechanisms versus muscle mechanics in promoting finger extension deficits following stroke. *Muscle Nerve* **28**, 309-318.

Kasser RJ and Cheney PD (1985) Characteristics of corticomotoneuronal postspike facilitation and reciprocal suppression of EMG activity in the monkey. *J Neurophysiol* **53**, 959-978.

Keizer K and Kuypers HG (1989) Distribution of corticospinal neurons with collaterals to the lower brain stem reticular formation in monkey (Macaca fascicularis). *Exp Brain Res* **74**, 311-318.

Kikuchi Y (2010) Comparative analysis of muscle architecture in primate arm and forearm. *Anat Histol Embryol* **39**, 93-106.

Kilner JM, Baker SN and Lemon RN (2002) A novel algorithm to remove electrical cross-talk between surface EMG recordings and its application to the measurement of short-term synchronisation in humans. *J Physiol* **538**, 919-930.

Klein Breteler MD, Simura KJ and Flanders M (2007) Timing of muscle activation in a hand movement sequence. *Cereb Cortex* **17**, 803-815.

Kohfeld DL (1969) Effects of the intensity of auditory and visual ready signals on simple reaction time. *J Exp Psychol* **82**, 88-95.

Komai H and McDowell TS (2001) Local anesthetic inhibition of voltage-activated potassium currents in rat dorsal root ganglion neurons. *Anesthesiology* **94**, 1089-1095.

Kumru H and Valls-Sole J (2006) Excitability of the pathways mediating the startle reaction before execution of a voluntary movement. *Exp Brain Res* **169**, 427-432.

Kuypers HG (1962) Corticospinal connections: postnatal development in the rhesus monkey. *Science* **138**, 678-680.

Kuypers HG 57 (1982) A New Look at the Organization of the Motor System. *Prog Brain Res* **57,** 381-403.

Kuypers HG (1987) Some aspects of the organization of the output of the motor cortex. *Ciba Foundation symposium* **132**, 63-82.

Lamas JA, Martinez L and Canedo A (1994) Pericruciate fibres to the red nucleus and to the medial bulbar reticular formation. *Neuroscience* **62**, 115-124.

Landgren S, Phillips CG and Porter R (1962) Cortical fields of origin of the monosynaptic pyramidal pathways to some alpha motoneurones of the baboon's hand and forearm. *J Physiol* **161**, 112-125.

Lang CE and Schieber MH (2003) Differential impairment of individuated finger movements in humans after damage to the motor cortex or the corticospinal tract. *J Neurophysiol* **90**, 1160-1170.

Lang CE and Schieber MH (2004) Human finger independence: limitations due to passive mechanical coupling versus active neuromuscular control. *J Neurophysiol* **92**, 2802-2810.

Lashley KS (1924) Studies of Cerebral Function in Learning (VI). *Psychol Rev* **31**, 369-375.

Lawrence DG and Hopkins DA (1976) The development of motor control in the rhesus monkey: evidence concerning the role of corticomotoneuronal connections. *Brain* **99**, 235-254.

Lawrence DG and Kuypers HG (1968) The functional organization of the motor system in the monkey. I. The effects of bilateral pyramidal lesions. *Brain* **91**, 1-14.

Leaton RN, Cassella JV and Borszcz GS (1985) Short-term and long-term habituation of the acoustic startle response in chronic decerebrate rats. *Behav Neurosci* **99**, 901-912.

Leigh SR (2004) Brain growth, life history, and cognition in primate and human evolution. *Am J Primatol* **62**, 139-164.

Lemon R (1984) *Methods for neuronal recording in conscious animals*. Chichester, West Sussex: John Wiley & Sons.

Lemon R, Sasaki S, Naito K, Yoshimura K, Isa T, Seki K, Pettersson LG, Alstermark B and Ohki Y (2004) Cortico-motoneuronal system and dexterous finger movements (multiple letters). *J Neurophysiol* **92**, 3601-3603.

Lemon RN (2008) Descending pathways in motor control. *Ann Rev Neurosci* **31**, 195-218.

Lemon RN, Muir RB and Mantel GW (1987) The effects upon the activity of hand and forearm muscles of intracortical stimulation in the vicinity of corticomotor neurones in the conscious monkey. *Exp Brain Res* **66**, 621-637.

Leocani L, Cohen LG, Wassermann EM, Ikoma K and Hallett M (2000) Human corticospinal excitability evaluated with transcranial magnetic stimulation during different reaction time paradigms. *Brain* **123**, 1161-1173.

Leyton ASF and Sherrington CS (1917) Observations on the excitable cortex of the chimpanzee, orangutan and gorilla. *Exp Physiol* **11**, 135-222.

Li L, Steidl S and Yeomans JS (2001) Contributions of the vestibular nucleus and vestibulospinal tract to the startle reflex. *Neuroscience* **106**, 811-821.

Loh MN, Kirsch L, Rothwell JC, Lemon RN and Davare M (2010) Information about the weight of grasped objects from vision and internal models interacts within the primary motor cortex. *J Neurosci* **30**, 6984-6990.

Madhavan S, Krishnan C, Jayaraman A, Rymer WZ and Stinear JW (2011) Corticospinal tract integrity correlates with knee extensor weakness in chronic stroke survivors. *Clin Neurophysiol* **122**, 1588-1594.

Maier MA, Olivier E, Baker SN, Kirkwood PA, Morris T and Lemon RN (1997) Direct and indirect corticospinal control of arm and hand motoneurons in the squirrel monkey (Saimiri sciureus). *J Neurophysiol* **78**, 721-733.

Martin RF and Bowden DM (1996) A stereotaxic template atlas of the macaque brain for digital imaging and quantitative neuroanatomy. *Neuroimage* **4**, 119-150.

Matsuyama K, Takakusaki K, Nakajima K and Mori S (1997) Multi-segmental innervation of single pontine reticulospinal axons in the cervico-thoracic region of the cat: anterograde PHA-L tracing study. *J Comp Neurol* **377**, 234-250.

McKiernan BJ, Marcario JK, Karrer JH and Cheney PD (1998) Corticomotoneuronal postspike effects in shoulder, elbow, wrist, digit, and intrinsic hand muscles during a reach and prehension task. *J Neurophysiol* **80**, 1961-1980.

Meier JD, Aflalo TN, Kastner S and Graziano MSA (2008) Complex organization of human primary motor cortex: A high-resolution fMRI study. *J Neurophysiol* **100**, 1800-1812.

Miller DM, Klein CS, Suresh NL and Rymer WZ (2014) Asymmetries in vestibular evoked myogenic potentials in chronic stroke survivors with spastic hypertonia: Evidence for a vestibulospinal role. *Clin Neurophysiol* 1388-2457.

Neckel N, Pelliccio M, Nichols D and Hidler J (2006) Quantification of functional weakness and abnormal synergy patterns in the lower limb of individuals with chronic stroke. *J Neuroeng Rehabil* **3**, 17.

Nonnekes J, Geurts ACH, Oude Nijhuis LB, Van Geel K, Snijders AH, Bloem BR and Weerdesteyn V (2014) Reduced StartReact effect and freezing of gait in Parkinson's disease: Two of a kind? *J Neurol* **261**, 943-50.

Nonnekes J, van Geel K, Oude Nijhuis LB, Bloem BR, Geurts AC and Weerdesteyn V (2013) Loading enhances the occurrence of startle responses in leg muscles. *Neuroscience* **240**,186-190.

Nudo RJ and Milliken GW (1996) Reorganization of movement representations in primary motor cortex following focal ischemic infarcts in adult squirrel monkeys. *J Neurophysiol* **75**, 2144-2149.

O Shea J, Boudrias MH, Stagg CJ, Bachtiar V, Kischka U, Blicher JU and Johansen-Berg H (2014) Predicting behavioural response to TDCS in chronic motor stroke. *Neuroimage*, **15**, 924-933.

Overduin SA, d Avella A, Carmena JM and Bizzi E (2012) Microstimulation activates a handful of muscle synergies. *Neuron*, **76**, 1071-1077.

Overduin SA, d Avella A, Roh J and Bizzi E (2008) Modulation of muscle synergy recruitment in primate grasping , *J Neurosci*, **28**, 880-892.

Pandian S and Arya KN (2013) Motor impairment of the ipsilesional body side in poststroke subjects. *J Bodyw Mov Ther* **17**, 495-503.

Park MC, Belhaj-Saif A and Cheney PD (2004) Properties of primary motor cortex output to forelimb muscles in rhesus macaques. *J Neurophysiol* **92**, 2968-2984.

Parvizi J and Damasio A (2001) Consciousness and the brainstem. *Cognition* **79**, 135-160.

Passingham R (2009) How good is the macaque monkey model of the human brain? *Curr Opin Neurobiol* **19**, 6-11.

Passingham R, Perry H and Wilkinson F (1978) Failure to develop a precision grip in monkeys with unilateral neocortical lesions made in infancy. *Brain Res* **145**, 410-414.

Pellet J (1990) Neural organization in the brainstem circuit mediating the primary acoustic head startle: an electrophysiological study in the rat. *Physiol Behav* **48**, 727-739.

Penfield W and Rasmussen T (1950) *The Cerebral Cortex of Man*. New York: MacMillan.

Perreault MC, Drew T and Rossignol S (1993) Activity of medullary reticulospinal neurons during fictive locomotion. *J Neurophysiol* **69**, 2232-2247.

Perreault MC, Rossignol S and Drew T (1994) Microstimulation of the medullary reticular formation during fictive locomotion. *J Neurophysiol* **71**, 229-245.

Peterson BW, Maunz RA, Pitts NG and Mackel RG (1975) Patterns of projection and branching of reticulospinal neurons. *Exp Brain Res* **23**, 333-351.

Peterson BW, Pitts NG and Fukushima K (1979) Reticulospinal connections with limb and axial motoneurons. *Exp Brain Res* **36**, 1-20.

Pflieger JF and Dubuc R (2004) Vestibulo-reticular projections in adult lamprey: their role in locomotion. *Neuroscience* **129**, 817-829.

Pilz PK, Caeser M and Ostwald J (1988) Comparative threshold studies of the acoustic pinna, jaw and startle reflex in the rat. *Physiol Behav* **43**, 411-415.

Pouydebat E, Gorce P, Coppens Y and Bels V (2009) Biomechanical study of grasping according to the volume of the object: human versus non-human primates. *J Biomech* **42**, 266-272.

Prentice SD and Drew T (2001) Contributions of the reticulospinal system to the postural adjustments occurring during voluntary gait modifications. *J Neurophysiol* **85**, 679-698.

Prut Y and Fetz EE (1999) Primate spinal interneurons show pre-movement instructed delay activity. *Nature* **401**, 590-594.

Raghavan P, Petra E, Krakauer JW and Gordon AM (2006) Patterns of impairment in digit independence after subcortical stroke. *J Neurophysiol* **95**, 369-378.

Rakic P (2009) Evolution of the neocortex: a perspective from developmental biology. *Nat Rev Neurosci* **10**, 724-735.

Rathelot JA and Strick PL (2006) Muscle representation in the macaque motor cortex: an anatomical perspective. *Proc Natl Acad Sci U S A* **103**, 8257-8262.

Rathelot JA and Strick PL (2009) Subdivisions of primary motor cortex based on cortico-motoneuronal cells. *Proc Natl Acad Sci U S A* **106**, 918-923.

Richards JE (2000) Development of multimodal attention in young infants: modification of the startle reflex by attention. *Psychophysiology* **37**, 65-75.

Riddle CN and Baker SN (2010) Convergence of pyramidal and medial brain stem descending pathways onto macaque cervical spinal interneurons. *J Neurophysiol* **103**, 2821-2832.

Riddle CN, Edgley SA and Baker SN (2009) Direct and indirect connections with upper limb motoneurons from the primate reticulospinal tract. *J Neurosci* **29**, 4993-4999.

Rimpel J, Geyer D and Hopf HC (1982) Changes in the blink responses to combined trigeminal, acoustic and visual repetitive stimulation, studied in the human subject. *Electroencephalogr Clin Neurophysiol* **54**, 552-560.

Rizzolatti G and Luppino G (2001) The cortical motor system. *Neuron* **36**, 889-901.

Rizzolatti G, Luppino G and Matelli M (1998) The organization of the cortical motor system: new concepts. *Electroencephalogr Clin Neurophysiol* **106**, 283-296.

Sacco RL, Kasner SE, Broderick JP, Caplan LR, Connors JJ, Culebras A, Elkind MS, George MG, Hamdan AD, Higashida RT, Hoh BL, Janis LS, Kase CS, Kleindorfer DO, Lee JM, Moseley ME, Peterson ED, Turan TN, Valderrama AL and Vinters HV (2013) An updated definition of stroke for the 21st century: a statement for healthcare professionals from the American Heart Association/American Stroke Association. *Stroke* **44**, 2064-2089.

Sakai ST, Davidson AG and Buford JA (2009) Reticulospinal neurons in the pontomedullary reticular formation of the monkey (Macaca fascicularis). *Neuroscience* **163**, 1158-1170.

Santello M, Flanders M and Soechting JF (2002) Patterns of hand motion during grasping and the influence of sensory guidance. *J Neurosci* **22**, 1426-1435.

Schepens B and Drew T (2004) Independent and convergent signals from the pontomedullary reticular formation contribute to the control of posture and movement during reaching in the cat. *J Neurophysiol* **92**, 2217-2238.

Schepens B and Drew T (2006) Descending signals from the pontomedullary reticular formation are bilateral, asymmetric, and gated during reaching movements in the cat. *J Neurophysiol* **96**, 2229-2252.

Schepens B, Stapley P and Drew T (2008) Neurons in the pontomedullary reticular formation signal posture and movement both as an integrated behavior and independently. *J Neurophysiol* **100**, 2235-2253.

Schicatano EJ and Blumenthal TD (1998) The effects of caffeine and directed attention on acoustic startle habituation. *Pharmacol Biochem Behav* **59**, 145-150.

Schieber MH (2001) Constraints on somatotopic organization in the primary motor cortex. *J Neurophysiol* **86**, 2125-43.

Schieber MH, Lang CE, Reilly KT, McNulty P and Sirigu A (2009) Selective activation of human finger muscles after stroke or amputation. *Adv Exp Med Biol* **629**, 559-575.

Shapovalov AI (1972) Extrapyramidal monosynaptic and disynaptic control of mammalian alpha-motoneurons. *Brain Res* **40**, 105-115.

Sharpe AN and Jackson A (2014) Upper-limb muscle responses to epidural, subdural and intraspinal stimulation of the cervical spinal cord. *J Neural Eng* **11**, 016005.

Shimamura M and Kogure I (1983) Discharge patterns of reticulospinal neurons corresponding with quadrupedal leg movements in thalamic cats. *Brain Res* **26**, 27-34.

Shimamura M, Kogure I and Wada S (1982) Reticular neuron activities associated with locomotion in thalamic cats. *Brain Res* **231**, 51-62.

Shinoda Y, Zarzecki P and Asanuma H (1979) Spinal branching of pyramidal tract neurons in the monkey. *Exp Brain Res* **34**, 59-72.

Siegmund GP, Inglis JT and Sanderson DJ (2001) Startle response of human neck muscles sculpted by readiness to perform ballistic head movements. *J Physiol* **535**, 289-300.

Soteropoulos DS, Williams ER and Baker SN (2012) Cells in the monkey ponto-medullary reticular formation modulate their activity with slow finger movements. *J Physiol* **590**, 4011-4027.

Spinks RL, Baker SN, Jackson A, Khaw PT and Lemon RN (2003) Problem of dural scarring in recording from awake, behaving monkeys: a solution using 5-fluorouracil. *J Neurophysiol* **90**, 1324-1332.

Stapley PJ and Drew T (2009) The pontomedullary reticular formation contributes to the compensatory postural responses observed following removal of the support surface in the standing cat. *J Neurophysiol* **101**, 1334-1350.

Starr A, Caramia M, Zarola F and Rossini PM (1988) Enhancement of motor cortical excitability in humans by non-invasive electrical stimulation appears prior to voluntary movement. *Electroencephalogr Clin Neurophysiol* **70**, 26-32.

Steeves JD, Sholomenko GN and Webster DM (1987) Stimulation of the pontomedullary reticular formation initiates locomotion in decerebrate birds. *Brain Res* **401**, 205-212.

Steinke W and Ley SC (2002) Lacunar stroke is the major cause of progressive motor deficits. *Stroke* **33**, 1510-1516.

Stoney SD, Jr., Thompson WD and Asanuma H (1968) Excitation of pyramidal tract cells by intracortical microstimulation: effective extent of stimulating current. *J Neurophysiol* **31**, 659-669.

Swerdlow NR and Geyer MA (1993) Prepulse inhibition of acoustic startle in rats after lesions of the pedunculopontine tegmental nucleus. *Behav Neurosci* **107**, 104-117.

Takakusaki K, Shimoda N, Matsuyama K and Mori S (1994) Discharge properties of medullary reticulospinal neurons during postural changes induced by intrapontine injections of carbachol, atropine and serotonin, and their functional linkages to hindlimb motoneurons in cats. *Exp Brain Res* **99**, 361-374.

Thompson RF and Spencer WA (1966) Habituation: A model phenomenon for the study of neuronal substrates of behavior. *Psychol Rev* **73**, 16-43.

Tresch MC, Cheung VC and d Avella A (2006) Matrix factorization algorithms for the identification of muscle synergies: evaluation on simulated and experimental data sets. *J Neurophysiol* **95**, 2199-2212.

Tresch MC and Jarc A (2009) The case for and against muscle synergies. *Curr Opin Neurobiol* **19**, 601-607.

Tufail Y, Matyushov A, Baldwin N, Tauchmann ML, Georges J, Yoshihiro A, Tillery SI and Tyler WJ (2010) Transcranial pulsed ultrasound stimulates intact brain circuits. *Neuron* **66**, 681-694.

Twitchell TE (1951) The restoration of motor function following hemiplegia in man. *Brain* **74**, 443-480.

Valls-Sole J, Kumru H and Kofler M (2008) Interaction between startle and voluntary reactions in humans. *Exp Brain Res* **187**, 497-507.

Valls-Sole J, Rothwell JC, Goulart F, Cossu G and Munoz E (1999) Patterned ballistic movements triggered by a startle in healthy humans. *J Physiol* **516**, 931-938.

Valls-Sole J, Sole A, Valldeoriola F, Munoz E, Gonzalez LE and Tolosa ES (1995) Reaction time and acoustic startle in normal human subjects. *Neurosci Lett* **195**, 97-100.

Valls-Sole J, Valldeoriola F, Tolosa E and Nobbe F (1997) Habituation of the auditory startle reaction is reduced during preparation for execution of a motor task in normal human subjects. *Brain Res* **751**, 155-159.

Valsamis B and Schmid S (2011) Habituation and prepulse inhibition of acoustic startle in rodents. *J Vis Exp*, 3446.

Vilensky JA (1987) Locomotor behavior and control in human and non-human primates: comparisons with cats and dogs. *Neurosci Biobehav Rev* **11**, 263-274.

Watson CJ, Lydic R and Baghdoyan HA (2011) Sleep duration varies as a function of glutamate and GABA in rat pontine reticular formation. *J Neurochem* **11**, 571-580.

Weiss EJ and Flanders M (2004) Muscular and postural synergies of the human hand. *J Neurophysiol* **92**, 523-535.

Woolsey CN, Settlage PH, Meyer DR, Sencer W, Pinto Hamuy T and Travis AM (1952) Patterns of localization in precentral and "supplementary" motor areas and their relation to the concept of a premotor area. *Res Publ Assoc Res Nerv Ment Dis* **30**, 238-264.

Wu MF, Suzuki SS and Siegel JM (1988) Anatomical distribution and response patterns of reticular neurons active in relation to acoustic startle. *Brain Res* **457**, 399-406.

Yakovenko S, Krouchev N and Drew T (2011) Sequential activation of motor cortical neurons contributes to intralimb coordination during reaching in the cat by modulating muscle synergies. *J Neurophysiol* **105**, 388-409.

Yang HS, Kwon HG, Hong JH, Hong CP and Jang SH (2011) The rubrospinal tract in the human brain: diffusion tensor imaging study. *Neurosci Lett* **504**, 45-48.

Yeo SS, Chang MC, Kwon YH, Jung YJ and Jang SH (2012) Corticoreticular pathway in the human brain: diffusion tensor tractography study. *Neurosci Lett* **508**, 9-12.

Yeomans JS and Frankland PW (1995) The acoustic startle reflex: neurons and connections. *Brain Res Brain Res Rev* **21**, 301-314.

Zaaimi B, Edgley SA, Soteropoulos DS and Baker SN (2012) Changes in descending motor pathway connectivity after corticospinal tract lesion in macaque monkey. *Brain* **135**, 2277-2289.

Zackowski KM, Dromerick AW, Sahrmann SA, Thach WT and Bastian AJ (2004) How do strength, sensation, spasticity and joint individuation relate to the reaching deficits of people with chronic hemiparesis? *Brain* **127**, 1035-1046.

Zimmermann JB, Seki K and Jackson A (2011) Reanimating the arm and hand with intraspinal microstimulation. *J Neural Eng* **8**, 054001.